

University of Warwick institutional repository: <http://go.warwick.ac.uk/wrap>

A Thesis Submitted for the Degree of PhD at the University of Warwick

<http://go.warwick.ac.uk/wrap/69397>

This thesis is made available online and is protected by original copyright.

Please scroll down to view the document itself.

Please refer to the repository record for this item for information to help you to cite it. Our policy information is available from the repository home page.

**NOVEL INSIGHTS IN IMAGING AND FUNCTION OF
HUMAN BROWN ADIPOSE TISSUE**

By

Dr Narendra Lakshmana Reddy

A thesis submitted to

The Faculty of Medicine

University of Warwick

For the degree of

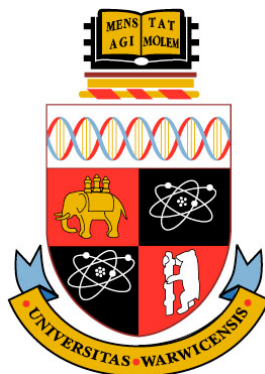
DOCTOR OF MEDICINE

Division of Metabolic and Vascular Health

Warwick Medical School

University of Warwick

May 2014



CONTENTS

Table of Contents.....	I
List of Figures and Tables.....	X
Acknowledgments.....	XIX
Dedication.....	XX
Declaration.....	XXI
Synopsis.....	XXII
Abbreviations.....	XXIV

TABLE OF CONTENTS

CHAPTER 1: Introduction	1
1.1 Obesity	2
1.1.1 Epidemiology of Obesity	2
1.1.2 Complications of Obesity	3
1.1.3 Economic Burden of Obesity	3
1.1.4 Measurement of Obesity	4
1.1.5 Management of Obesity	7
1.2 Insulin Resistance	8
1.2.1 Physiology of Insulin Resistance	8
1.2.2 Measures of Insulin Resistance	11
1.2.3 Risk factors for Insulin Resistance	12
1.2.4 Metabolic Syndrome	12

1.2.5	Insulin Resistant States	15
1.3	Dietary Patterns and Obesity	16
1.4	Adipose Tissue	18
1.4.1	Adipose Tissue: a cause of Insulin Resistance	18
1.4.2	Types of Adipose Tissue	21
1.4.3	White, Brown and Beige Adipose Tissue	23
1.5	Brown adipose tissue	24
1.5.1	Evolution of Brown adipose tissue	24
1.5.2	Anatomy of Brown adipose tissue	26
1.5.3	Function of Brown adipose tissue	28
1.5.4	Prevalence of Brown adipose tissue	30
1.5.5	Origin of Brown Adipose Tissue	31
1.6	Imaging of Brown adipose tissue	34
1.6.1	Positron Emission Tomography-Computed Tomography (PET-CT) Imaging of Brown Adipose Tissue	34
1.6.2	Magnetic Resonance (MR) Imaging of Brown Adipose Tissue	37
1.7	Brown Adipose Tissue and Energy Expenditure	39
1.7.1	Energy Expenditure	39
1.7.2	Brown Adipose Tissue: Cold and Diet Induced Thermogenesis	42
1.7.3	Metabolic Significance of Brown Adipose Tissue	43

1.8	Regulators of Brown Adipose Tissue	45
1.8.1	Environmental temperature and Brown Adipose Tissue	45
1.8.2	Sympathetic Nervous System and Brown Adipose Tissue	46
1.8.3	Thyroid hormones and Brown Adipose Tissue	47
1.8.4	Transcriptional Regulation	48
1.9	Neurohormonal Adiposity Signals	50
1.9.1	Central regulation of body weight	50
1.9.2	Ghrelin	51
1.9.3	Glucagon-like peptide 1	52
1.9.4	Peptide YY	53
1.9.5	Pancreatic polypeptide	54
1.9.6	Leptin	55
1.9.7	Adiponectin	56
1.9.8	Non-esterified Fatty Acids	56
1.10	General Aims of the Study	50
CHAPTER 2: Methods and Materials		61
2.1.1	Positron Emission Tomography (PET) detected Brown Adipose Tissue (BAT) study	61
2.1.2	Basic principles of PET imaging	62
2.1.3	Image reconstruction from PET	64

2.1.4	Principles of Computed tomography (CT)	65
2.1.5	Integration of PET with CT	69
2.1.6	PET-CT imaging protocol	70
2.1.7	Patient Records Data collection	71
2.1.8	Image analyses	73
2.1.9	Significance of Standardised Uptake Value (SUV)	73
2.1.10	BAT activity, BAT volume and BAT mass quantification	74
2.1.11	Statistical analyses	76
2.2	Materials and Methods for Magnetic Resonance Imaging of Brown Adipose Tissue (BAT) Study	77
2.2.1	Introduction	77
2.2.2	Basic principles of Magnetic Resonance Imaging	78
2.2.3	Iterative Decomposition with Echo Asymmetry and Least Squares Estimation (IDEAL) MRI	81
2.2.4	Proof of concept of IDEAL MRI study on Rat fat samples	82
2.2.5	Subject recruitment and Positron-emission tomography scanning	83
2.2.6	Magnetic resonance scanning of the study subject	83
2.2.7	Histology and Immunohistochemistry	84
2.3	Meal Duration Study	85
2.3.1	Introduction	85
2.3.2	Inclusion and Exclusion Criteria	86
2.3.3	Meal Duration Study Protocol	87
2.3.4	Anthropometric Assessment	90

2.3.5	Assessment of Body Composition Using the BODPOD	90
2.3.6	Assessment of Energy Expenditure using Whole Body Calorimeter	90
2.3.7	Calculation of Energy Expenditure including Diet Induced Thermogenesis (DIT)	93
2.3.8	Assessment of Hunger, Fullness, Appetite and Satiety	93
2.3.9	Buffet meal	94
2.7.10	Statistical analyses and power calculation	94
2.7.11	Collection of Human Blood samples	94
2.7.12	Biochemical evaluation	95
2.7.13	Multiplex assay	96
2.7.14	Endotoxin assay	96
2.7.15	Measurement of Insulin resistance	97
CHAPTER 3: Determinants of human brown adipose tissue		98
based on physiologic ¹⁸F-FDG uptake in		
sequential PET-CT examinations		
3.1	Introduction	99
3.2	Methods	103
3.2.1	Subjects data collection	103
3.2.2	PET-CT imaging protocol	104
3.2.2	Image analyses	105
3.2.3	Statistical analyses	105

3.3	Results	106
3.3.1	General Characteristics and overall study parameters	106
3.3.2	Prevalence of ¹⁸ FDG detected BAT	108
3.3.3	BAT mass and BAT activity (SUV _{max}) analyses	109
3.3.4	Influence of Age on BAT prevalence, BAT activity and BAT mass	113
3.3.5	Influence of Gender factor on BAT prevalence, BAT activity and BAT mass	115
3.3.6	Influence of Body Mass Index (BMI) on BAT prevalence, BAT activity and BAT mass	118
3.3.7	Influence of Fasting Glucose on BAT prevalence, BAT activity and BAT mass	119
3.3.8	Influence of Outdoor temperature on BAT prevalence, BAT activity and BAT mass	120
3.3.9	Influence of Thyroxine on BAT prevalence	122
3.4	Discussion	126
CHAPTER 4: Identification of brown adipose tissue using MR Imaging		131
4.1	Introduction	132
4.2	Materials and Methods	135
4.2.1	Proof of concept of IDEAL MRI study on Rat fat samples	135
4.2.2	Subject recruitment and case study	136

4.2.3	Positron-emission tomography scanning	138
4.2.4	Magnetic resonance scanning	139
4.2.5	Retrospective image analysis	139
4.2.6	Prospective image analysis	141
4.2.7	Histology and Immunohistochemistry	141
4.3	Results	142
4.3.1	IDEAL MRI results from Rat imaging	142
4.3.2	IDEAL MRI results from Human imaging- Retrospective image analyses	143
4.3.3	IDEAL MRI results from Human imaging- Prospective image analyses	148
4.3.4	Histology and Immunohistochemistry	149
4.4	Discussion	151
	CHAPTER 5: Effect of meal duration on diet induced thermogenesis and biochemical metabolic markers	155
5.1	Introduction	156
5.2	Methods	160
5.2.1	Subjects	160
5.2.2	Protocol: Anthropometry, calorimetry and meal duration	161
5.2.3	Protocol: Postprandial phase	162

5.2.4	Biochemical evaluation	163
5.2.5	Statistical analyses and power calculations	163
5.3	Results	164
5.3.1	Baseline anthropometric, clinical and biochemical data	164
5.3.2	The Effect of 10-minute Meals or 40-minute Meals on Diet Induced Thermogenesis in Obese Subjects	166
5.3.3	The Effect of 10-minute Meals or 40-minute Meals on Delta Energy Expenditure rates in Obese Subjects	168
5.3.4	The Effect of 10-minute Meals or 40-minute Meals on Serum Glucose and Insulin in Obese Female Subjects	168
5.3.5	The Effect of 10-minute Meals or 40-minute Meals on Serum Adiponectin and Serum NEFA in Obese Female Subjects	169
5.3.6	The Effect of 10-minute Meals or 40-minute Meals on Pancreatic, Gut hormones and Cortisol in Obese Female Subjects	170
5.3.7	Postprandial Appetite (Visual Analogue Scale and <i>ad libitum</i> evening buffet)	172
5.4	Discussion	175
CHAPTER 6: Discussion		181
6.1	Introduction	181

6.2	Future directions	185
6.3	Conclusion	187
	BIBLIOGRAPHY	188
	APPENDIX	214

LIST OF FIGURES AND TABLES

CHAPTER 1

Table 1.1.4

Classification of Weight Categories Based on BMI

Figure 1.2.1

Pathophysiology of insulin resistance

Table 1.2.4.1

International Diabetes Federation (IDF) Criteria for Diagnosis of Metabolic Syndrome

Table 1.2.4.2

Ethnic specific values for waist circumference

Figure 1.4.1

Chronic inflammation in adipose tissue triggers insulin resistance in skeletal muscle

Figure 1.4.2

Amount and activity of brown adipose tissue as shown in PET (left), CT (centre) and combined PET-CT (right).

Table 1.5.1

Timeline and summary of major developments in Human BAT research

Table 1.5.2

Morphological features of BAT, WAT and BeAT

Figure 1.5.2:

a) Haematoxylin and Eosin staining preparations of adipose tissues on 3 subjects demonstrating multilocular and intracellular lipid droplets in BAT, absent in WAT;

b) Immunohistochemistry demonstrating high UCP-1 uptake in BAT for UCP-1 antispecific sera, which is absent in WAT.

Figure 1.5.3

Molecular mechanism of Brown Adipose tissue

Figure 1.5.5

Development of Brown Adipose tissue

Figure 1.6.1

Coronal image of a 25-year old female following curative surgery for neck malignancy resection demonstrating avid ¹⁸F¹⁸FDG uptake in supraclavicular, cervical, mediastinal and axillary region

Table 1.6.1

Comparison of prevalence rate of BAT detection in retrospective PET studies

Figure 1.6.2

IDEAL results from excised tissues imaged placing in water filled petri dish. a) Macroscopic brown and white adipose tissue (BAT, WAT) in vials; b) water; c) fat, and d) fat-fraction map. Mean fat-fraction map for the 4 samples (from left to right) 92%, 51%, 93%, and 62%.

Table 1.7.1

Components of Human Energy Expenditure

Table 1.7.3

Metabolic significance of BAT in Adult Humans

Figure 1.8.3

Illustration of origin and cellular receptor pathways of some of the secreted endocrine regulators, which recruit brown and/or beige adipocytes.

Figure 1.9.8

NEFA release from adipocytes causes reduced glucose uptake in adipocyte and skeletal muscle; acutely, NEFA causes insulin release, but chronic exposure causes insulin resistance.

CHAPTER 2**Figure 2.1.2**

Basic principles of PET imaging

Figure 2.1.3

Illustration showing two photons from a single annihilation event interacting simultaneously with opposing scintillation crystals along a single Line of Response (LOR). The light photons are converted into electrical impulses by a photomultiplier tube and are computer processed to produce a Pet image.

Figure 2.1.4.1

Illustration of a CT arrangement.

Table 2.1.4.2

Range of CT attenuation values for various tissues

Figure 2.1.5

Schematic representation of dual PET-CT scanner with respective positions in a common gantry.

Figure 2.1.10.a

Semi-automatic selection of ^{18}F -FDG regions of interest by defining an isocontour set at SUV of 2.5 g/ml

Figure 2.1.10.b

Coronal PET Maximum intensity projection (MIP) image, showing isocontours around BAT from which volumes were derived

Figure 2.2.2

Basics principles of MRI

CHAPTER 3

Table 3.3.1

Characteristics of BAT positive and BAT negative patients based on ^{18}F -FDG BAT

Table 3.3.2.1

Logistic regression analyses on predictors of Brown Adipose Tissue prevalence based on ^{18}F -FDG scanning (n=2685.)

Table 3.3.2.2

Stepwise regression analyses on predictors of BAT prevalence based on ^{18}F -FDG scanning (n=2685).

Figure 3.3.3.1

Illustration of Normal Q-Q plot with Kolmogorov-Smirnov test being statistical significant 0.200 (>0.05) for BAT mass

Table 3.3.3.2

Illustration of BAT mass determinants on ^{18}F -FDG PET scans based on Tobit model univariate and multivariate analyses

Table 3.3.3.3

Illustration of BAT activity determinants on ^{18}F -FDG PET scans based on Tobit model univariate and multivariate analyses

Table 3.3.4.1

Age decade wise ¹⁸F-DG detected BAT positive scans

Figure 3.3.4.2

Schematic representation of effect of Age on BAT prevalence expressed in percentage of BAT detection rate according to decade

Figure 3.3.4.3

Schematic representation of effect of Age on BAT activity

Figure 3.3.4.4

Schematic representation of effect of Age on BAT mass

Figure 3.3.5.1

Schematic representation of effect of sex on BAT prevalence

Figure 3.3.5.2

Illustration of brown fat mass in males and females on ¹⁸F-FDG PET scanning

Table 3.3.5.3

Comparison of biophysical, PET scan and environmental parameters related to ¹⁸F-FDG BAT uptake

Figure 3.3.6.1

Bar graph of BAT prevalence in PET scans according to Body Mass Index

Figure 3.3.6.2.

Bar graph of BAT mass in PET scans according to Body Mass Index categories

Figure 3.3.7

Bar graph of PET BAT detected patients in various glycaemic groups

Figure 3.3.8.1

Graph representing the relation of mean monthly temperature with BAT FDG uptake prevalence rates.

Figure 3.3.8.2

Seasonal variation of BAT detection from PET scanning

Figure 3.3.8.3

Monthly variation of BAT detection from PET scanning

Table 3.3.9.1

Comparison data of patients' characteristics in Thyrotoxic, Euthyroid and total ^{18}F -FDG BAT +ve patients

Figure 3.3.9.2

Correlation of Thyroid Stimulating Hormone and BAT activity

(SUV_{max}) in ^{18}F -FDG BAT uptake positive patients

Figure 3.3.9.3

Correlation of Free T4 Hormone and BAT activity

(SUV_{max}) in ^{18}F -FDG BAT uptake positive patients

CHAPTER 4

Figure 4.2.1.1

IDEAL results from dissected tissues. (a) Brown and white adipose tissue (BAT, WAT) are macroscopically distinct. (b) Water-only IDEAL, (c) Fat-only IDEAL, and (d) Fat-fraction map: 92%, 51%, 93%, and 62% mean fat-fraction from left to right.

Figure 4.2.1.2

Macroscopic BAT and WAT samples dissected from Wistar rats kept at thermoneutrality (30 °C) and cold (4 °C).

Figure 4.2.2.1

Coronal image of ^{18}F -FDG PET scan of the study subject exhibiting high physiological ^{18}F -FDG BAT uptake in cervical, mediastinal and axillary areas

Table 4.2.2.2

Phenotypical characteristics of the human subject

Figure 4.3.1.1

a) Fat-fraction images of dissected BAT, Subcutaneous WAT and Omental WAT (from left to right), from rats kept at 4°C , and, b) at 30°C . Images are coloured in 10% increments. The areas of blue correspond to skeletal muscle, orange is WAT and green/yellow is BAT

Figure 4.3.1.2

Axial MR slices through the upper thorax showing a) Fat-IDEAL and b) Low fat-fraction corresponding to BAT in the interscapular region

Figure 4.3.2.1

(a): Axial PET-CT image showing ^{18}F -FDG uptake consistent with BAT in mediastinum (arrowed); (b): Fat:IDEAL MR image demonstrating low signal areas within the mediastinal fat (arrows) corresponding to BAT on PET-CT; (c): ROIs drawn around high ^{18}F -FDG uptake and transferred onto registered fat-only images.

Table 4.3.2.2

For each anatomical region the number of $\text{BAT}_{\text{retro}}$ ROIs with low and normal signal intensity on MR is tabulated. The ROIs were retrospectively drawn on MR from areas of corresponding high ^{18}F -FDG uptake on the PET-CT images.

Table 4.3.2.3

Variation in $\text{BAT}_{\text{retro}}$ and $\text{WAT}_{\text{retro}}$ MR signal intensity and BAT:WAT signal ratio according to anatomical region

Figure 4.3.2.4: Variation in BATretro and WATretro signal according to slice and anatomical site, showing a ten-fold increase in signal intensity between cranial (neck) and caudal (mediastinal) MR slices.

Figure 4.3.2.5

Variation in BATretro:WATretro signal ratio according to anatomical location, with significantly lower signal ratio within mediastinum and neck. The shaded area represents a ratio >1 (i.e. WATretro signal > BATretro signal).

Figure 4.3.2.6

a) Baseline MR; b) Repeat axial fat:IDEAL MR image of the upper thorax performed 2 months after the baseline MR scan, showing a similar distribution of putative BAT within the anterior mediastinum and suprasternal notch

Figure 4.3.4:

a) ¹⁸F-FDG uptake within the suprasternal notch on PET-CT (arrow); (b) fat:IDEAL MR at the same level showing corresponding low signal in the suprasternal notch; (c) Haematoxylin-Eosin staining and (d) UCP1 immunostaining providing confirmation of BAT obtained from this area.

CHAPTER 5

Table 5.3.1

Baseline anthropometric, clinical and biochemical (fasting) data for all subjects (n=10) taken prior to entry into WBC at first metabolic study

Table 5.3.2.1

Diet Induced Thermogenesis of 10-minute and 40-minute meals

Figure 5.3.2.2

Comparison of diet induced thermogenesis between 10-minute meals and 40-minute meals in obese females

Figure 5.3.2.3

Comparison of diet induced thermogenesis (expressed in percentage of the total meal calories ingested) between 10-minute meals and 40-minute meals in obese females.

Figure 5.3.3

Comparison of energy expenditure rate difference between pre- and post 10-minute meals and 40-minute meals in obese females.

Figure 5.3.4

Comparison between the effect of 10-minute meals and 40-minute meals on serum insulin and serum glucose in obese females.

Figure 5.3.5

Comparison between the effect of 10-minute meals and 40-minute meals on serum adiponectin and serum NEFA in obese females.

Figure 5.3.6

Comparison between the effect of 10-minute meals and 40-minute meals on serum pancreatic, gut hormones, serum cortisol and HOMA-IR in obese females.

Table 5.3.7

Postprandial biochemical data of study subjects following each standard meal (D10 versus D40)

Table 5.3.8

Data showing measures of appetite (visual analogue scales) in the postprandial phase, consumption of *ad libitum* evening meal data and energy expenditure in the postprandial phase

ACKNOWLEDGEMENTS

I would like to thank my supervisors Dr Thomas Barber and Dr Harpal Randeva for their excellent support and guidance over the past two years, and for making me a critical thinker. I thank Professor Sudhesh Kumar for the HMRU facility in UHCW. I thank profoundly Milan Piya and Terry Jones and, who have been my research critics and for giving me constant support.

I would also like to express my gratitude to the Diabetes Team of the Division of Metabolic and Vascular Health of Warwick Medical School, as well as my clinical colleagues in WISDEM centre in UHCW for their constant help and encouragement.

John Hattersley, Alison Campbell and Dr Chen Peng in the HMRU unit have been extremely helpful with energy expenditure experiments. I thank Sean James for help in samples storage and for his expertise in immunohistochemical staining. I also would like to thank Dr Olu Adesanya, Sarah Wayte and Professor Charles Hutchinson for teaching me radiology concepts.

I would like to thank Alison Harte, Marcos Carreira, Felipe Casanueva and the UHCW NHS Biochemistry department staff for their expertise in analysing the analysis of samples. I would also like to thank the NHS R&D team at UHCW.

This thesis could not have been written without the generous assistance of countless volunteers, patients and colleagues and I would like to convey best wishes.

DEDICATION

To my parents Shivamma and Lakshmana Reddy, who have made me what I am, and for continuing to inspire.

To my soul mate Sandhya, for being the pillar of my strength, for pushing me along during moments of despair, and for enduring my long absences.

To my just born son Advaith, for failing to wipe the smile off my face even in times of extreme duress.

DECLARATION

I declare that this thesis is an accurate record of results obtained from the Human Metabolism Research Unit, Warwick Medical School collaboration, and the Department of Radiology at University Hospitals Coventry and Warwickshire NHS Trust. The data that has arisen is detailed in this thesis. I confirm that I collected the entire data from Human Metabolism Research Unit relevant for the studies presented in the thesis. The radiology data was jointly collected and analysed by myself, and by Dr Terry Jones, Research Fellow at Warwick Medical School. All sources of support and technical assistance have been stated in the text of the acknowledgements. None of the work has been previously submitted for a higher degree.

All sources have been specifically acknowledged by means of reference.

SYNOPSIS

Phenomenal rise in prevalence of obesity and its complications has made it imperative to tackle the issue on a war footing, especially given the failure of current life style and medical approaches. Clearly, alternate means of treating obesity need to be explored. In contrast to white adipose tissue (WAT), which stores excess energy, brown adipose tissue (BAT) dissipates chemical energy in the form of heat by uncoupling oxidative phosphorylation from electron transport chain, to maintain body temperature homeostasis. Recent revelation of functionality of BAT in adult humans provides an excellent opportunity of stimulating it to increase energy expenditure, in turn causing weight loss alongside improving lipid and glucose homeostasis. This thesis sought to investigate the physiological nature of brown fat, by exploring the environmental, biophysical and behavioural factors that can activate BAT.

¹⁸Fluoro-labelled-2-deoxyglucose Positron Emission Tomography (¹⁸F-FDG PET) is currently the gold standard and the most sensitive method to study BAT and its function. These studies concluded that younger-age, lower body mass index, female sex and cooler outdoor temperatures are strong determinant factors of BAT prevalence, activity and mass. Interestingly, modest elevation of thyroid hormones in a sustained iatrogenically created thyrotoxic state did not influence any of the BAT indices, contrary to conventional wisdom of strong stimulation, thus highlighting the complexity of BAT metabolism. Arguably, BAT has a role in diet-induced thermogenesis. Manipulation of diet-induced thermogenesis by prolonging meal duration to 40 minutes resulted in excess postprandial energy expenditure loss than shorter meal duration of 10 minutes. However, prolonged meal duration had weakly

positive effect on metabolic biochemical markers and no influence on pancreatic and gut hormones relevant to appetite. These studies advocate life style and behavioural public health messages of lowering thermostat in living spaces and chewing the food adequately in order to obtain potential metabolic benefits. As a follow-up of exploring BAT's physiology, a successful attempt at characterising BAT's anatomy was made through novel imaging technique of Iterative Decomposition of Echo Asymmetry and Least Squares Estimation (IDEAL) Magnetic Resonance Imaging. The first ever non-PET imaging demonstration of adult human BAT using IDEAL MRI was achieved with immunohistochemical confirmation, and provided proof of concept for developing MR as a safe, non-radiation exposure imaging biomarker of BAT.

In summary, this thesis provided useful insights into environmental, anthropometrical, behavioural, and hormonal factors regulating BAT, whilst also providing a proof of principle of an imaging tool to visualise full extent of both metabolically active and inactive BAT, aiding future pursuits of BAT therapeutics to combat the global obesity epidemic.

ABBREVIATIONS

ARB3	Adrenoreceptor
ADRB3	β 3 adrenergic receptor
AEE	Activity related energy expenditure
AgRP	Agouti-related protein
ATP	Adenosine tri-phosphate
ANP	Atrial Natriuretic Peptide
ARC	Arcuate nucleus
AUC	Area under the curve
BAT	Brown Adipose Tissue
BeAT	Beige Adipose Tissue
BMI	Body mass index
BMP	Bone morphogenic proteins
BMP7	Bone Morphogenic Protein-7
BGO	Bismuth germinate
B_0	External magnetic field
CI	Confidence Interval
c-AMP	Cyclic adenosine monophosphate
CIT	Cold induced thermogenesis
CHO	Carbohydrate
CVD	Cardiovascular disease
CT	Computed Tomography
γ	Constant
DIT	Diet induced thermogenesis

DEXA	Dual Energy X-ray Absorption
D2	Type 2 iodothyronine deiodinase
DPP- IV	Dipeptidyl dipeptidase –IV
EE	Energy expenditure
EDTA	Ethylenediaminetetraacetic acid
ER	Endoplasmic reticulum
EN1	Engrailed-1
¹⁸ FDG	18-Fluoro-labelled -2-deoxy-glucose
FPG	Fasting plasma glucose
FFA	Free fatty acids
FGFs	Fibroblast growth factors
FNDC5	Fibronectin type III domain containing 5
FOXC2	Forkhead box C2
FGF-21	Fibroblast Derived Growth Factor-21
g	Grams
GDM	Gestational Diabetes Mellitus
GLP- 1	Glucagon-like peptide-1
GLP- 2	Glucagon like peptide-2
GLUT4	Glucose Transporter Protein 4
HbA1C	Glycated haemoglobin
HE	Haematoxylin-eosin
Hrs	Hours
HDL	High Density Lipoprotein
HIV	Human Immunodeficiency Virus
HOMA-IR	Homeostasis model assessment insulin resistance

HMRU	Human Metabolism Research Unit
HPT- JT	Hyperparathyroidism-Jaw Tumour
HRPT2	HPT-JT gene
IDEAL	Iterative decomposition of water and fat with echo asymmetry and least-squares estimation
IFG	Impaired fasting Glycaemia
IGT	Impaired Glucose Tolerance
IVGTT	Intravenous Glucose Tolerance Test
ITT	Insulin Tolerance Test
ISI	Insulin sensitivity index
IDF	International Diabetes Federation
IL-10	Interleukin-10
IL-4	Interleukin-4
IL-13	Interleukin-13
IL- 6	Interleukin-6
IGF1	Insulin like growth factor - 1
IKK β	Kappa B Kinase catalytic subunit- β
IASO/IOTF	International Association for the Study of Obesity/International Obesity Taskforce analysis
IU	International units
JNK	Jun N-terminal Kinase
Kcal	Kilo calories
LBW	Lean body weight
LDL	Low Density Lipoprotein
LSO	Lutetium oxyorthosilicate

LYSO	Lutetium yttrium oxyorthosilicate
LOR	Line of Response
Mz	Longitudinal magnetization
Mxy	Transverse magnetization
MR	Magnetic resonance
MRI	Magnetic Resonance Imaging
MCP- 1	Monocyte chemoattractant protein-1
Myf5	Myogenic regulating factor-5
NHS	National Health Service
NMR	Nuclear magnetization resonance
NMV	Net Magnetic Vector
NPY	Neuropeptide Y
NEFAs	Non-esterified fatty acids
NFκB	Nuclear Factor Kappa B
NAFLD	Non-Alcoholic Fatty Liver Disease
NCEP: ATP III	National Cholesterol Education Program's Adult Treatment Panel III
NS	Not significant
OGTT	Oral Glucose Tolerance Test
PACS	Picture archiving and communication system
PTH	Parathyroid hormone
PAI-1	Plasminogen Activator Inhibitor-1
PCOS	Polycystic Ovarian Syndrome
PET	Positron Emission Tomography
PHA	Pulse height analyzer (PHA)

pNA	<i>p</i> -nitroaniline
PYY	Peptide-YY
PP	Pancreatic polypeptide
PPAR- γ	Proliferator-Activated receptor Gamma Alpha
PGC1 α	Peroxisome Proliferator-Activated receptor-Gamma-Coactivator-1-alpha
PRDM16	PR domain containing 16
POMC	Pro-opiomelanocortin Precession frequency
PKA	Protein kinase –A
ω_0	Precession frequency
QUICKI	Quantitative Insulin Sensitivity Check Index
REE	Resting energy expenditure
RF	Radiofrequency
RIP140	Receptor-Interacting Protein 140
RMR	Resting metabolic rate
ROIs	Region of interests
SD	Standard deviation
SEM	Standard error of mean
SMR	Sleeping metabolic rate
SNS	Sympathetic nervous system
SHBG	Sex hormone binding globulin
SUV	Standardised uptake value
TLG	Total lesion glycolysis
TEE	Total energy expenditure
TNF- α	Tumour Necrosis Factor- α

T1DM	Type 1 Diabetes mellitus
T2DM	Type 2 diabetes mellitus
TG	Triglycerides
TGF β	Transformation Growth Factor- β
TH	Thyroid hormone
TSH	Thyroid stimulating hormone
T4	Thyroxine
T3	Thyronin
TR β	Thyroid Receptor Beta
TR	Repetition time
UCP1	Uncoupling Protein-1
UHCW	University Hospitals Coventry and Warwickshire
VO ₂	Volume of oxygen consumption
VCO ₂	Volume of carbon dioxide consumption
VLDL	Very Low Density Lipoprotein
VAS	Visual analogue scale
WBCs	Whole body calorimeters
WHO	World Health Organization
WHR	Waist-to-hip ratio
WAT	White Adipose Tissue
WISDEM	Warwickshire Institute for the Study of Diabetes, Endocrinology and Metabolism
25-OH Vit D	25-hydroxycholecalciferol

Chapter 1

INTRODUCTION

1.1 Obesity

1.1.1 Epidemiology of Obesity

According to the World Health Organization (WHO) report, worldwide obesity rates have more than doubled since 1980. Global figures from 2008 showed that 1.46 billion adults were overweight and that obesity affected 200 million men and 300 million women, with the numbers expected to rise exponentially (World Health Organization, Obesity and overweight, Fact sheet No 311 Updated March 2013¹). As per the New International Association for the Study of Obesity/International Obesity Taskforce analysis (IASO/IOTF) 2010, it is estimated that approximately 1 billion overweight adults (Body Mass Index [BMI] 25-29.9 kg/m²), and a further 475 million adults are obese (BMI 30 kg/m² or over). With an Asian-specific definition of obesity (BMI >28 kg/m²), global obesity prevalence in adults is estimated at >600 million (International Association for the Study of Obesity/ International Obesity Taskforce analysis 2010²). The prevalence of clinical obesity in United Kingdom is highest in Europe and is expected to rise to more than 1 in every 2 adults by 2050 (Foresight 2007³). Almost a quarter of adults (24% of men and 25% of women aged 16 or over) in England are classified as obese, and the prevalence increased from 14.9% to 24.9% between 1993 and 2013 (Health Survey England 2010⁴, National Obesity Observatory 2013⁵).

1.1.2 Complications of Obesity

Obesity is associated with increased risk of number of chronic conditions including type 2 diabetes mellitus (T2DM), coronary heart disease, heart failure, stroke, hypertension, dyslipidaemia, reproductive and gastrointestinal cancers, fatty liver disease, osteoarthritis and obstructive sleep apnoea (Padwal, R et al Cochrane review 2004⁶), resulting in overall increase of mortality rates (Calle et al 1999⁷). Sims and colleagues in 1970's aptly coined the term 'diabesity' as around 90% of T2DM patients have a BMI of more than 23 kg/m² and the risk increases further with family history of diabetes, gestational diabetes and early weight gain especially in childhood (Wannamethee, S, G et al⁸). The number one cause of mortality remains cardiovascular disease (CVD), and obesity is a key factor in increased rates of CVD associated morbidity and mortality (Flegal et al 2007⁹, Kenchaiah et al 2002¹⁰). Obesity is a significant determinant for increased rates of cancer (Guh et al 2009¹¹, Basen-Engquist et al 2011¹²), obstructive sleep apnoea, asthma, gall bladder disease and osteoarthritis (Anandam et al 2013¹³, Gami et al 2003¹⁴, Guh et al 2009¹¹). It is also associated with significant psychological morbidity, including depression (Hryhorczuk et al 2013¹⁵).

1.1.3 Economic Burden of Obesity

The medical costs of obesity represent the monetary value of health-care resources devoted to managing obesity-related disorders, including the costs incurred by excess use of ambulatory care, hospitalization, drugs, radiological or laboratory tests, and long-term care including that of nursing homes (Wang et al 2011¹⁶). A

systematic review of worldwide economic burden of direct health-care costs of obesity reveals that it accounts for 0.7–2.8% of a country's total health-care costs, and that obese individuals had 30% higher medical costs than those with normal weight (Withrow et al 2011¹⁷). Compared with normal-weight individuals, obese patients incur 46% increased inpatient costs, 27% more physician visits and outpatient costs, and 80% increased spending on prescription drugs (Finkelstein et al 2009¹⁸). Loss of productivity accounting for the indirect costs, further adds to this financial burden. The direct cost of treating overweight and obesity in England has risen from £479.3 million to £4.2 billion in 2007, and estimates of indirect costs ranges from £2.6 to £15.8 billion (Economic Burden of Obesity, National Obesity Observatory, October 2010⁴, Foresight 2007³). It is expected to rise to £9.7 billion in direct costs, and £49.9 billion in indirect costs (Foresight 2007³).

1.1.4 Measurement of Obesity

There are various ways in which to measure different aspects of obesity. They include BMI, skin fold thickness, waist circumference, waist-to-hip ratio, bio-impedance and radiological methods. The most widely used method of measuring obesity is BMI due to the ease of measurement; established cut-offs and existing published statistics. BMI is calculated as weight in kilograms divided by height in metres squared ($BMI = \text{weight [kg]} / \text{height [m}^2\text{]}$). WHO classification of weight categories based on BMI is shown in Table 1.1.4. BMI is a good predictor of health risk, such as CVD mortality, in white Caucasian populations - as described in two separate meta-analyses (Whitlock et al, Prospective Studies Collaboration 2009¹⁹, Berrington de Gonzalez et al 2010¹⁹⁻²¹). Both these studies demonstrated an overall

increased mortality risk in both overweight and obese populations, with an estimated loss of 2-4 years of life for BMI 30-35 kg/m², and 8-10 years for BMI 40-45 kg/m² compared to an optimum BMI of 22.5-25 kg/m². However, BMI is only a proxy indicator of body fatness; factors such as fitness (muscle mass), ethnic origin and puberty can alter the relationship between BMI and body fatness whilst also underestimating mortality risk (WHO Expert Consultation 2004²²). Abdominal or centripetal obesity is shown to be a better predictor of health risk than BMI alone (National Obesity Observatory²³, Pischon et al 2008²⁴, Koster et al 2008²⁵). Waist circumference or waist-to-hip ratio is shown to be more strongly associated with the risk of myocardial infarction than BMI (Yusuf S et al 2005²⁶), and also seem to be better predictors of risk of insulin resistance and future risk of T2DM than BMI alone (Langenberg et al 2012²⁷).

Bioelectrical impedance measures body fat percentage, by recording the impedance or opposition to the flow of a very small electric current as it passes through the body. As lean mass is made up of 73% water and fat has no water content, this method estimates lean tissue mass (which acts as a conductor) and fat mass (which acts as an insulator), through changes in voltage (Pietilainen et al 2013²⁸). More accurate measurement of body fat percentage is by underwater weighing and air displacement plethysmography, but inherits practical limitations for general population assessment (Ginde et al 2005²⁹, Koda et al 2000³⁰).

Radiological methods such as Computed Tomography (CT), Dual Energy X-ray Absorption (DEXA) or Magnetic Resonance Imaging (MRI) assess adiposity and obesity more accurately, but are expensive and cumbersome, and therefore used for

research purposes only (Seidell et al 1988³¹, Kaul et al 2012³², Pietilainen et al 2013²⁸).

Table 1.1.4 Classification of Weight Categories Based on BMI

	White Europeans	Asians
Classification	BMI (Kg/m²)	BMI (Kg/m²)
Normal weight	18.5-24.9	18.5-22.9
		23-24.9
Pre-obese	25-29.9	25-27.4
		27.5-29.9
Class I Obesity	30-34.9	30.0-32.4
		32.5-34.9
Class II Obesity	35-39.9	35.0-37.4
		37.5-39.9
Class III Obesity	>40.0	>40.0

For Asian populations, classifications remain the same as the international classification, but the public action points are set at 23, 27.5, 32.5 and 37.5 kg/m² for intervention purposes³³. Source: International Diabetes Federation (IDF) position statement on bariatric surgery 2011³⁴, as adapted from World Health Organization (WHO) 2004³⁵.

1.1.5 Management of Obesity

The multi-pronged management approach of obesity includes lifestyle changes, pharmacological interventions, and in extreme obesity, surgical approaches are warranted. The management of obesity through changes to lifestyle is notoriously difficult and the resulting effects on weight are variable and often transient. Weight regain following weight loss is common and results from a number of mechanisms that redress any loss of energy storage capacity (Geldszus et al 1996³⁶, Cummings et al 2002³⁷, Chearskul et al 2008³⁸). Current therapeutic options for obesity management are very limited following the recent withdrawal of sibutramine and rimonabant amid safety concerns. Orlistat, which is the only licensed medication in UK, faces problems relating to the supply, unacceptable side-effect profile and long-term efficacy (Padwal et al 2004⁶). Bariatric surgery is the only effective treatment modality that appears to have sustained weight loss maintenance, but is reserved for selected population with morbid obesity, and does not represent a practical solution to the global obesity epidemic (Buchwald et al 2004³⁹, Sjöström et al⁴⁰, Pontiroli et al 2011⁴¹, O'Brien et al 2013⁴²). Given the limitations of current therapeutic approaches to obesity, and the current global obesity epidemic and escalating incidence of obesity-related deaths, it is imperative to identify novel and effective therapeutic options. Adipose tissue, a multifarious endocrine organ with multiple signalling capabilities to both central and peripheral systems, is currently targeted for research-based solutions for the obesity epidemic.

1.2 Insulin Resistance

1.2.1 Physiology of Insulin Resistance

Insulin is produced by β beta cells of pancreas in response to increased circulating levels of glucose and amino acids after a meal. The major sites of action of insulin are liver, skeletal muscle and adipose tissue. In liver, insulin increases glycogen synthesis, inhibits gluconeogenesis and promotes *de novo* lipogenesis. In skeletal muscle, insulin promotes glucose uptake and glycogen synthesis. In adipose tissue, it promotes lipogenesis and inhibits lipolysis. The opposite happens in the fasted state when insulin level is reduced. Insulin resistance is a state of subnormal response of target tissues to normal concentrations of insulin hormone. The pathophysiology of insulin resistance is depicted in Figure 1.2.1 (Eckel et al 2005⁴³). Abundant free fatty acids (FFA) released from expanded adipose tissue mass, acts on liver to cause increased production of glucose, triglycerides and secretion of Very Low Density Lipoprotein (VLDL). This results in low High Density Lipoprotein (HDL) and high Low Density Lipoprotein (LDL). FFA also reduce insulin sensitivity in muscle by inhibiting insulin mediated glucose uptake, reduced glycogen synthesis and increased triglyceride accumulation (Eckel et al 2005⁴³). Increase in glucose and increase in FFA stimulates excess insulin secretion from pancreas causing hyperinsulinaemia, which in turn simultaneously contributes to hypertension from sodium reabsorption and increase sympathetic nervous system activity caused by hyperinsulinaemia. Increased lipogenesis action of hyperinsulinaemia causes fat deposition in liver resulting in Non-Alcoholic Fatty Liver Disease (NAFLD), where as poor glucose uptake over long duration causes β -cell fatigue, resulting in Impaired

fasting Glycaemia (IFG), Impaired Glucose Tolerance (IGT) and T2DM (Stumvoll et al 2005⁴⁴). Autocrine and paracrine effect of proinflammatory cytokines, such as Tumour Necrosis Factor- α (TNF- α) and Interleukin- 6 may enhance hepatic glucose production, hepatic VLDL production and skeletal muscle insulin resistance. Increased circulating adipocytokines and FFA may also contribute to prothrombotic state as shown in the Figure 1.2.1.

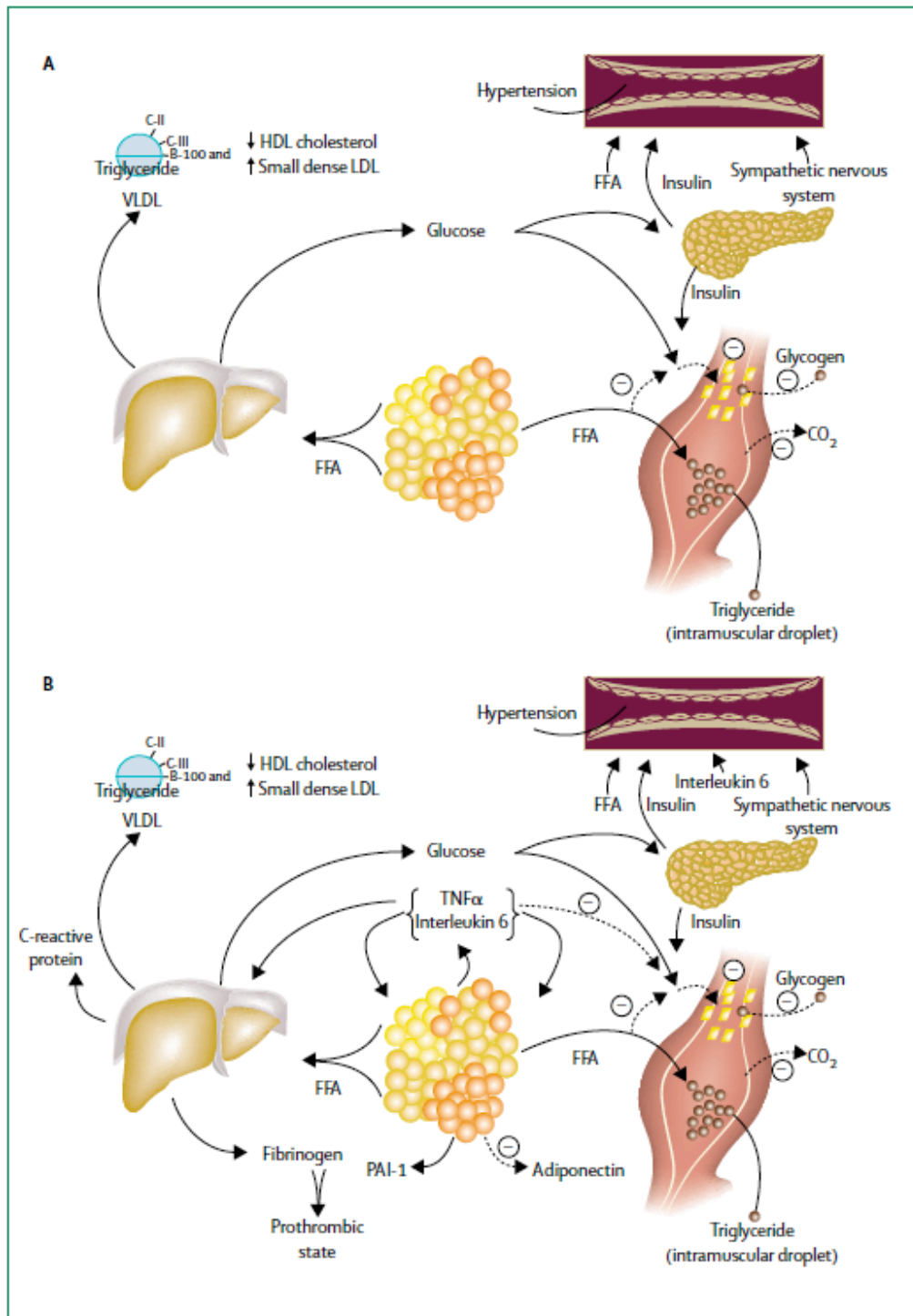


Figure 1.2.1 Pathophysiology of insulin resistance (Eckel et al 2005⁴³)
 Abbreviations- HDL: High Density Lipoprotein, LDL: Low Density Lipoprotein,
 VLDL: Very Low Density Lipoprotein, FFA: Free Fatty Acids, PAI-1: Plasminogen
 Activator Inhibitor-1, TNF- α : Tumour Necrosis Factor- α

1.2.2 Measures of Insulin Resistance

Although there are various methods to measure insulin resistance, there are no validated methods currently to undertake in a clinical setting for widespread usage. Hyperinsulinaemic euglycaemic clamp is a type of dynamic test, considered as the gold-standard for measurement of insulin resistance (DeFronzo et al 1979⁴⁵, Borai et al 2011⁴⁶). Other dynamic tests include Intravenous Glucose Tolerance Test (IVGTT) and Insulin Tolerance Test (ITT) (Buchanan et al 2010⁴⁷, Bergman et al 1985⁴⁸). Insulin sensitivity index (ISI), homeostasis model assessment insulin resistance (HOMA-IR) and Quantitative Insulin Sensitivity Check Index (QUICKI) (Matthews et al 1985⁴⁹, Katz et al 2000⁵⁰, Wallace et al 2004⁵¹) are few of the most commonly used indices. Although HOMA-IR and QUICKI are well-validated simple and practical fasting blood test assessments, which can be used in large population studies in clinical settings, they are considered a reflection of hepatic insulin resistance than peripheral insulin resistance (Hoffman et al 2008⁵²). Also, they are not well validated in conditions where insulin reserve is reduced, such as in patients with uncontrolled T2DM or Type 1 Diabetes Mellitus (T1DM). Serum insulin levels, intact and total pro-insulin levels are also used as surrogate markers of insulin resistance, but are not well validated (Pfützner et al 2008⁵³). Matsuda index is another index derived from Oral Glucose Tolerance Test (OGTT) (Matsuda et al 1999⁵⁴) which is found to correlate well with euglycaemic clamp, especially in south Asian population (Trikudanathan et al 2013⁵⁵).

1.2.3 Risk factors for Insulin Resistance

Insulin resistance, which is the main cause of metabolic syndrome co-exists with obesity or may be a significant aetiological factor for obesity. Diet and life style along with genetic predisposition are established causes of obesity and insulin resistance. Family history of T2DM and presence of Polycystic Ovarian Syndrome (PCOS) can increase the risk of developing insulin resistance. Insulin resistance may be physiological as noted in puberty, pregnancy and ageing population (DeFronzo et al 1979, Buchanan et al 1990, Moran et al 1999⁵⁶⁻⁶⁰). Incidence of insulin resistance is high in South Asians, Hispanics and Afro-Caribbean ethnic groups (Farooqi et al 1994⁶¹, Kramer et al 2013⁶²). Extreme form of insulin resistance is found in inherited disorders like leptin receptor defects, SH2B1 and LAMIN-A mutations leading to lipodystrophic states (Patricia et al 2012⁶³, Duan et al 2004⁶⁴, Farooqi et al 1999⁶⁵).

Certain medications, such as corticosteroids, anti-retro viral drugs used in treatment of Human Immunodeficiency Virus (HIV) have shown to cause insulin resistance as a side effect (Yasuda et al 1982⁶⁶, Tebas et al 2008⁶⁷).

1.2.4 Metabolic Syndrome

The metabolic syndrome is also known as Syndrome X (Reaven et al 1988⁶⁸), the insulin resistance syndrome (DeFronzo et al 1991⁶⁹), and the deadly quartet (Kaplan et al 1989⁷⁰). The constellation of metabolic abnormalities includes glucose intolerance (T2DM, impaired glucose tolerance, impaired fasting glycaemia), insulin resistance, central obesity, dyslipidaemia, and hypertension, all well recognized risk

factors for CVD (Eckel et al 2005⁴³). The central component is obesity which is included as the main parameter in majority of accepted definitions of metabolic syndrome: WHO (Alberti et al 1998⁷¹), European Group for the Study of Insulin Resistance (Balkau et al 1999⁷²), National Cholesterol Education Program's Adult Treatment Panel III (NCEP: ATP III) (JAMA 2001⁷³) and International Diabetes Federation (IDF) (Alberti et al 2005⁷⁴). The most currently accepted and clinically easy to use definition is that of IDF's which is shown in Table 1.2.4.

Insulin resistance remains to be the vital factor leading to insulin resistant states such as T2DM and Gestational Diabetes Mellitus (GDM). More than 90% of diabetes patients are of T2DM variety and are at increased risk of macro-vascular (Stroke, CVD, Peripheral Vascular Disease) and micro-vascular complications (Retinopathy, Nephropathy, Peripheral neuropathy, and Autonomic neuropathy) (Turner et al 1998⁷⁵, UKPDS 1998⁷⁶).

Table 1.2.4.1 International Diabetes Federation (IDF) Criteria for Diagnosis of Metabolic Syndrome

<p>1. Central obesity (waist circumference of ≥ 94 cm for European men and ≥ 80 cm for European women, with ethnicity specific values for other groups)</p>
<p>In addition to any two of the following four factors</p> <p>2. Raised triglyceride level (TG): (≥ 150 mg/dL or 1.7 mmol/L) Or specific treatment for this lipid abnormality</p> <p>3. Reduced high density lipoprotein (HDL): (< 40 mg/dL or 1.03 mmol/L in males) and (< 50 mg/dL or 1.29 mmol/L in females) Or specific treatment for this lipid abnormality</p> <p>4. Raised blood pressure: (systolic BP ≥ 130 or diastolic BP ≥ 85 mm Hg) Or treatment of previously diagnosed hypertension</p> <p>5. Raised fasting plasma glucose, FPG: (≥ 100 mg/dL or 5.6 mmol/L) Or previously diagnosed type 2 diabetes</p>

Table 1.2.4.2 Ethnic specific values for waist circumference

Country/Ethnic group	Sex	Waist circumference
Europeans In USA, the ATP III values (102 cm ♂; 88 cm ♀) are to continue	Male	≥ 94
	Female	≥ 80
South Asians Based on the Chinese, Malay and Asian-Indian population	Male	≥ 90
	Female	≥ 80
Chinese	Male	≥ 90
	Female	≥ 80
Japanese	Male	≥ 90
	Female	≥ 80
Ethnic South and Central Americans	Use South Asian recommendations until more specific data are available	
Sub-Saharan Africans	Use European data until more specific data are available	
Eastern Mediterranean and Middle East (Arab) populations	Use European data until more specific data are available	

1.2.5 Insulin Resistant States

T2DM is an insulin resistant state in the presence of relative insulin deficiency resulting in hyperglycaemia. More than 90% of diabetes patients are of T2DM variety and are at increased risk of macro-vascular (Stroke, CVD, Peripheral Vascular Disease) and micro-vascular complications (Retinopathy, Nephropathy, Peripheral neuropathy, and Autonomic neuropathy), the risks of which can be substantially reduced on optimal glycaemic management (Turner et al 1998⁷⁵, UKPDS 1998⁷⁶).

GDM is defined as glucose intolerance noted during pregnancy and the aetiology is not similar to that of T2DM (American Diabetes Association 2004⁷⁷). It is generally accepted that glucose lowering, in combination with life style changes has better pregnancy outcomes (Crowther et al 2005⁷⁸ Metzger et al 2008⁷⁹, Rowan et al 2008⁸⁰, Lautatzis et al 2013⁸¹).

PCOS is another insulin resistant metabolic disorder comprising menstrual irregularities, hyperandrogenism and multiple cysts in ovaries. On satisfying any 2 of the 3 following components of Rotterdam 2003 criteria, remains the most acceptable diagnosis of PCOS: oligo- or anovulation, clinical or biochemical signs of hyperandrogenism, and sonographic visualisation of multiple cysts in ovaries (Rotterdam ESHRE/ASRM-Sponsored PCOS consensus workshop group 2004⁸²). Approximately 40 to 85% of PCOS women are overweight or obese compared to age matched controls and carry increased CV risk (Randeve et al 2012⁸³).

1.3 Dietary Patterns and Obesity

To mitigate the adverse impact of obesity on global health and health-care economies, a multi-faceted approach is required. Such an approach should incorporate the development of novel pharmacological strategies, re-design of our living spaces for enhanced energy expenditure, governmental approaches to improve our diet and obesogenic environment and cultural and lifestyle changes. Diet is a major determinant of fat mass, and an obvious target for the prevention and management of obesity (Forget et al 2013⁸⁴). It is well known that dietary behaviour patterns is closely linked with obesity/insulin resistance, in turn results in increased CV risk. The evidence for effects of meal quality, meal size, meal frequency and meal duration over obesity and human metabolism is discussed below.

Meal quality, particularly constituting high fat diet results in dyslipidaemic profile: elevated serum cholesterol, elevated LDL, elevated triglycerides (TG), HDL resulting in increasing CV risk, reversing the same substantially reduces the risk (4S-Study Group 1994⁸⁵, LIPID-Study-Group 1998⁸⁶). Dietary cholesterol, trans fatty acids and saturated fatty acids increase atherogenic lipoproteins and are recommended to reduce intake to lower CV risk (Kris-Etherton et al 2001⁸⁷). The UK dietary reference value for total recommended fat intake is less than 35% of total energy required (Dietary reference values for energy, Scientific Advisory Committee of Nutrition 2011⁸⁸). It is shown that nutritional factors inherent to fast food, such as low levels of dietary fibre, high palatability, high energy density, high fat content, high glycaemic load, and high content of sugar in liquid form promote excess energy intake (Ebbeling et al 2007⁸⁹).

Meal quantity in excess over prolonged period, even in recommended proportions, is fundamental to weight gain and the development of obesity (Mayer et al 1967⁹⁰). However methodological constraints may appear in proving this concept due to under-reporting of dietary exposures (Rennie et al 2005⁹¹). In a series of studies, it is shown that larger meal size increases energy intake and aids more deposition of fat (Kral et al 2004⁹², Rolls et al 1998⁹³, Rolls et al 2000⁹⁴).

Meal frequency is linked with weight and metabolic diseases, as suggested by Fabry et al in 1960's. The authors inferred that men eating 3 or fewer meals per day were heavier, had higher incidence of hypercholesterolaemia and glucose intolerance, compared to men eating 5 or more meals a day (Fabry et al 1964). Contrarily, rodent studies (Anson et al 2003⁹⁵, Mattson et al 2005⁹⁶) and human studies (Harvie et al 2011⁹⁷, Harvie et al 2013⁹⁸) have shown intermittent fasting with fewer meal frequency have beneficial metabolic profile and lesser weight gain. So evidence for higher or lower meal frequency is conflicting (Summerbell et al 1996⁹⁹, Crawley et al 1997¹⁰⁰, Dreon et al 1998¹⁰¹, Cameron et al 2010¹⁰², La Bounty et al 2011¹⁰³). However, erratic meal patterns are shown to be detrimental than regular meal pattern (6 meals per day), in healthy lean and obese women (Farshchi et al 2004¹⁰⁴, Farshchi et al 2005¹⁰⁵).

Meal duration and its effect on weight, appetite, food ingestion and metabolism remain to be fully clarified. Faster eating rate is shown to increase energy intake, (Andrade et al 2008¹⁰⁶, Martin et al 2007¹⁰⁷, Zandian et al 2009¹⁰⁸) lower satiating efficiency index, and is associated with increased BMI (Hill et al 1984¹⁰⁹, Otsuka et al 2006¹¹⁰, Maruyama et al 2008¹¹¹). Subsequent study did not back up the same

finding, as longer meal duration did not alter the energy intake in lone diners (Brindal et al 2011¹¹²). Appetite is mediated by a variety of neural and endocrine signals including several pancreatic and gut hormones such as insulin, Glucagon-like peptide-1 (GLP-1), peptide-YY (PYY), pancreatic polypeptide (PP) and ghrelin (Cummings et al 2007¹¹³). The effect of meal duration/eating rate on energy intake and on the pancreatic and gut hormones that influence energy intake and appetite are undetermined. The role of brown adipose tissue on diet-activated energy expenditure is discussed in section 1.7.2. There is a need for well-designed studies to assess gut hormone responses to meal duration, in conjunction with energy expenditure assessment to evaluate any beneficial metabolic effects.

1.4 Adipose Tissue

1.4.1 Adipose Tissue: A cause of Insulin Resistance

An unwanted by product of contemporary human behaviour related to eating and physical activity is excess adipose tissue accumulation in comparison to lean body mass (Guilherme et al 2008¹¹⁴). It is well established that lipid overload and lipotoxicity promotes obesity by perturbing insulin signalling pathways resulting in disturbed homeostasis of glucose, lipids and lipoprotein pathways (Unger et al 1995¹¹⁵). Insulin resistance develops because of the effects of inflammatory and hormonal factors, endoplasmic reticulum (ER) stress, and accumulation of by-products of nutritional ‘overload’ in insulin-sensing tissues (Muoio et al 2008¹¹⁶), such as in skeletal muscle as depicted in Figure 1.4.1. Adipose tissue, a crucial site of inflammation produces preferential anti-inflammatory adipocytokines in lean

individuals, such as Transformation Growth Factor- β (TGF β), Interleukin-10 (IL-10), Interleukin-4 (IL-4), Interleukin-13 (IL-13), and Apelin; whilst producing pro-inflammatory adipocytokines in obese individuals, such as tumour necrosis factor- α (TNF α), Interleukin-6 (IL-6), leptin, visfatin, resistin, angiotensin-II, Plasminogen Activator Inhibitor-1 (PAI-1), in addition to several interleukins (Ouchi et al 2011¹¹⁷). Furthermore, the above adipocytokines directly modulate insulin resistance by affecting insulin signalling pathways, or indirectly, via stimulating inflammatory pathways. The inter-organ communication between liver, skeletal muscle adipose tissue and other insulin sensitive organs occur through combined effect of adipokines and inflammatory mediators. This results in insulin resistance via activation of I-Kappa B Kinase catalytic subunit- β (IKK β)/Nuclear Factor Kappa B (NF κ B) and c-Jun N-terminal Kinases (JNK) pathways (Harte et al 2013¹¹⁸, Pirola et al 2004¹¹⁹, Tilg et al 2008¹²⁰, Kalupahana et al 2012¹²¹).

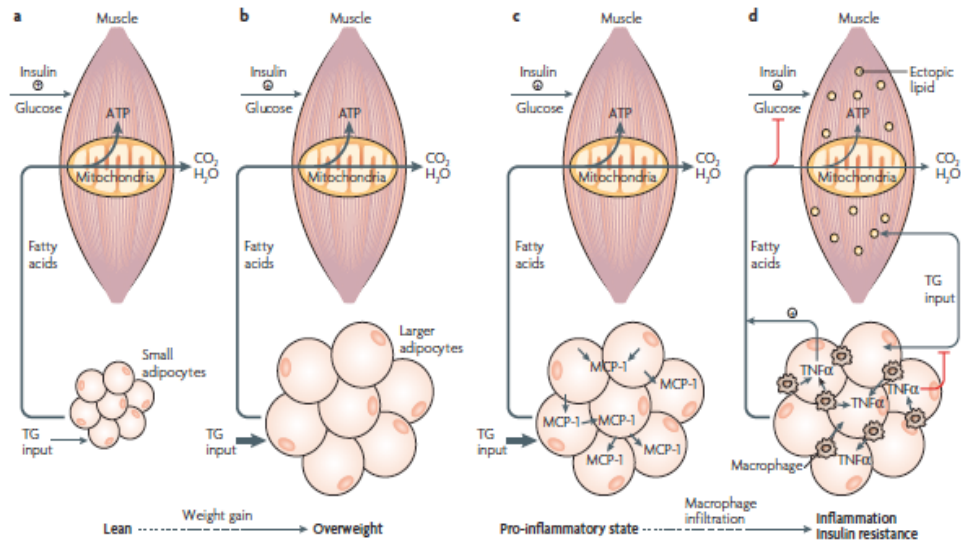


Figure 1.4.1 Guilherme et al 2008¹¹⁴ Nature reviews

Chronic inflammation in adipose tissue triggers insulin resistance in skeletal muscle.

a) In the lean state, small adipocytes efficiently store fatty acids as triglyceride (TG input, arrow), which can be mobilized and used to generate ATP through the mitochondrial β -oxidation pathway in muscle during periods of caloric need. Insulin-stimulated glucose uptake under these conditions is normal. **b)** Excess caloric intake leads to metabolic overload, increased TG input and adipocyte enlargement. Nonetheless, in non-diabetic overweight individuals, TG storage by adipose cells and β -oxidation in muscle is maintained to prevent insulin resistance. **c)** On further overloading with TG, hypertrophy of adipocytes and increased secretion of macrophage chemoattractants occurs, including the secretion of monocyte chemoattractant protein-1 (MCP1; arrows), which recruits additional macrophages. **d)** Macrophage recruitment in turn results in a pro-inflammatory state in obese adipose tissue. Infiltrating macrophages secrete large amounts of $\text{TNF}\alpha$, which results in a chronic inflammatory state with impaired TG deposition and increased lipolysis (arrow and plus signal). The excess of circulating TG and free fatty acids results in the accumulation of activated lipids in the muscle (yellow dots), disrupting

functions such as mitochondrial oxidative phosphorylation and insulin-stimulated glucose transport, thus triggering insulin resistance.

1.4.2 Types of Adipose Tissue

Although excess adipose tissue as observed in obesity, is a recognized site of inflammation and adipokine dysregulation, leading to chronic subclinical inflammation and in turn resulting in insulin resistance (Shoelson et al 2006¹²²), the location of the tissue also determines the degree of inflammation.

Central fat distribution (apple-shaped, android, abdominal) is considered more inflammatory and confers considerable metabolic risks, compared to peripheral fat distribution (pear-shaped, gynoid, gluteo-femoral), which may even be protective (Vega et al 2006¹²³, Snijder et al 2005¹²⁴, Fox et al 2007¹²⁵, Azuma et al 2007¹²⁶, Koster et al 2008²⁵, St-Pierre et al 2007¹²⁷). Thus, better identification of abdominally obese subjects at risk of developing metabolic diseases is measurement of waist and hip circumferences and calculating waist-to-hip ratio (WHR). Waist circumferences greater than 94 cm in European men and 80 cm in European women, and WHR greater than 1.0 in men and 0.8 in women define those at increased risk (Alberti et al 2009¹²⁸). Waist circumference cut-offs of respective ethnicities are illustrated in Table 1.2.4.2.

Adipose tissue can also be grossly divided into subcutaneous adipose tissue and visceral adipose tissue based on the location. Subcutaneous deposits include abdomen, thigh, mammary and gluteo-femoral regions. Visceral depots are located

around internal organs, such as stomach (omental), intestine (mesenteric), peri-renal (kidney) and heart (epicardial). Computed tomography (CT) or Magnetic Resonance (MR) images taken at L2-3 and/or L4-5 to distinguish visceral and abdominal subcutaneous depots indicate strong negative effects of visceral fat mass that are independent of total body fat on metabolic risks (Despres and Lemieux, 2006¹²⁹). Sex differences in metabolic risk can also partially attributed to the higher visceral fat mass in men compared to women (Despres and Lemieux, 2006¹²⁹). Ethnic minority populations such as in South Asians have tendency of central obesity, which explains the higher CV risk than compared to Caucasians of similar BMI (WHO-Expert-Consultation 2004²², Bellary et al 2008¹³⁰). Abdominal subcutaneous adipose tissue appears to be more active than it was previously thought, secreting multiple pro-inflammatory adipocytokines. (McTernan et al 2002¹³¹, McTernan et al 2003¹³², Fischer et al 2002¹³³, Harte et al 2003¹³⁴).

Another classification of adipose tissue based on the histology and function is: White Adipose Tissue (WAT) and Brown Adipose Tissue (BAT). WAT stores energy in the form of triglycerides and BAT expends energy due to presence of a specialised protein Uncoupling Protein-1 (UCP1), in its mitochondria, which uncouples respiration dissipating energy in the form of heat (Hull et al 1966¹³⁵, Nicholls et al 1984¹³⁶, Feldman et al 2009¹³⁷).

Traditionally, it was thought that BAT was present only in infants. The advent of Positron Emission Tomography (PET), demonstrated metabolically active BAT in human adults as evident by physiological uptake of 18-Fluoro-labelled -2-deoxy-glucose (¹⁸FDG) dye, as shown in Figure 1.4.2 (Hany et al 2002¹³⁸, Nedergaard et al

2007¹³⁹, Virtanen et al 2009¹⁴⁰, Cypess et al 2009¹⁴¹, van Marken Lichtenbelt et al 2009¹⁴², Saito et al 2009^{143,144}, Zingaretti et al 2009¹⁴⁴). This led to renewed interest in BAT, as it is currently considered as a potential anti-obesity therapeutic target due to its energy expending properties.

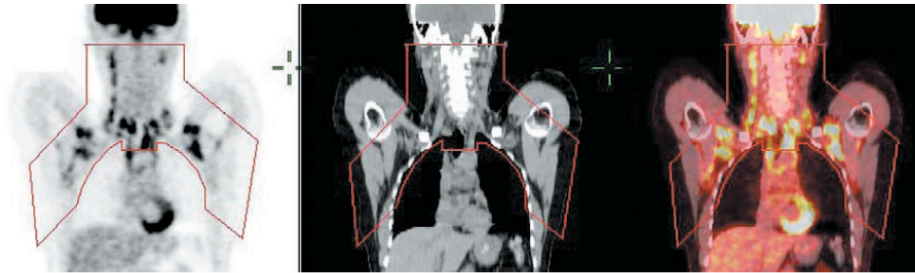


Figure 1.4.2: Amount and activity of brown adipose tissue as shown in PET (left), CT (centre) and combined PET-CT (right). Cypess et al 2009¹⁴¹

1.4.3 White, Brown and Beige Adipose Tissue

There are two main types of adipose tissue: WAT and BAT that have evolved for completely different purposes: to survive famine and prevent hypothermia respectively. WAT and BAT, as energy storage and thermogenic tissues respectively, therefore evolved to protect mammalian organisms from important environmental threats including lack of food and exposure to cold climates (Enerback et al 2010¹⁴⁵). Humans are therefore evolutionarily maladapted to our modern obesogenic and thermo-regulated environment, with abundance of food and adoption of sedentary lifestyles resulting in WAT excess. This is likely to be an important explanation for the current obesity epidemic.

In addition to WAT and BAT, a third intermediate-type of adipose tissue termed ‘beige’ or ‘brite’ is identified (Wu et al 2012¹⁴⁶), referred in text as Beige Adipose Tissue (BeAT). Adipocytes from BeAT depots resemble white adipocytes but possess the classical properties of brown adipocytes (Wu et al 2012¹⁴⁶). The histological and morphological properties of each of the types of adipose tissue are further elaborated in section 1.5.2.

1.5 Brown adipose tissue

1.5.1 Evolution of Brown adipose tissue

Konrad von Gesner first identified brown fat in 1551 in European marmots *Muris alpines*, but it was not until the 1960’s and 70’s that the importance of BAT as a thermoregulatory organ was appreciated (Prusiner et al 1968¹⁴⁷, Cannon et al 1978¹⁴⁸, Cannon et al 2004¹⁴⁹). BAT seen in human neonates and small mammals on several necropsy studies, was thought to be absent in human adults. Juliet Heaton in 1972 demonstrated its presence in humans through autopsy studies of over 50 corpses and concluded that BAT incidence is high in neonates and declines with age but can still be present even in the eighth decade (Heaton et al 1972^{150,151}). Later in 1979, Rothwell & Stock alluded to its presence in humans through infrared thermography following ephedrine administration (although the increase in surface temperature may have resulted from the effect of ephedrine on cutaneous blood flow) (Rothwell et al 1979¹⁵²). The timeline and summary of major developments in BAT research are depicted in Table 1.5.1 modified from Lee et al 2013¹⁵³.

Table 1.5.1: Timeline of major developments in BAT research: Lee et al 2013¹⁵³

Year	Authors	Findings
1902	Hatai et al ¹⁵⁴	Similarity between cervical fat of human neonate and interscapular BAT in hibernating mammals
1908	Bonnot et al ¹⁵⁵	Detailed description of the interscapular gland in an adult human
1922	Rasmussen et al ¹⁵⁶	Morphological similarity between paediatric peri-renal and animal BAT
1964	Silverman et al ¹⁵⁷	Maintenance of warm temperature in nape of infants during cold exposure, providing first evidence of BAT function in humans
1965	Dawkins and Scopes et al ¹⁵⁸	Demonstration of non-shivering thermogenesis in infants, indicating BAT as thermogenic organ
1972	Heaton et al ¹⁵⁰	Histological evidence that BAT is present in humans throughout adult life
1983	Bouillaud et al ¹⁵⁹	Discovery of UCPI in human BAT
1984	Astrup et al ¹⁶⁰	No evidence in human that interscapular fat is thermogenic or functional
2002	Hany et al ¹⁶¹	FDG uptake in cervical/supraclavicular region of PET-CT scan may be BAT
2004	Garcia et al ¹⁶²	FDG uptake in BAT during PET-CT is influenced by ambient temperature
2006	Chiba et al ¹⁶³	Inverse relationships between BAT activity and BMI, suggesting metabolic significance of BAT
2009	Saito et al ¹⁴³	High incidence of metabolically active BAT in adult humans
2009	Cypess et al ¹⁴¹	Higher prevalence of BAT in women than men and during winter; inverse relationships between BAT activity, age, and BMI
2009	Van Marken Lichtenbelt et al ¹⁴²	Quantification of BAT activation in adult humans during cold exposure
2009	Virtanen et al ¹⁴⁰	Signature genes of FDG-avid BAT in human
2011	Lee et al ¹⁶⁴	Universal presence of BAT from supraclavicular fat in humans regardless of PET imaging status
2011	Lee et al ¹⁶⁵	Inducible brown adipogenesis of human supraclavicular BAT in vitro
2012	Ouellet et al ¹⁶⁶	Contribution of BAT oxidative metabolism to energy expenditure
2012	Wu et al ¹⁴⁶ and Sharp et al ¹⁶⁷	Identification of beige adipocytes; evidence supporting developmental origin of human BAT from this lineage
2013	Orava et al ¹⁶⁸	Insulin-stimulated glucose uptake rate and cold-induced glucose uptake rate are attenuated in obese humans
2013	Chen et al ¹⁶⁹	A slight decrease in ambient temperature (19 °C) is sufficient to activate BAT with a significant energy consuming impact in healthy males and females
2013	Van der Lans et al ¹⁷⁰	A 10-day, 6-hour daily cold exposure at 15–16 °C increases BAT SUV and volume in healthy lean adults
2014	Blondin et al ¹⁷¹	A 4-week, 2-hour daily cold exposure at 10 °C results in 45% increase in BAT volume of activity and 2.2-fold increase in cold-induced BAT oxidative metabolism.

PET- Positron Emission tomography; SUV- Standard uptake value

1.5.2 Anatomy of Brown adipose tissue

The presence of BAT in human adults is now incontrovertible following recent radiological and histological confirmation of BAT depots in the axillary, paravertebral, supraclavicular and cervical regions (Nedergaard et al 2007¹³⁹, Cypess et al 2009¹⁴¹, van Marken Lichtenbelt et al 2009¹⁴², Virtanen et al 2009¹⁴⁰, Saito et al 2009¹⁴³, Zingaretti et al 2009¹⁴⁴). Adult human BAT is composed of brown adipocytes with a matrix rich in blood vessels and nerves, in keeping with its primary function of supplying heat to the body in response to sympathetic nervous activity (Cinti et al 2000¹⁷²). Although brown adipocytes contain enzymes required for synthesis and storage of triglycerides, lipids within brown adipocytes are usually stored in multiple (multilocular) small fat droplets, in contrast to white adipocytes that contain one large (unilocular) droplet of triglyceride (Cinti et al 2000¹⁷²). Brown adipocytes are comparatively smaller (15-60µm in diameter) than white adipocytes (25-200µm) (Cinti et al 2000¹⁷²). In contrast to white adipocytes which have few mitochondria, brown adipocytes contain abundant mitochondria that are crucial for heat generation (Napolitano et al¹⁷³). Abundant mitochondria with iron as cofactor in their respiratory chain cytochrome enzymes, along with vasculature within BAT impart a dark red (brown) discolouration to the tissue and is therefore responsible for its name, compared to pale hue colour of WAT (Cinti et al 2000¹⁷²). Adipocytes from beige adipose tissue (BeAT) depots resemble white adipocytes but possess the classical properties of brown adipocytes (Wu et al¹⁴⁶). The characteristic features of WAT, BAT and BeAT are illustrated in Table 1.5.2, and histological differences between WAT and BAT are depicted in Figure 1.5.2.

Table 1.5.2: Morphological features of BAT, WAT and BeAT

	WAT	BAT	BeAT
Cell shape	Variable, but classically spherical	Polygonal	Resembles WAT
Cell size	Variable, but large (25-200µm)	Comparatively small (15-60µm)	Variable
Nucleus	Peripheral, flattened	Central, round or oval in shape	Not studied
Cytoplasm	Thin, peripheral rim	Large volume evenly distributed throughout	Not studied
Lipid content	Single large droplet occupying 90% cell volume	Multiple small lipid droplets	Not studied
Mitochondria	Few	Abundant	Intermediate
Endoplasmic reticulum (ER)	Little, but recognizable as rough and smooth ER	Present, but poorly developed	Not studied
Tissue organisation	Small lobules of densely packed cells	Lobular, gland-like	Not studied
Cell content	Multiple cell types present	Few other cell types present	Not studied
Vascularity	Adequate	Highly vascularised	Not studied
Gene expression	PPAR-gamma, aP2, Adiponectin, adipon, perilipin	UCP-1, PGC-1alpha, β-3 adreno receptor (ARB3), PRDM16, Iodothyronine type II (D2)	Low UCP1, but activated by cAMP stimulation
Cell markers	CD34, ABCG2, ALDH	EVA1, EBF3, FBXO31	CD137, TMEM26, TBX1

BAT- Brown adipose tissue; WAT- White adipose tissue; BeAT- Beige adipose tissue; ER- Endoplasmic reticulum

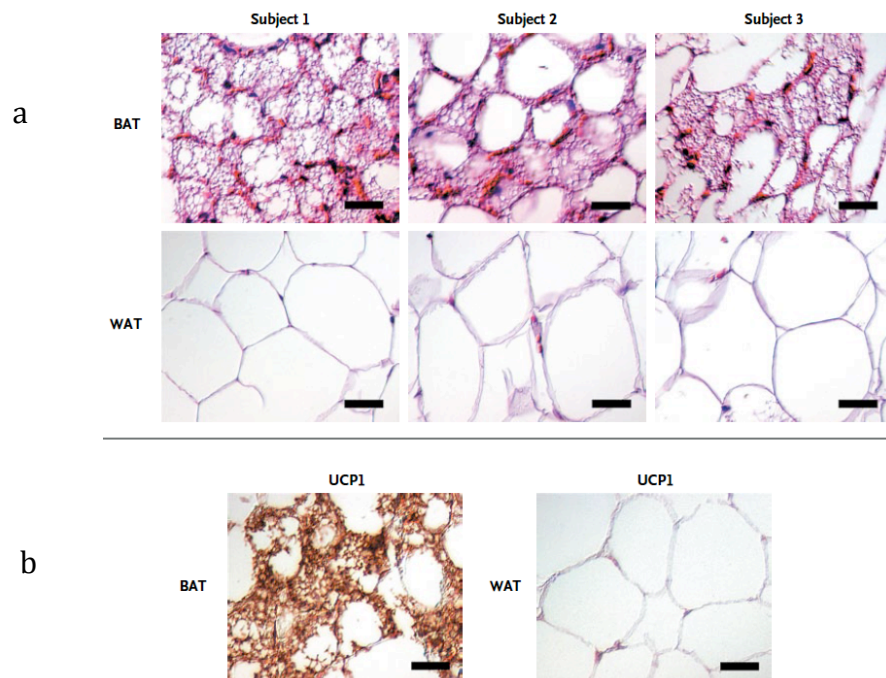


Figure 1.5.2: Virtanen et al NEJM 2009¹⁴⁰: a) Haematoxylin and Eosin staining preparations of adipose tissues on 3 subjects demonstrating multilocular and intracellular lipid droplets in brown adipose tissue, absent in WAT; b) Immunohistochemistry demonstrating high UCP-1 uptake in BAT for UCP-1 anti-specific sera, which is absent in WAT.

1.5.3 Function of Brown adipose tissue

The presence of the 32 kDa UCP-1 in BAT mitochondria enables the inward translocation of protons across the mitochondrial inner membrane. This process enables uncoupling of oxidative phosphorylation from the electron transport chain, resulting in dissipation of heat rather than the generation of adenosine tri-phosphate (ATP) (Nicholls et al 1984¹³⁶), as depicted in Figure 1.5.3. The generation of heat

from uncoupled oxidative phosphorylation, termed adaptive thermogenesis, has been demonstrated in rodent studies to be essential for the homeostasis of body temperature (Enerback et al 1997¹⁷⁴). Adaptive thermogenesis refers to production of heat in responses to environmental temperature changes (cold induced temperature [CIT]¹⁷⁵) and diet (diet induced thermogenesis[DIT]), and BAT is implicated in both CIT (Orava et al 2011¹⁷⁶) and DIT (Vrieze et al 2012¹⁷⁷). Adaptive thermogenesis may also play a role in the control of body weight through enhancement of energy expenditure and may therefore also protect against the development of obesity, although such a role would presumably not have been particularly important for survival and reproduction during our famine-prone and food-deprived evolutionary past (Guerra et al 1998¹⁷⁸, Feldmann et al 2009¹³⁷). It seems likely therefore that manipulating BAT activity and BAT volume may offer solution to combat obesity through regulating adaptive thermogenesis.

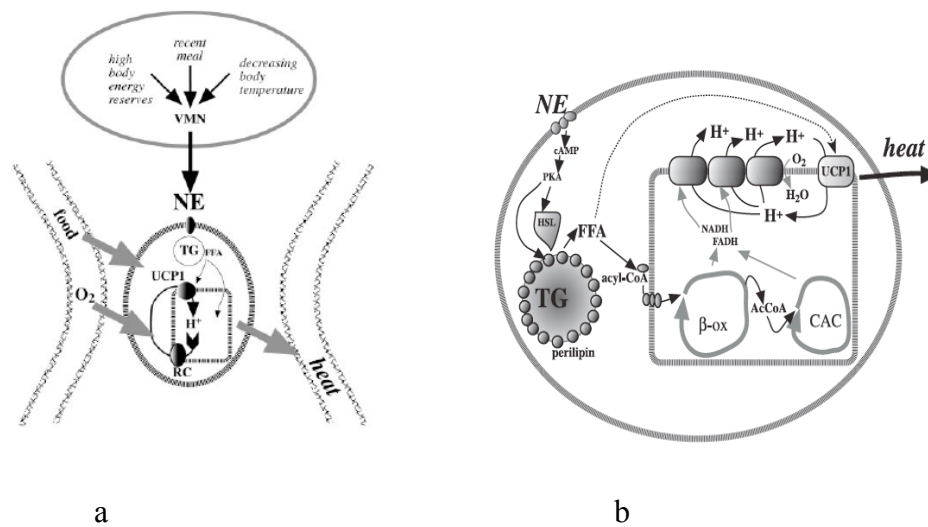


Figure 1.5.3: Cannon et al 2004¹⁴⁹: a) Food, cold and high body energy reserves stimulate ventromedial nucleus in hypothalamus triggering nor-epinephrine release via sympathetic nervous system, which initiates triglyceride breakdown in brown adipocytes, predominantly through β_3 adrenergic receptors. This releases free fatty acids, which are substrate of thermogenesis and regulators of uncoupling protein-1

activity; b) Intracellular signalling following nor-epinephrine stimulation in brown adipocyte, resulting in release of free fatty acids, which in turn transferred on to respiratory chain resulting in pumping out of protons. This leads to formation of proton-motive force that drives back the protons back into mitochondrial matrix through UCP-1. The energy stored in proton motive force is then released as heat.

1.5.4 Prevalence of Brown adipose tissue

BAT was originally thought to be present in between 3.5 and 60% of adult humans (Cypess et al 2009¹⁴¹, Saito et al 2009¹⁴³). More recent studies have demonstrated the presence of BAT in 96% of adult humans following cold-induced activation (van Marken Lichtenbelt et al¹⁴²). PET-CT currently remains the gold standard technique for detection of BAT, but is associated with exposure to ionizing radiation, and images are dependent on factors such as environmental temperature resulting in intra-individual variability over time (Cypess et al 2009¹⁴¹ and van Marken Lichtenbelt et al¹⁴²). It would therefore be desirable for safer and more reliable imaging modalities for BAT to be developed. One important unanswered question is the extent to which BAT occurs in adult humans (regardless of its activity). To date, we do not have a reliable means of imaging inactive BAT, and it remains possible that in the majority of adult humans with no apparent BAT activity on PET-CT imaging, inactive BAT is still present. Having an estimate for the proportion of the population with inactive BAT depots present would clearly have important implications for and inform the direction of future therapeutic developments to manipulate human BAT as a weight-loss strategy: strategies to enhance existing

BAT activity versus those to stimulate the formation of new BAT from other fat depots for example.

1.5.5 Origin of Brown adipose tissue

Adipose tissue develops from the mesoderm along with bone, cartilage and skeletal muscle (Gossler et al 1998¹⁷⁹). It was proposed that WAT and BAT develop from common progenitors and then diverge along their own lineages (Gossler et al 1998¹⁷⁹). More recent studies have challenged the notion of a common progenitor for white and brown adipocytes (Atit et al 2006¹⁸⁰). Gene profiling has identified a myogenic gene signature within brown fat preadipocytes suggesting that brown fat and skeletal muscle share a common progenitor (Timmons et al 2007¹⁸¹). Furthermore, it has been shown that brown fat bundles originate from progenitors within the central dermatomyotome (derived from paraxial mesoderm) that express engrailed-1 (En1), while others have suggested that brown adipocytes originate from progenitors expressing myogenic regulating factor-5 (Myf5) (Atit et al 2006¹⁸⁰, Seale et al 2008¹⁸²).

An alternative origin of brown adipocytes is trans-differentiation from WAT. WAT-derived brown adipocytes tend to be BeAT, and do not seem to arise from Myf5+ progenitors, but rather develop through re-programming of white progenitors (Seale et al 2008¹⁸²). BeAT resemble white fat cells in having low UCP1, but respond to cAMP stimulation with high UCP1 expression like classical brown fat (Wu et al 2012¹⁸³). The functional characteristics of BeAT and how these relate to those of brown fat should be a focus for further research. The origin of adipocytes appears to

be influenced by location: brown adipocytes that are present in classical locations such as perirenal or interscapular regions are derived from Myf5+ cells (Seale et al 2008¹⁸²). Conversely, the origin of white adipocytes is linked to mural cells (pericytes) of the vasculature of WAT, but not the vasculature of other tissues (Tang et al 2008¹⁸⁴), whilst white adipocytes in the cephalic region derive their origin from the cranial neural crest (Billon et al 2007¹⁸⁵). Whilst both WAT and BAT express high levels of Peroxisome Proliferator-Activated receptor Gamma Alpha (PPAR- γ) (Farmer et al 2006¹⁸⁶), BAT expresses UCP-1 (Heaton et al 1978¹⁵⁰), Peroxisome Proliferator-Activated receptor Gamma Coactivator 1 alpha (PGC1 α) (Puigserver et al 1998¹⁸⁷), type 2 deiodinase (D2) (Silva et al 1983¹⁸⁸), PR domain containing 16 (PRDM16) (Seale et al 2008¹⁸²) and β 3 adrenergic receptor (Arch et al 1989¹⁷⁵) (ADRB3), the presence of which are now also confirmed in human BAT (Virtanen et al 2009¹⁴⁰). The origin of brown adipocyte is depicted in Figure 1.5.5.

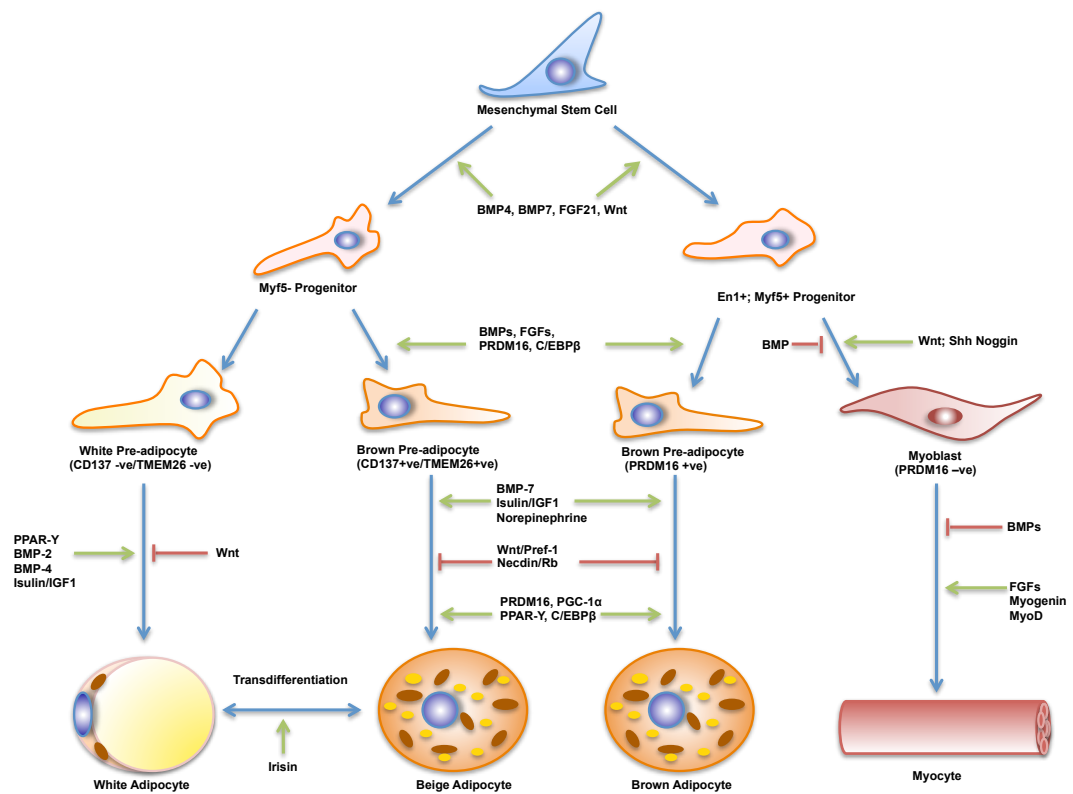


Figure 1.5.5: Multipotent mesenchymal stem cells commit to brown adipocyte lineage following developmental triggers such as bone morphogenic proteins (BMP) and fibroblast growth factors (FGFs) leading on to cascade resulting in a fully developed brown adipocyte. Distinct progenitors give rise to preformed versus systemic brown adipocytes. Myf5-expressing progenitors give rise to skeletal muscle and brown adipocytes in traditional sites such as interscapular area. Myf5-negative progenitors are common precursors for both white adipocyte and recruitable brown adipocyte or beige adipocyte. Beige adipocyte is formed from either the transdifferentiation from white adipose tissue in response to cues such as Irisin or from recruitable brown preadipocyte.

1.6 Imaging of Brown adipose tissue

1.6.1 Positron Emission-Tomography-Computed Tomography (PET-CT)

Imaging of Brown Adipose Tissue

PET-CT is a non-invasive molecular imaging used for whole body scanning and functional assessment. PET imaging was introduced in 1980's for the diagnosis and staging of cancers, and hybridized CT was combined for better anatomical definition. It is based on the principle, that tumours have high metabolic rates, and increased glycolytic activity will result in avid uptake of glucose tagged radiolabelled tracers such as ^{18}F FDG. This will aid to differentiate tissues of high activity (cancers) from that of lesser or no activity (non-cancerous tissues). Serendipitously, low-density tissues of higher metabolic activity were noted in supraclavicular area which were subsequently confirmed to be of BAT, providing renewed evidence of BAT presence in adult life (Hany et al 2002¹⁶¹, Nedergaard et al 2007¹³⁹). PET detected BAT is seen in cervical, supraclavicular, paravertebral, axillary, mediastinal, pericardial, perirenal/adrenal, trachea-oesophageal, intercostal and mesenteric areas, correlating well with previous post-mortem studies (Heaton et al 1972¹⁵¹, Cypess et al 2009¹⁴¹). FDG avid uptake BAT areas are depicted in Figure 1.6. 1.

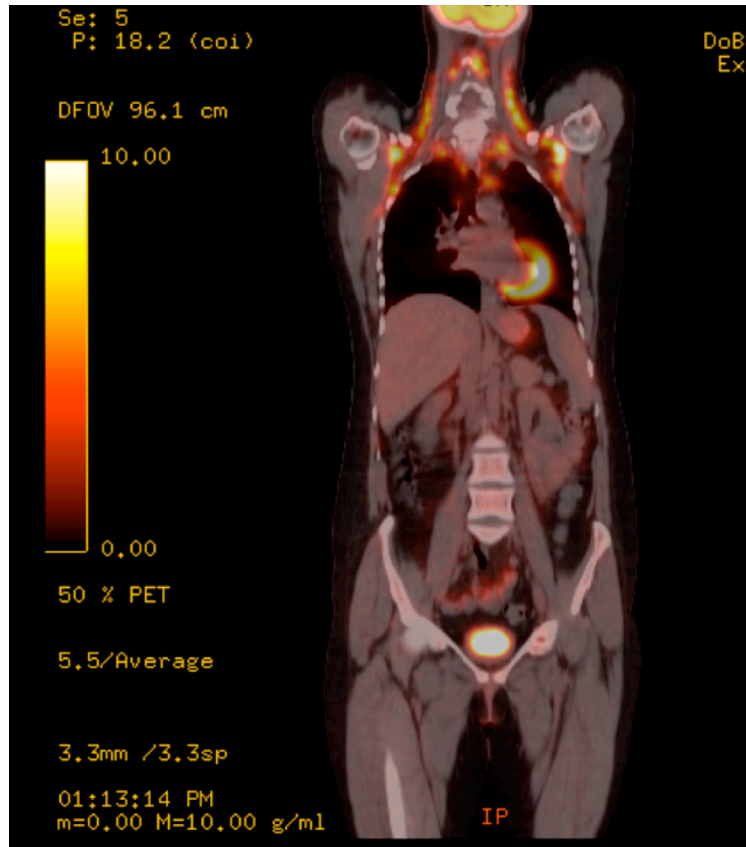


Figure 1.6.1: Coronal image of a 25-year old female following curative surgery for neck malignancy resection demonstrating avid ^{18}F FDG uptake in supraclavicular, cervical, mediastinal and axillary region.

BAT prevalence in humans in large cohort PET studies in ambient temperature range from 2% to 7% (Yeung et al 2003¹⁸⁹, Au-Young et al 2009¹⁹⁰, Pfannenbergl et al 2010¹⁹¹, Ouellet et al 2011¹⁶⁶, Turong et al 2004¹⁹², Kim et al 2008¹⁹³, Williams et al 2008¹⁹⁴, Stefan et al 2009¹⁹⁵), and 36% to 96% in cold activated PET studies (van Marken Lichtenbelt et al 2009¹⁴², Saito et al 2009¹⁴³, Yoneshiro et al 2011¹⁹⁶, Yoneshiro et al 2011¹⁹⁷, Orava et al 2011¹⁷⁶). A comparison of prevalence rate of BAT detection in retrospective PET studies is shown in Table 1.6.1. BAT prevalence

correlates positively to young age, female sex, low BMI and cooler outdoor temperature (Cypess et al 2009¹⁴¹, Ouellet et al 2011¹⁶⁶).

Table 1.6.1: Comparison of prevalence rate of BAT detection in retrospective PET studies

Year	Authors	Location	No of BAT+ve subjects	No of BAT-ve subjects	Prevalence
2002	Hany et al ¹⁶¹	Zurich, Switzerland	17	638	2.5%
2003	Cohade et al ¹⁹⁸	Baltimore, USA	68	107	6.7%
2004	Truong et al ¹⁹²	Houston, USA	15	845	1.8%
2009	Au-Yong et al ¹⁹⁰	Nottingham, UK	167	3614	4.6%
2009	Cypess et al ¹⁴¹	Boston, USA	106	1972	5.4%
2009	Cheng et al ¹⁹⁹	Beijing, China	41	1080	3.8%
2010	Jacene et al ²⁰⁰	Baltimore, USA	56	908	6.2%
2011	Pace et al ²⁰¹	Naples, Italy	73	848	8.6%
2011	Ouellet et al ¹⁶⁶	Sherbrooke, Canada	328	4842	6.8%
2012	Cronin et al ²⁰²	Boston, USA	298	6867	4.3%

PET- Positron Emission tomography; BAT- Brown adipose tissue

Limitations of PET in assessment of BAT include: It is a useful tool to detect BAT activity, but is not yet shown to reliably quantify human BAT volume/mass. Images derived from PET are influenced heavily by environmental temperature, given the

temperature-dependence of BAT activity (which increases in cold conditions) (Ouellet et al 2011¹⁶⁶, Zukotynski et al 2009²⁰³) Furthermore, PET involves exposure to potentially harmful ionizing radiation, and is an expensive technique for imaging BAT in humans (Ouellet et al 2011¹⁶⁶). A safe alternative to PET as an imaging modality for human BAT, and one that can potentially overcome the obstacles outlined above is Magnetic Resonance (MR) imaging.

1.6.2 Magnetic Resonance Imaging of Brown Adipose Tissue

Magnetic Resonance Imaging (MRI), also called as Nuclear Magnetic Resonance, Magnetic Resonance Topography, is a technique that uses a magnetic field and radio waves to create detailed images of organs and tissues. This technique has had enormous influence in radiology field and has generated more than one Nobel Prize. From the first development of MRI awarded to Felix Bloch (Bloch, 1946) and Edward Mills Purcell (Bloembergen, 1948) in the 1952 Physics prize, to the latest recognition of Paul C. Lauterbur (Lauterbur,1986) and Sir Peter Mansfield (Mansfield and Maudsley, 1977) in the 2003 prize for Physiology or Medicine. The advantages of MRI over PET are: non-invasive, less cumbersome, no radiation involved, less expensive, and finally it detects both metabolically inactive and active tissue.

Several attempts to differentiate BAT from WAT in rodents using techniques such as magnetic resonance (MR) spectroscopy and chemical shift MR are proven successful (Hamilton et al 2011²⁰⁴). However, the delineation of BAT and WAT in human adults has so far remained elusive.

BAT and WAT differ in their water:fat ratios due to the different functions of these two tissue types. Whilst BAT contains abundant mitochondria, WAT consists mainly of triglyceride (Cinti et al 2005²⁰⁵). Therefore, BAT contains proportionately more water and less fat than WAT. This important difference provides a rationale for exploring MR as a potential imaging modality to discern BAT from WAT. MR technique of iterative decomposition of water and fat with echo asymmetry and least-squares estimation (IDEAL) has been used successfully in rats to clearly delineate BAT from WAT (Hu et al 2010²⁰⁶). The lower signal intensity of BAT compared to WAT has been exploited to obtain IDEAL fat-water imaging in rats. With reconstructed fat-fraction images, a broad fat-fraction range was observed for BAT (37-70%), in contrast to a higher and smaller range for WAT (90-93%), in both excised tissue samples and *in situ* (Hu et al 2010²⁰⁶). The excised adipose samples from rats and their mean fat-fractions are depicted in Figure 1.6.2.

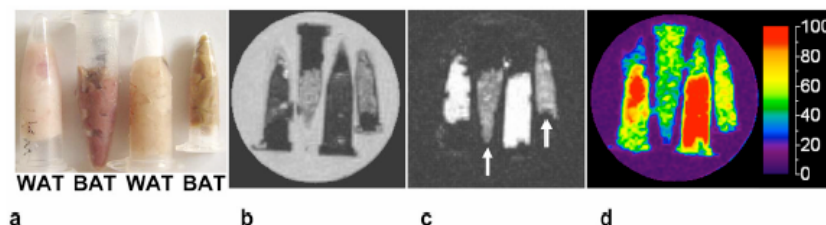


Figure 1.6.2: Hu et al 2010²⁰⁶ IDEAL results from excised tissues imaged placing in water filled petri dish. a) Macroscopic brown and white adipose tissue (BAT, WAT) in vials; b) water; c) fat, and d) fat-fraction map. Mean fat-fraction map for the 4 samples (from left to right) 92%, 51%, 93%, and 62%.

Intermediate signal intensity in comparison with hypointense subcutaneous fat and hyperintense muscle was noted on T2- weighted MR images of presumed BAT in supraclavicular and axillary region of a 13-day old neonate (Carter et al 2008²⁰⁷). Recently, using water-fat imaging in 11 healthy human volunteers, a paired

difference in fat fraction of 16.3% (4.9%) was noted between BAT and WAT, and on dynamic T2* imaging, cold stimulation revealed signal fluctuations that were sensitive to BAT activation (van Rooijen et al 2012²⁰⁸). But histological confirmation was not adopted to conclusively confirm BAT presence.

In summary, an MRI-based methodology to identify and also quantify BAT is highly desirable step in addressing the role of BAT in obesity related disorders. MRI studies conducted so far have not conclusively confirmed BAT presence in living human adults based on both histological and imaging parameters.

1.7 Brown Adipose Tissue and Energy Expenditure

1.7.1 Energy Expenditure

Obesity is as a result of chronic imbalance between energy intake and energy expenditure. The human body's energy balance between energy intake (food) and energy expenditure (heat and work) is a complex phenomenon. It is estimated that 4-8% of the ingested energy is lost in digestion (faeces), and another 3-5% is lost in urine and via skin, leaving approximately 90% of metabolizable ingested energy. A large part of this metabolizable energy is expended in the form of heat (Blaxter et al 1989²⁰⁹).

Heat production plus external work account for the average daily metabolic rate or total energy expenditure (TEE). TEE can be classically divided into resting metabolic rate (RMR; normally 55–65% of TEE), activity related energy expenditure

(AEE; normally 25–35% of TEE), and DIT (about 10% of TEE) (van Marken Lichtenbelt et al 2011²¹⁰, Westerterp et al 1999²¹¹).

RMR is the energy spent when a person is awake in a fasting rested state (Ravussin et al 1982²¹², Prentice et al 1986²¹³, Ravussin et al 1986²¹⁴, Riggs et al 2007²¹⁵). Sleeping metabolic rate (SMR) is 3 consecutive hours of resting energy expenditure measured when asleep (Schoffelen et al 2008²¹⁶). Although it is generally considered that SMR is equal to RMR (FAO/WHO/UNO 1985. Report of a joint expert consultation, Energy and protein requirement WHO technical report series no 724 . WHO:Geneva²¹⁷), the rate of SMR was noted to be higher than RMR at the beginning of sleeping period, and lower than RMR in early morning hours. Furthermore, average SMR is noted to be lower than RMR in obese subjects, and higher than average RMR in non-obese subjects (Zhang et al 2002²¹⁸).

AEE is a composite of planned physical exercise, and that related to daily activities such as fidgeting and pacing (Rumpler et al 1990²¹⁹). AEE accounts for approximately 30% of TEE and is the most modifiable part of TEE (Rumpler et al 1990²¹⁹). Hence exercise and physical activity escalation is a standard recommendation for any weight loss programme.

DIT is the increase in heat production by the body after eating. It is due to both the metabolic energy cost of digestion (the secretion of digestive enzymes, active transport of nutrients from the gut, and gut motility) and the energy cost of forming tissue reserves of fat, glycogen, and protein (Marino et al 2002²²⁰). DIT is highest for alcohol and protein, followed by carbohydrates and then fat (Westerterp et al

1999²¹¹, Westerterp et al 2004²²¹). Although DIT constitutes only 10% of TEE, some studies suggest that bigger meal size and increased meal frequency result in higher DIT (Kinabo et al 1990²²², Tai et al 1991²²³).

Alternative classification is obligatory energy expenditure, which includes RMR, involuntary AEE and obligatory part of DIT, and facultative thermogenesis, which includes voluntary AEE, cold-induced non-shivering thermogenesis (NST), cold-induced shivering thermogenesis, and facultative part of DIT (van Marken Lichtenbelt et al 2011²¹⁰).

Table 1.7.1 Components of Human Energy Expenditure

Total Energy Expenditure (TEE) 100%	=	Resting Metabolic Rate (RMR) 55-65%	+	Activity Energy Expenditure (AEE) 25-35%	+	Diet Induced Thermogenesis (DIT) 10%
Obligatory Energy Expenditure				Facultative Energy Expenditure		
Resting Metabolic Rate				Cold Induced Thermogenesis or Non-shivering Thermogenesis		
Involuntary Activity related energy expenditure				Voluntary Activity related energy expenditure		
Obligatory part of Diet Induced Thermogenesis				Facultative part of Diet Induced Thermogenesis		

Table depicting components of human energy expenditure, as adapted from van Marken Lichtenbelt et al 2011²¹⁰.

There are various ways of measuring energy expenditure, and the most accurate way is by whole room indirect calorimetry (Schoffelen et al 1997²²⁴, Westerterp et al 1999²¹¹, Bonomi et al 2013²²⁵, Westerterp et al 2013²²⁶) and is measured in Kilo

calories (Kcal) per 24 hours. Indirect calorimetry is the method by which energy expenditure is calculated on the basis of total oxygen consumed (VO_2) is converted into carbon dioxide (VCO_2) and water. Technological advances have yielded more accurate measurements of oxygen and carbon dioxide, whilst preventing ambient air mixing with the gases that are being measured. Room calorimeters are airtight to prevent leakages of air, with large fans to enable adequate mixing of air, as it is measured when exiting the room.

1.7.2 Role of Brown Adipose Tissue in Cold and Diet Induced Thermogenesis

As stated in chapter 1.5.3, studies in animals have established that cold exposure acutely elevates UCP1 mRNA expression (Jacobsson et al 1994²²⁷, Griggio et al 1999²²⁸), whereas prolonged exposure induces BAT hypertrophy and hyperplasia (Mory et al 1980²²⁹, Mineo et al 2012²³⁰). Cold exposure also induces UCP-1 immunoreactive BAT emergence in WAT (Barbatelli et al 2012²³¹). BAT is shown to have a role in adaptive thermogenesis through CIT and DIT by a common regulation of sympathetic nervous system (Feldmann et al 2009¹³⁷, van Marken Lichtenbelt et al 2009¹⁴², Marino et al 2002²²⁰). Recent human PET-CT studies using radio-labelled tracers have further confirmed BAT's role in CIT (also called non-shivering thermogenesis) through mitochondrial uncoupling property of UCP-1 (Ouellet et al 2012²³², Muzik et al 2012²³³).

In mice, nutrient ingestion acutely raises energy expenditure by 20%, along with doubling of blood flow in BAT, in absence of enhanced blood flow to other metabolic tissues (Glick et al 1984²³⁴, Glick et al 1984²³⁵). In humans, insulin

mediated 5-fold increase in FDG uptake in BAT indirectly suggests that BAT has a role in postprandial energy metabolism (Orava et al 2011¹⁷⁶). More recently, PET studies following high-calorie meal in lean men have shown increased FDG uptake in brown fat, implicating BAT in DIT (Vosselman et al 2013²³⁶).

1.7.3 Metabolic significance of Brown Adipose Tissue in Humans

BAT provides persuasive evidence for a metabolic role of potential significance, given the recent evidence that BAT is present in most humans, if not all, and at least in a small proportion. (Lee et al 2011²³⁷, van Marken Lichtenbelt et al 2009¹⁴²). BAT's contribution to energy expenditure (CIT and DIT), a chief determinant of energy balance, offers a possible anti-obesity strategy through cellular bio-energetic route.

Some of the mice studies claim the thermogenic potential of BAT when maximally activated is 300 W/kg (Cannon et al 2004¹⁴⁹, Rothwell et al 1983²³⁸). On this basis, Rothwell and Stock extrapolated that 40-50 g of BAT in humans can account to 20% of energy expenditure (Rothwell and Stock et al¹⁵²). Human studies by Virtanen and colleagues estimated 4.1 kg of weight loss over one year through maximally activating 63 g of BAT (Virtanen et al 2009¹⁴⁰). BAT can potentially be activated for prolonged periods based on rodent studies demonstrating sustained CIT (Golozoubova et al 2001²³⁹). Two independent but congruent human PET studies estimated an energy expenditure of 200-400 kcal/day, a 10 to 20% rise in daily basal metabolic rate through BAT activation (Yoneshiro et al 2011¹⁹⁶, Muzik et al 2012²⁴⁰). Therefore, the glucose disposal (Orava et al 2011²⁴¹) and triglyceride

clearance properties of BAT Bartelt et al 2011²⁴²), when fully utilized may act as an energy sink. Further evidence of BAT's contribution to TEE is provided in Table 1.7.3. BAT prevalence is higher in leaner subjects and is inversely correlated to BMI in multiple retrospective PET studies (Cypess et al 2009¹⁴¹, Ouellet et al 2011¹⁶⁶). In summary, these studies provide strong evidence that BAT's contribution to TEE, although small in proportion, is significant and sufficient to contribute to weight loss over time. There are three ways of enhanced energy expenditure through manipulation of BAT could be theoretically achieved: i) maximal and continual activation of BAT; ii) trans-differentiation of WAT to BAT (to form BeAT), and; iii) transplantation of BAT stem cells.

Table 1.7.3: Metabolic significance of BAT in Adult Humans, Lee et al 2013¹⁵³

Author	Year	Extrapolated parameter	Magnitude	Contribution of BAT to TEE
Virtanen et al ¹⁴⁰	2009	Glucose uptake into cold stimulated BAT	12.2µmol/100 g/min	7%
Yoneshiro et al ¹⁹⁶	2011	Difference in cold-stimulated EE in BAT positive and negative individuals	368 kcal/d	25%
Orava et al ¹⁷⁶	2011	Increase in glucose uptake into BAT after cold stimulation	8µmol/100 g/min	5%
		Difference in cold-stimulated EE between BAT positive and negative individuals	286 kcal/d	22%
Ouellet et al ²³²	2012	Glucose uptake into cold-stimulated BAT	10.8µmol/100 g/min	6.7%
		Difference in EE in BAT positive individuals in cold and warm environments	2001 kcal/d	77%

BAT- Brown adipose tissue; TEE- Total energy expenditure

1.8 Regulators of Brown Adipose Tissue

1.8.1 Environmental Temperature and Brown Adipose Tissue

To capitalize BAT as an anti-obesity target, it is vital to know the factors, which stimulate and increase BAT activity/volume and/or aid transcription of WAT to beige. There are several regulatory factors identified over years, but most studied ones are environmental temperature and sympathetic nervous system.

Cold is classically known to stimulate rodent BAT activity, BAT hypertrophy, BAT hyperplasia whilst causing morphological transformation of WAT to beige (Jacobsson et al 1994²²⁷, Griggio et al 1982²²⁸, Mory et al 1980²²⁹, Mineo et al 2012²³⁰, Barbatelli et al 2010²³¹). Several cooling protocols in human PET examinations involving a temperature range from 16°C to 20°C, have increased the PET detection rate up to 100%, and increased FDG uptake by 15 fold (Feldmann et al 2009¹³⁷, van Marken Lichtenbelt et al 2009¹⁴², Marino et al 2002²²⁰, Ouellet et al 2012²³², Muzik et al 2012²³³). Studies using ¹¹C-Acetate (Ouellet et al 2012²³²) and ¹⁵O₂ tracers (Muzik et al 2012²³³) to measure oxidative metabolism and oxygen extraction in human PET studies, unequivocally prove cold exposure stimulate BAT activity. Contrarily, inverse correlation is noted that PET detected BAT prevalence is lesser in summer and on increasing room temperature (Cypess et al 2009¹⁴¹).

1.8.2 Sympathetic Nervous System and Brown Adipose Tissue

Sympathetic nerves richly innervate BAT. Cold exposure increases sympathetic drive and doubles plasma noradrenaline levels (Celi et al²⁴³). Lateral hypothalamus area is shown to influence sympathetic nerves in BAT and BAT induced thermogenesis, hypothesized through central melanocortin signalling (Cerri et al 2005²⁴⁴, Fan et al 2007²⁴⁵). Contrarily, central nervous depressants such as isoflurane (Fueger et al 2006²⁴⁶), halothane (and diazepam suppress BAT detection (and hence activation) in PET imaging.

Epinephrine causes vasodilatation and enhances glucose and oxygen consumption in skeletal muscle (Simonsen et al 1992²⁴⁷) whilst also enhancing thermogenesis in humans (Simonsen et al 1993²⁴⁸). BAT is also activated in patients with pheochromocytoma, with increased UCP1 expression similar to levels in cold-exposed rodents (Ricquier et al 1982²⁴⁹, Lean et al²⁵⁰). BAT activity is greater in patients with pheochromocytoma (English et al 1973²⁵¹, Melicow et al 2002²⁵²) due to over-activity of the SNS and elevated levels of circulating catecholamines, that in turn stimulate β_3 adrenergic receptors, thereby activating *UCP1* expression via cyclic adenosine monophosphate (cAMP) and protein kinase-A (PKA) pathways (Bouillaud et al²⁵³). Hadi *et al.* demonstrated active BAT to be present in 27% (26/96) of pheochromocytoma patients undergoing FDG PET/CT scans (Hadi et al 2007²⁵⁴), indicating higher detection rates compared to 5.37% (106/1972) of all cause PET/CT studies reported by Cypess and colleagues (Cypess et al 2009¹⁴¹). Recent human observational studies demonstrate a correlation between plasma metanephrine levels and BAT activity (Wang et al 2011²⁵⁵).

1.8.3 Thyroid hormones and Brown Adipose Tissue

We have known for over a century that thyroid hormone (TH) increases metabolic rate and thermogenesis in homeothermic species, and hence is an important physiological modulator of energy homeostasis (Klitgaard et al 1952²⁵⁶, Klieverik et al 2009²⁵⁷). TH not only stimulates both obligatory and facultative thermogenesis (Silva et al 2006²⁵⁸), but also enhances oxidative phosphorylation through induction of mitochondrial biogenesis and modulation of the expression of genes implicated in the regulation of the mitochondrial respiratory chain (Sheehan et al 2004²⁵⁹). The weight gain and decreased cold tolerance observed in individuals with hypothyroidism, and the weight loss and sweating/heat intolerance observed in patients with hyperthyroidism, are predictable clinical manifestations of alterations in BAT activity (Lopez et al 2010²⁶⁰). It follows therefore that differences in BAT quantity and/or activity between individuals may also influence the clinical manifestations of hypo- or hyperthyroid states. This may also explain the inter-individual variability of weight changes and heterogeneity of other clinical manifestations of dysthyroid states. Type 2 deiodinase (D2) is present abundantly in BAT, and plays an essential role in mediating the full thermogenic response of BAT to adrenergic stimulation via increased thyroxine (T4) to thyronine (T3) conversion within this tissue (Bianco et al 1988²⁶¹). A thyroid hormone analogue, GC-1 compound, a selective Thyroid Receptor Beta (TR β) agonist, induces *UCPI* gene expression in rats (Rebeiro et al 2001²⁶²), improves glucose homeostasis (Bryzgalova 2008²⁶³), increases energy expenditure and reduces fat mass and plasma cholesterol (Grover 2004²⁶⁴).

Promising data from human studies implicate thyroid hormones of having important effects on BAT activity. T3 treatment of differentiated human multipotent adipose-derived stem cells *in vitro* induces UCP1 expression and mitochondrial biogenesis through effects on TR β (Lee et al 2011²⁶⁵). Following thyroidectomy and subsequent treatment with thyroxine replacement therapy in a patient with papillary carcinoma, BAT activity was enhanced with concurrent weight-loss and remission of T2DM (Skarulis et al 2010²⁶⁶). Thyroxine may cause ‘brownification’ of WAT (Lee et al 2011²⁶⁵), although this remains a hypothesis.

1.8.4 Transcriptional Regulation

Given that adult humans have BAT, it is important to explore BAT manipulation as a means of promoting weight-loss through enhanced energy expenditure via BAT manipulation. In addition to augmentation of BAT content and/or enhancement of BAT activity, other approaches include trans-differentiation of non-BAT progenitors into BAT pre-adipocytes, and surgical implantation of BAT. Development of novel BAT-related therapies will require a complete understanding of the embryological and transcriptional mechanisms of BAT specification and development in human models. We also need to characterize and confirm the physical and genetic attributes of BAT including anatomical and histological distributions of human BAT. Further challenges will be to develop a sustained long-term BAT stimulating or recruiting molecular circuit with adequate knowledge of counter-regulatory mechanisms for an acceptable safety profile, and to identify a reliable and safe imaging modality to monitor the effects of such therapies on BAT once developed and administered.

Several transcriptional regulators of brown adipocyte differentiation are described in rodents, with some revealing promising effects even in human models. Irisin is a 112-amino-acid polypeptide hormone, and is a cleaved and secreted fragment of fibronectin type III domain containing 5 (FNDC5) membrane protein, in turn released by muscle through increased PGC-1 α expression following exercise in both rodents and humans (Bostrom et al 2012²⁶⁷). Irisin showed a powerful browning effect on certain white adipose tissues in mice, both in culture and *in vivo* (Bostrom et al 2012²⁶⁷). Human irisin is believed to be identical to mouse irisin, and in healthy adult subjects showed a 2-fold increase in plasma levels following 10 weeks of supervised endurance exercise training, as compared to the non-exercised state (Bostrom et al 2012²⁶⁷). This PGC-1 α dependent myokine alludes to the super-added beneficial effects of exercise via BAT, which need to be further explored.

The PRDM16-C/EBP- β transcriptional complex acts in Myf5-positive myoblastic precursors or pre-adipocytes to drive the thermogenic program with co-activation of PPAR- γ and PGC-1 α (Seale et al 2008¹⁸², Kajimura et al 2009²⁶⁸). The cAMP-dependent thermogenic program is potentiated by Forkhead box C2 (FOXC2) (Cederberg et al 2001²⁶⁹) and PRDM16 and repressed by Receptor-Interacting Protein 140 (RIP140) (Hallberg et al 2008²⁷⁰). Other transcriptional regulators of Bone Morphogenic Protein-7 (BMP7) (Tseng et al 2008²⁷¹), Fibroblast Derived Growth Factor-21 (FGF-21) (Beenken et al 2009²⁷²), PPAR- γ ligands (Wilson-Fritch et al 2004²⁷³) and Atrial Natriuretic Peptide (ANP) (Bordicchia et al 2012²⁷⁴), have been described in rodents. Successful transcription of WAT through these various regulators result in BeAT, as opposed to classical BAT and success of these compounds depend upon extrapolating the gains in human studies. The cellular

mechanisms of some of these endocrine factors are shown in Figure 1.8.3.

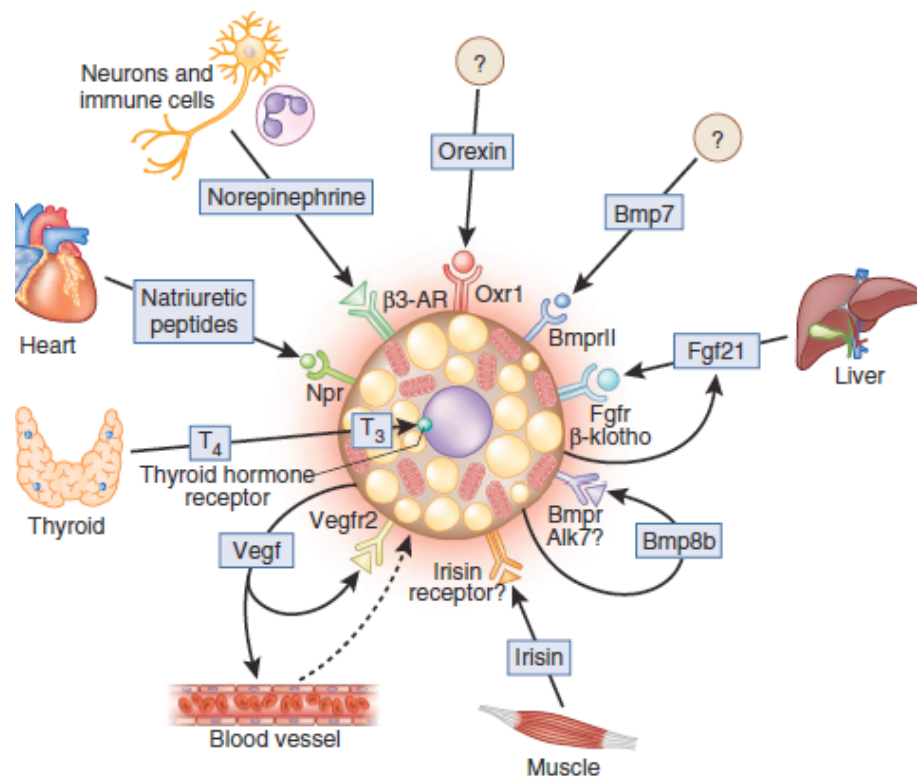


Figure 1.8.3: Harms et al 2013²⁷⁵- Illustration of origin and cellular receptor pathways of some of the secreted endocrine regulators, which recruit brown and/or beige adipocytes.

1.9 Neurohormonal Adiposity Signals

1.9.1 Central regulation of body weight

The regulation of feeding, energy intake and expenditure, and body weight is a homeostatic process (Wilding 2002²⁷⁶). Neurohormonal signals and adipokines from the gut and adipose tissue respectively converge and integrate in hypothalamus, resulting in energy intake and expenditure regulation (Wren et al 2007²⁷⁷). Two

neuronal populations in arcuate nucleus (ARC) of hypothalamus, possessing opposite effects on energy balance forms the basis of central integration of peripheral adiposity signals. Medial arcuate nucleus consists of neurons that express Neuropeptide Y (NPY) and Agouti-Related Peptide (AgRP), which act to stimulate food intake and weight gain. In contrast, lateral arcuate nucleus contains pro-opiomelanocortin (POMC) and cocaine- and amphetamine-regulated transcript co-expressing neurons that inhibit food intake and promote weight loss (Williams et al 2001²⁷⁸, Cone et al 2001²⁷⁹, Wren et al 2007²⁷⁷). In response to peripheral adiposity signals, relative activity of these appetite stimulating and appetite suppressing hypothalamic neurons results in release of respective neuropeptides, which in turn regulate feeding behaviour and body weight regulation (Williams et al 2001²⁷⁸, Cone et al 2001²⁷⁹, Wren et al 2007²⁷⁷).

1.9.2 Leptin

Leptin is a long-term adiposity signal and was the first discovered adipokine in 1994 (Zhang et al²⁸⁰). Secreted by WAT, circulating level of leptin is proportional to fat mass. Mice lacking leptin develop hyperphagia, obesity, insulin resistance and hypogonadism (Friedman et al 1998). Regular central or peripheral administration of leptin or leptin agonists in *ob/ob* mice induces weight loss by satiety suppression and increase in energy expenditure, whilst recovering euglycaemia and reproductive function (Halaas et al 1995²⁸¹, Campfield et al 1995²⁸², Pelleymounter et al 1995²⁸³). In humans, leptin is shown to inhibit orexigenic NPY/AgRP co-expressing neurons, and to stimulate anorexigenic POMC-expressing neurons of the hypothalamic arcuate nucleus (Sahu et al 2003²⁸⁴). Obesity caused by congenital leptin deficiency,

which alleviates on treatment with recombinant leptin, is very rare (Farooqi et al 1999²⁸⁵). On the contrary, leptin levels are found to be higher in obese individuals, probably as a result of insulin resistance and recombinant leptin use in such individuals are unfavourable (Maffei et al 1995²⁸⁶, Moon et al 2011²⁸⁷, Vazier et al 2012²⁸⁸). It proportionally correlates with BMI and has been implicated in multiple cardiovascular pathologies including myocardial infarction, stroke, hypertension and atherosclerosis, where it is said to act synergistically with other inflammatory mediators (Gualillo et al 2007²⁸⁹, Lawlor et al 2007²⁹⁰, Sattar et al 2009²⁹¹). Overall, leptin acts as ‘adipostat’ and regulates food intake and energy expenditure through its actions on hypothalamus.

1.9.3 Adiponectin

Adiponectin, most abundant protein secreted by adipose tissue (Scherer et al 1995²⁹²), unlike many other adipokines, is known to increase insulin sensitivity and vascular function, thus possessing both anti-diabetic and anti-atherogenic (Trujillo et al 2003²⁹³, Ouchi et al 1999²⁹⁴) properties. Administration of recombinant adiponectin in rodent models increases insulin sensitivity (Yamauchi et al 2001²⁹⁵), and adiponectin transgenic mice showed partial amelioration of insulin resistance (Yamauchi et al 2003²⁹⁶). In contrast, adiponectin deficient mice displayed glucose intolerance and insulin resistance (Kubota et al 2002²⁹⁷). Low levels of plasma adiponectin in humans correlate to CVD (Von Enyatten et al 2008²⁹⁸) and metabolic syndrome (Salmenniemi et al 2004²⁹⁹). High adiponectin levels are protective towards atherosclerosis because of anti-inflammatory properties (Gualillo et al 2007²⁸⁹). It is hypothesized that adiponectin acts as a starvation signal, increases in

fasting state and stimulates appetite, having an opposite to leptin's satiety action, thus indicating a role in energy homeostasis (Kubota et al 2007³⁰⁰). However, a definitive role of adiponectin in energy homeostasis is yet to be fully determined.

1.9.4 Ghrelin

Ghrelin, a 28-amino acid peptide produced primarily in gastric fundus and proximal small intestine, is the only orexigenic hormone identified till date, that powerfully triggers hunger in a diverse of species including humans (Kojima et al 1999³⁰¹, Tschop et al 2000³⁰², Wren et al 2001³⁰³). Ghrelin is an endogenous ligand for growth hormone secretagogue receptor and hence releases growth hormone (Wren et al 2001³⁰³). Although the precise mechanisms are unclear, it is speculated to act on hypothalamic medial arcuate nucleus and triggers NPY/AgRP co-expressing neurons to stimulate food intake and is known as a meal initiator (Wren et al 2001³⁰⁴). Ghrelin is implicated in meal-time hunger and meal initiation in both lean and obese individuals (Druce et al 2005³⁰⁵), and on intravenous infusion is noted to increase dietary intake by 30% in human volunteers (Murphy et al 2004³⁰⁶). Circulating plasma ghrelin levels surge before meals and suppress on ingestion of nutrients (carbohydrates, protein and fats in order of effectiveness of suppression) (Weigle et al 2003³⁰⁷, Mohlig et al 2002³⁰⁸). The typically expected post-prandial suppression of ghrelin is attenuated or absent in obese individuals (English et al 2002³⁰⁹). Ghrelin status following gastric bypass surgery remains to be determined, as studies report levels to be increased (Cummings et al 2002³¹⁰), same (Karamanakos et al 2008³¹¹, Couce et al 2006³¹²) or reduced (Garcia-Fuentes et al 2008³¹³). However, ghrelin blockade studies show promise both in rodent models (Wortley et al 2005³¹⁴, Zigman

et al 2005³¹⁵) and in humans (Foster-Schubert et al 2006³¹⁶), convincing us the role of ghrelin in energy homeostasis. The most promising strategy for an anti-obesity agent through ghrelin pathway would be to attempt pre-prandial receptor blockade.

1.9.5 Peptide YY

PYY, is secreted in full-length 36-amino acid form from L-cells of distal gastrointestinal tract (primarily colon), circulates in 34-amino acid active PYY₃₋₃₆ form. It acts via Y2 receptor (G-protein coupled receptor family) in hypothalamus, inhibiting the release of NPY, the most potent CNS stimulant of appetite (Batterham et al 2002³¹⁷). Circulating levels of PYY₃₋₃₆ become elevated 1 hour post-meal, and are influenced by diet composition and calorie content (Adrian et al 1985³¹⁸). Endogenous fasting and post-prandial concentrations were lower in obese than in lean subjects, and fasting level negatively correlated with BMI (Batterham et al 2003³¹⁹). Increased level of PYY₃₋₃₆ is noted following gastric bypass surgery indicating to long-term success of these procedures in causing weight loss in humans (Korner et al 2005³²⁰). Intravenous infusion of exogenous PYY₃₋₃₆ induced lower 24-hour food intake by 30% and suppress satiety in humans (Batterham et al 2002³¹⁷, Batterham et al 2003³¹⁹). Intranasal PYY₃₋₃₆ administration thrice daily results in modest weight loss in humans (Gantz et al 2007³²¹). Limitations of PYY₃₋₃₆ or Y2 receptor agonists use are severe nausea and vomiting noted in these studies (Halatchev et al 2005³²²). More work is needed before using PYY₃₋₃₆ as biomarker of satiety. A combined approach of other novel agents along with PYY₃₋₃₆ may usher in an anti-obesity drug.

1.9.6 Glucagon Like Peptide-1

GLP-1 is a cleaved product from proglucagon, produced by L-cells primarily in distal small intestine and colon, where it colocalizes with oxyntomodulin and PYY (Verdich et al 2001³²³). Other proglucagon products include glucagon (a counter regulatory hormone), Glucagon like peptide-2 (GLP-2)(an intestinal growth factor), glicentin (a gastric acid inhibitor), and oxyntomodulin (Verdich et al 2001³²³). Several of these products are implicated in satiation, but the strongest of these are GLP-1 and oxyntomodulin (Herrmann et al 1995³²⁴). Two equipotent bioactive forms of GLP-1₇₋₃₆ and GLP-1₇₋₃₇, are inactivated by Dipeptidyl dipeptidase -IV (DPP-IV), rendering the half-life of GLP-1 to 5 minutes (Kieffer et al 1995³²⁵). Ingestion of nutrients triggers GLP-1 release from L cells, which applies 'ileal brake' by reducing gastric and intestinal motility. In addition to delaying gastric emptying, GLP-1 accentuates glucose dependent insulin release, inhibits glucagon release, stimulates β -cell growth (Tourell et al 2001³²⁶) and suppresses satiety through central pathways (Turton et al 1996³²⁷). Both centrally and peripherally administered GLP-1 and GLP-1 receptor agonists exert profound anorexigenic effects in several species (John Eng et al 1992³²⁸) including normal-weight (Gutzwiller et al 1996³²⁹) obese (Naslund et al 1999³³⁰) and diabetic humans (Toft-Nielsen et al 1999³³¹). Anorectic effects are mediated specifically by GLP1R, as they are absent in GLP1R-deficient mice and are reversed with selective GLP1R antagonists (Baggio et al 2004³³²). GLP-1 levels are increased following gastric bypass (le Roux et al 2007³³³). The GLP-1 analog, exendin-4, discovered from the venom of the Gila monster, *Heloderma suspectum*, is an established anti-diabetic agent (Eng et al 1992³²⁸). It is also currently being investigated as an anti-obesity agent in non-

diabetic humans. DPP-IV inhibition is a beneficial approach in treatment of T2DM (Ahren et al 2007³³⁴). Overall, evidence suggests that plasma GLP-1 level is a useful marker for satiation, and use of GLP-1 receptor agonists alleviates glucose intolerance and induces weight loss in humans (Verdich et al 2001³²³).

1.9.7 Pancreatic Polypeptide

Pancreatic polypeptide (PP) is a 36-amino acid anorexigenic peptide, primarily synthesized and released from the endocrine pancreas, to a lesser extent from colon and rectum (Chaudhri et al 2008³³⁵). Levels are low during the fasting state and rise in proportion to nutrient load (Track et al 1980³³⁶). PP acts predominantly via Y4 receptor (Lin et al 2009)³³⁷. Peripheral administration of PP causes reduced food intake and weight loss in rodents (Malaisse-Lagae et al 1977³³⁸) and humans (Batterham et al 2003³³⁹). Although the hypothalamically-regulated anorexigenic effects of PP remain to be fully characterized, a product with the capacity to increase endogenous PP production while avoiding degradation in the circulation, or to increase Y4-mediated signalling, would certainly hold promise as a future anti-obesity tool (Perry et al 2012³⁴⁰).

1.9.8 Non-esterified Fatty Acids

Non-esterified fatty acids (NEFAs) are adipocyte-derived products, secreted primarily during fasting as a nutrient source for the rest of the body. NEFAs constitute the primary energy fuel for most tissues during starvation. Their release into circulation is partly through hydrolysis of triacylglycerol-rich lipids by

activation of lipoprotein lipase, and the rest from tissue triacylglycerol depots, which are under the influence of hormone sensitive lipase. NEFA removal is dependent on tissue uptake or esterification (Ferrannini et al 1997³⁴¹). Insulin is a potent regulator of NEFA and causes profound suppression through its stimulatory effect on lipoprotein lipase and inhibitory effect of hormone sensitive lipase, besides also providing α -glycerophosphate, the substrate for NEFA re-esterification (Campbell et al 1992³⁴²). This action of insulin marks the switch over of energy production from dominant fat oxidation to prevalent glucose utilization. Elevated fasting NEFA levels are noted in T2DM subjects (Golay et al 1986³⁴³), as impaired insulin activity is noted, and also in non-diabetic obese subjects despite normal levels of insulin (Golay et al 1986³⁴³, Frayn et al 1996³⁴⁴). NEFAs effect glucose homeostasis by reducing adipocyte and skeletal muscle glucose uptake, and promoting hepatic glucose output (Rosen et al 2006³⁴⁵) as shown in Figure 1.9.8. Because lipolysis in adipocytes is repressed by insulin, and insulin resistance from any cause can lead to chronic NEFA elevation, which in turn results in lipotoxicity of β -cells (McGarry et al 1999³⁴⁶), reduced glucose dependent insulin excretion (Sako et al 1990³⁴⁷, Zhou et al 1995³⁴⁸, Mason et al 1999³⁴⁹), impaired insulin gene expression (Gremlich et al 1997³⁵⁰), and increased β -cell apoptosis (Milburn et al 1995³⁵¹, Shimabukuro et al 1998³⁵², Randle et al 1963³⁵³). In summary, acute effect of NEFA is to release insulin, but chronic effect of NEFA is to reduce insulin secretion as shown in Figure 1.9.8.

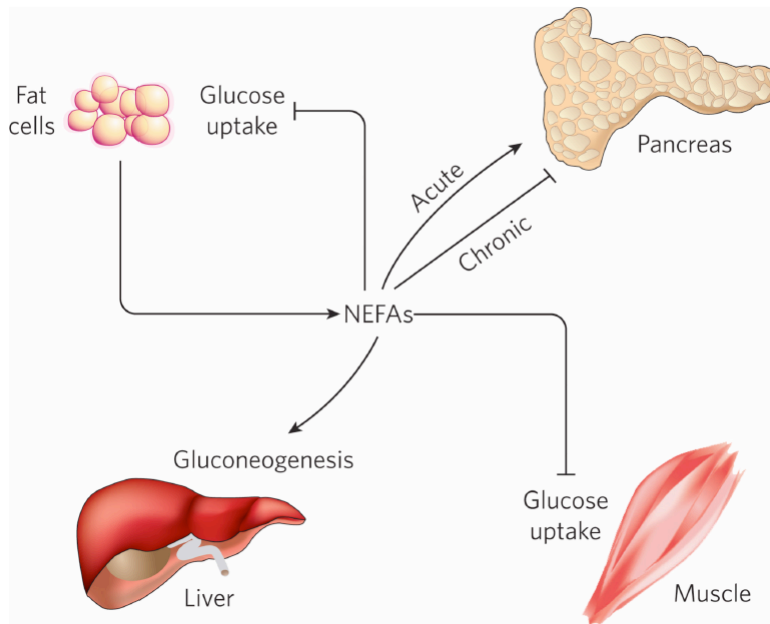


Figure 1.9.8: Rosen et al 2006³⁴⁵ - NEFA release from adipocytes causes reduced glucose uptake in adipocyte and skeletal muscle; acutely, NEFA causes insulin release, but chronic exposure causes insulin resistance.

1.10 General Aims of the Study

The aims of this thesis are:

1. To develop IDEAL MRI as a novel imaging tool for characterization of BAT in humans. This innovation would enable to detect BAT irrespective of its activity, and without radiation exposure or interference from external factors such as environmental temperature, which would represent a significant advantage over ^{18}F -FDG PET/CT as a means of imaging human BAT.
2. To explore the effect of various determinants such as age, sex, BMI, fasting glucose, outdoor temperature *etc.*, on BAT prevalence and volume in sequential ^{18}F -FDG PET/CT examinations.
3. To investigate the impact of meal duration (eating rate) on BAT implicated diet-induced thermogenesis, and on pancreatic and gut hormones.

The combination of these aims will seek to accurately detect human BAT using safe radiological means, whilst exploring various factors of BAT activity and its impact on energy expenditure, providing new insights and understanding of BAT on human physiology for an ultimate aim to manipulate BAT as an anti-obesity measure.

Chapter 2

METHODS AND MATERIALS

2.1 Methods and Materials

This chapter details the methods and materials used for the individual chapters of this thesis. Each appropriate chapter has further information outlining specific methods for each study.

2.1.1 Positron Emission Tomography (PET) detected Brown Adipose Tissue (BAT) study

Retrospective analyses of 3295 consecutive PET-CT scans at the PET centre in University Hospitals Coventry and Warwickshire (UHCW) National Health Service (NHS) Trust, was undertaken. PET scans were ordered for various diagnostic reasons and were largely conducted for clinical evaluation of different malignancies. The data collection period was between June 2007 and August 2012. Substantial physiologic ^{18}F -FDG uptake at recognized BAT areas were considered to be putative BAT. The influence of outdoor temperature, sex, age, body mass index (BMI), fasting plasma glucose level and thyroid status on the prevalence, volume and activity of BAT was investigated. UHCW Human Metabolism and Research Unit (HMRU) ethics approved by the Black County Research Ethics Committee (Rec No. 11/H1206/3) was applied for the study, and the requirement for consent was waived under exempt review, given the retrospective observational nature of the study.

2.1.2 Basic principles of PET imaging

Positron emission tomography (PET) is a non-invasive functional nuclear imaging technique that captures functional, physiological and molecular processes of the body tissue (tumour), by producing a three-dimensional picture.

To acquire a PET scan, a positron-emitting radionuclide tracer (e.g., F-18) is tagged on a biologically active molecule (e.g., Deoxyglucose) and is intravenously injected into the body. Following a waiting period, the tracer thus concentrated in the tissues of interest emits gamma photons, which are detected by sensors to construct a three-dimensional image by computer analysis.

Radionuclides are unstable compounds due to the unsuitable composition of neutrons and protons or excess energy. Therefore, they decay by emitting radiations such as α particles, β^- particles, β^+ particles, electron capture, and isomeric transition.

A range of radioactive nuclei of positron-emitting radionuclide tracers, also called as PET radiopharmaceuticals (^{11}C , ^{13}N , ^{15}O , ^{18}F , ^{68}Ga and ^{82}Rb), emit positively charged electrons (positrons), referred as β^+ . This process is also called as 'Positron Emission Decay' or 'Beta Emission Decay'. A positron is an antiparticle of an electron with opposite charge (Basu et al 2011³⁵⁴).

Usually the radiotracers have a short half-life. The most common PET tracer used is a radiolabelled glucose analog, 2-deoxy-2- [^{18}F] Fluoro-D-Glucose (^{18}F -FDG). ^{18}F -FDG has a relatively long half-life of 110 minutes, and provides a waiting period of

approximately one-hour for clinical purposes of PET imaging. The waiting period is for the active molecule to be concentrated in the tissues of interest. Like glucose, ^{18}F -FDG is phosphorylated by hexokinase as part of the glycolysis, and therefore is taken up by mitochondria of all metabolically active tissues (tumour, heart, brain, liver, BAT etc.). Unlike glucose, ^{18}F -FDG is intracellularly trapped as it lacks the requisite hydroxyl group at position 2', therefore not undergoing further glycolysis by phosphohexokinase isomerase (Basu et al 2011³⁵⁴).

A positron thus emitted travels to certain distance in the tissue and loses energy by interaction with an electron of an absorber atom and comes to rest by a process called 'Annihilation'. Both particles (β^+ and e^-) are annihilated as a result of matter-antimatter encounter to produce two Photons of 511 keV, which are emitted in opposite directions (approximately 180°), and this forms the basic molecular process of PET as shown in Figure 2.1.2.

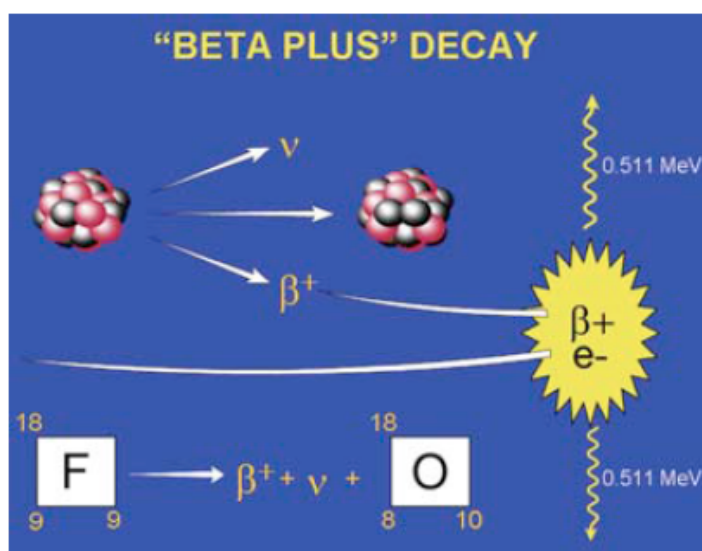


Figure 2.1.2 Saha et al, Basics of PET imaging 2nd edition, 2010³⁵⁵: A schematic illustration of the annihilation of a positron and an electron in the medium. Two 511-keV photons are produced and emitted in opposite directions (180°).

2.1.3 Image reconstruction from PET

The released Gamma photons (also termed as Gamma rays) are detected by scintillation counter to form light photons. The common detectors in PET system are bismuth germinate (BGO), lutetium oxyorthosilicate (LSO) and lutetium yttrium oxyorthosilicate (LYSO). A true coincidence occurs when two Gamma Photons of 511-keV from a single annihilation, are sensed simultaneously by a pair of diametrically opposite detectors along a Line of Response (LOR), as shown in Figure 2.1.3. The light photons are converted to electrical impulse by a photomultiplier tube, which contains a photocathode. The anode end of the photocathode, which is made of alloy of cesium and antimony, absorbs the light photons and emits electrons. The pulse height analyzer (PHA) further discriminates the signals, such that only selected energy photons are permitted which is in turn computer-processed and stored as a PET image (Saha et al 2010³⁵⁵).

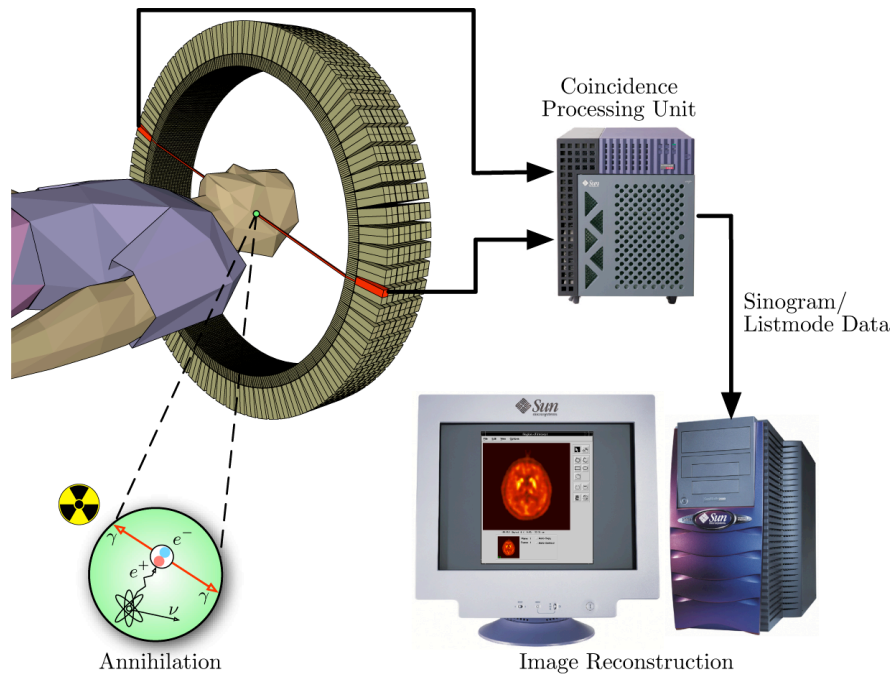


Figure 2.1.3 Illustration showing two photons from a single annihilation event interacting simultaneously with opposing scintillation crystals along a single Line of Response (LOR). The light photons are converted into electrical impulses by a photomultiplier tube and are computer processed to produce a PET image. Image downloaded from [http://en.wikipedia.org/wiki/File: PET-schema.png](http://en.wikipedia.org/wiki/File:PET-schema.png)

The image thus produced however, is a functional image with no anatomical reference and low spatial resolution. This is circumvented with integration with Computed tomography (CT).

2.1.4 Principles of Computed tomography (CT)

The fact that CT was one of the greatest innovations in the field of radiology since the discovery of X-rays in 1895, was duly acknowledged by awarding Nobel prizes in medicine to Sir Godfrey Hounsfield and Alan McLeod Cormack in 1979 (Ghonge

et al 2013³⁵⁶).

CT is a medical imaging procedure that utilizes computer-processed X-rays to produce tomographic images or 'slices' of specific regions of interest of the body. 'Tomography' is derived from Greek words *tomos* (to slice) and *graphien* (to write). CT is based on the basic principle that the density of the tissue passed by the X-ray beam can be measured from calculation of the attenuation co-efficient.

CT is composed of a moving x-ray tube mounted on a rotating gantry and a ring of thousands of detectors. The detectors are made of ceramics, gadolinium oxysulfide and gemstone, etc. A high voltage is applied to the cathode filament of the x-ray tube. These electrons from the cathode impinge to the rotating anode made of tungsten, rhenium or molybdenum, producing X-rays. X-ray tube rotates around the subject and transmits X-ray beams through the subject's body (Goldman et al 2007³⁵⁷) as illustrated in Figure 2.1.4.1.

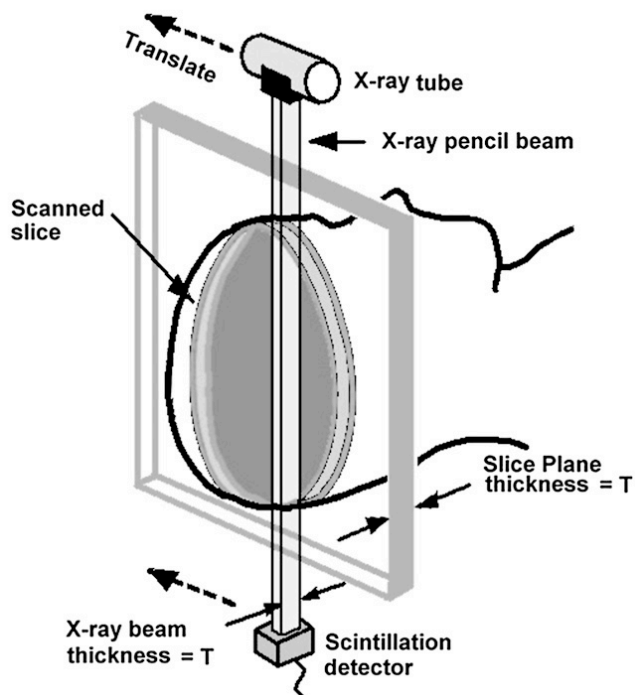


Figure 2.1.4.1 Goldman et al 2007³⁵⁷: Illustration of a CT arrangement. Axial slice through patient is swept out by narrow (pencil-width) x-ray beam as linked x-ray tube–detector apparatus scans across patient in linear translation. Translations are repeated at many angles. Thickness of narrow beam is equivalent to slice thickness.

The detectors measure the transmission of a thin beam (1-10mm) of X-rays through a full scan of the body, unlike an X-ray radiography where an image is produced directly following the transmission of X-rays. The light signals then are computer-processed by the photodiode and stored in the form a CT image. Since there are distinct atomic masses within the subject, the x-rays will have differential attenuation through the subject. The image of the section of the object irradiated by the X-ray, is reconstructed from a large number of measurements of attenuation coefficient of various tissues obtained (Ghonge et al 2013³⁵⁶, Saha et al 2010³⁵⁵). The average attenuation values of various tissues are called ‘Hounsfield units’ named

after CT pioneer Sir Godfrey Hounsfield.

Table 2.1.4.2: Range of CT attenuation values for various tissues

Tissue	Range of CT numbers (Hounsfield units)
Bone	500-1500
Muscle	40-60
Brain	35-45
Water	0
Adipose tissue	-60 to -150
Lung	-300 to -800
Air	-1000

2.1.5 Integration of PET with CT

Even though the PET method was developed in the 50's, and the first commercial tomographs were available in the 80's, the real breakthrough of technology occurred in late 90's with integration of PET with Computed tomography (CT) (Beyer et al 2000³⁵⁸, Wagner et al 1998³⁵⁹). This gave an ideal platform of integrating functional with anatomical imaging, resulting in wide clinical use of PET-CTs since 2001 (Beyer et al 2000³⁵⁸).

The scanning table goes through the front CT scanner and back PET scanner in a common support and gantry. To ensure the images of PET and CT scans can be fused together, the subject is kept in the same position throughout the scan, as

demonstrated in Figure 2.1.5.

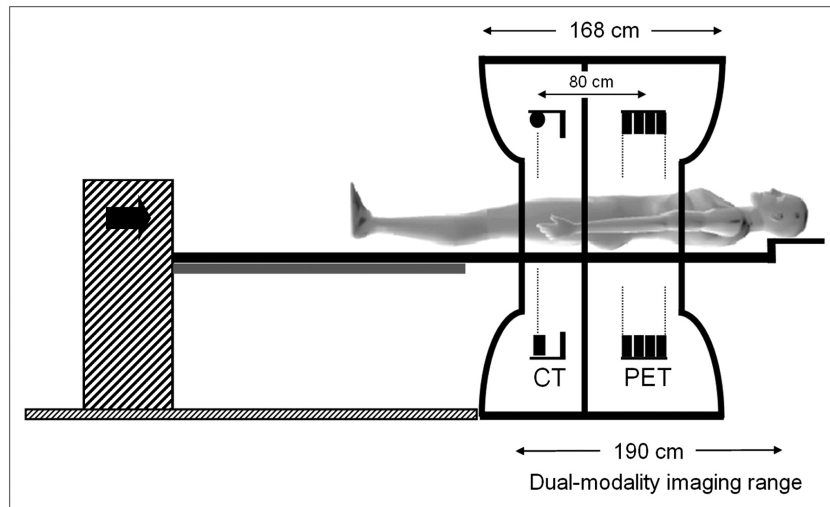


Figure 2.1.5: Schematic representation of dual PET-CT scanner with respective positions in a common gantry.

Combining CT with PET not only provides anatomical information, it also provides attenuation correction for the reconstructed PET images, adding value to PET interpretation. The attenuation correction factor bases on the photon energy of CT X-ray and PET photon. The CT 70keV X-rays are scaled to match the PET 511keV photons by applying a scaling factor which is mass attenuation coefficient ratio in a given tissue of 511keV photons to that of 70keV X-rays (Saha et al 2010³⁵⁵). This reduces CT scan time to few seconds and thereby reducing the overall PET-CT imaging time. This increases the diagnostic accuracy to 84% sensitivity and 88% specificity for any cancer evaluation (Saha et al 2010³⁵⁵). In summary, PET-CT is a standard imaging modality in cancer evaluation and is the preferred method to detect metastases.

2.1.6 PET-CT imaging protocol

Scanning was performed on a combined GE Discovery STE PET/CT scanner (General Electric Medical Systems, Milwaukee, USA) at UHCW PET centre. Patients were fasted for at least 6 hours prior to scanning in accordance with standard administration and acquisition protocol. After administration of the ^{18}F -FDG isotope, patients rested for 60 minutes in the waiting room within the PET/CT suite, where ambient temperature was maintained at 24°C. Prior to administration of the ^{18}F -FDG dye, capillary blood glucose was checked, and 2 to 5 IU of insulin administered subcutaneously in cases of hyperglycaemia. ^{18}F -FDG was administered intravenously one hour prior to the scan (mean injected dose 362.1 MBq, standard deviation 33.2 MBq; range 103 – 505 MBq). Static emission data were obtained from the skull base to mid thigh with the arms elevated whenever possible. In cases of head and neck cancer a second set of emission data were obtained of the head and neck with the arms by the patients' side. Emission data were obtained for 3 minutes in each bed position (each covering between 10 and 20 cm) with 2-dimensional acquisition. PET images were reconstructed using the computerised tomography (CT) data for attenuation correction. Unenhanced spiral CT scans were acquired from the skull base to the mid-thighs using 3.3 mm slice thickness. All oncology patients with the exception of those being scanned for the purposes of head and neck cancer were given water-soluble iodinated contrast media (Gastrografin®, Bayer plc, Newbury, UK) for bowel opacification. Images were reconstructed using the filtered back-protection algorithm.

2.1.7 Patient Records Data collection

3295 consecutive ^{18}F -FDG-PET/CT whole-body scans were performed on 2685 patients (1497 males, 1188 females) for various diagnostic reasons between June 2007 and August 2012, at UHCW NHS Trust PET centre. Data on age, sex, BMI, fasting glucose level, scan date and scan timing were obtained for all patients. BMI was categorised based on WHO (as illustrated in Chapter 1.1.4) and National Institute of Health criteria into 4 groups (Underweight ≤ 18.5 ; Normal=18.6-24.9; Overweight=25-29.9; Obese ≥ 30 , The Evidence Report, National Institutes of Health 1998³⁶⁰). Glycaemic group was categorised based on American Diabetes Association's criteria (Normoglycaemia < 5.5 mmol/L; Impaired Fasting Glycaemia ≥ 5.5 -6.9 mmol/L; Diabetes Mellitus ≥ 7.0 mmol/L).

Lean body weight (LBW) was calculated using the following validated formulas (Ouellet et al 2011¹⁶⁶):

$$\text{LBW (Males)} = [1.10 \times \text{Weight (kgs)}] - [128 \times (\text{Weight [kgs]} / \text{Height [cm]})^2]$$

$$\text{LBW (Females)} = [1.07 \times \text{weight (kilograms)}] - [148 \times (\text{weight [kilograms]} / \text{height [centimeters]})^2].$$

Basal Metabolic Rate was calculated using revised Harris Benedict equation (Roza et al 1984³⁶¹):

$BMR \text{ (Males)} = 88.362 + (13.397 \times \text{Weight in kg}) + (4.799 \times \text{Height in cm}) - (5.677 \times \text{Age in years})$

$BMR \text{ (Females)} = 447.593 + (9.247 \times \text{weight in kg}) + (3.098 \times \text{height in cm}) - (4.330 \times \text{age in years})$

Outdoor temperature in Coventry for the day of the scan was obtained from United Kingdom Meteorological Society. PET/CT reports and medical records were reviewed for cancer diagnosis. If the diagnosis was not available, it was classified as non-cancerous diagnosis.

For the 151 patients who were detected to have putative BAT, electronic and medical records were reviewed for other relevant past medical history, drug history, smoking status, fasting lipid profile, and biochemical thyroid profile.

Post-thyroidectomy patients in thyroid cancer are iatrogenically rendered mildly thyrotoxic by thyroxine replacement therapy (Levothyroxine and Liothyronine) to suppress TSH, in order to prevent reactivation of thyroid malignancy.

Out of 229 patients who were treated for thyroid cancer in UHCW during the same period, 34 patients underwent PET scans, whose notes and electronic records were reviewed irrespective of their BAT status. This small group was further classified into Thyrotoxic and Euthyroid subgroups, depending upon patients' biochemical thyroid status (Thyrotoxic: $TSH < 0.35 \text{ mU/L}$, Euthyroid: $0.035 - 6.0 \text{ mU/L}$) at the time of PET scan. The thyroid profiles were collected only if they were within 6

weeks range from the date of PET scan. The summary of this methodology is discussed further in Chapter 3.2.1.

2.1.8 Image analyses

All PET/CT scans were initially reported by a Consultant Radiologist with expertise in nuclear imaging as part of the patients' routine clinical care using a Centricity PACS workstation (GE Healthcare, USA), and ^{18}F -FDG BAT recorded in the report if present. For the purposes of this study each PET/CT scan was re-evaluated by second radiologist using a GE ADW Advantage Workstation 4.3 (GE Healthcare, USA) to confirm the presence of ^{18}F -FDG BAT. ^{18}F -FDG BAT was considered present when there was avid ^{18}F -FDG uptake at a greater-than background level (i.e. Standardised Uptake Value [SUV] > 2.5 g/ml) in areas corresponding to the attenuation of adipose tissue on CT (i.e. an attenuation of between -100 and -10 Hounsfield units).

2.1.9 Significance of Standardised Uptake Value (SUV)

SUV, which is corrected for body weight and injected ^{18}F -FDG doses, is a semi-quantitative measurement for ^{18}F -FDG uptake (Lucignani et al 2004³⁶²).

SUV is commonly defined as the ratio of (1) tissue radioactivity concentration 'c' (MegaBequerel [MBq]/kg) at time point 't', and (2) the injected activity (MBq, extrapolated to the same time 't') divided by body weight (kg). SUV (g/ml) =

[Average activity in region of interest (ROI) (MBq/ml)/injected dose (MBq)] X body weight (kg).

In simple terms, SUV is a way of determining PET activity. It is used to measure response of cancers to treatment and is considered a semi-quantitative value because it is vulnerable to various factors such as, image noise, low image resolution and variable user-biased ROI selection. The SUV cut-off between benign and malignant lesion is 2.0 or 2.5 g/ml, and can also be raised in inflammatory processes (Thie et al 2004³⁶³). In absence of malignancy, if a ROI measured SUV of >2.5 g/ml in the usual BAT areas of neck, mediastinum, axilla, suprarenal areas, then this was considered BAT as detailed in Chapter 1.6.1 in keeping with other BAT PET studies (Saito et al 2009¹⁴³, Cypess et al 2009¹⁴¹).

Total Lesion Glycolysis (TLG) is another recent FDG-PET parameter, which represents a combined metabolic and morphologic tumour burden parameter, and hence is a reflection of BAT activity for this study purposes (Larson 1999³⁶⁴). It is calculated by multiplying SUV_{mean} by tumour volume.

2.1.10 BAT activity, BAT volume and BAT mass quantification

Out of the 2685 patients who underwent 3295 scans, 151 patients were identified to have positive ¹⁸F-FDG BAT uptake on 175 scans, and hence were categorized as BAT responders, and the remaining 2533 patients as BAT non-responders. 2685 scans with highest SUV_{max} were included in the analysis to avoid confounding of factors such as BMI, age and sex in analyses of BAT prevalence, activity and mass.

BAT activity was measured utilizing SUV_{max} , which denotes the highest concentration of the ^{18}F -FDG dye greater than 2.5 g/ml in ROI at the given time 't', a reflection of maximal putative BAT activity if ROI coincides with BAT recognized areas, in absence of malignancy diagnosis (Ouellet et al 2011¹⁶⁶).

BAT volume was measured using commercially available image fusion software (Mirada XD 4.3, Mirada Ltd, Oxford, UK). It semi-automatically defined isocontours around putative ^{18}F -FDG BAT depots on axial PET/CT scans (Figure 2.1.10 a and Figure 2.1.10.b) with a threshold set at an SUV of 2.5 g/ml, using a similar technique to that described by Huang *et al*³⁶⁵ and van Marken Lichtenbelt *et al*³⁶⁶. We found that this threshold provided the best compromise between capturing the extent of ^{18}F -FDG uptake within BAT, whilst minimising artefactual 'bleeding' of signal into adjacent tissues. From this the volume and SUV_{max} were calculated for each depot. For BAT mass calculation, an assumption of fat having a density of 0.92 g/ml was made as per validated methods used in literature (Ross et al 1991³⁶⁷).



Figure 2.1.10.a: Semi-automatic selection of ^{18}F -FDG regions of interest by defining an isocontour set at SUV of 2.5 g/ml

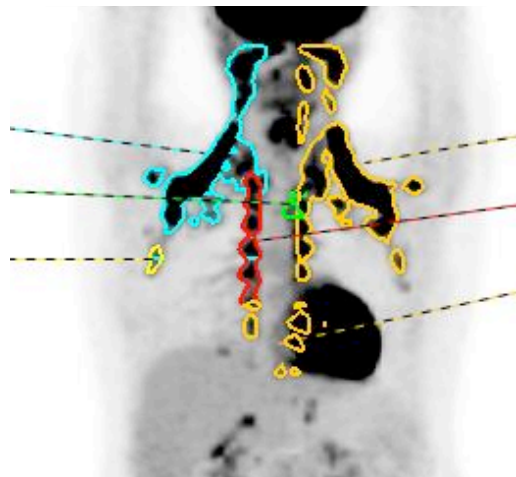


Figure 2.1.10.b: Coronal PET Maximum intensity projection (MIP) image, showing isocontours around BAT from which volumes were derived. The colours depicted in the figure are automated and are generated by computer software for distinction purposes and bears no clinical relevance.

2.1.11 Statistical analyses

The recorded data were entered into Microsoft excel spreadsheet. The data were analysed using SPSS IBM software Version 22 (SPSS Chicago, IL). Normally distributed continuous variables were compared between study groups with the use

of Student's t-test, and non-normally distributed variables were compared with Mann-Whitney U test. The roles of sex, age, BMI, fasting glucose, outdoor temperature as predictors of BAT prevalence were tested by logistic regression with the use of univariate and multivariate models. The patients were also divided into four BMI groups (Underweight, Normal, Overweight and Obese), and also Fasting Glucose level (Normoglycaemia, Impaired Fasting Glycaemia, and Diabetes); Kruskal Wallis was used to compare between the categories for BAT mass and BAT activity. Missing values were dealt with pairwise deletion using SPSS software. Odds ratio and Confidence Intervals were estimated as measures of magnitude of associations. All P values presented are two-tailed, and values less than 0.05 are considered to be statistically significant.

2.1 Materials and Methods for Magnetic Resonance Imaging of Brown Adipose Tissue (BAT) Study

2.2.1 Introduction

¹⁸F-FDG PET scan detects only metabolically active BAT and therefore grossly underestimates BAT's prevalence and extent. Besides, it is not reliably reproducible and involves radiation exposure. This study was aimed at providing a proof of concept for a novel MRI imaging technique- Iterative Decomposition with Echo Asymmetry and Least Squares Estimation (IDEAL) to visualize BAT in humans. The concept of IDEAL MRI, which was shown to work in rat models to demonstrate BAT by Houchun Hu et al²⁰⁶ was reproduced in our centre, on a rat carcass. The same methodology was adopted in an adult human volunteer, who had already

undergone PET-CT for clinical indication. PET-CT images were co-registered with IDEAL MRI images using image fusion software, and the combined images were analysed by two radiologists. BAT presence in the region of interest was confirmed by histological and immunohistochemical staining. Black County Research Ethics Committee (Rec No. 11/H1206/3) provided ethics for this study.

2.2.2 Basic principles of Magnetic Resonance Imaging

Magnetic Resonance Imaging (MRI) or Nuclear Magnetic Resonance (NMR) is a non-ionising radiation method, which utilises strong magnetic fields and radiowaves to create diagnostic images. Two physicists Felix Bloch and Edward Mills Purcell simultaneously discovered MRI, for which they received Nobel Prize for Physics in 1952. Herman Carr in 1952 first produced a 2-dimensional image in his Harvard thesis (Carr 1952³⁶⁸). Sir Peter Mansfield, Professor in University of Nottingham, United Kingdom developed a mathematical technique for speedy imaging acquisition and was awarded Nobel Prize in 2003 along with Paul Lauterber.

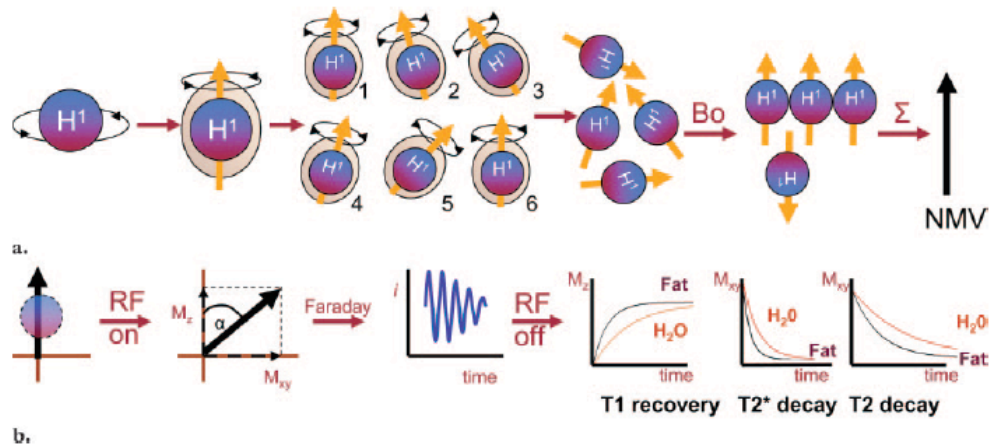


Figure 2.2.2 Bitar et al 2006³⁶⁹: Basic physics of the MR signal. (a) As ^1H nuclei spin, they induce their own magnetic field (tan), the direction (magnetic axis) of which is depicted by an arrow (yellow). The ^1H nuclei initially precess with a wobble at various angles (1–6), but when they are exposed to an external magnetic field (B_0), they align with it. The sum of all magnetic moments is called the net magnetization vector (NMV). (b) When an RF pulse is applied, the net magnetization vector is flipped at an angle ‘ α ’, which produces two magnetization components: longitudinal magnetization (M_z) and transverse magnetization (M_{xy}). As the transverse magnetization precesses around a receiver coil, it induces a current (i). When the RF generator is turned off, T1 recovery and T2 and T2* decay occur.

MRI is based on electromagnetic activity of atomic nuclei. Atomic nucleus has protons and neutrons, which have spins (wobbles). Odd numbered protons (Hydrogen, Fluorine, Phosphorous etc.) are preferred in MRI, as they do not cancel out with their neutron counterparts (Bouni et al 1992³⁷⁰). Hydrogen nuclei are most commonly used because of their abundance in the body (water). Protons are positively charged and their spin creates a magnetic field. When an external magnetic field is applied in a particular direction (B_0), horizontally by an electric current in the case of MRI scanner, protons start to spin along, or wobble along the

lines of magnetic field, a phenomenon called ‘precess’. The frequency in which they precess is obtained from Larmor equation (Sands et al 2004³⁷¹).

$$\begin{array}{ccc} \text{Precession frequency } (\omega_0) & = & \text{External magnetic field } (B_0) \times \text{Constant } (\gamma) \\ \text{(MHz)} & & \text{(Tesla)} \qquad \qquad \qquad (42.5) \end{array}$$

The precession frequency of Hydrogen proton is 42.5 MHz in a magnetic field strength of 1 Tesla (42 million times per second). As illustrated in Figure 2.2.2, following the external magnetic field B_0 , all protons arrange themselves parallel or antiparallel to B_0 , and following cancellations of both parallel and antiparallel proton charges, the net effective direction is called Net Magnetic Vector (NMV), which is usually in the direction of B_0 , which is called ‘Longitudinal Magnetization’ (Sands et al 2004³⁷¹).

When a radiofrequency (RF) wave is applied transversely in this field imparting ‘in phase’, NMV flips to a certain angle towards the direction of RF impulse causing ‘Transverse Magnetization’. The protons continue to spin albeit facing the coil in the MRI from which RF is transmitted, and this moving magnetic field results in creation of current/electric impulse, which is the Magnetic Resonance (MR) signal (Bouni et al 1992³⁷⁰).

When RF signal is switched off, NMV gradually reverts back to Longitudinal magnetization direction of B_0 . The time taken by NMV for 63% of Longitudinal relaxation to occur is called T1, or ‘Longitudinal Relaxation Time’ or ‘Spin-Lattice Relaxation Time’. Spin-lattice relaxation occurs as a result of exchange of thermal

energy to surrounding lattice from protons, which received energy originally from the RF waves. T1 depends on i) Water quantity ii) structure iii) surroundings of the tissue (Bitar et al 2006³⁶⁹).

A simultaneous phenomenon when the RF signal is switched off is the Transversal relaxation when the NMV reverts to its original longitudinal direction from transverse position, and the time taken for 37% of this transversal relaxation process to happen is called T2, also called 'Spin-Spin relaxation'. T2 depends on i) External magnetic fields and ii) Local magnetic fields. (Sands et al 2004³⁷¹).

Various tissues exhibit different T1 and T2 times, coupled along with proton density of Hydrogen nuclei in the tissue forms the basis for different contrast obtained in MR images. T1 (300-2000 milliseconds) is 2 to 10 times as long as T2 (30-150 milliseconds). Water has a long T1 and T2, and fat has short T1 and T2 times.

Repetition Time (TR) and Echo Time (TE) are the two key parameters in creation of a contrast image. TR is the time to repeat RF pulse sequence, and TE is the time from RF pulse to the time to detect a peak echo. The factors that influence signal intensity are T1, T2, proton density, flow, pulse sequence, TR, TE, flip angle and use of contrast media. Larger flip angles produce more T1-weighting, and longer TEs produce more T2*-weighting, which are special type of Gradient Echo sequences (Bitar et al 2006³⁶⁹). The imaging time is obtained from the equation:

Acquisition time (a.t) = Repetition time (TR) x No of rows in an image (N) x No of excitations ($N_{\text{excitations}}$).

2.2.3 Iterative Decomposition with Echo Asymmetry and Least Squares Estimation (IDEAL) MRI

WAT is a lipid reservoir, and is made of cells with single large intracellular lipid droplet, whereas BAT is highly vascularised iron containing tissue possessing smaller intracellular lipid droplets and more water content. This difference in water-fat content is exploited in a special form of MR imaging called IDEAL MRI. It is a type of chemical shift MRI (modified Dixon technique), which delivers computationally robust, consistent and accurate fat/water separation. This clear advantage of uniform fat suppression is clinically used in diagnosing and characterizing adrenal adenomas, hepatic steatosis, renal angioliipomas, soft tissue lipomas and ovarian teratomas.

2.2.4 Proof of concept of IDEAL MRI study on Rat fat samples

BAT and WAT from samples taken from sacrificed rats can be clearly delineated from one another, and provide distinct signals when imaged with existing technology. This has already been demonstrated by Hu *et al.* using 6-echo IDEAL MRI (Hu et al 2011²⁰⁶).

For this purpose, following a normal feeding regimen 2 male Wistar rats (mean mass 300g, age 6-8 weeks) were used. One was kept at thermoneutrality (30°C) for 8 hours; the other was kept in the cold (4°C) for 8 hours. Both rats were sacrificed, and fat samples were dissected to extract Interscapular BAT, Subcutaneous WAT and Omental WAT. The samples were collected into 2 sets of 3 x 2 ml eppendorfs (cold and thermoneutral), and were photographed to demonstrate the macroscopic

difference between BAT and WAT. The specimens from rat kept in the cold, was transported to the MRI scanner on ice, while those from the rat kept at thermoneutrality, was transported at ambient temperature.

All MR imaging was carried on 3T GE HDxt scanner (GE, Milwaukee, USA). *Ex vivo* MR scanning of the cold and thermoneutral rat carcasses, and dissected phantom samples (“*rat test tubes*”) was performed on Optima MR360 3T MR scanner using the IDEAL settings. The images had a 2.0mm slice width and 150mm square field of view and 256x256 matrix.

2.2.5 Subject recruitment and Positron-emission tomography scanning

Following written informed consent, a 25-year old female who underwent parathyroidectomy surgery for primary hyperparathyroidism, was recruited for MRI study. She underwent PET scan first for clinical indication to rule out malignancy. PET-CT image acquisition was conducted as per the protocol outlined in Chapter 2.1.6. PET images were reconstructed using the computed tomography (CT) data for attenuation correction. PET image analyses, including BAT volume and BAT SUV_{max} estimation was done as outlined in Chapter 2.1.8. This part of methodology is further discussed in Chapter 4.2. The study was reviewed and approved by the Black County Research Ethics Committee (Rec No. 11/H1206/3).

2.2.6 Magnetic resonance scanning of the study subject

A 3-echo IDEAL sequence (Reeder et al 2005, Reeder et al 2004)^{372,373} was

performed on a 3T GE HDxt scanner (General Electric Medical Systems, Milwaukee, USA). The cardiac coil was placed around the cervical and upper thoracic regions. Axial images with a 5mm slice thickness were obtained from the upper cervical to mid-thoracic level. The T1 weighted IDEAL sequence parameters were: TR 440 ms, TE 10.8 ms, acquisition matrix size 320 x 256, NEX 3 and field of view of 30 cm. This generated water-only and fat-only (fat:IDEAL) images, of which the latter were used for subsequent analysis.

A baseline MR scan was performed the same month as the PET-CT (December), upon which subsequent image analysis was performed. A second MR was performed 2 months later using identical imaging parameters (apart from the field of view which was 34 cm), to determine whether there was any temporal variation in the distribution of BAT.

PET-MR image co-registration, prospective and retrospective image analyses are further outlined in Chapter 4.2.

2.2.7 Histology and Immunohistochemistry

Histology and immunohistochemistry were performed on tissue obtained during parathyroidectomy, corresponding with high ^{18}F -FDG uptake on the PET-CT scan and low-signal intensity on the fat-only MRI. Samples were prepared for morphology by keeping in formalin until moulded in paraffin and stained with haematoxylin-eosin (HE). For immunohistochemistry, Vectastain Elite ABC Kit (Vector Laboratories, PK-6101) and rabbit anti-UCP1 (1:500, Sigma U6382) were

used according to the manufacturer's protocol. UHCW Histopathology department undertook the above examination and staining of the tissue as per hospital protocols.

2.3 Meal Duration Study

2.3.1 Introduction

A clinical trial was conducted with obese female subjects. Only White Caucasian women were included in the study to reduce variability with gender and ethnicity. Each subject attended for two visits within a two-week period, and spent 8 hours in room calorimeters (9am to 5pm) for the assessment of energy expenditure and repeated blood sampling. Balanced standard meal was provided, and the subjects were instructed to eat the entire meal in 40 minutes in the first visit and in 10 minutes in the subsequent visit. Regular blood sampling was conducted at fixed times over the 4-hour postprandial period. Complete data from each visit was available for the 10 subjects. The study was reviewed and approved by the Black County Research Ethics Committee (Rec No. 11/H1206/3).

2.3.2 Inclusion and Exclusion Criteria

Inclusion Criteria

White Caucasian women

Age 18-50 years

BMI 30-50 kg/m²

Premenopausal

Exclusion Criteria

Age <18 or >50 years

Diabetes or dysglycaemia (HbA1c >6.0% or fasting glucose >6mmol/L)

Any medical/endocrine problem that could affect energy expenditure (*e.g.* thyroid problems, Cushing's syndrome, PCOS, Obstructive Sleep apnoea etc)

Prior bariatric surgery

Chronic inflammatory disorders *e.g.* rheumatoid arthritis, or long term use of steroids or other immunomodulators like cyclosporine, azathioprine.

Cholesterol lowering medication, anti-diabetes medications (oral or injectable),

Beta-blockers

Recent significant change in weight (>2.5 kg in 3 months)

Vegans or vegetarians

Depression or any psychiatric illness

Claustrophobia or needle phobia

Participants were recruited from Obesity Clinic in University Hospitals Coventry and Warwickshire (UHCW) National Health Service (NHS) Trust. Only women

subjects were recruited to study a focused group with the intent of reducing variability. Also, at the time of recruitment, approximately 78% of overall patients attending UHCW obesity clinics were women. Obese subjects were chosen for study participation, as the effects of meal duration intervention was intended to be studied first in the obese population, prior to exploration in lean and male subjects. As per the power calculations, 10 subjects had >80% power to detect a between-meal duration difference exceeding 50% of a Standard Deviation (SD) for plasma glucose from D10 and D40 ($\alpha=0.05$). A total of 53 consecutive women in the age range of 18-50 years, and BMI range of 30-50 kg/m² were approached during their outpatient visits. 21 women declined to participate, and 22 had one or more exclusion criteria, and therefore excluded. A total of 10 were recruited following written consent.

2.3.3 Meal Duration Study Protocol

The 10 study subjects were advised not to undertake vigorous exercise, or alter their lifestyle between visits. They were given lifestyle and dietary advice at the end of the study. Fasting glucose and HbA1c was measured in all subjects to rule out diabetes or dysglycaemia. Subjects with HbA1c <6.0% and fasting glucose <6mmol/L were considered not to have diabetes or dysglycaemia in accordance with the WHO criteria for diagnosis of diabetes (WHO guidance on use of HbA1c to diagnose diabetes mellitus 2011³⁷⁴).

Study Visit 1

Recruitment/Consent

Following scrutiny of the inclusion/exclusion criteria, informed consent was obtained from eligible subjects. Baseline demographic information was collected as well as anthropometry including: weight, height, BMI, waist circumference, neck circumference (for obstructive sleep apnoea), hip circumference, blood pressure and BODPOD measurement. Fasting blood was taken for glucose, HbA1c, complete lipid profile, renal function, liver function, thyroid function, insulin growth factor-1 (IGF-1) and bone profile as well as Vitamin D status. The subjects were shown around Human Metabolism Research Unit (HMRU) at UHCW.

Study Visit 2

Subjects attended HMRU at 8am after a light evening meal and overnight fast from 10 pm the previous night. Following body composition measurement in the BODPOD, an intravenous cannula was inserted and fasting blood test obtained. Subjects were allowed to enter the calorimeter room at 8.45am. Measurements of energy expenditure began at 9am. On entry into the WBC and for the first 120 minutes of the metabolic study, each subject was requested to lie still on the bed to allow for equilibration and to provide an estimate of baseline resting energy expenditure (REE). At 12 pm, the standard meal (ham sandwich, yoghurt, banana, crisps, and orange juice drink) was given. The caloric content was divided equally into eight separate food boxes, the food contents of each box eaten over 5 minutes for a total meal duration of 40 minutes (the lunch being completed by 12:40 pm). This is referred to as 'D40'. Subjects were provided with timers and were monitored

to ensure compliance with eating rate. Subjects were instructed to vary chewing speed accordingly. Blood was drawn from indwelling cannula at baseline, 30, 60-, 90-, 120-, 180- and 240-minute intervals- a total of 7 times. During pre- and postprandial periods, subjects watched TV or read quietly with minimal ambulation. At 5 pm, after total duration of 8 hours in the room calorimeters, subjects were invited to leave and offered an *ad libitum* standard buffet meal, consisting of various cold foods (sandwiches, chocolate bars, fruit, sausage rolls and drinks). The caloric content and macronutrient composition of the *ad libitum* food ingested was calculated. They also completed a visual analogue scale (hunger, satiety and fullness) at 10 set time points throughout the study including post-buffet meal.

Study Visit 3

For the second metabolic assessment, as in the previous visit, subjects attended the HMRU at 8am after a light evening meal and overnight fast from 10pm. An identical protocol was followed except that the duration of the standard lunch was 10 minutes rather than 40 minutes. For this assessment, the caloric content of the standard meal was divided into two halves, with the food contents of each box being eaten over 5 minutes for a total meal duration of 10 minutes (the lunch being completed by 12:10 pm). This is referred to as 'D10'. Again with an indwelling intravenous cannula, blood samples were taken at 7 time points in the 4-hr postprandial period similar to the Visit 2. The subjects also completed the visual analogue scale similar to Visit 2.

2.3.4 Anthropometric Assessment

Anthropometric assessments were undertaken in all subjects at the start of the study, with measurements of height on a wall mounted stadiometer, weight, waist circumference, hip circumference including calculation of body mass index (BMI in kg/m^2) and waist hip ratio.

2.3.5 Assessment of Body Composition Using the BODPOD

At visit 2, accurate assessment of body composition was undertaken using the BODPOD (Air displacement plethysmography, Cosmed Inc, USA)³⁷⁵ (Fields et al 2002). A finely calibrated weighing scale initially calculated the total mass, and the body volume was calculated using air volume displacement to calculate density. For these calculations, estimated lung volumes were used. All subjects wore swimming costumes or tight fitting lycra with a swimming cap, as advised by the manufacturer, as volume is affected by clothing and hair. Fat mass and fat free mass (lean mass) was calculated using the Siri equation, with a reported margin of error of only 1% (Siri et al 1961³⁷⁶). The Siri equation is as follows,

$$\text{Body fat percentage} = (4.95/\text{density} - 4.50) \times 100 \quad (\text{density measured in gm/cm}^3)$$

2.3.6 Assessment of Energy Expenditure using Whole Body Calorimeter

HMRU, a UHCW NHS Trust facility, houses two Whole-Body Calorimeter (WBC) rooms, built in partnership with Warwick Medical School, University of Warwick. The twin rooms are approximately 2m X 3m X 2.5m in dimensions, each equipped

with a bed, desk, chair, television, computer with internet connection, telephone, sink and toilet. Each WBC room replicates free-living environment, and is hermetically-sealed to the outside environment. Double-doored hatches enable food to be delivered in and waste out. The rooms are linked to both the hospital fire alarm and emergency life support crash call system, for safety purposes. Experiments were held under constant supervision, and all subjects were given a health and safety briefing prior to entering the room.

Throughout the experiment, the temperature in WBC room was regulated at 24°C, maintained within 0.5°C, and humidity was maintained at 57 ± 5%. The room was at a slight under pressure, 250 Pa below ambient. There was a constant flow of air going into the room at 117 L/min to ensure the air was thoroughly mixed to give more accurate readings of air that came out of the room. Physical activity was measured utilising analog ultrasound doppler system (Advisor DU160, Aritech BV, Roermond, Netherlands). Thermoneutral temperature (24°C) and relative humidity (57%) were kept constant.

Automated calibration was performed in the WBC rooms, during the studies, every 5 minutes in 3 ways. Initially nitrogen was passed into the analyser to give a 0 reading of O₂ and CO₂, subsequently scientific air was passed into the analyser to give a known concentration of 18% O₂ and 0.8% CO₂, and finally fresh air was passed into the analyser to give known concentrations of 21% O₂ and 0.3% CO₂ (Schofflen et al 1997³⁷⁷). Using methanol combustion, whole room calibration was undertaken once a month. Pure methanol was burnt in each room for 24 hours, and the weight of methanol burnt was calibrated to the amount of O₂ consumed and CO₂ produced.

Methanol when burnt uses O₂ and gives out CO₂ whilst also producing small amount of moisture, replicating human respiration levels.

Air coming out of WBC was analysed by the system consisting of model A0 2020 dual pairs of infrared CO₂ (ABB/Hartmann and Braun Uras, Frankfurt A.M., Germany) and paramagnetic O₂ analysers (Servomex 4100, Crowborough, England and ABB/Hartmann and Braun Uras, Frankfurt A.M., Germany). Flow was measured utilising electronically modified dry gasmeters (G6, gasmeterfabriek Schlumberger, Dordrecht, Netherlands). Data acquisition was performed using custom built interfaces (IDEE, University of Maastricht, Netherlands), a computer (Apple Macintosh, Cupertino, United States) and graphical programming environment (Labview, National Instruments, Austin, United States). The vital gas levels of O₂ and CO₂ were sampled every minute and analysed, and an average reading was calculated for every 30 minutes to reduce variability in data inherent to such a large volume of air in the room compared to the small differences in respired air. Accurate minute-by-minute measurements of CO₂ and O₂ from air entering at inlet and air leaving the WBCs at outlet was undertaken. These gas measurements were used to calculate energy expenditure (including DIT) by using Weir's equation (Weir et al 1949³⁷⁸).

The Weir Formula used to calculate Energy Expenditure (EE) is:

$$EE \text{ (Kcal)} = [3.941 \times \text{O}_2 \text{ consumed (L)}] + [1.106 \times \text{CO}_2 \text{ produced (L)}].$$

2.3.7 Calculation of Energy Expenditure including Diet Induced Thermogenesis (DIT)

Pre- and postprandial energy expenditure (Kcal) was calculated using O₂ and CO₂ gases using Weir's equation. Resting Metabolic rate (RMR) was calculated using the lowest 30 minutes during the first 120 minutes of the study when the subjects were lying still on the bed. DIT (difference between postprandial and baseline EE) was calculated using validated methods reported in literature, and also expressed in percentage of energy intake ($[\text{Postprandial EE} - \text{Baseline EE}] / \text{Amount of calorie ingested}$) (Marno et al 2002²²⁰, Ravn et al 2013³⁷⁹). Although the units for EE represents power (Kcal/24 hours) instead of energy (Kcal), EE is used throughout the script without mentioning 'over the 24 hours', in order to be consistent with the literature.

2.3.8 Assessment of Hunger, Fullness, Appetite and Satiety

Visual analogue scales for hunger, fullness and satiety were completed by subjects at 10 time points at both visits: -180 min, -60 min, -10 min, 0 min, 30 min, 60 min, 120 min, 180 min, 240 min, and post buffet, with '0' being the meal reference point. Mean and standard deviation of the scores at the above set time points pre- and postprandial were analysed.

2.3.9 Buffet meal

At 1700h, subjects were invited to leave the WBC and offered an *ad libitum* standard buffet meal, consisting of various cold foods (sandwiches, chocolate bars, fruit, sausage rolls and drinks). The caloric content and macronutrient composition of the *ad libitum* food ingested was calculated.

2.7.10 Statistical analyses and power calculation

Statistical analyses were conducted in SPSS (version 21 Windows; SPSS Inc., Chicago, IL) and Microsoft Excel. Paired sample t-tests were used for comparisons of 4-hour postprandial ‘Area Under the Curve’ (AUC) metabolic and biochemical data between D40 and D10. Each subject acted as their own control thereby limiting confounding. We had >80% power to detect a between-meal duration difference exceeding 50% of a Standard Deviation (SD) for plasma glucose from D10 and D40 ($\alpha=0.05$). A P-value <0.05 was considered significant. AUC was calculated using the validated Trapezoid method in Excel (Pruessner et al 2003³⁸⁰). Variables are expressed as mean \pm standard error of mean (SEM) unless otherwise specified.

2.7.11 Collection of Human Blood samples

For serum sample preparations, whole blood was drawn into a BD-vacutainer® (BD, UK) serum tube containing silica clot activator. Blood was allowed to clot at room temperature for 30 minutes. Once clotted, the samples were centrifuged at 20°C and

2000rpm for 10 minutes. Supernatant was carefully drawn off; flash frozen and then stored in labelled 1.5 mL eppendorfs at -80°C.

For plasma sample preparations, whole blood was similarly drawn into a BD-vacutainer® (BD, UK) plasma tube containing EDTA. Samples were immediately centrifuged at 20°C and 2000rpm for 10 minutes. Supernatant was carefully drawn off; flash frozen and then stored in labelled 1.5 mL eppendorfs at -80°C. 4-(2-aminoethyl)-benzenesulfonylfluoride hydrochloride (Pefabloc SC) and dipeptidyl peptidase-IV inhibitor were added to chilled EDTA tubes for measurements of pancreatic and gut hormones.

2.7.12 Biochemical evaluation

Fasting baseline serum samples taken at the first metabolic study for each subject were analysed for lipid profile (Total Cholesterol, LDL Cholesterol, HDL Cholesterol and Triglycerides), HbA1C, glucose, 9 am cortisol, IGF1, TSH, free T4, Testosterone, Sex Hormone Binding Globulin (SHBG) and 25-hydroxycholecalciferol. Postprandial and pre-lunch blood samples (D40 and D10) were analysed for Insulin, Glucose, Total Cholesterol, LDL Cholesterol, HDL Cholesterol, Triglycerides, Endotoxin and NEFA. The analyses for these two panel of analytes were undertaken by the biochemistry department of UHCW NHS Trust laboratories. The individual assay techniques and kits used are mentioned further in Chapter 5.

2.7.13 Multiplex assay

Postprandial and pre-lunch blood samples (D40 and D10) were also analysed for Ghrelin, Leptin, PYY, PP, GLP-1, Adiponectin, Cortisol were undertaken by researchers in CIBER Fisiopatología Obesidad y Nutrición (CB06/03), Instituto de Salud Carlos III (ISCIII), Santiago de Compostela, Spain (F·F·C, M·C·C). The gut hormone panel was analysed using Luminex Multiplex Assay technique.

Using a 96-well format, a multiplex assay is a type of assay that simultaneously is capable of providing quantitative measurements of multiple analytes in a single run/cycle of the assay. Luminex-XMAP is bead based multiplexing, where beads are internally dyed using fluorescent dyes to produce a specific spectral address. Biomolecules (such as an oligo or antibody) can be conjugated to the surface of beads in order to capture analytes of interest. This technology uses flow cytometric or imaging technologies for characterization of the beads as well as detection of phycoerythrin emission due to analyte presence (Elshal et al 2006³⁸¹).

2.7.14 Endotoxin assay

Serum endotoxin was analysed using a chromogenic limulus amoebocyte lysate (LAL) test, which is a quantitative test for gram-negative bacterial endotoxin (Cambrex, New Jersey, USA). This assay is based on an ELISA principle. Gram-negative bacterial endotoxin catalyzes the activation of a proenzyme in the LAL. The initial rate of activation is directly determined by the concentration of endotoxin. The activated enzyme catalyzes the splitting of *p*-nitroaniline (pNA) from the colourless

substrate Ac-Ile-Glu-Ala-Arg-pNA. The pNA released was measured photometrically at 405–410 nm following termination of the reaction. The correlation between the absorbance and the endotoxin concentration is linear in the 0.1–1.0 EU/mL range (intra-assay CV $3.9 \pm 0.46\%$, inter-assay CV $9.6 \pm 0.75\%$) (Creely et al 2007³⁸²). Lyophilized endotoxin (*E. coli* origin) was utilised to generate a standard curve with chromogenic LAL test kit from Cambrex, and this produced a corresponding curve in keeping with the manufacturer's instructions. All samples were run in duplicate within the same plate; therefore, no inter-assay variability was observed in this study.

2.7.15 Measurement of Insulin Resistance

Insulin resistance was calculated as per Homeostatic model assessment method (HOMA-IR) (Matthews et al 1985⁴⁹) using the following equation:

$$\text{HOMA-IR} = [\text{Fasting glucose (mmol/L)} \times \text{Fasting Insulin (pmol/L)}] / 22.5$$

Chapter 3

DETERMINANTS OF HUMAN BROWN ADIPOSE TISSUE BASED ON PHYSIOLOGIC ^{18}F -FDG UPTAKE IN SEQUENTIAL PET-CT EXAMINATIONS

3.1 Introduction

The formidable interest in BAT is from the hope that it is probably thought to be the panacea for obesity, given the energy expending, glucose and lipid clearance properties (Orava et al 2013¹⁶⁸, Bartelt et al 2011²⁴², Ouellet et al 2012²³²). Hybridisation of CT and PET was probably the defining moment in BAT research field. This technological advance resulted in anatomical integration of CT into the functional element of PET. The cervical and mediastinal high physiological uptake, which was noted for several decades in PET studies alone, was actually proven to be arising from adipose tissue, contrary to conventional thinking of skeletal muscle origin (Hany et al 2002)¹⁶¹. As discussed in Chapter 1.4.2 and illustrated in Table 1.5.1, this led to series of PET-CT studies (also involving immunohistochemical methodologies) which proved BAT presence in adults, and banished the myth of BAT disappearance from infants on reaching adulthood (Cypess et al 2009, Hadi et al 2007, Saito et al 2009, Virtanen et al 2009, Zingaretti et al)^{140,141,143,144,254}. The challenge now is to manipulate BAT activity in order to achieve the hypothesized metabolic benefits.

Current PET-BAT research is trying to address this particular challenge, and evidence from last few years whilst promising, has largely remained inconclusive, specifically as to the role of determining factors of BAT prevalence and activity. The reported prevalence of BAT taking up ¹⁸F-FDG in adults varies considerably. In the observational studies with large cohorts of patients evaluated for cancer, ¹⁸F-FDG BAT prevalence is low (ranging between 2 and 10%), whereas in prospective studies involving young subjects, the prevalence is reported to be very high (close to

100%)(van Marken Lichtenbelt et al 2009)¹⁴². Interventional studies examining two important triggers of BAT activation: cold exposure and increased sympathetic drive (Cannon et al 2004)¹⁴⁹ showed higher prevalence (40 to close to 100%).

BAT's role in CIT is well validated and cold exposure increases BAT prevalence as noted in prospective as well as retrospective observational studies (Cypess et al 2009¹⁴¹, Persichetti et al 2013³⁸³van Marken Lichtenbelt et al 2009)¹⁴². A review analysis of 8 retrospective PET studies suggested outdoor temperature to be the most vital determining factor of PET detected BAT uptake (Huang et al 2011)³⁸⁴. There was also seasonal variation noted with BAT detection increased in winter months than in summer (Au-Yong et al 2009¹⁹⁰). It was thought that only temperate countries would have higher prevalence, but a recent Chinese study analysing over 30,000 scans showed similar prevalence rates (2.6%), albeit slightly lower (Zhang et al 2014³⁸⁵). Mediterranean BAT prevalence rate (3.4%) also reflected the general trend.

Perhaps, lifestyle parameters and other clinical factors dictate PET detected BAT prevalence and activity. Factors such as sex (Cypess et al 2009¹⁴¹, Persichetti et al 2013³⁸³van Marken Lichtenbelt et al 2009)¹⁴², age (Cypess et al 2009¹⁴¹, Virtanen et al 2009¹⁴⁰, Persichetti et al 2013³⁸³, van Marken Lichtenbelt et al 2009¹⁴², Ouellet et al 2011¹⁶⁶), and body mass index (BMI) (Cypess et al 2009¹⁴¹, Virtanen et al 2009¹⁴⁰, Persichetti et al 2013³⁸³, van Marken Lichtenbelt et al 2009¹⁴², Ouellet et al 2011¹⁶⁶) have known to play a role in BAT's detection through PET. Plasma glucose (Jacene et al 2011²⁰⁰, van der Veen et al 2012³⁸⁶), and day length (Au-Yong et al 2009¹⁹⁰) are also suggested to be determinants of 18 F-FDG uptake in BAT. Nonetheless, there is

still controversy with regard to the relative importance of all those factors in determining the prevalence, mass, and glucose-uptake activity of 18 F-FDG PET BAT.

Thyroid hormones are vital regulators of basal metabolism and play a significant role in thermogenesis during both shivering and non-shivering adaptation to cold. A small alteration in free thyroid hormone levels cause significant changes in tissue oxygen consumption, lipid oxidation and heat production (al-Adsani et al 1997³⁸⁷). As mentioned in Chapter 1 Section 1.8.3, role of thyroid hormones on BAT regulation is well recognized in animal studies: D2 is required for conversion of T4 to T3, and TR β receptor is required for UCP1 induction (Cannon et al 2004¹⁴⁹). In a case report, BAT activation on PET was noted following thyroxine replacement therapy in a post-thyroidectomy hypothyroid patient with papillary carcinoma (Skarulis et al 2010²⁶⁶). In the only dedicated human study so far investigating direct role of thyroid hormones on BAT, 10 hyperthyroid patients showed 3-fold higher glucose uptake on PET, which was reversed on treatment of thyrotoxicosis. However, the study also showed 90% higher skeletal muscle glucose uptake and significantly higher skeletal muscle perfusion than BAT. The study concluded, that thyroid hormones of free T4 and Free T3 activated BAT, but to a lesser degree than BAT activation by cold exposure (Thyrotoxic state BAT glucose uptake versus Cold exposure BAT glucose uptake: 3-fold versus 10- to 15-fold respectively). Whether these findings can be replicated in a clinical setting needs to be determined. One can currently hypothesise that thyroid hormones may play a role in BAT stimulation in humans, but this needs to be further clarified.

Therefore the hypothesis for this set of studies was that:

1. Cold outdoor temperatures stimulate BAT through cold induced thermogenesis, and therefore may result in weight loss.
2. Age, Sex, BMI may have a role in human BAT prevalence, quantity and function.
3. Thyroxine hormone may have a role in stimulating BAT activity and mass.

Therefore the aims of these studies were:

1. To examine the determinants of the prevalence, mass, and glucose-uptake activity of ^{18}F -FDG-detected BAT in a large cohort of subjects who underwent PET/CT examination for cancer diagnosis and staging.
2. To ascertain whether iatrogenic thyrotoxic state resulting from levothyroxine/levothyronine therapy in post-thyroidectomy patients, increases ^{18}F -FDG-detected BAT prevalence, activity and mass.

3.2 Methods

3.2.1 Subjects data collection

Methodology for this part of the study was discussed in detail in Chapter 2.1. In brief, consecutive ^{18}F -FDG-PET/CT whole-body scans were performed on 2685 patients (1497 males, 1188 females) for various diagnostic reasons between June 2007 and August 2012, at UHCW NHS Trust PET centre. Data on age, sex, BMI, fasting glucose level, scan date and scan timing were obtained for all patients. BMI was categorised based on WHO (as illustrated in Chapter 1.1.4) and National Institute of Health criteria into 4 groups (Underweight ≤ 18.5 ; Normal = 18.6-24.9; Overweight = 25-29.9; Obese ≥ 30 , The Evidence Report, National Institutes of Health³⁶⁰). Glycaemic group was categorised on American Diabetes Association's criteria (Normoglycaemia < 5.5 mmol/L; Impaired Fasting Glycaemia ≥ 5.5 -6.9 mmol/L; Diabetes Mellitus ≥ 7.0 mmol/L). Lean Body Weight and Basal Metabolic rate was calculated using validated equations (Ouellet et al 2011¹⁶⁶, Roza et al 1984³⁶¹). Outdoor temperature in Coventry for the day of the scan was obtained from United Kingdom Meteorological Society. For the 151 patients who were detected to have putative BAT, electronic and medical records were reviewed for other relevant past medical history, drug history, smoking status, fasting lipid profile, and biochemical thyroid profile.

Out of 229 patients who were treated for thyroid cancer in UHCW during the same period, 34 patients underwent PET scans, whose notes and electronic records were reviewed irrespective of their BAT status. This small group was further classified

into Thyrotoxic and Euthyroid subgroups, depending upon patients' biochemical thyroid status at the time of the scan.

3.2.2 PET-CT imaging protocol

As outlined in Chapter 2.1.6, in accordance with standard administration and acquisition protocol, the subject was fasted for 6 hours, weight adjusted amount of ^{18}F -FDG radiotracer was injected one hour prior to the PET scan. PET was performed on a GE Discovery STE PET-CT scanner (General Electric Medical Systems, Milwaukee, USA). Two sets of emission data were obtained for 3 minutes in each bed position; from the skull base to mid thigh (with arms elevated).

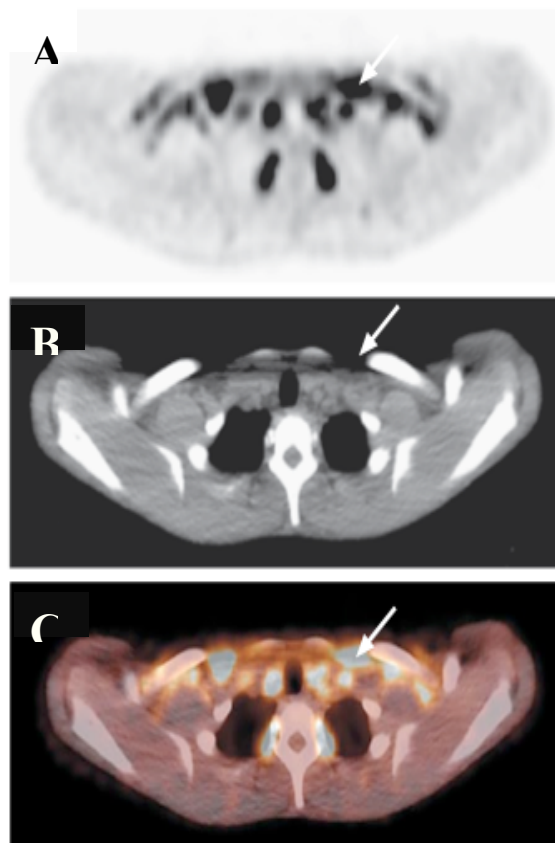


Figure 3.2.2 van Marken Lichtenbelt et al 2009 (A) PET, (B) CT, and (C) integrated PET-CT scans, with BAT location indicated

3.2.3 Image analyses

The protocol for this part of the methodology is as detailed in Chapter 2.1.8. All PET/CT scans were initially reported by a Consultant Radiologist, possessing expertise in nuclear imaging as part of the patients' routine clinical care. For the purposes of this study each PET/CT scan was re-evaluated by second radiologist to confirm the presence of ^{18}F -FDG BAT. PET images were reconstructed using the CT data for attenuation correction. Areas of more than 5 mm with a CT density of adipose tissue (-100 to -10 Hounsfield units), and had maximal Standard Uptake Value (SUV) of ^{18}F -FDG of at least 2.5 g per milliliter was considered as ^{18}F -FDG detected BAT. Volume and activity of BAT were quantified with image fusion software Mirada XD 4.3 (Mirada Medical Ltd, Oxford, UK) in user-defined regions of interest by autocontouring in the cervical, supraclavicular and superior mediastinal depots as illustrated in Chapter 2, Figure 2.1.10.a and Figure 2.1.10.b. BAT mass was calculated based on assumption of density of fat being 0.92 g per milliliter (Ross et al 1984³⁶⁷).

3.2.4 Statistical analyses

The recorded data were entered into Microsoft excel spreadsheet. The data were analysed using SPSS IBM software Version 22 (SPSS Chicago, IL). Normally distributed continuous variables were compared between study groups with the use of Student's t-test, and non-normally distributed variables were compared with Mann-Whitney U test. The roles of sex, age, BMI, fasting glucose, outdoor temperature as predictors of BAT prevalence were tested by logistic regression with

the use of univariate and multivariate models. For multivariate analyses of BAT mass, logarithmic transformation of the data was done as the scores were non-normally distributed. The patients were also divided into four BMI groups (Underweight, Normal, Overweight and Obese), and also Fasting Glucose level (Normoglycaemia, Impaired Fasting Glycaemia, and Diabetes); Kruskal Wallis was used to compare between the categories for BAT mass and BAT activity. Missing values were dealt with pairwise deletion method using SPSS software. Odds ratio and Confidence Intervals were estimated as measures of magnitude of associations. All P values presented are two-tailed, and values less than 0.05 are considered to be statistically significant.

3.3 Results

3.3.1 General Characteristics and overall study parameters

¹⁸F-FDG BAT was observed in 151 out of 2685 patients (5.6%) in a total of 175 out of 3295 scans (5.3%). The main biophysical, PET scan and environmental parameters are enlisted in Table 3.3.1. Generally individuals with BAT ¹⁸F-FDG uptake were on an average younger, had lower BMI, and had lower fasting glucose levels than BAT negative group. Lower outdoors temperatures and lesser sunshine was also noted in the BAT positive group.

Table 3.3.1 Characteristics of BAT positive and BAT negative patients based on ¹⁸F-FDG BAT uptake

Total ¹⁸ F-FDG PET scans (n=2685)	BAT Negative PET scans (n=2534)		BAT Positive PET scans (n=151)	
	Mean	SEM	Mean	SEM
Characteristics				
Age (yrs)	63.4	0.3	50.8	1.5
Weight (kg)	76.1	0.3	66.6	1.1
Height (cm)	168.7	0.2	165.0	0.8
Body Mass Index (kg/m ²)	26.7	0.1	24.4	0.4
Lean body mass (kg)	54.2	0.2	47.8	0.7
Basal Metabolic rate	1505	6	1395	19
Fasting Glucose	5.7	0.0	5.3	0.1
Diabetes (%)	10.3	NA	3.9	NA
No of PETs undertaken	1.2	0.0	1.6	0.1
¹⁸ F-FDG dose (MBq)	363.3	0.6	360.6	2.7
SUV mean (g/ml)	NA	NA	3.0	0.0
SUV maximum (g/ml)	NA	NA	7.4	0.3
SUV volume (cm ³)	NA	NA	77.5	8.5
BAT mass (0.92g/ml)	NA	NA	71.3	7.8
Total Lesion Glycolysis	NA	NA	263.1	32.3
Minimum temp on scan	6.1	0.1	4.3	0.4
Mean temp on scan date	9.9	0.1	7.9	0.4
Preceding week's mean	9.9	0.1	7.8	0.4
Mean monthly temp	10.4	0.1	9.0	0.4
Mean sunshine on scan	4.1	0.1	3.6	0.2
Total monthly sunshine	130.2	1.0	117.8	4.2

BAT-Brown adipose tissue; SUV-Standard uptake value; ¹⁸F-FDG – 18 Fluoro-labelled -2-deoxy-glucose; PET- Positron emission tomography; MBq- Megabecquerel; NA-Not applicable

3.3.2 Prevalence of ¹⁸F-DG detected BAT

Table 3.3.2.1 Logistic regression analyses on predictors of Brown Adipose Tissue prevalence based on ¹⁸F-FDG PET scanning (n=2685)

Variable	Univariate analysis		Multivariate analysis	
	Odds ratio (95%CI)	P value	Odds ratio (95%CI)	P value
Age	0.952 (0.949-0.955)	<0.001	0.965 (0.955-0.976)	<0.001
Sex	0.025 (0.018-0.035)	<0.001	0.135 (0.075-0.242)	<0.001
BMI	0.895 (0.889-0.901)	<0.001	0.894 (0.845-0.946)	<0.001
Fasting Glucose	0.595 (0.577-0.614)	<0.001	1.130 (0.987-1.294)	0.07
Diabetes status	0.023 (0.010-0.051)	<0.001	0.305 (0.100-0.929)	0.03
Basal Metabolic rate	0.998 (0.998-0.998)	<0.001	1.002 (1.001-1.003)	0.001
Mean day temp	0.757 (0.742-0.771)	<0.001	0.917 (0.861-0.977)	0.007
Mean monthly temp	0.752 (0.737-0.767)	<0.001	1.130 (0.953-1.114)	NS
Mean monthly sunshine	0.496 (0.473-0.519)	<0.001	NS	NS

NS-Not significant (p>0.05); BMI- Body mass index; ¹⁸F-FDG- 18 Fluoro-labelled - 2-deoxy-glucose; PET-Positron emission tomography; P<0.05 is significant

As depicted in Table 3.3.2.1, from univariate analyses, lower age, female sex, lower BMI, lower fasting glucose, non-diabetic status, lower outdoor day and month temperatures, and lesser monthly sunshine hours were all predictive of a higher prevalence of ¹⁸F-FDG BAT. In multivariate analyses, following adjustment of all other variables, lower age (P<0.001), female sex (P<0.001), lower BMI (P<0.001),

diabetes status (P=0.03), outdoor day temperature (P=0.007) remained significant. Fasting glucose was seemingly trending towards significance (P<0.07). Interestingly, BMR was noted to be lower in BAT positive group as against conventional findings of higher BMR in this group owing to the metabolically active nature of BAT. The same determinants for BAT ¹⁸F-FDG uptake identified by multivariate, were consistently detected once again on performing the stepwise backward regression analyses as illustrated in Table 3.3.2.2 However, forward stepwise regression analyses only identified lower age, female sex and mean daily outdoor temperature.

Table 3.3.2.2 Stepwise regression analyses on predictors of BAT prevalence based on ¹⁸F-FDG PET scanning (n=2685)

Variable	Stepwise regression P-values	
	Backward regression	Forward regression
Age	<0.001	<0.001
Sex	<0.001	<0.001
BMI	<0.001	
Fasting Glucose	0.090	
Diabetes status	<0.02	
Basal Metabolic	<0.001	
Mean day temp	<0.001	0.003

PET-positron emission tomography; P<0.05 is significant; ¹⁸FDG- ¹⁸F-Fluorodeoxy-glucose; BMI- Body mass index

3.3.3 BAT mass and BAT activity (SUV_{max}) analyses

The scores of BAT mass (0.92 x BAT volume) failed tests of normality. Hence, the scores were log10 transformed to satisfy normality criteria, and the Figure 3.3.3.1

illustrates Normal Q-Q plot with Kolmogorov-Smirnov test being statistical significant 0.200 (>0.05) for BAT mass. However, BAT activity reflecting SUVmax was not normally distributed despite log transformation or square root application. Therefore, multivariate Tobit model (Tobin et al 1958³⁸⁸), a recognised statistic model specifically designed for variables distributed with a large percentage of cases at lower limit or upper limit was used.

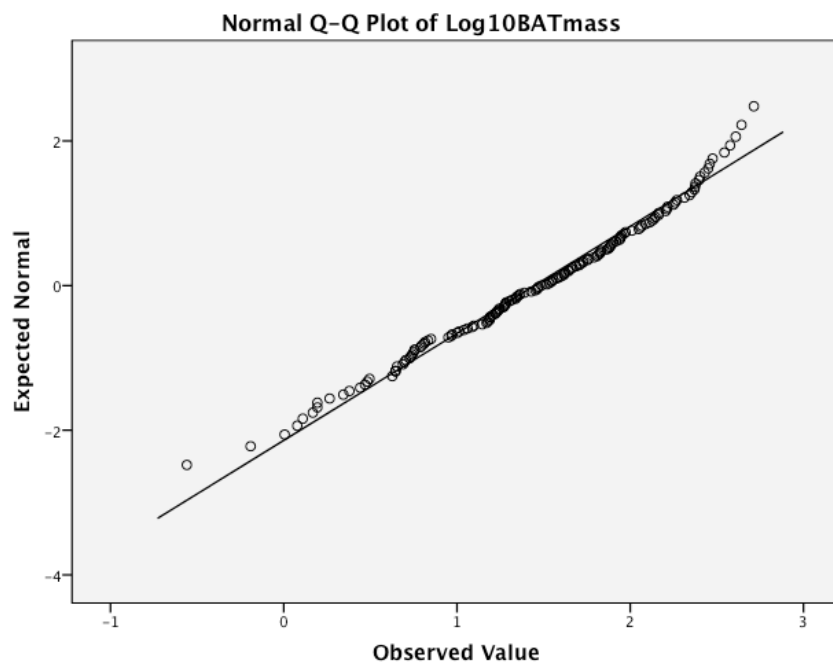


Figure 3.3.3.1 Illustration of Normal Q-Q plot with Kolmogorov-Smirnov test being statistical significant 0.200 (>0.05) for BAT mass.

Table 3.3.3.2 Illustration of BAT mass determinants on ¹⁸F-FDG PET scans based on Tobit model univariate and multivariate analyses

Variable	Univariate P-value	Multivariate P-value
Age (years)	<0.001	<0.001
Gender	<0.001	<0.001
Fasting Glucose (mmol/L)	<0.001	0.214
BMI (kg/m²)	<0.001	<0.001
Min daily temp (°C)	<0.001	0.302
Mean daily temp (°C)	<0.001	0.884
Max daily temp (°C)	<0.001	0.008
Mean monthly temp (°C)	0.001	0.067
Daily sunlight hours	0.030	0.783
Mean monthly sunlight hours	0.009	0.904
Scan time	0.002	<0.001
Max previous day temp (°C)	<0.001	0.020
Mean previous week temp (°C)	<0.001	0.025

PET-positron emission tomography; p<0.05 is significant; BAT-Brown adipose tissue; ¹⁸FDG- 18F-Fluorodeoxy-glucose; PET-Positron emission tomography; MBq-Megabecquerel; NA-Not applicable

Table 3.3.3.3 Illustration of BAT activity determinants on ¹⁸F-FDG PET scans based on Tobit model univariate and multivariate analyses

Variable	Univariate P-value	Multivariate P-value
Age (years)	<0.001	<0.001
Gender	<0.001	<0.001
Scan Date	0.226	0.923
Fasting Glucose (mmol/L)	<0.001	0.129
BMI (kg/m²)	<0.001	<0.001
Min daily temp (°C)	<0.001	0.263
Mean daily temp (°C)	<0.001	0.827
Max daily temp (°C)	<0.001	0.008
Mean monthly temp (°C)	<0.001	0.039
Daily sunlight hours	0.021	0.608
Mean monthly sunlight hours	0.005	0.908
Scan time	0.002	0.001
Max previous day temp (°C)	<0.001	0.024
Mean previous week temp (°C)	<0.001	0.016

BMI- Body mass index; ¹⁸F-FDG- 18 Fluoro-labelled -2-deoxy-glucose; PET- Positron emission tomography; P<0.05 is significant; BAT- Brown adipose tissue

In line with logistic regression and stepwise regression for BAT prevalence, Tobit model analyses also show age (<0.001), sex (<0.001) and BMI (<0.001) as strong determinants of BAT mass and BAT activity. In summary, for this part of the

chapter, BAT prevalence, BAT mass and BAT activity are strongly determined by age, sex and BMI and moderately influenced by outdoor temperature.

3.3.4 Influence of Age on BAT prevalence, BAT activity and BAT mass

Increasing age was negatively correlated with BAT prevalence ($P < 0.001$), BAT activity ($P < 0.001$) and BAT mass ($P < 0.001$) as depicted in Table 3.3.2.1 and Figures 3.3.2.

Table 3.3.4.1 Age decade wise ^{18}F FDG detected BAT positive scans

Age (decade)	Total PET scans	BAT +ve scans	%age of BAT +ve scans
1st	1	0	0
2nd	19	7	36.8
3rd	65	21	32.3
4th	118	17	14.4
5th	253	21	8.3
6th	499	29	5.8
7th	851	32	3.8
8th	686	19	2.8
9th	191	5	2.6
10th	2	0	0
Total	2685	151	5.6

^{18}F -FDG- 18 Fluoro-labelled -2-deoxy-glucose; PET-Positron emission tomography; BAT- Brown adipose tissue

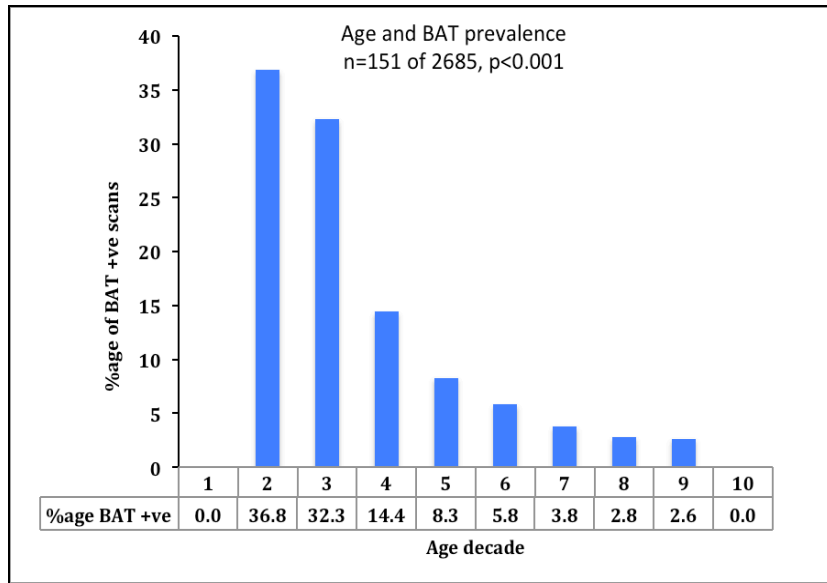


Figure 3.3.4.2 Schematic representation of effect of Age on BAT prevalence expressed in %age of BAT detection rate according to decade

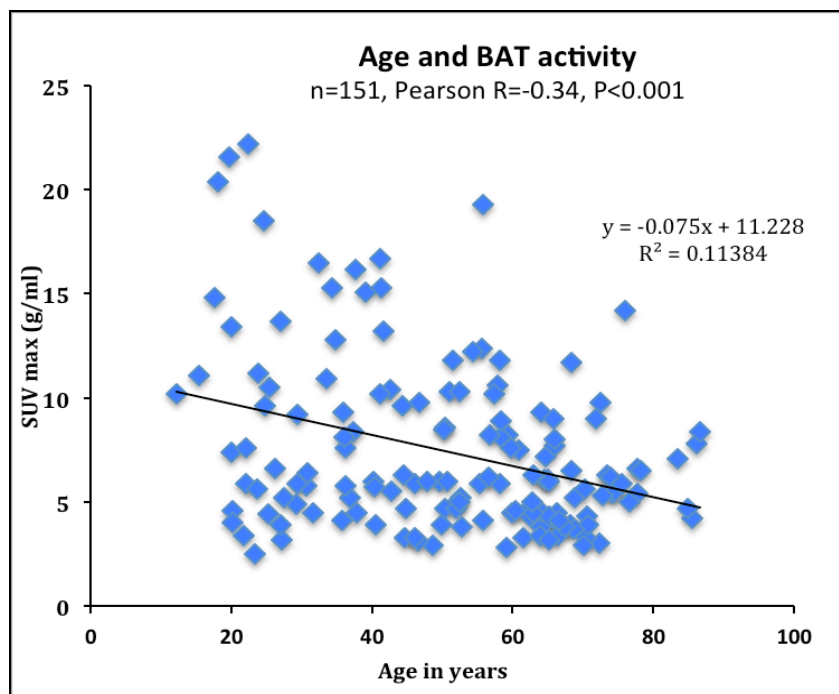


Figure 3.3.4.3 Schematic representation of effect of Age on BAT activity

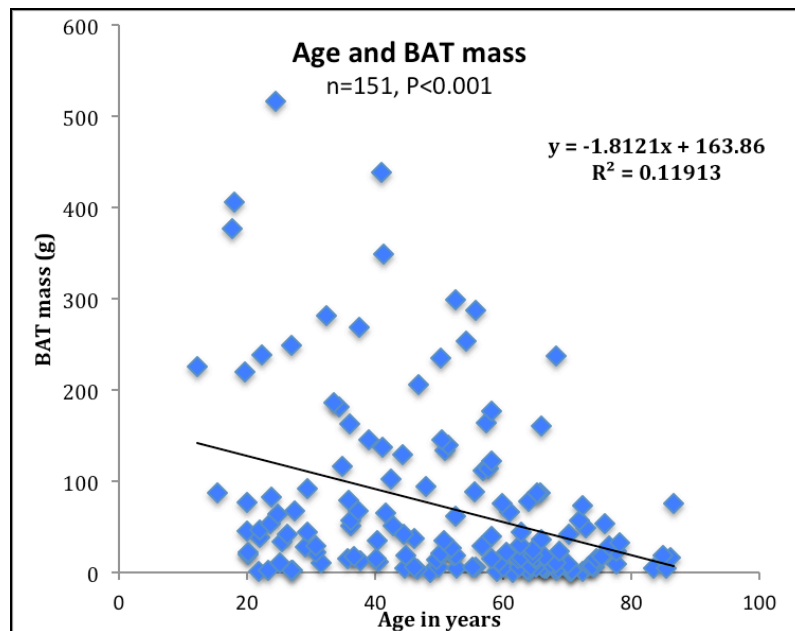


Figure 3.3.4.4 Schematic representation of effect of Age on BAT mass

3.3.5 Influence of Gender factor on BAT prevalence, BAT activity and BAT mass

Out of 2685 patients (1188 females and 1497 males), 151 patients had BAT 18F-FDG uptake on PET scans. 114 (9.6%) were females and 37 (2.5%) were males as shown in Figure 3.3.5.1. Younger leaner females were at increased chance of being detected to have 18F-FDG BAT uptake ($P<0.001$) and also showed significantly increased BAT activity ($P<0.001$) as shown in Table 3.3.2.

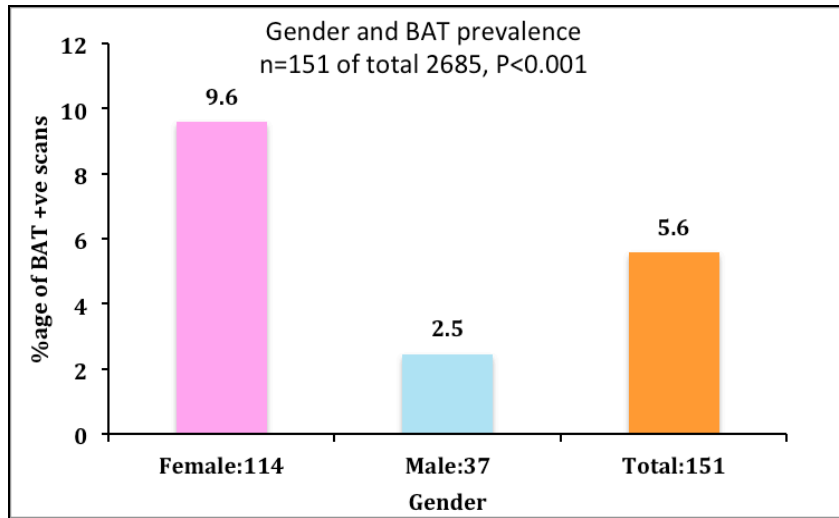


Figure 3.3.5.1 Schematic representation of effect of sex on BAT prevalence

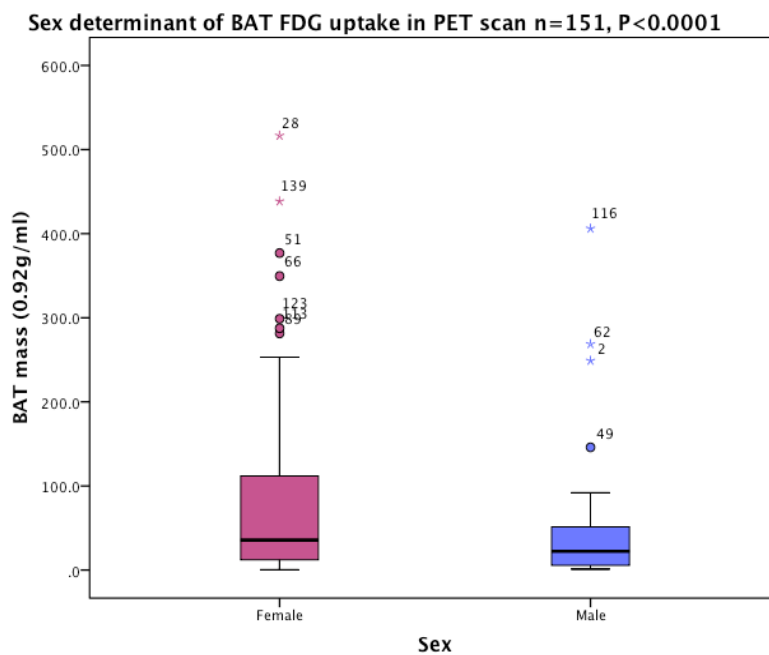


Figure 3.3.5.2 Illustration of brown fat mass in males and females on 18F-FDG PET scanning

BAT mass, which is calculated from measured BAT volume, was noted to be higher in females when compared to males (Mean \pm Standard Error of Mean: Females 77.8 grams \pm 9.3; Males 53.3 \pm 14.1 grams respectively, $P < 0.001$), as illustrated in Table 3.3.3.2.1 and Figure 3.4.2. Total lesion glycolysis, reflector of BAT activity was also noted to be higher in females, but was not statistically significant. Some of the anthropometry and PET scan related parameters comparing males and females in BAT positive PET scans are outlined in Table 3.4.3.

Table 3.3.5.3 Comparison of biophysical, PET scan and environmental parameters related to ^{18}F -FDG BAT uptake

Characteristics	Male		Female	
	Mean	SEM	Mean	SEM
Age (yrs)	49.8	3.6	51.1	1.6
Weight (kg)	73.7	2.5	64.3	1.1
Height (cm)	176.3	1.3	161.3	0.7
BMI (kg/m²)	23.6	0.6	24.7	0.4
Lean body mass (kg)	58.1	1.3	44.4	0.4
No of PET scans	1.9	0.3	1.5	0.1
Basal Metabolic Rate (Kcal/24)	1639.5	45.0	1316.0	13.1
SUVmean (g/ml)	2.9	0.1	3.1	0.0
SUV max (g/ml)	6.8	0.6	7.6	0.4
SUVvolume (cm³)	57.9	15.3	84.6	10.1
BAT mass (0.92g/ml)	53.3	14.1	77.8	9.3
Total Lesion Glycolysis (g)	192.1	55.4	288.5	39.0
Mean temp on scan date	6.8	0.9	8.3	0.5
Mean monthly temp	8.2	0.7	9.3	0.4
Daily sunshine (hours)	3.8	0.4	3.5	0.2
Total monthly sunshine (hrs)	122.3	9.3	116.7	4.7

BMI- Body mass index; ^{18}F -FDG- 18 Fluoro-labelled -2-deoxy-glucose; PET- Positron emission tomography; BAT- Brown adipose tissue; SUV- Standard uptake value; SEM- Standard Error of Mean

3.3.6 Influence of Body Mass Index (BMI) on BAT prevalence, BAT activity and BAT mass

Lower BMI is statistically significant in detecting ^{18}F -FDG BAT uptake as noted in both univariate ($P < 0.001$, OR 0.895, 0.889-0.901 CI), and multivariate analyses ($P < 0.001$, OR 0.894, 0.845-0.901 CI). BAT mass and BAT activity was not statistically significant when BMI was categorised to WHO classification of obesity ($P = \text{NS}$) as demonstrated in Figure 3.3.6.2.

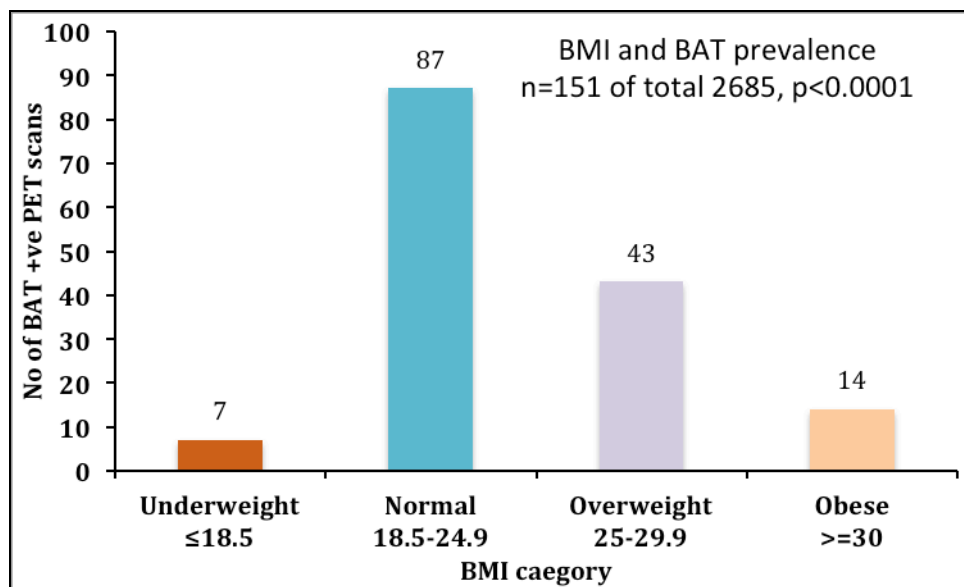


Figure 3.3.6.1 Bar graph of BAT prevalence in PET scans according to Body Mass Index categories

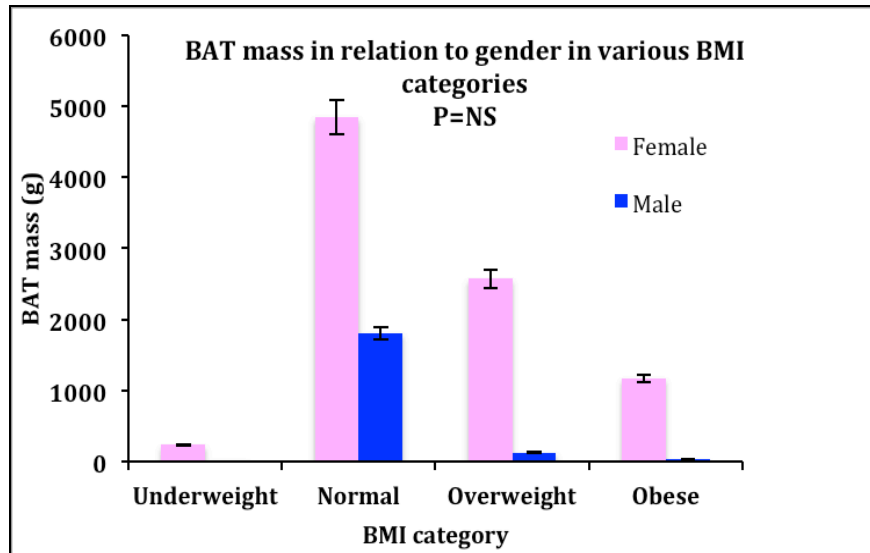


Figure 3.3.6.2. Bar graph of BAT mass in PET scans according to Body Mass Index categories

3.3.7 Influence of Fasting Glucose on BAT prevalence, BAT activity and BAT mass

11 missing fasting glucose values were assorted with paired deletion method using SPSS software. Univariate analysis showed lower fasting glucose to enhance BAT FDG uptake ($P < 0.001$), and when combined with rest of the variables it showed a trend towards significance ($P = 0.07$). The different glycaemic groups did not show influence on BAT activity, however BAT mass was noted to be lesser in diabetes patients than in non-diabetics, specifically in females ($P = 0.03$).

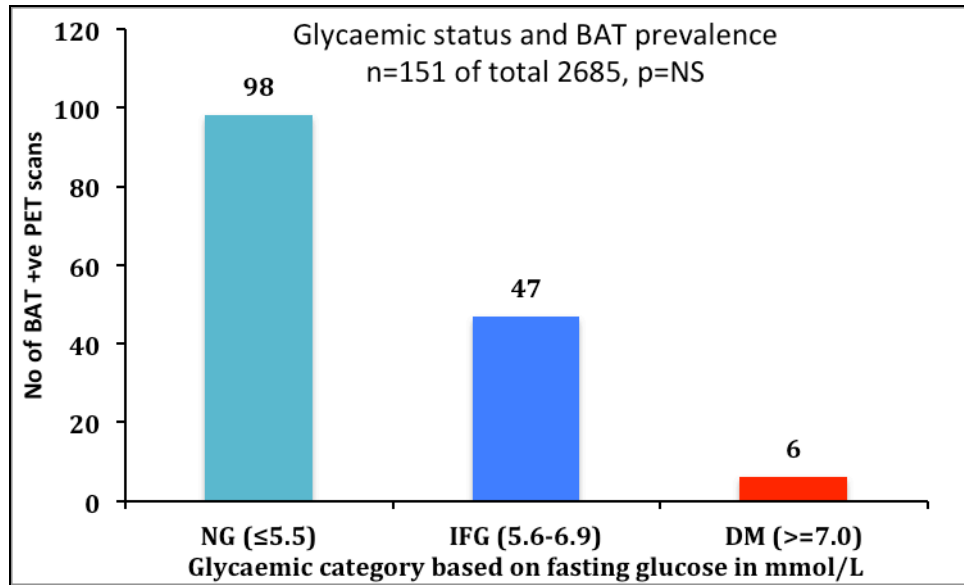


Figure 3.3.7 Bar graph of PET BAT detected patients in various glycaemic groups

3.3.8 Influence of Outdoor temperature on BAT prevalence, BAT activity and BAT mass

Exposure to colder temperature at the time of scanning seems to be the critical most triggering factor in PET BAT detection. An inverse correlation was noted in our study between mean monthly temperature and BAT FDG uptake prevalence (Pearson R= -0.72) and is shown in Figure 3.3.8. Summer months BAT prevalence markedly reduced as temperature rose, and winter BAT detection rates were higher (P=NS). We also noted that mean daily temperature irrespective of the season, can influence BAT detection (P=0.007). As illustrated in Tobit analyses in Table 3.3.3.2.2, previous day mean temperature and previous week's mean temperature bore some influence on BAT mass and BAT activity (P=0.024).

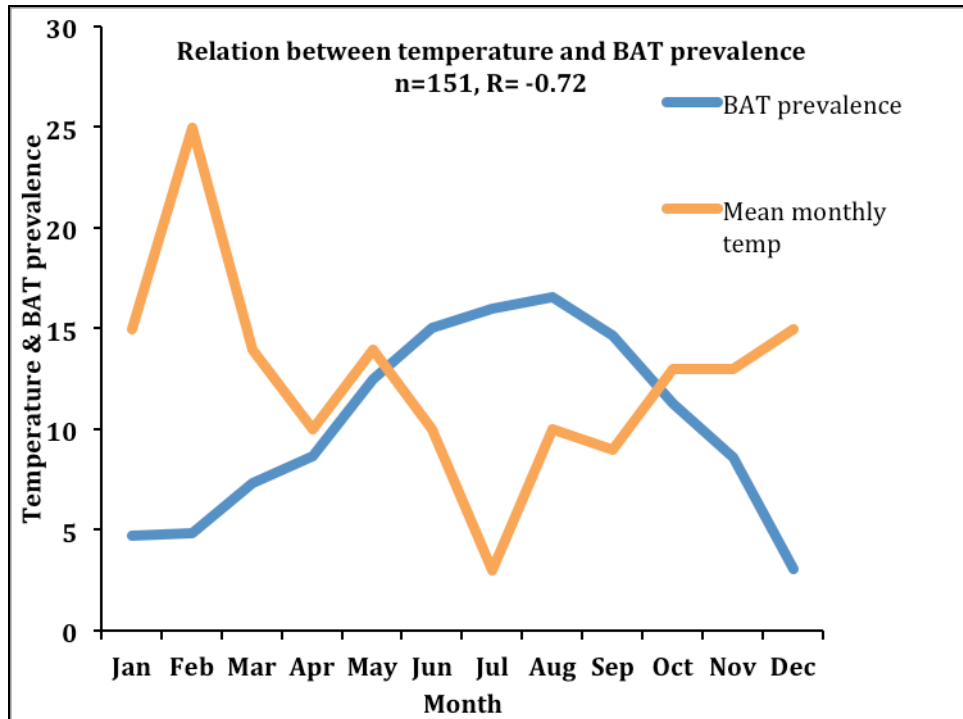


Figure 3.3.8.1 Graph representing the relation of mean monthly temperature with BAT FDG uptake prevalence rates.

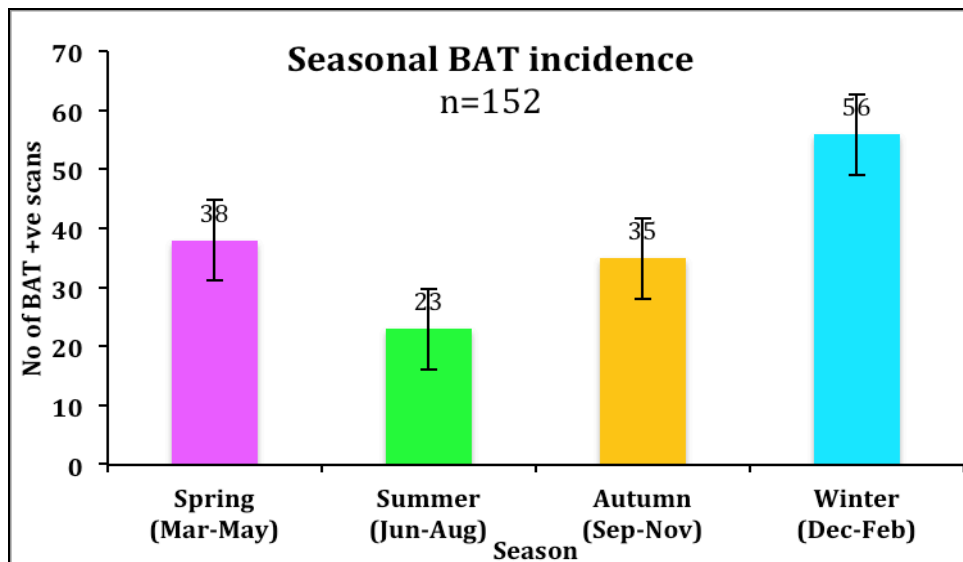


Figure 3.3.8.2 Seasonal variation of BAT detection from PET scanning

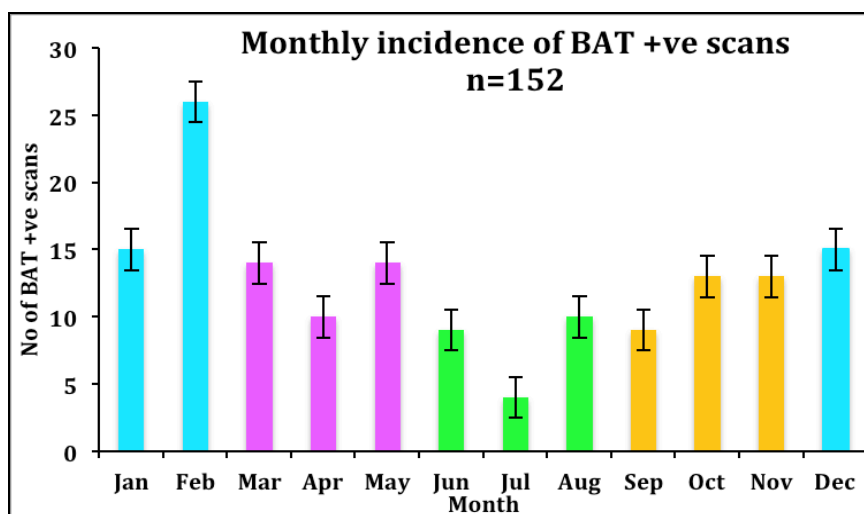


Figure 3.3.8.3 Monthly variation of BAT detection from PET scanning

3.3.9 Influence of Thyroxine on BAT prevalence

Out of 229 thyroid cancer patients treated in UHCW, 34 patients (8 male, 26 female) underwent ^{18}F -FDG PET scanning. Biochemical thyroid profile, anthropometry and other PET scan parameters are depicted in Table 3.3.9.

19 patients were rendered iatrogenically thyrotoxic (TSH [Mean \pm SEM]: 0.05 \pm 0.01 mU/L, Normal range 0.35-6.0) using thyroid replacement therapy to suppress TSH, and were classified as Thyrotoxic group. The remaining 15 patients were Euthyroid (TSH [Mean \pm SEM]: 2.52 \pm 0.65 mU/L, Normal range 0.35-6.0), and there was statistical significance between both groups ($P < 0.001$). Only one patient in Thyrotoxic group (34-year old female, BMI 14, BAT mass 112 grams), and one patient in Euthyroid group (77-yr old lady, BMI 26, BAT mass 23 grams) demonstrated ^{18}F -FDG BAT uptake. BAT prevalence rate of 5.3% in the Thyrotoxic

group, 6.6% in Euthyroid group is comparable to overall BAT prevalence of 5.6% for total 2685 patients.

Thyroid profile was available for analysis on 126 out of 151 ¹⁸F-FDG BAT positive patients. 7 out of 126 BAT positive patients were mildly thyrotoxic (TSH [Mean ± SEM]: 0.16 ± 0.06 mU/L). 2 were thyroid cancer patients on thyroxine replacement. The remaining 5 patients were incidentally thyrotoxic secondary to unintentional levothyroxine drug over-replacement. Despite TSH being significantly different in both groups, no correlation was noted between TSH and BAT activity (P=NS, Pearson R=0.04), as demonstrated in Figure 3.9.9.2, or with BAT mass (P=NS, Pearson R=0.08). Free T4 did not show correlation with either BAT activity (P=NS, Pearson R= -0.07), or with BAT mass (P=NS, R= -0.16).

In summary, no correlation was noted between thyroid hormones and BAT indices in this study.

Table 3.3.9.1 Comparison data of patients' characteristics in Thyrotoxic, Euthyroid and total ¹⁸F-FDG BAT +ve patients

Characteristics	Thyrotoxic patients (n=19)		Euthyroid patients (n=15)		¹⁸ F-FDG BAT +ve patients (n=152)	
	Mean	SEM	Mean	SEM	Mean	SEM
TSH (mU/L) (0.35-6.0)	0.05	0.01	2.52	1.90	1.90	0.01
Free T4 (pmol/L) (9-26)	26.8	1.6	18.1	18.1	18.1	0.3
Free T3 (pmol/L) (2.8-7.1)	11.2	1.2	4.8	5.0	5.0	0.1
Age (yrs)	58.3	4.3	49.8	4.0	50.8	1.5
Fasting Glucose (mmol/L)	5.1	0.1	5.2	0.2	5.3	0.1
Weight (kg)	80.8	5.1	73.8	7.2	66.1	1.1
BMI (kg/m²)	28.8	1.8	26.7	2.4	24.4	0.4
Basal Metabolic Rate (Kcal/24hr)	1527	81	1483	83	1395	19
SUVmax (g/ml)	0.4	0.4	0.8	0.8	7.4	0.3
BAT mass (g)	1.3	1.3	7.3	7.3	71.3	7.8
BAT +ve %age	5.3		6.7		100	
Total Lesion Glycolysis (g)	4.4	4.4	27.7	27.7	263.1	32.3
Mean day temp (°C)	11.1	1.0	8.3	1.6	7.9	0.4
Mean monthly temp (°C)	11.3	1.0	8.6	1.3	9.0	0.4

BMI- Body mass index; ¹⁸F-FDG- 18 Fluoro-labelled -2-deoxy-glucose; PET- Positron emission tomography; BAT- Brown adipose tissue; SUV- Standard uptake value; SEM- Standard Error of Mean; TSH- Thyroid stimulating hormone

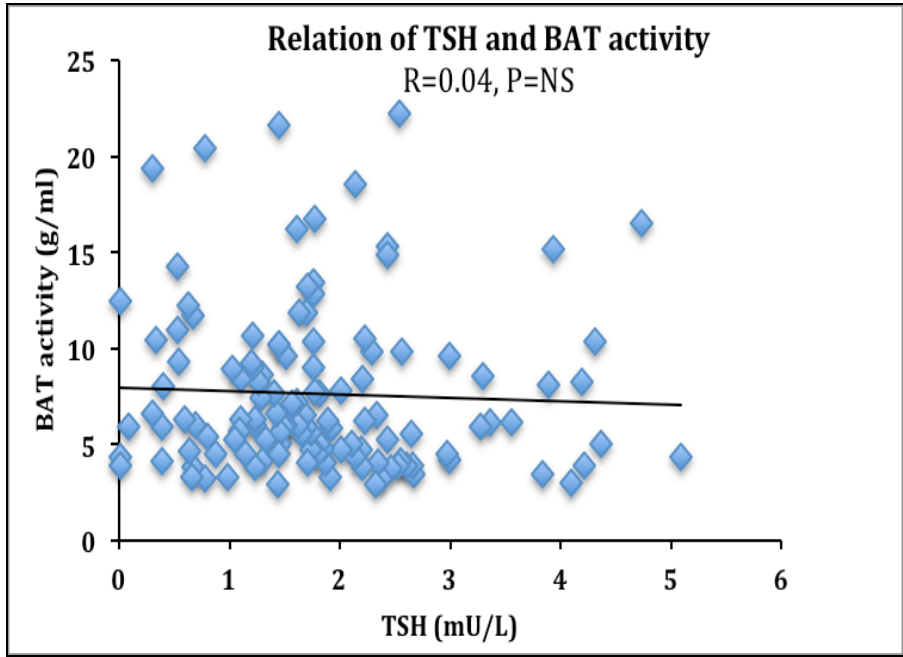


Figure 3.3.9.2 Correlation of Thyroid Stimulating Hormone and BAT activity (SUV_{max}) in ¹⁸F-FDG BAT uptake positive patients

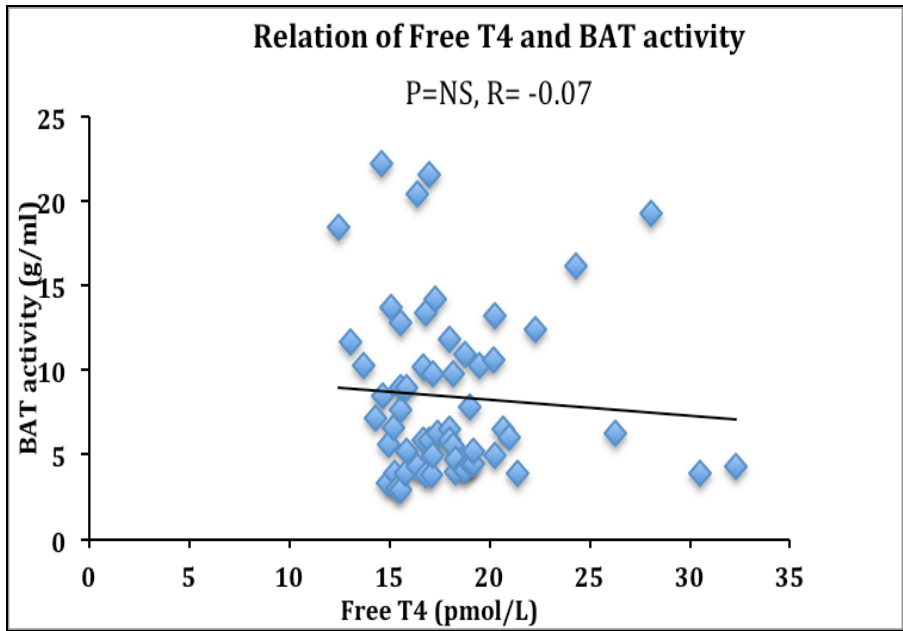


Figure 3.3.9.3 Correlation of Free T4 Hormone and BAT activity (SUV_{max}) in ¹⁸F-FDG BAT uptake positive patients

3.4 Discussion

Many studies have indicated that BAT in rodents has profound effects on body weight, energy balance, and glucose metabolism, and therefore BAT route is worth pursuing in adults (Cannon et al 2004)¹⁴⁹. Human PET studies based on ¹⁸F-FDG uptake by BAT have been successful in a sense, that they conclusively prove BAT's presence in adults, but so far have not reached consensus regarding the determining factors of BAT prevalence, BAT activity and BAT mass (Cypess et al 2009³⁸⁹, Cronin et al 2009²⁰²). This study based on a large cohort of patients (n=2685) in a single centre, was carried out to further disentangle these anthropometric and environmental factors using robust statistical methods. The study concludes that lower age, female sex, lower BMI, lower outdoor temperatures and absent diabetes status influence ¹⁸F-FDG detected BAT prevalence; and lower age, female sex, lower BMI and lower outdoor temperatures influence BAT mass and BAT activity. There is no influence of thyroxine hormone on BAT uptake in a mild thyrotoxic state.

The study's BAT prevalence of 5.6%, is comparable to similar large retrospective PET-series studies (Cypess et al 2009¹⁴¹, Cronin et al 2012²⁰², Perishetti et al 2013³⁸³, Zhang et al 2013³⁸⁵). Prospective studies indicate a higher prevalence (40% to 96%) (van Marken Lichtenbelt et al 2011¹⁴², Saito et al 2009¹⁴³). Also, postmortem studies have shown higher incidence, 26 out of 31 cases in over 30-year olds (84%) (Heaton et al 1972¹⁵¹). Furthermore, out of 6 patients who had incidental histological confirmation of BAT during routine pathological examination of their neck-dissection samples, only one revealed ¹⁸F-FDG detected BAT (data not

shown), indicating much higher actual BAT prevalence. It is an inherent nature of retrospective PET studies to underestimate the true BAT prevalence, as PET-CT shows only incidental metabolically activated BAT, as opposed to deliberately stimulated BAT. PET scans are usually performed in fasting and thermal comfort conditions with the room temperature set in the range between 22°C-25°C, depending upon the individual centre's PET image acquisition protocol. Both these factors switch off BAT, as cold and diet are recognised stimulators of BAT as mentioned in detail Chapter 1.8.2. The PET-scans in the current study were done at thermo-neutral condition with the room temperature kept constant at 23°C. However, following adjustment of all other variables, multivariate analyses yielded lower age, female sex, BMI and diabetes status, as significant factors suggesting their independent influence on BAT activation, other than cold temperature and diet.

The study also confirms the findings of other major case series, and adds to the evidence that sex, age, BMI, diabetes status and outdoor temperature are significant determinants of BAT prevalence (Cypess et al 2009¹⁴¹, Cronin et al 2012²⁰², Perishetti et al 2013³⁸³, Zhang et al 2013³⁸⁵, Jacene et al 2011²⁰⁰, Pace et al 2011²⁰¹). Majority of the PET-studies studied BAT prevalence, and only few studied BAT volume or mass (Ouellet et al 2011)¹⁶⁶. We found BAT mass to be higher compared to other studies (70 grams versus 11 grams) (Cypess et al 2009¹⁴¹), indicating that other studies may be underestimating true BAT quantity. This can be attributed to advanced technology of imaging analysis MIRADA software, which yielded reasonably accurate automatic estimation of SUV volume, and hence BAT volume, when compared to other softwares used in the previous studies. Sexual dimorphism was clearly evident in both BAT prevalence (Female to male: 9.6% versus 2.5%

respectively) and BAT mass (Mean \pm Standard Error of Mean: Females 77.8 grams \pm 9.3; Males 53.3 \pm 14.1 grams respectively, $P < 0.001$).

One of the striking findings of our study is the pronounced variation of outdoor temperature to BAT prevalence, in this large case series. Although this confirms evidence from previous studies, it is an important reaffirmation of this vital outcome, given global warming and global obesity epidemic. Whilst a correlation between these two phenomena needs exploration, it is an important public health message to lower our living room thermostats in order to activate BAT. The study did not show correlation between sunshine hours and BAT indices, but found strong correlation between Season and BAT prevalence. This evokes speculations, that changes in diurnal, or possibly circannual rhythm variations of hormones such as prolactin and melatonin, may explain the increased BAT incidence in winter more than in summer. The endocrine mechanisms such as these and that related to sexual dimorphism may be complex, and it is imperative that we learn more about BAT's physiology if at all we aim to use BAT as an anti-obesity strategy.

Although our study (in line with other major PET series studies) did not show a strong correlation between glucose and all BAT indices, overall evidence of effect of BMI points towards active BAT to offer protection against diabetes and obesity. This interpretation is substantiated by several animal studies, where BAT-deficient mice develop obesity, hyperphagia, and insulin resistance (Hamann et al 1995, Hamann et al 1996, Lowell et al 1993³⁹⁰⁻³⁹²). Furthermore, overall mean levels of fasting glucose was lower in FDG BAT detected groups than in FDG BAT negative groups in several other studies (Ouellet et al 2011) including that of ours.

We found unexpected findings of no correlation of thyroid hormones on BAT FDG uptake on PET scans, against conventional speculations. Only one of the 19 thyrotoxic patients (34-year old female, BMI 14 kg/m⁻²) was detected to have significant BAT depots, but it could be argued that younger age, female sex and lower BMI may have had some influence, rather than thyroid status alone. Furthermore, BAT prevalence rates were similar across the Thyrotoxic, Euthyroid and BAT positive groups (approximately 5%), indicating co-incidental BAT detection, as opposed to thyroxine-stimulated detection. These findings are contrary to the evidence shown by Finnish group (Lahesmaa et al 2014³⁹³), where BAT showed increased glucose uptake in hyperthyroid patients, independent of BAT perfusion. However, the authors noted that skeletal muscle perfusion and glucose uptake was far higher than BAT perfusion and glucose uptake. One explanation is, skeletal muscle has more D2 and significantly contributes for facultative thermogenesis (van Marken Lichtenbelt et al 2011)²¹⁰. Furthermore, thyroid hormones up-regulate glucose transporter protein type 4 (GLUT-4), which mediates the rate-limiting step of glucose metabolism in the skeletal muscle, resulting in more thermogenesis (Ezaki et al 1997)³⁹⁴. This excess thermogenesis from the skeletal route in hyperthyroid patients may centrally inhibit BAT pathway of non-shivering thermogenesis, which is usually modest even in maximal stimulated conditions. BAT contains high amounts of Type II 5' Iodothyronine deiodinase (D2), which is required for T4 to T3 conversion. High local tissue T3 concentrations are necessary for up-regulation of UCP-1 in BAT as already highlighted in Chapter 3.1 (Silva et al 1983)¹⁸⁸. D2 levels of skeletal muscle in humans when compared to BAT are far higher than noted in mice, pointing out the diversification of tissue variations between the two species (Salvatore et al 1996³⁹⁵, Croteau et al 1996³⁹⁶). This might

explain the failure of replication of animal data in humans in our current study. To our knowledge, this is the first ever study evaluating thyroid hormones' influence on BAT in a clinical setting. Interestingly, two pheochromocytoma patients were in the 2685 patients cohort, and both did not exhibit BAT despite, one being a metastatic pheochromocytoma with grossly elevated metanephrines.

The major limitation is retrospective nature of the study, and lack of control groups which did not allow registration of complete clinical histories, including diabetes and metabolic profiles evaluation. Majority of the PET studies conducted was for evaluation of malignancy and it is possible that various malignancies may have confounding variables, including influence from chemotherapy agents, which could alter the outcome of PET BAT detection. Only patients who had biochemical thyroid profiles within 6 weeks of range from the date of PET scan were included in the study, which may result in a selection bias.

In conclusion, the results of this large PET case series study showed that the main determinants of ^{18}F -FDG detected BAT prevalence, mass, and activity are age, sex, BMI, outdoor temperature and diabetes status. Thyroid hormones have no influence on BAT activation in mild thyrotoxic state. Major implications of these findings are public health messages: escalation of weight losing life style measures of exercise to reduce BMI, which will also may encourage environmental cold exposure; and reducing thermostat of indoor living spaces. Whilst awaiting the solutions of anti-obesity BAT therapeutic manipulation methods/drugs, it cannot be ignored that perhaps the safest and simplest way to activate BAT is reducing thermal comfort through mild cold exposure.

Chapter 4

IDENTIFICATION OF BROWN ADIPOSE TISSUE USING MR IMAGING

4.1 Introduction

As stated in Chapter 1.7.3, BAT is postulated as a holy grail for metabolic disease, enhanced and sustained activity of which can potentially prevent obesity, hyperlipidaemia and type 2 diabetes mellitus. It is over a century that BAT was first discovered, described as ‘mulberry cells’ by Dr Betty H Shaw in 1901 (Shaw et al 1901³⁹⁷), yet we do not know its entire anatomy, let alone physiology and therapeutics.

A significant obstacle to the progress of research on human BAT has been the lack of a safe, sensitive, specific and reproducible imaging technique to quantify BAT volume and/or mass. Such a tool would be essential to evaluate the efficacy of novel therapies based on the manipulation of BAT. The mainstay research on human BAT in recent years, including that of our study as described in Chapter 3, have been based on retrospective assessments of images using the technique of ¹⁸Fluoro-2-Deoxyglucose Positron Emission Tomography (¹⁸F-FDG PET), performed clinically mainly for the assessment of tumours and metastases (van Marken Lichtenbelt et al 2009¹⁴², Cypess et al 2009¹⁴¹, Virtanen et al 2009¹⁴⁰). The advent of PET technique has demonstrated BAT in human adults and it delineated the depots: supraclavicular, mediastinal and paravertebral (Virtanen et al 2009¹⁴⁰). Another advantage of PET is that it shows metabolic activity of BAT, focusing on function and metabolism aspects of BAT research. However, ¹⁸F-FDG PET has got limitations as it may not be a reliable research technique to accurately identify BAT in all subjects, or accurately quantify human BAT volume/mas. Images derived from ¹⁸F-FDG PET are therefore influenced heavily by environmental temperature, given the

temperature-dependence of BAT activity as shown in Chapter 3 and in other studies (Zukotynski et al 2009²⁰³, Ouellet et al 2011¹⁶⁶). Furthermore, ¹⁸F-FDG PET involves exposure to potentially harmful ionizing radiation, and is an expensive technique for imaging BAT in humans (Ouellet et al 2011¹⁶⁶).

Several attempts to differentiate BAT from WAT in rodents using techniques such as MR spectroscopy and chemical shift MR have been successful (Lunati et al 1999³⁹⁸, Hamilton et al 2011³⁹⁹). However, the delineation of BAT and WAT in human adults has so far remained elusive. A safe alternative to ¹⁸F-FDG PET as an imaging modality for human BAT, and one that can potentially overcome the obstacles outlined above is MR imaging. BAT and white adipose tissue (WAT) differ in their water:fat ratios due to the different functions of these two tissue types. As illustrated in Figure 1.5.2 and Table 1.5.2, BAT contains abundant mitochondria, whereas WAT consists mainly of triglyceride (Cinti et al 2005²⁰⁵). Therefore, BAT contains proportionately more water and less fat than WAT. This important difference provides a rationale for exploring MR as a potential imaging modality to discern BAT from WAT. As discussed in Chapter 1.6.2 and Chapter 2.2.3, MR technique of Iterative Decomposition of water and fat with Echo Asymmetry and Least-squares estimation (IDEAL) has been used successfully in rats to clearly delineate BAT from WAT (Hu et al 2010²⁰⁶). The lower signal intensity of BAT compared to WAT has been exploited to obtain IDEAL fat-water imaging in rats. As illustrated in Figure 4.2.1.1, reconstructed fat-fraction images, show a broad fat-fraction range for BAT (37-70%), in contrast to a higher and smaller range for WAT (90-93%), in both excised tissue samples and *in situ* (Hu et al 2010²⁰⁶). Intermediate signal intensity in comparison with hypointense subcutaneous fat and hyperintense muscle was noted

on T2- weighted MR images of presumed BAT in supraclavicular and axillary region of a 13-day old neonate (Carter et al 2008²⁰⁷).

The aim of our study was to explore the use of IDEAL MR as a means of identifying BAT in human adults. A further aim was to demonstrate proof of principle that MR is a potential future biomarker for human BAT. This would be an essential step for future novel therapeutic developments for the prevention and management of human obesity through manipulation of BAT.

Therefore the hypothesis for this set of studies was that:

1. Brown Adipose Tissue (BAT) contains more water content than White Adipose Tissue (WAT). IDEAL MRI, with its robust fat-water separation technique, may potentially discern BAT from WAT.
2. Human BAT and WAT may possess similar characteristics as that of rat species, and may aid IDEAL MRI to delineate the two tissues as shown in rodent models.

Therefore the aims of these studies were:

1. To identify brown adipose tissue using IDEAL MR imaging in rat carcass, and reconfirm the results shown by Hu et al 2010
2. To utilise the same IDEAL technique to identify BAT in a human adult volunteer to provide proof of concept.
3. To provide confirmation with histological and immunohistochemical staining.

4.2 Materials and Methods

4.2.1 Proof of concept of IDEAL MRI study on Rat fat samples

BAT and WAT from samples taken from sacrificed rats can be clearly delineated from one another, and provide distinct signals when imaged with existing technology. This has already been demonstrated by Hu *et al.* using 6-echo IDEAL MRI as outlined in Figure 4.2.1.1 (Hu et al 2011²⁰⁶).

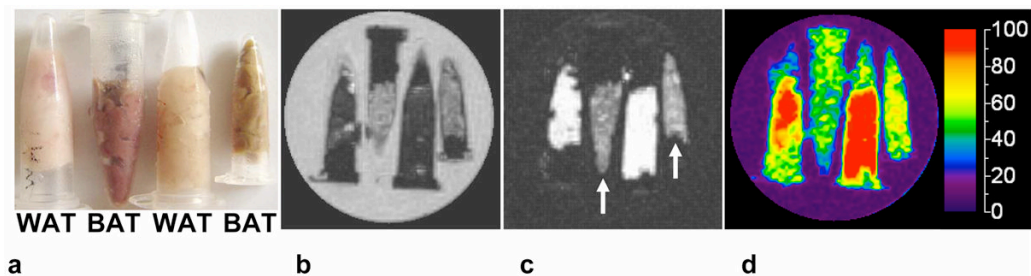


Figure 4.2.1.1 (Hu et al 2011²⁰⁶), IDEAL results from dissected tissues. (a) Brown and white adipose tissue (BAT, WAT) are macroscopically distinct. (b) Water-Only IDEAL, (c) Fat-only IDEAL, and (d) Fat-fraction map: 92%, 51%, 93%, and 62% mean fat-fraction from left to right.

To confirm the concept of IDEAL MRI technique, we chose to reproduce the above Hu *et al* experiment results on a rodent model, the methodology of which is outline in Chapter 2.2.4. In brief, following a normal feeding regimen 2 male Wistar rats (mean mass 300g, age 6-8 weeks), one kept at thermoneutrality (30°C) for 8 hours; the other was kept in the cold (4°C) for 8 hours were sacrificed. The fat samples were dissected to extract Interscapular BAT, Subcutaneous WAT and Omental WAT. The samples were collected into 2 sets of 3 x 2 ml eppendorfs (cold and thermoneutral), and were photographed to demonstrate the macroscopic difference

between BAT and WAT (Figure 4.2.2). The specimens from rat kept in the cold, was transported to the MRI scanner on ice, while those from the rat kept at thermoneutrality, was transported at ambient temperature.

As described in Chapter 2.2.4, MR imaging of cold and thermoneutral rat carcasses, and phantom rat samples were carried on 3T GE MR scanner using IDEAL settings. Images had 2.0mm slice width, 150mm square field of view and 256x256 matrix.

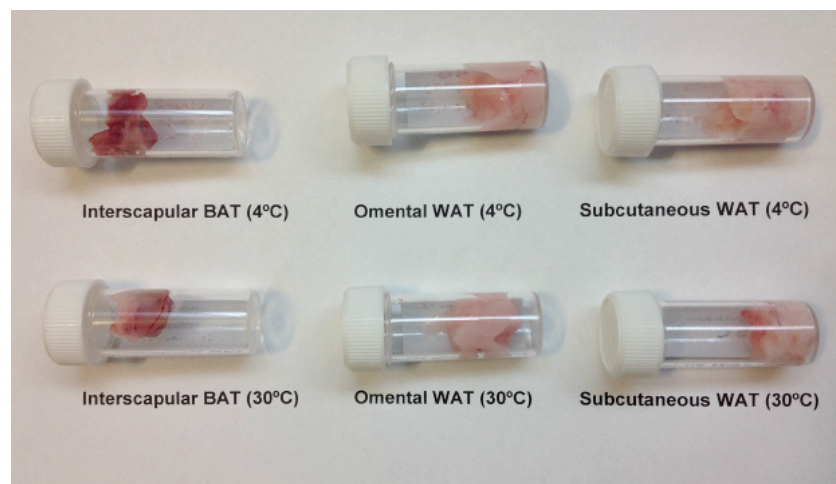


Figure 4.2.1.2: Macroscopic BAT and WAT samples dissected from Wistar rats kept at thermoneutrality (30 °C) and cold (4 °C).

4.2.2 Subject recruitment and case study

A 25-year old Caucasian female (BMI 22.6 kg/m²; waist circumference 90.5 cm; waist/hip ratio 0.93; fasting glucose 4.6 mmol/L; total cholesterol 3.9 mmol/L) was diagnosed with Hyperparathyroidism-Jaw Tumour (HPT-JT) syndrome based on biochemistry and imaging. She was not on regular medication and there was no other

medical history to note. Nuclear imaging detected a 0.5 mm right inferior parathyroid adenoma. In addition, a right-sided mandibular lesion was identified, and following surgical resection, histopathology revealed this to be a giant cell granuloma. HPT-JT syndrome was confirmed genetically, and the mutation shown to be heterozygous for a T to C nucleotide substitution in exon 2 of the gene, *CDC73* (c.191T>C), also called HRPT2 gene, which encodes for parafibromin was identified (Carpten et al 2002⁴⁰⁰). Following successful and complete enucleation of the parathyroid adenoma, the serum parathyroid hormone (PTH) level was partially and transiently elevated, raising a concern of parathyroid carcinoma. The patient therefore subsequently underwent an ¹⁸F-FDG PET-CT scan. This scan was negative for malignancy, but did reveal multiple areas of high ¹⁸F-FDG uptake within suprasternal and mediastinal fat (Figure 4.2.2). Written informed consent for study recruitment was obtained and appropriate ethical approval to perform an IDEAL MR scan was obtained from a Black County Research Ethics Committee (Rec No. 11/H1206/3).

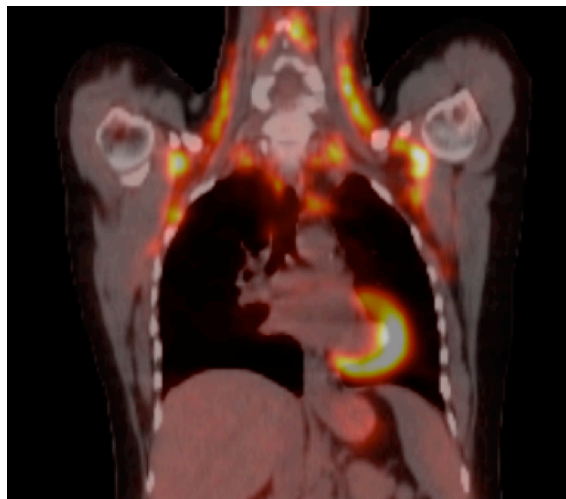


Figure 4.2.2.1 Coronal image of ¹⁸F-FDG PET scan of the study subject exhibiting high physiological ¹⁸F-FDG BAT uptake in cervical, mediastinal and axillary areas

Table 4.2.2.2 Phenotypical characteristics of the human subject

Phenotypical characteristics	Values
Age	25 years
BMI	22.6 kg/m ²
Waist:hip ratio	0.93
Fasting glucose	5 mmol/L
Fasting insulin	105 pmol/L
Total cholesterol	3.9 mmol/L
HOMA2-IR	1.9
Resting metabolic rate	1403 kCal/day
Genetic diagnosis	HRPT2 gene: T to C nucleotide substitution in exon 2 of the gene, <i>CDC73</i> (c.191T>C)
Brown fat mass	516 grams
Brown fat Total Lesion glycolysis (TLG)	2414 grams
Brown fat tissue activity	14556 kBq
Temperature on the day of PET scan	Outdoor temperature: 8.5° Celsius Room temperature: 23° Celsius

BMI- Body mass index; HOMA2-IR- Homeostatic model assessment 2-Insulin resistance; PET- Positron emission tomography

4.2.3 Positron-emission tomography scanning

PET was performed on a GE Discovery STE PET-CT scanner (General Electric Medical Systems, Milwaukee, USA). Two sets of emission data were obtained; from the skull base to mid thigh (with arms elevated); and the head and neck protocol (without elevation of arms). In accordance with standard administration and acquisition protocol, the subject was fasted for 6 hours, and 375 MBq of ¹⁸F-FDG

radiotracer was injected one hour prior to the scan. Emission data was obtained for 3 minutes in each bed position. PET images were reconstructed using the computed tomography (CT) data for attenuation correction.

4.2.4 Magnetic resonance scanning

A 3-echo IDEAL sequence (Reeder et al 2004⁴⁰¹, Reeder et al 2005³⁷²) was performed on a 3T GE HDxt scanner (General Electric Medical Systems, Milwaukee, USA). The cardiac coil was placed around the cervical and upper thoracic regions. Axial images with a 5mm slice thickness were obtained from the upper cervical to mid-thoracic level. The T1 weighted IDEAL sequence parameters were: TR 440 ms, TE 10.8 ms, acquisition matrix size 320 x 256, NEX 3 and field of view of 30 cm. This generated water-only and fat-only (fat:IDEAL) images, of which the latter were used for subsequent analysis.

A baseline MR scan was performed the same month as the PET-CT (December) upon which subsequent image analysis was performed. A second MR was performed 2 months later using identical imaging parameters (apart from the field of view which was 34 cm), to determine whether there was any temporal variation in the distribution of BAT.

4.2.5 Retrospective image analysis

This analysis used Region of Interests (ROIs) of high radiotracer uptake on the PET-CT (considered to be BAT) transposed onto the fat:IDEAL MR images. To achieve

this, the PET-CT and enhanced MR images were co-registered using a combination of multi-modal rigid and non-rigid registration, employing image fusion software Mirada XD 4.3 (Mirada Medical Ltd, Oxford, UK) to facilitate direct positioning of ROIs between the images. Visual comparison and manual registration using vascular landmarks was employed when there was doubt.

Image analysis was then performed on the MR images using ImageJ 1.45s (National Institutes of Health, USA). MR images were enhanced using the automated contrast enhancement and sharpen algorithms within ImageJ. ROIs were drawn on the MR scans around areas corresponding to greater-than-background levels of ^{18}F -FDG uptake within adipose tissue on the PET-CT scans, indicating BAT. These ROIs on the MR images, derived from ^{18}F -FDG uptake on PET, will be referred to as 'BAT_{retro}'. Radiotracer uptake in paravertebral regions was not assessed due to the difficulties of accurately identifying these areas on MR.

The MR signals within the BAT_{retro} ROIs were compared with those from immediately adjacent adipose tissue to determine differences in signal intensity. These areas will be referred to as WAT_{retro}. The MR images were scrutinized with regard to adjacent image slices to ensure that any perceived variation in MR signal did not represent partial volume (or volume averaging) artefact.

Differences in signal intensity in BAT_{retro} and WAT_{retro} ROIs were compared using the Wilcoxon matched pairs test (or paired t test) using GraphPad Prism version 5.00 (GraphPad Software, San Diego California USA). Subsequently, a one-way

ANOVA was performed to determine whether the $BAT_{\text{retro}}:WAT_{\text{retro}}$ signal ratios varied according to anatomical location.

4.2.6 Prospective image analysis

This analysis method positioned ROIs directly on the MR images, based on differences in signal intensity observed between BAT_{retro} and adjacent adipose tissue identified during the retrospective analysis. To reduce recall bias, 4 months later a single radiologist drew ROIs around areas of adipose tissue on the baseline MR scans that exhibited discrete low signal intensities in relation to neighbouring adipose tissue postulated to represent islands of BAT (BAT_{prosp}). ROIs were restricted to adipose tissue within the upper mediastinum, base of the neck and supraclavicular fossae.

4.2.7 Histology and Immunohistochemistry

Histology and immunohistochemistry were performed on tissue obtained during parathyroidectomy, corresponding with high ^{18}F -FDG uptake on the PET-CT scan and low-signal intensity on the fat-only MR scan. Samples were prepared for morphology by keeping in formalin until moulded in paraffin and stained with haematoxylin-eosin (HE). For immunohistochemistry, Vectastain Elite ABC Kit (Vector Laboratories, PK-6101) and rabbit anti-UCP1 (1:500, Sigma U6382) were used according to the manufacturer's protocol.

4.3 Results

4.3.1 IDEAL MRI results from Rat imaging

Fat-fraction map on the rat phantom samples, showed BAT (40-60%) in fluorescent green, clearly delineated from WAT (>80%) in orange, based on fat-fraction map as shown in Figure 4.3.1.1. Skeletal muscle tissue contains more water than fat, and incidental presence of muscle displayed blue. There was no difference in mean fat fraction between interscapular BAT at 4°C and 30°C. Both fat-only IDEAL images and fat-fraction IDEAL images of rat carcass samples exhibited clear delineation of BAT from WAT as illustrated in Figure 4.3.1.2. This confirms the reliability and reproducibility of IDEAL technique in differentiation of BAT and WAT in rats.

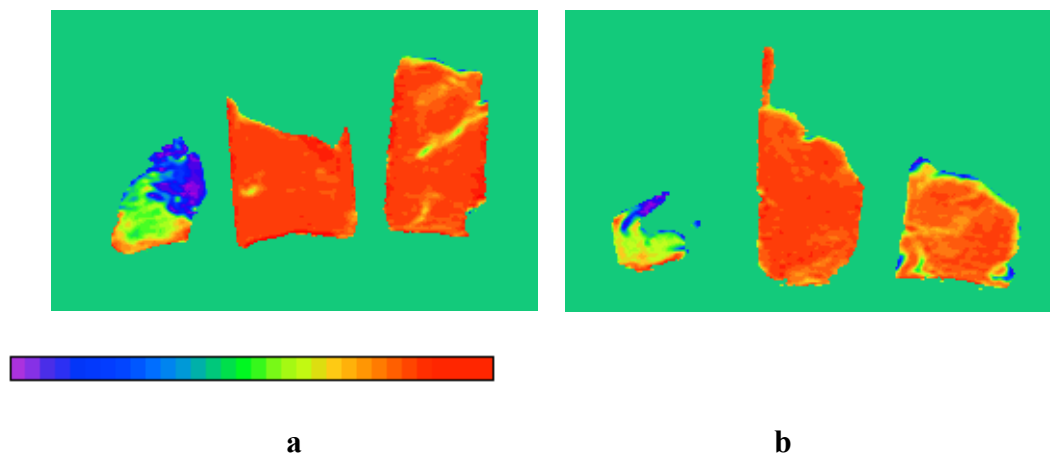


Figure 4.3.1.1 a) Fat-fraction images of dissected BAT, Subcutaneous WAT and Omental WAT (from left to right), from rats kept at 4°C, and, **b)** at 30°C. Images are coloured in 10% increments. The areas of blue correspond to skeletal muscle, orange is WAT and green/yellow is BAT.

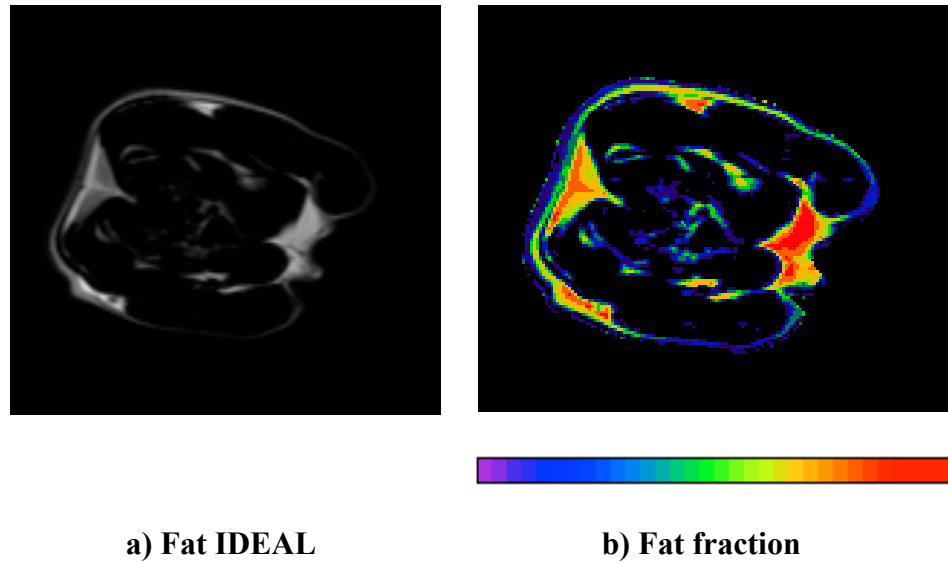


Figure 4.3.1.2 Axial MR slices through the upper thorax showing a) Fat-IDEAL and b) Low fat-fraction corresponding to BAT in the interscapular region

4.3.2 IDEAL MRI results from Human imaging- Retrospective image analyses

111 regions of ^{18}F -FDG uptake on PET were identified which were consistent with BAT (Figure 4.3.2.1). 25 ROIs were within the upper mediastinum, 41 within the supraclavicular fossae, 31 within the neck, and 14 in the axillae (Table 1). These ROIs of increased ^{18}F -FDG uptake had a total cumulative surface area of $9,031 \text{ mm}^2$, of which the majority occurred within the mediastinum and supraclavicular regions.

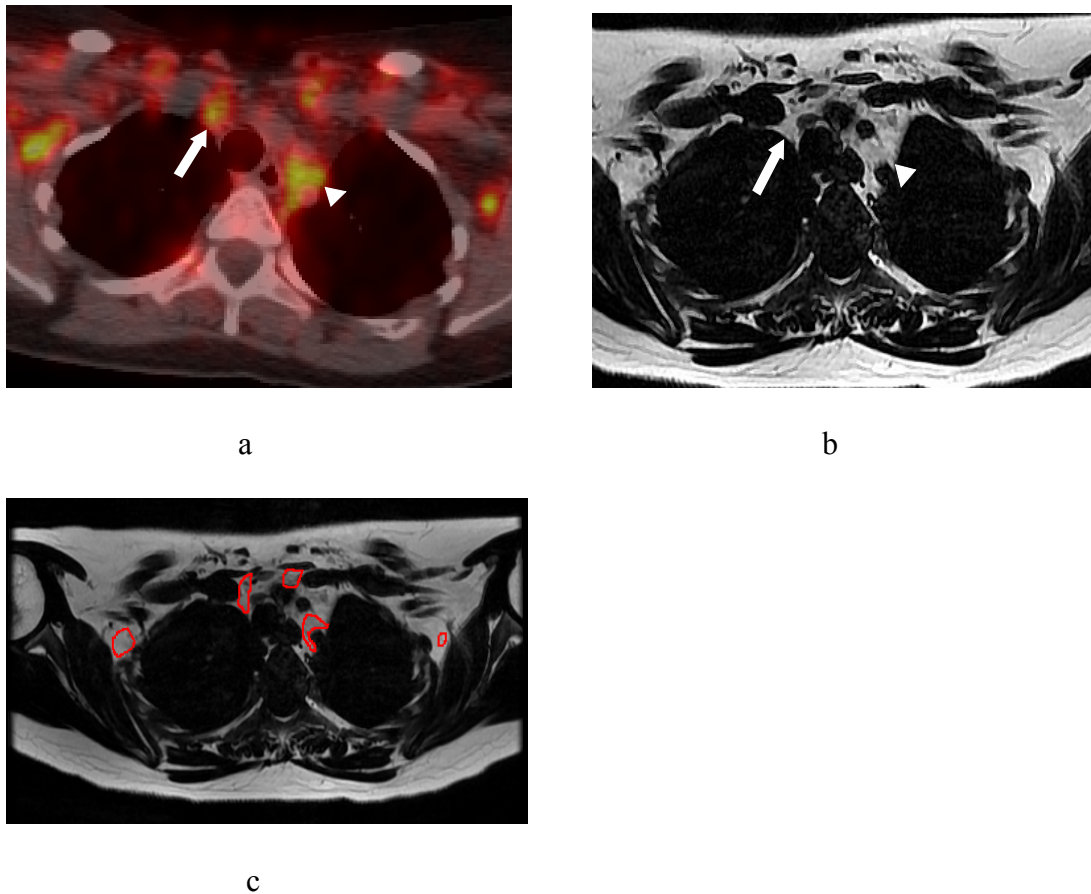


Figure 4.3.2.1 (a): Axial PET-CT image showing 18F-FDG uptake consistent with BAT in mediastinum (arrowed); **(b):** Fat:IDEAL MR image demonstrating low signal areas within the mediastinal fat (arrows) corresponding to BAT on PET-CT; **(c):** ROIs were drawn around high 18F-FDG uptake and transferred onto registered fat-only images.

Visual comparison of the MR signal within these BAT_{retro} ROIs and adjacent adipose tissue (WAT_{retro}) revealed differences in signal between the two. The BAT_{retro} ROIs had a lower signal than surrounding adipose tissue, and were often delineated by a discrete margin, as shown in Figure 4.3.2.1.b.

Overall 93 of the 111 BAT_{retro} ROIs (83.8%) had a lower MR signal than adjacent adipose tissue, although this did vary according to anatomical site (Table 4.3.2.2).

25/25 (100%) of the BAT_{retro} ROIs in the upper mediastinum had a lower MR signal than adjacent adipose tissue, 29/31 in the neck (93.5%), 31/41 in the supraclavicular fossae (75.6%) and 8/14 in the axillae (57%). A significant difference was found between the MR signal within BAT_{retro} and WAT_{retro} ROIs (Table 4.3.2.3) using the Wilcoxon matched pairs test, in all but the axillary region. Signal intensity varied considerably along the B₀ axis (*i.e.* in a cranio-caudal direction), with a ten-fold difference in signal intensity between the cranial (neck) images and the caudal (mediastinal) images (Figure 4.3.2.4). There was no correlation between the level of the MR slice and the BAT:WAT signal ratio. There was, however, variation in the BAT_{retro}:WAT_{retro} signal ratio according to anatomical region (Figure 4.3.2.5), with significantly lower signal ratio ($p < 0.0001$ found using the one-way ANOVA) within the mediastinum and neck (*i.e.* lower BAT signal with respect to WAT) than in the supraclavicular fossae and axillae.

Table 4.3.2.2 For each anatomical region the number of BAT_{retro} ROIs with low and normal signal intensity on MR is tabulated. The ROIs were retrospectively drawn on MR from areas of corresponding high ¹⁸F-FDG uptake on the PET-CT images.

Anatomical region	No of BAT_{retro} ROIs with lower signal with lower MR signal than adjacent fat	Number of BAT_{retro} ROIs with similar MR signal to adjacent fat	Total number of ROIs	Total area of ROIs (mm²)
All regions	93	18	111	9,030
Mediastinum	25	0	25	2,348
Supraclavicular	31	10	41	3,313
Neck	29	2	31	1,451
Axillae	8	6	14	1,918

Table 4.3.2.3 Variation in BAT_{retro} and WAT_{retro} MR signal intensity and BAT:WAT signal ratio according to anatomical region

Anatomical region	Mean BAT_{retro} MR signal	Mean WAT_{retro} MR signal	Significance P value	Signal ratio BAT:WAT
All	485 (±229)	549 (± 260)	<0.0001	0.89 ± 0.12
Mediastinum	586 (±145)	750 (±197)	<0.0001	0.79 ± 0.11
Supraclavicular	541 (± 68)	594 (±90)	<0.0001	0.92 ± 0.12
Neck	196 (± 116)	219 (± 125)	<0.0001	0.89 ± 0.09
Axillae	783 (± 189)	788 (±184)	NS	0.99 ± 0.08

BAT- Brown adipose tissue; WAT- White adipose tissue; ROI-Region of interest; MR- Magnetic Resonance; P<0.05- significant

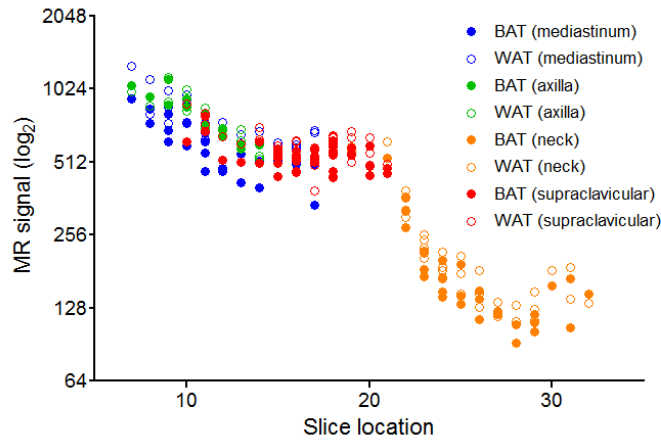


Figure 4.3.2.4: Variation in BATretro and WATretro signal according to slice and anatomical site, showing a ten-fold increase in signal intensity between cranial (neck) and caudal (mediastinal) MR slices

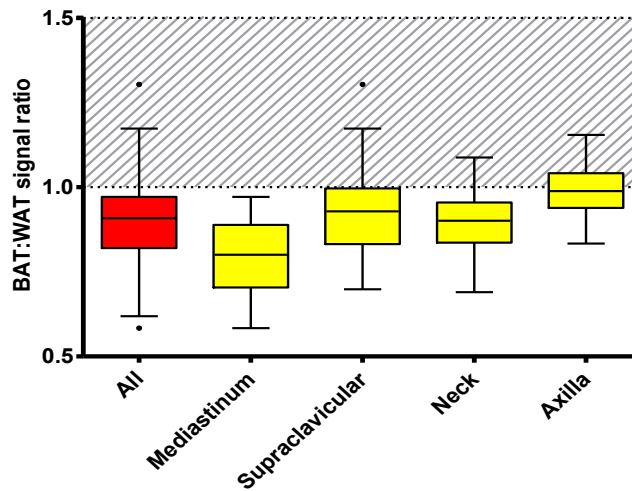


Figure 4.3.2.5: Variation in BATretro:WATretro signal ratio according to anatomical location, with significantly lower signal ratio within mediastinum and neck. The shaded area represents a ratio >1 (i.e. WATretro signal > BATretro signal).

The repeat IDEAL MR scan demonstrated little change in the distribution of low signal regions. There are persistent areas of well-circumscribed low signal change

within the anterior mediastinum and suprasternal notch in a similar distribution to those identified on the comparable slice from the baseline MR (Figure 4.3.2.6).

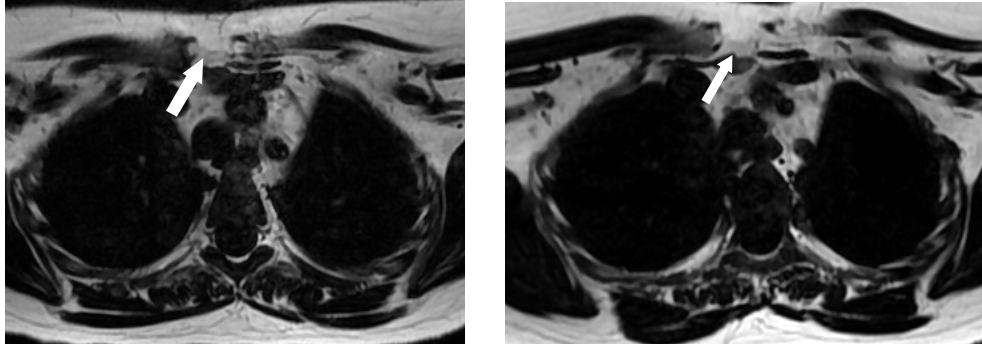


Figure 4.3.2.6: a) Baseline MR; b) Repeat axial fat:IDEAL MR image of the upper thorax performed 2 months after the baseline MR scan, showing a similar distribution of putative BAT within the anterior mediastinum and suprasternal notch.

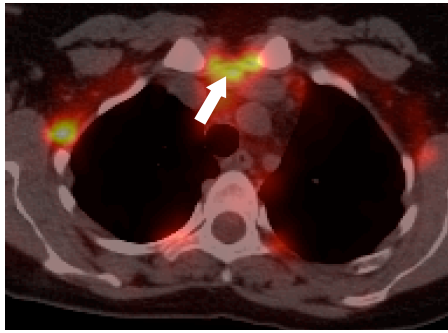
4.3.3 IDEAL MRI results from Human imaging- Prospective image analyses

Fifty-four ROIs were prospectively identified on MR by a single investigator on the basis of having discrete areas of low signal intensity with respect to adjacent adipose tissue, and were presumed to represent BAT ('BAT_{prosp}'). The total cumulative surface area of these BAT_{prosp} ROIs was 6,207mm², compared with 5,661 mm² in the mediastinum and supraclavicular fossae in BAT_{retro} ROIs. The total surface area of the 54 BAT_{prosp} ROIs comprised 2.4% of the total surface area of adipose tissue examined (257,181mm²). When these BAT_{prosp} ROIs were then compared with the PET-CT scans, 47/54 ROIs (87%) coincided with areas of ¹⁸F-FDG uptake.

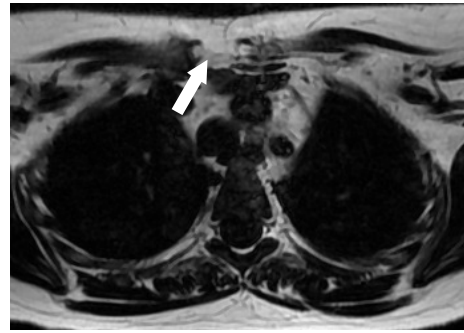
4.3.4 Histology and Immunohistochemistry

Haematoxylin-eosin staining of fat tissue obtained from the suprasternal area (as marked by the white arrowhead in Figure 4.3.4) demonstrates smaller multilocular cells with multiple small lipid droplets (yellow arrowhead in Figure 4.3.4.c) consistent with BAT as opposed to larger unilocular WAT (white arrowhead in 4.3.4.c) (Cinti et al 2005²⁰⁵). BAT was also unequivocally confirmed on immunostaining with anti-serum against rabbit UCP1, (Figure 4.3.4.d) as BAT has abundant mitochondria containing UCP1, as elegantly shown in multiple rodent as well as human studies (as illustrated in Chapter 1.5.2, Chapter 1.5.3) (Heaton et al 1978¹⁵⁰, Aquila et al 1985⁴⁰², Saito et al 2009¹⁴³, Lowell et al 1993³⁹², Zingaretti et al 2009¹⁴⁴).

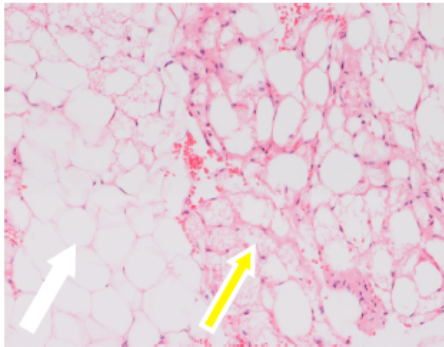
Although samples were collected prior imaging procedures, our study subject amply demonstrates morphological and immuno-histological correlation in the ROI corresponding to brown fat in both PET and MRI, thus also corroborating the presence of BAT in humans.



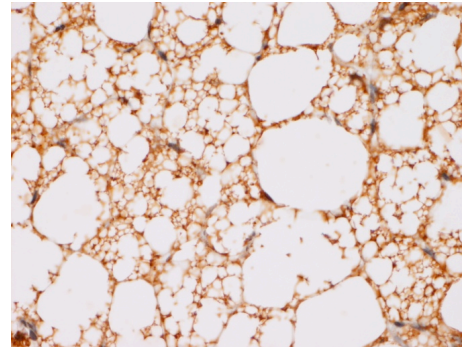
a



b



c



d

Figure 4.3.4: (a) ^{18}F -FDG uptake within the suprasternal notch on PET-CT (arrow); (b) fat:IDEAL MR at the same level showing corresponding low signal in the suprasternal notch; (c) Haematoxylin-Eosin staining and (d) UCP1 immunostaining providing confirmation of BAT obtained from this area.

4.4 Discussion

At the time of publication of this study, we reported for the first time, verification of BAT in a living human adult using MR imaging. We have shown MR scanning confirmation of presumed BAT from comparisons with ^{18}F -FDG PET images. We also provided histological and immunohistochemical confirmation of BAT in samples taken from a low fat signal region identified prospectively on the MR images. The $\text{BAT}_{\text{prosp}}$ images revealed clear delineation and unequivocal differences ($p < 0.001$) in signal intensities between BAT and the adjacent WAT. The $\text{BAT}_{\text{prosp}}$ ROI signals appeared more heterogeneous than the surrounding WAT signals, particularly in the mediastinal and midline neck areas. We believe that this signal pattern is entirely consistent with these ROIs being from BAT, and indeed the pattern that what one would expect given the characteristic histological appearance of human BAT often occurring in many islets within surrounding WAT (Cinti et al 2000)

The technique of ^{18}F -FDG PET currently represents the gold standard for imaging human BAT in the research setting. PET-CT is also performed for clinical reasons, often for identification and monitoring of malignancy. PET-CT provides data on the metabolic activity of tissues, and therefore only provides information on BAT activity. It follows therefore, that inactive BAT would not be identified on PET-CT. MR differs fundamentally from PET-CT in that MR provides anatomical information, and the images generated are not dependent upon tissue activity. Therefore, a key advantage of MR over PET-CT is that this imaging modality offers the potential to measure BAT volume regardless of its activity, and thereby could be

developed, to provide an accurate and reliable biomarker for human BAT. Another advantage of this approach is that BAT activity (resulting from variations in daily temperatures for example) would not be expected to influence the measurements derived from the MR images. Furthermore, MR is an entirely safe imaging modality with no associated exposure to harmful ionizing radiation, in contrast to ^{18}F -FDG PET-CT, MR is also comparatively cheap.

Previous MR studies have successfully identified BAT in rodents both in inactive (Lunati et al 1999³⁹⁸, Hu et al 2010²⁰⁶, Sbarbati et al 1997^{206,403,404}) and in active state (Sbarbati et al 2006⁴⁰⁵). We based our study on Houchun Hu's study using IDEAL MR fat-water imaging technique, which observed a broad fat fraction range (37-70%) in mouse BAT, in comparison to a tighter and higher range for WAT (90-93%) (Hu et al 2010²⁰⁶). The same group have also shown lower T2* relaxation and Proton-density fat fraction in BAT compared to WAT in mice (Hu et al 2012⁴⁰⁶). The challenge lies in extrapolating these gains on to *in vivo* human studies to non-invasively characterise inactive BAT. BAT in rodents is well localised and hence easily studied, whereas anatomy and function of BAT in humans are yet to be characterised. Furthermore, WAT in some areas is thought to be amenable for transcription into BAT (Wu et al 2012¹⁴⁶, Seale et al 2008¹⁸²), which poses new challenges to image a constantly dynamic tissue. In general, *in vivo* BAT in humans using non-invasive modalities is yet to be demonstrated and our study aims to address this relevant question.

T2-weighted images of presumed BAT found bilaterally in supraclavicular and axillary region of a prematurely born 13-day old live neonate, demonstrated

intermediate signal intensity on a clinical MR sequence in comparison to hyperintense muscle and hypointense subcutaneous fat (Carter et al 2008²⁰⁷). MR appearances of 8 consecutive hibernomas (benign, slow-growing, soft-tissue tumours resembling brown adipose tissue) detected in human adults, demonstrated diffusely hypointense signals compared to the surrounding subcutaneous WAT (Lee et al 2006⁴⁰⁷). In a postmortem study of a 3-month old infant, Hu et al demonstrated a lower fat-fraction for BAT (41.9+/-6.25%) in comparison to higher fat-fraction for WAT (>90%), using chemical shift two-point 3D spoiled gradient echo pulse sequence on a 3-Tesla MR scanner (Hu et al 2012⁴⁰⁸). In comparison to previous MR studies which were done on mouse and postmortem human models, our study demonstrates unequivocal identification of adult human inactive BAT *in vivo*, whilst also reiterating the feasibility of BAT imaging by IDEAL MR.

Our study has some unavoidable limitations. It is possible (although not likely) that adipose tissue may be affected in some way in HPT-JT syndrome, which may in turn affect signal intensity on MR imaging. However, the histology and immunohistochemistry of fat samples obtained from this patient showed the characteristic features of BAT and WAT, similar to those from other studies on human adults without HPT-JT syndrome, thus proving that the morphology demonstrated is not disease related (van Marken Lichtenbelt et al 2009¹⁴², Saito et al 2009¹⁴³, Virtanen et al 2009¹⁴⁰). A further potential limitation is that transposing areas of ¹⁸F-FDG uptake on PET-CT onto MR images may introduce bias. To limit this potential bias, the ¹⁸F-FDG PET-CT and MR scans were performed with the patient adopting a similar position with their arms down in accordance with the standard head and neck PET-CT protocol. Another limitation is that the MR axial

images had a 5-mm slice thickness. It is possible that greater differentiation of BAT from WAT signal could be obtained through a smaller slice thickness. Regardless of slice thickness, this does not detract from the main outcome of this study, which is the clear identification of BAT and delineation from WAT on MR images.

In summary, at the time of publication of this study, we reported for the first time, demonstration of BAT, clearly delineated from adjacent WAT, in a living human adult using the technique of IDEAL MR. Our study provides a framework for future studies on MR-based detection of BAT in human adults. We provide proof of principle that IDEAL MR could be developed as a tool to provide an accurate, reliable and reproducible radiological tool for human BAT. Such a tool would be invaluable in the future pursuit of novel therapeutics to combat the global obesity epidemic through manipulation of facultative energy expenditure, BAT volume being a key modifiable contributor to such an approach.

Chapter 5

EFFECT OF MEAL DURATION ON DIET INDUCED THERMOGENESIS AND BIOCHEMICAL METABOLIC MARKERS

Definition of Fletcherism:

*.... the practice of eating in small amounts and only when hungry, and of chewing
one's food thoroughly*

Merriam-Webster dictionary

Fletcher, Horace (1849-1919), American dietician.

Fletcher was plagued by obesity and indigestion most of his life. Then in 1895 he set out to find the key to good health. He developed a set of principles, which he proceeded to propagate. The basic tenets were these: one should eat only when genuinely hungry and never when anxious, depressed, or otherwise preoccupied; one may eat only food that appeals to the appetite; one should chew each mouthful of food 32 times or, ideally, until the food liquefies; one should enjoy one's food.

5.1 Introduction

The global obesity epidemic is showing no signs of abating. Obesity and its associated problems constitute the biggest threat to the health of our species, and form a major component of the global healthcare economy (Danaei G et al 2011⁴⁰⁹). It is imperative that novel strategies to tackle obesity are developed and implemented. To mitigate the adverse impact of obesity on global health and health-care economies, a multi-faceted approach is required. Such an approach should incorporate the development of novel pharmacological strategies, re-design of our living spaces for enhanced energy expenditure (EE), governmental approaches to improve our diet and obesogenic environment and cultural and lifestyle changes, particularly for our children.

Diet is a major determinant of fat mass, and an obvious target for the prevention and management of obesity (Forget et al 2013⁸⁴). It appears that behavioural and nutritional strategies that can help control appetite and energy intake should be developed and tested for their efficacy in body-weight management. Food-related lifestyle factors such as meal frequency (La Bounty et al 2011¹⁰³), macronutrient composition (Karhunen et al 2008⁴¹⁰), and viscosity (Juvonen et al 2009⁴¹¹) are studied. Other dietary factors are worthy of further exploration, and this includes duration of meal.

Many characteristics of meals have been shown to promote energy intake in feeding studies, including large portion size (Orlet Fisher et al 2003⁴¹², Levitsky et al 2004⁴¹³) rapid eating rate (Kral et al 2001⁴¹⁴), energy density (Kral et al 2004⁴¹⁵,

Karl et al 2013⁴¹⁵) low levels of dietary fibre (Burton-Freeman et al 2000⁴¹⁶), high palatability (McCroy et al 2006⁴¹⁷), high fat content (Prentice et al 1998⁴¹⁸), high glycaemic load Ludwig et al 1999⁴¹⁹), and high sugar content of diet in liquid form (DiMaggio et al 2000⁴²⁰). It appears that meal duration is perhaps the only non-nutritional factor amongst the above key parameters, and along with meal frequency constitutes a potentially modifiable behavioural entity towards reduced energy intake.

According to Webster dictionary, 'to gorge' means 'to swallow in large mouthfuls or quantities' or 'with greediness'. Ubiquity of fast foods has encouraged excess 'gorging', reflecting increased portion size and quicker eating rates, resulting in increased energy intake (French et al 2001⁴²¹). In a large self-reported survey conducted on Japanese civil servants, faster eating was directly proportional to BMI, and the survey concluded that faster eating leads to obesity (Otsuka et al 2006¹¹⁰). Multiple feeding studies in humans show faster eating rates increase energy intake during single meals (Andrade et al 2008¹⁰⁶, Martin et al 2007¹⁰⁷, Zandian et al 2009¹⁰⁸ and is associated with higher BMI (Hill et al 1984¹⁰⁹, Otsuka et al 2006¹¹⁰, Maruyama et al 2008¹¹⁰). This observation is also supported by several animal studies (Clifton et al 1984⁴²², Sclafani et al 1994⁴²³, Lucas et al 1988⁴²⁴).

Contrarily, eating slowly is often advised for weight management as slower eating is thought to allow satiation to be perceived before too much energy is further consumed (Stuart et al 1972⁴²⁵). Appetite is regulated by a variety of neuro-endocrine signals including gut and pancreatic hormones such as glucagon-like peptide-1 (GLP-1), ghrelin, pancreatic polypeptide (PP), peptide-YY (PYY), insulin,

adiponectin, leptin and non-esterified fatty acids (NEFA) (Wren et al 2007²⁷⁷). It has been proposed that slower rates of ingestion allow more time for these peripheral signals to act, lengthen satiety's duration, and reduce total energy intake (Martin et al 2007¹⁰⁷, Stuart et al 1972⁴²⁵).

Controversy exists in the current literature regarding the effects of meal duration on weight, appetite, food ingestion and metabolism (Tanihara et al 2011⁴²⁶, Sasaki et al 2003⁴²⁷, Otsuka et al 2006¹¹⁰, Maruyama et al 2008¹¹¹, Pliner et al 2006⁴²⁸, Sobki et al 2010⁴²⁹, Brindal et al 2011¹¹²). As mentioned in chapter 1.7.1, manipulation of BAT may provide an answer to obesity, and BAT is implicated in DIT (which constitutes 10% of TEE) as demonstrated extensively in both animal studies (Glick et al 1984²³⁵, Glick et al 1984²³⁴), as well as human PET studies (Orava et al 2011¹⁷⁶, Vosselman et al 2013²³⁶). There are no studies so far in the literature looking at the effect of meal duration on DIT. It is therefore timely to develop a clearer understanding and insight into the metabolic effects of slower eating, including postprandial energy expenditure. Such insight will aid formulating future public health messages regarding population-wide weight-loss strategies based on food-related behaviour such as meal duration to tackle the worsening obesity epidemic.

Therefore the hypothesis for this set of studies was that:

1. Slower eating rate (increased meal duration) increases postprandial energy expenditure (through prolonged increase in DIT) in obese subjects.
2. Change in meal duration may cause metabolically favourable postprandial pancreatic and gut hormonal effects in obese subjects.
3. Hunger and satiety are not affected by meal duration since the overall calorie intake remains the same.

Therefore the aims of these studies were:

1. To establish whether longer meal duration compared to shorter duration increases energy expenditure in obese normoglycaemic females.
2. To ascertain whether meal duration affects circulating insulin, glucose, lipids, GLP-1, ghrelin, PYY, PP, leptin and adiponectin levels in obese normoglycaemic females.
3. To ascertain whether meal duration affects appetite (assessed both on a visual analogue scale [VAS] and through ingestion of a standard buffet).

5.2 Methods

5.2.1 Subjects

The methodology for this study is discussed in detail in Chapter 2.3. All subjects (n=10) were recruited from the Obesity clinic at the Warwickshire Institute for the Study of Diabetes, Endocrinology and Metabolism (WISDEM) centre at the University Hospitals Coventry and Warwickshire (UHCW), as described in Chapter 2.3.2. In brief, all 10 subjects were obese (BMI $>30\text{Kg m}^{-2}$) adult pre-menopausal women, with normoglycaemia (based on fasting and postprandial plasma glucose measurements, and no past history of dysglycaemia). All subjects were white Caucasian non-smokers and none had any other medical problems. Specifically, none had any weight-related conditions such as Polycystic Ovary Syndrome, Cushings Syndrome, Obstructive Sleep Apnoea or other adverse metabolic sequelae. Exclusion criteria included prior bariatric surgery, weight-loss medication or actual weight-loss of $>2.5\text{kg}$ up to three months prior to recruitment and dislike of the standard meal. Inclusion and exclusion criteria are as outlined in section 2.3.2. All subjects had received standard lifestyle advice (dietary modification and exercise) from a specialist dietician prior to inclusion in the study. All clinical investigations were conducted in accordance with the guidelines in the Declaration of Helsinki. All subjects provided fully informed written consent, and a local Research Ethics Committee in the United Kingdom approved the study.

5.2.2 Protocol: Anthropometry, calorimetry and meal duration

Following informed consent, each subject was invited to undergo metabolic studies on two separate days in Whole-Body Calorimeters (WBC) at the Human Metabolism Research Unit (HMRU), a University of Warwick and UHCW NHS Trust facility. HMRU facility and mechanism of WBCs are discussed in detail in Chapter 2.3.6.

The two WBC metabolic studies were executed within 2 weeks of each other. Subjects were instructed to avoid caffeine ingestion and strenuous physical activity for 24-hours preceding each visit, and to adhere to their normal diet and physical activity schedules. Subjects were fasted for 12 hours prior to commencement of each metabolic study. On each study day, the subject was requested to arrive at HMRU in a fasted state on the morning of their study. Prior to their first WBC metabolic study, waist circumference, BMI and body composition (fat mass and fat percentage) was measured, the latter with a BodPod using air displacement plethysmography as outlined in Chapter 2.3.5.

Baseline fasting blood tests were taken following which the subject entered the WBC at 0900h. On entry into the WBC and for the first 120 minutes of the metabolic study, each subject was requested to lie still on the bed to allow for equilibration and to provide an estimate of baseline resting EE. During postprandial periods, subjects watched TV or read quietly with minimal ambulation.

For each study day, standard lunch was provided at 1200h. The same standardised lunch (designed and prepared by a specialist weight-management dietician) was

served for all the metabolic studies. The standard lunch (ham sandwich, yoghurt, banana, biscuit and orange juice drink) contained a total of 763kcal; 50% carbohydrate, 18% protein, and 32% fat. On their first metabolic assessment day, each subject was served standard lunch, with caloric content of the meal divided equally into eight separate food boxes, the food contents of each box eaten over 5 minutes for a total meal duration of 40 minutes (the lunch being completed by 1240h). This is referred to as 'D40'. For the second metabolic assessment (on a different day), an identical protocol was followed except that the duration of the standard lunch was 10 minutes rather than 40 minutes. For this assessment, the caloric content of the standard meal was divided into two halves, with the food contents of each box being eaten over 5 minutes for a total meal duration of 10 minutes (the lunch being completed by 1210h). This is referred to as 'D10'. Subjects were provided with timers and were monitored by study investigators to ensure compliance with eating rate. Subjects were instructed to vary chewing speed accordingly.

5.2.3 Protocol: Postprandial phase

During the 4-hour postprandial phase, subjects were requested to remain seated in the WBC with minimal activity and to refrain from ingestion of food or drink. Blood tests were taken at pre-defined time-points (at baseline, 30-, 60-, 90-, 120-, 180- and 240-minute intervals). The timing of the postprandial blood tests was determined by the *end-point* of the standard meal (to avoid taking any blood tests during the D40 meal), ie. time '0' was defined by the *end* of the meal: for D40 at 1240h and for D10 at 1210h. Blood was taken from an arm placed through a hatch of the WBC, a plastic

cover used to avoid any air exchange with the WBC. All samples were spun in a centrifuge immediately, and serum samples frozen at -80°C. Appetite was assessed just prior to each blood test through use of VAS. At 1700h, subjects were invited to leave the WBC and offered an *ad libitum* standard buffet meal, consisting of various cold foods (sandwiches, chocolate bars, fruit, sausage rolls and drinks). The caloric content and macronutrient composition of the *ad libitum* food ingested was calculated. DIT ($[\text{Postprandial EE} - \text{Baseline EE}]/\text{Amount of calorie ingested}$) was calculated using validated methods reported in literature, as outlined in Chapter 2.3.7.

5.2.4 Biochemical evaluation

Fasting baseline serum samples taken at the first metabolic study for each subject were analysed for lipid profile (Total Cholesterol, LDL Cholesterol, HDL Cholesterol and Triglycerides), HbA1C, glucose, 0900h cortisol, Insulin-like Growth Factor 1 (IGF1), Thyroid Stimulating Hormone (TSH), free T4, Testosterone, Sex Hormone Binding Globulin (SHBG) and 25-hydroxycholecalciferol. Postprandial and pre-lunch blood samples (D40 and D10) were analysed for Ghrelin, Leptin, PYY, GLP-1, Adiponectin, Cortisol, Insulin, Glucose, Total Cholesterol, LDL Cholesterol, HDL Cholesterol, Triglycerides, Endotoxin and NEFA, at predefined time points (at baseline, 30-, 60-, 90-, 120-, 180- and 240-minute intervals). The methodology of collection of blood samples and laboratory analyses are outlined in Chapter 2.7.11, Chapter 2.7.12, Chapter 2.7.13 and Chapter 2.7.14. Insulin resistance was calculated using HOMA-IR method as outlined in Chapter 2.7.15.

5.2.5 Statistical analyses and power calculations

Statistical analyses were conducted in SPSS (version 21 Windows; SPSS Inc., Chicago, IL) and Microsoft Excel. Paired sample t-tests were used for comparisons of 4-hour postprandial 'Area Under the Curve' (AUC) metabolic and biochemical data between D40 and D10. Each subject acted as their own control thereby limiting confounding. We had >80% power to detect a between-meal duration difference exceeding 50% of a Standard Deviation (SD) for plasma glucose from D10 and D40 ($\alpha=0.05$). A P-value <0.05 was considered significant. Data are shown as mean and SD. AUC was calculated using the validated Trapezoid method in Excel (Pruessner et al 2003³⁸⁰).

5.3 Results

5.3.1 Baseline anthropometric, clinical and biochemical data

Baseline anthropometric, clinical and biochemical (fasting) data from measurements taken prior to entry into the WBC on the first visit are shown in Table 5.3.1. The age [mean (SD)] of the subjects was 41.8 years (6.9). All subjects were obese by definition with BMI [mean (SD)] of 42.1Kgm⁻² (4.6), and fat percentage [mean (SD)] of 50.7% (7.4). By definition, all subjects had normal fasting glucose and HbA1C, with mean (SD) values being 4.7mmol/l (0.6) [84.7mg/dl (10.8)], and 5.6% (0.3) respectively. All subjects were biochemically euthyroid and normoandrogenaemic.

Table 5.3.1: Baseline anthropometric, clinical and biochemical (fasting) data for all subjects (n=10) taken prior to entry into WBC at first metabolic study

Subject parameters	Mean	SD
Age (years)	41.8	6.7
Weight (Kg)	116.5	16.2
BMI (Kgm ⁻²)	42.1	4.6
Waist Circumference (m)	1.20	0.09
Hip Circumference (m)	1.35	0.13
Waist:Hip Ratio	0.90	0.1
Fat mass (Kg)	59.5	14.5
Lean mass (Kg)	57.0	8.7
Fat %	50.7	7.4
Glucose (mmol/l)	4.7	0.6
Total Cholesterol (mmol/l)	5.0	0.9
LDL Cholesterol (mmol/l)	3.2	0.8
HDL Cholesterol (mmol/l)	1.3	0.1
Triglycerides (mmol/l)	1.2	0.3
HbA1C (%)	5.6	0.3
9am Cortisol (nmol/l)	356	165
IGF1 (nmol/ml)	20.7	5.8
TSH (mIU/l)	2.4	1.1
Free T4 (pmol/l)	15.2	1.6
Testosterone (nmol/l)	0.8	0.6
SHBG (nmol/l/ml)	54.4	31.5
25-OH vit D (nmol/ml)	36	18

25-OH vit D-25-hydroxycholecalciferol; SHBG-Sex Hormone Binding Globulin; TSH-Thyroid Stimulating Hormone; IGF1-Insulin-like Growth Factor-1; HDL-High Density Lipoprotein; LDL-Low Density Lipoprotein; SD-Standard deviation; HbA1c- Glycated haemoglobin

5.3.2 The Effect of 10-minute Meals or 40-minute Meals on Diet Induced Thermogenesis in Obese Subjects

RMR for D40 and D10 were equivalent (RMR [SD]: 37.4 Kcal/hr [2.5] versus 38.6 Kcal/hr [3.7] respectively, P=NS). DIT for 4-hr postprandial duration was significantly greater in D40 than D10 (DIT mean [SEM]: 80.9Kcal [1.4] versus 29.9Kcal [1.2] respectively, P=0.006; DIT AUC 71.7 Kcal versus 22.4 Kcal respectively, P=0.02). When calculated as a proportion of energy intake during the meal, DIT was also significantly higher in D40 than D10 (DIT mean % [SEM]: 10.6% [0.2] vs 3.9% [0.2] respectively, P=0.006).

Table 5.3.2.1 Diet Induced Thermogenesis (DIT) of 10-minute and 40-minute meals

Time (min)	DIT-D10 (Kcal/hr)	DIT-D40 (Kcal/hr)	Significance
30	6.2	11.1	
60	6.7	14.4	
90	3.9	12.1	
120	2.6	11.4	
150	1.3	14.1	
180	2.2	3.4	
210	-1.8	7.2	
240	8.7	7.2	
Total DIT	29.9	80.9	P=0.006
SD	3.4	3.8	
SEM	1.2	1.4	
AUC	22.4	71.7	P=0.02

SD-Standard deviation; SEM- Standard error of mean; AUC- Area under the curve;
DIT- Diet induced thermogenesis

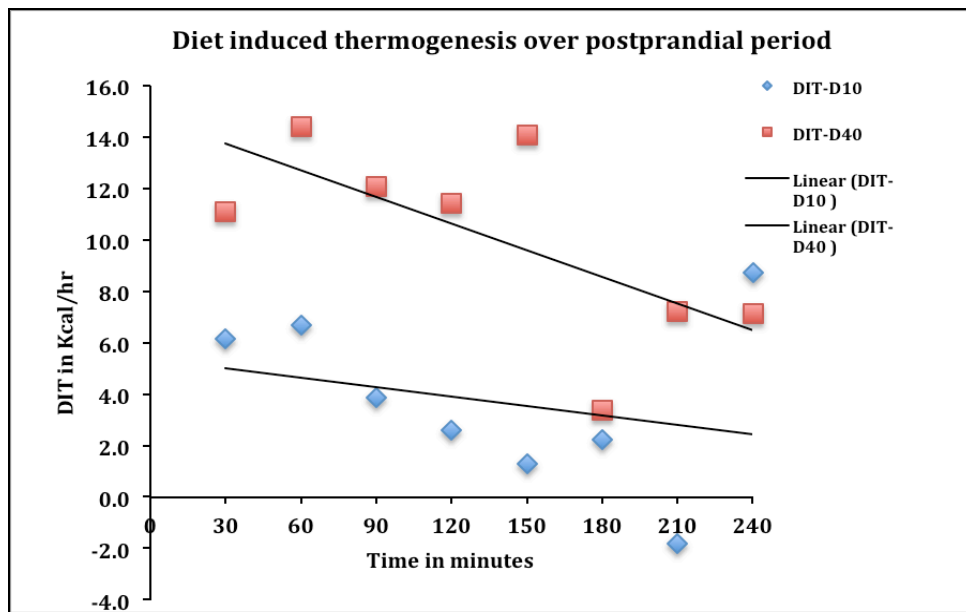


Figure 5.3.2.2 Comparison of diet induced thermogenesis between 10-minute meals and 40-minute meals in obese females.

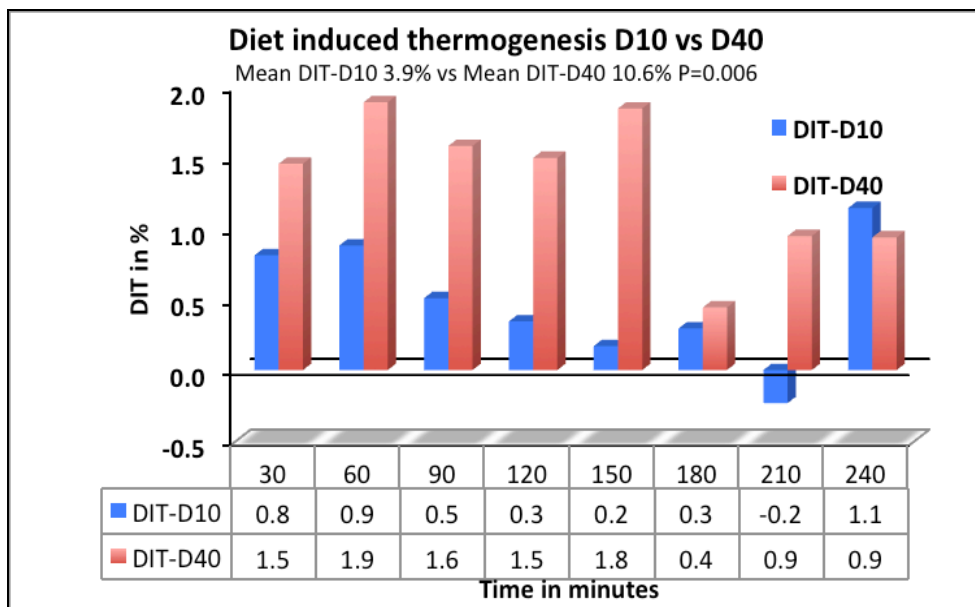


Figure 5.3.2.3 Comparison of diet induced thermogenesis (expressed in percentage of the total meal calories ingested) between 10-minute meals and 40-minute meals in obese females.

5.3.3 The Effect of 10-minute Meals or 40-minute Meals on Delta Energy Expenditure rates in Obese Subjects

The post-D40 energy expenditure rate was significantly higher than D10 (Mean Δ EE rate-D40 24.3 Kcal/hr [3.2] versus 20.2 Kcal/hr [3.7]).

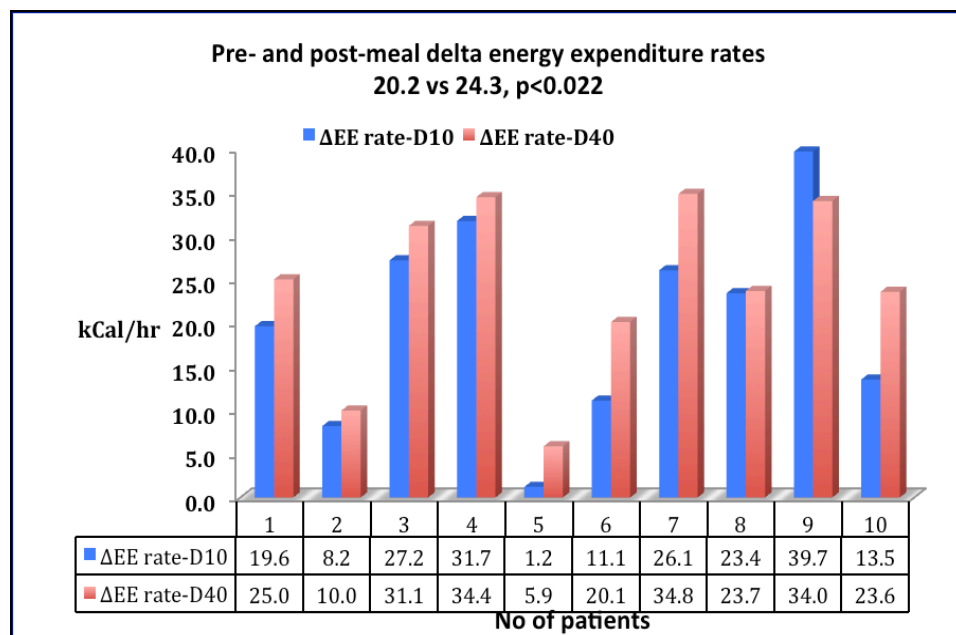


Figure 5.3.3 Comparison of energy expenditure rate difference between pre- and post 10-minute meals and 40-minute meals in obese females.

5.3.4 The Effect of 10-minute Meals or 40-minute Meals on Serum Glucose and Insulin in Obese Female Subjects

Postprandial serum glucose levels were lower and trending towards significance in D40 compared with D10 groups (Mean Glucose [SEM] 6.0 mmol/L [0.4] versus 6.4 mmol/L [0.3], $P = 0.07$; Glucose AUC [SEM] 23.8 mmol.hr/L [0.7] versus

25.2mmol.hr/dl [0.9] respectively, $P=0.07$). Postprandial insulin levels were statistically equivalent between D40 and D10 (Mean Insulin 615pmol/L [143] versus 693 pmol/L [130], $P=0.24$; Insulin AUC 2416pmol/L/hr [301] versus 2853pmol/L/hr [537] respectively, $P=0.29$).

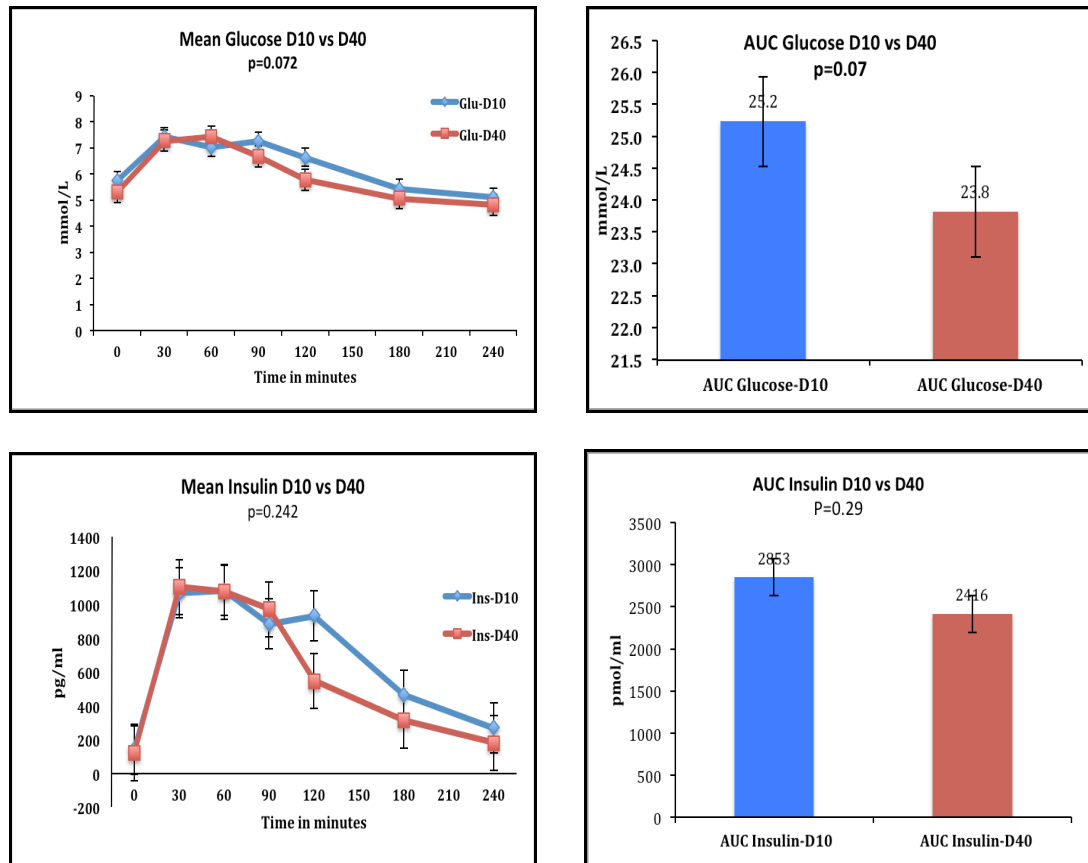


Figure 5.3.4 Comparison between the effect of 10-minute meals and 40-minute meals on serum insulin and serum glucose in obese females.

5.3.5 The Effect of 10-minute Meals or 40-minute Meals on Serum Adiponectin and Serum NEFA in Obese Female Subjects

Postprandial adiponectin was significantly higher for D40 than D10 (Adiponectin AUC 33385ng.hr/ml [3939] versus 27293 ng.hr/ml [3775] respectively, $P=0.04$;

Mean Adiponectin [SEM]: 8382ng/ml [1262] versus 6880ng/ml [389], P=NS)). Plasma NEFA in the postprandial period was significantly lower for D40 than D10 (NEFA AUC 627μmol/L/hr [56] versus 769μmol/L/hr [60] respectively, P=0.02; Mean NEFA [SEM] 191μmol/L [50] versus 242μmol/L [69] respectively, P=NS)

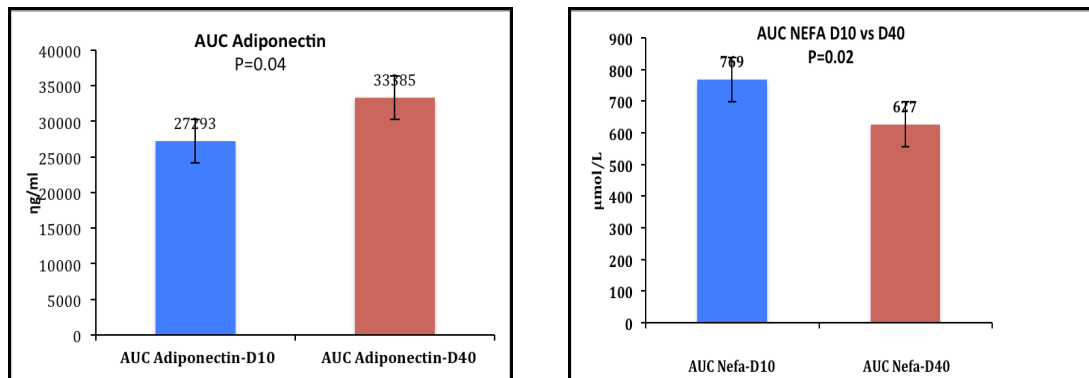


Figure 5.3.5 Comparison between the effect of 10-minute meals and 40-minute meals on serum adiponectin and serum NEFA in obese females.

5.3.6 The Effect of 10-minute Meals or 40-minute Meals on Pancreatic, Gut hormones, Cortisol and HOMA-IR in Obese Female Subjects

Ghrelin was significantly higher in D40 compared to D10 (Mean Ghrelin 78 pg/ml [5.3] versus 54pg/ml [5.7], P=0.04; Ghrelin AUC 305pg/ml/hr [77] versus 226pg/ml/hr [43], P=NS). For all other postprandial analytes including leptin, GLP-1, PYY, PP, cortisol, lipid profile, endotoxin and HOMA-IR, mean data and AUC data between D40 and D10 were equivalent.

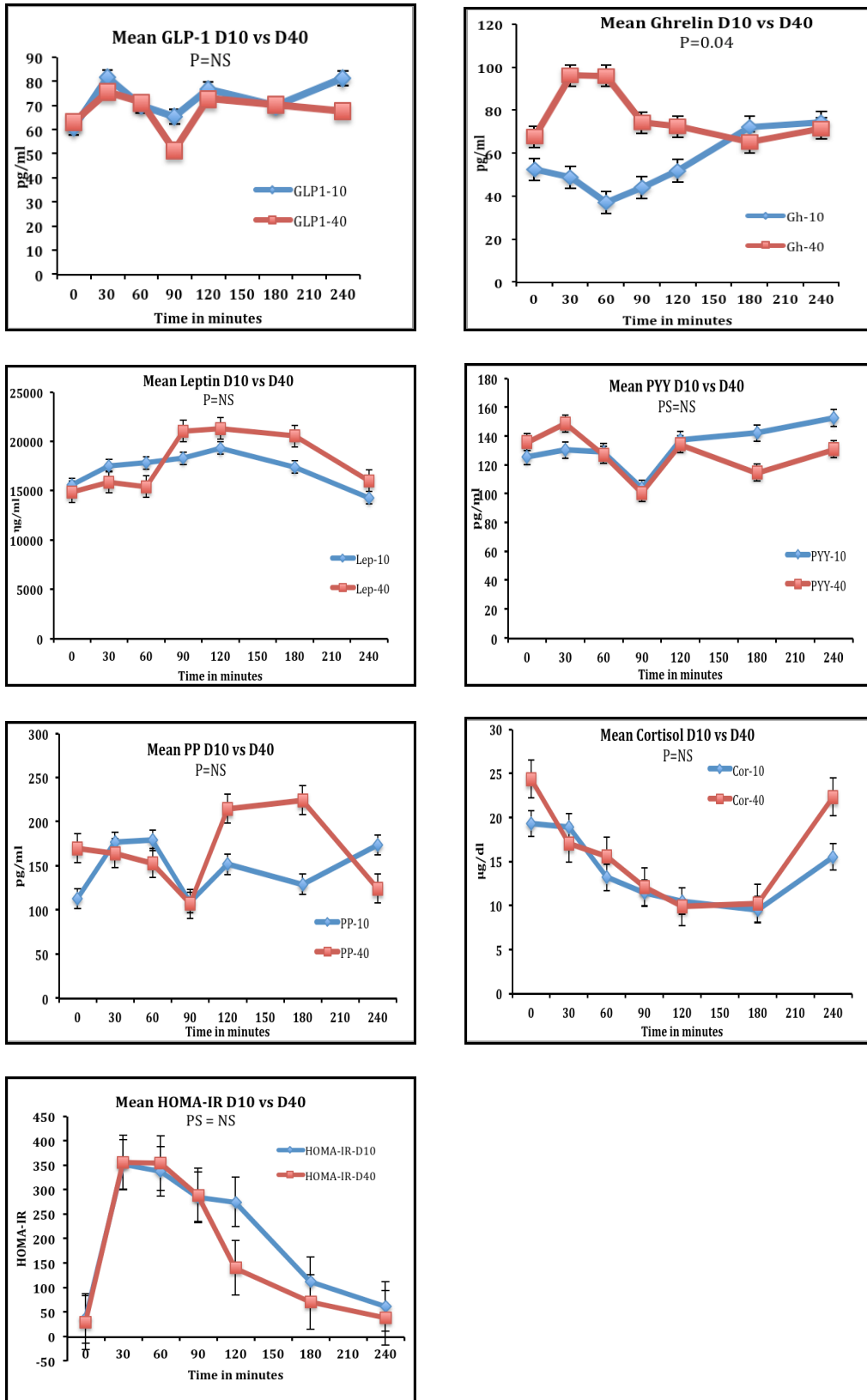


Figure 5.3.6 Comparison between the effect of 10-minute meals and 40-minute meals on serum pancreatic, gut hormones, cortisol, HOMA-IR in obese females.

Table 5.3.7: Postprandial biochemical data of study subjects following each standard meal (D10 versus D40)

Analyte	D10 AUC (SEM)	D40 AUC (SEM)	P- value	D10 Mean (SEM)	D40 Mean (SEM)	P- value
Glucose (mmol/l)	25.2 (0.9)	23.8 (0.7)	0.07	6.4 (0.3)	6.0 (0.4)	0.07
Insulin (pmol/l)	2853 (537)	2416 (301)	NS	693 (130)	615 (143)	NS
NEFA (μmol/l)	769 (60)	627 (56)	0.02	242 (69)	191 (50)	NS
Ghrelin (pg/ml)	226 (43)	305 (77)	NS	54 (5.7)	78 (5.3)	0.04
Leptin (ng/ml)	69645 (19352)	74291 (15718)	NS	17154 (693)	17837 (1194)	NS
GLP1 (pg/ml)	292 (34)	274 (29)	NS	72 (3.2)	67 (3.3)	NS
PYY (pg/ml)	535 (37)	503 (34)	NS	132 (6.2)	127 (6.4)	NS
Adiponectin (ng/ml)	27293 (3775)	33385 (3939)	0.04	6880 (389)	8382 (1262)	NS
Cortisol (nmol/l)	1424 (241)	1575 (93)	NS	387 (45)	438 (64)	NS
Total Cholesterol (mmol/l)	18.9 (0.8)	18.8 (1.1)	NS	4.7 (0.03)	4.7 (0.01)	NS
LDL Cholesterol (nmol/l)	12.0 (0.8)	11.8 (1.0)	NS	3.0 (0.04)	3.0 (0.02)	NS
HDL Cholesterol (nmol/l)	4.1 (0.1)	4.1 (0.2)	NS	1.03 (0.01)	1.03 (0.01)	NS
Triglycerides (nmol/l)	5.7 (1.3)	5.7 (1.3)	NS	1.4 (0.05)	1.4 (0.06)	NS
Endotoxin (EU/ml)	23.4 (3.5)	23.2 (3.5)	NS	6.0 (0.4)	5.9 (0.4)	NS
HOMA-IR	846 (11.0)	701 (5.5)	NS	209 (50.7)	182 (55.6)	NS

AUC=Area Under the Curve; SEM=Standard Error of Mean; HDL Cholesterol=High Density Lipoprotein Cholesterol; LDL Cholesterol=Low Density Lipoprotein Cholesterol; NEFA=Non-Esterified Fatty Acids; GLP1=Glucagon-Like Peptide 1; PYY=Peptide YY; For the AUC data, the units are multiplied by time (hours); HOMA-IR=Homeostatic model assessment estimated insulin resistance.

5.3.7 Postprandial Appetite (Visual Analogue Scale and ad libitum evening buffet)

Postprandial data on appetite (VAS) and evening buffet consumption are as shown below in Table 5.3.7. As expected, appetite was at its height pre-meal (standard lunch), and was most suppressed in the early postprandial phase (0-90 minutes) following lunch. VAS for D40 and D10 however were equivalent throughout. For the early evening *ad libitum* buffet following the standard lunch, total calories ingested and macroconstituent food fractions for D40 and D10 were equivalent (mean [SD] total calories ingested 482Kcal [274] versus 448Kcal [243] respectively, P=NS).

Table 5.3.7 Data showing measures of appetite (visual analogue scales) in the postprandial phase, consumption of *ad libitum* evening meal data and energy expenditure in the postprandial phase

Variable	D10 Mean (SD)	D40 Mean (SD)	P-value
Pre-meal appetite VAS	7.4 (2.4)	7.5 (2.6)	NS
Early postprandial appetite VAS (0-90 mins)	1.7 (0.9)	1.6 (1.1)	NS
Late postprandial appetite VAS (120-240 mins)	3.3 (2.1)	3.2 (2.2)	NS
Post-buffet VAS	4.1 (3.1)	2.6 (3.0)	NS
Buffet total calories ingested (Kcal)	448 (243)	482 (274)	NS
Buffet total protein ingested (g)	21 (9.0)	24 (7.6)	NS
Buffet total CHO ingested (g)	41 (24.1)	45 (29.6)	NS
Buffet total fat ingested (g)	23 (16.4)	23 (17.6)	NS

VAS- visual analogue scale (0- no hunger and fully satiated; 10- extremely hungry);
g-grams; CHO- carbohydrate; Kcal- Kilocalories; SD-standard deviation

5.4 Discussion

We have demonstrated in a well-phenotyped, well-controlled and objective study on meal duration, that eating a standard lunch over 40-minutes versus the same lunch over 10-minutes, is associated with significantly enhanced DIT, postprandial suppression of plasma NEFA and elevated adiponectin levels in obese women. Our study is the most comprehensive one to date on the metabolic and appetitive effects of meal duration, and to our knowledge this is the first report of effects of meal duration on DIT in a WBC.

Adoption of a consistently slow eating rate over time may, through effects on serum adiponectin levels, confer positive metabolic effects (including improved insulin sensitivity) given the known beneficial functions of adiponectin (Turer et al 2012⁴³⁰). We hypothesize that the importance of the relative changes in postprandial serum adiponectin levels in D40 compared with D10 may facilitate an increased action of insulin on NEFA through enhanced peripheral lipoprotein lipase activity (Lambert et al 2012⁴³¹, Farese et al 1991⁴³²). This in turn may result in reduced ‘spill-over’ of NEFA within adipose tissue, and associated increased uptake of fatty acids from chylomicrons into adipocytes (Padwal et al 2007⁴³³). As such the enhanced postprandial suppression of NEFA associated with slower eating behaviors would, over time, result in reduced exposure of organs such as the liver and heart to fatty acids. Reduced ectopic fat deposition within these organs would improve insulin sensitivity and risk of future development of T2D and other features of the metabolic syndrome. Previous studies support this, highlighting an association between short meal duration and development of impaired glucose tolerance, T2D and other

cardiometabolic risk factors (Totsuka et al 2011⁴³⁴, Sakurai et al 2012⁴³⁵). The effects of slow duodenal infusion of a fat-containing, stable isotope-labelled liquid meal versus a bolus oral meal-feeding paradigm on NEFA ‘spill over’ in healthy men was reported by Barrows and colleagues (Khanna et al 2012⁴³⁶). The quantity of NEFA ‘spill over’ over 9-hours was similar between the two regimes. The effects of meal duration on NEFA levels could therefore be influenced by macronutrients (with variable effects on insulin release according to duration of ingestion).

Ingestion of food results in increased oxygen consumption and body temperature primarily from digestive processes accounting for DIT (Westerterp-Plantenga et al 1999⁴³⁷). Between D40 and D10, a mean difference in DIT of 51Kcal per 763Kcal standard lunchtime meal was observed during the 4-hour postprandial period. If extrapolated for an entire year, the expected difference in DIT between D40 and D10 would be 18,626Kcal. Assuming that 3500 Kcal is equivalent to 395g of fat (Wishnofsky et al 1958⁴³⁸), this equates to a difference in body weight of 2.1 kg/year. Although varying the protein content of meals may also influence DIT and body weight (Veldhorst et al 2008⁴³⁹), the macronutrient constituents (including protein) of the lunch in our study was fixed, suggesting that this disparity in DIT is a reflection of the difference in meal duration between D40 and D10.

Furthermore, in a recent study involving eleven healthy human subjects, following a single meal, brown adipose tissue was postprandially activated, and maximal glucose uptake in brown adipose tissue was noted in comparison to rest of peripheral tissues, as demonstrated in 18-FDG-PET scans, implicating its role in DIT and hence energy homeostasis (Vosselman et al 2013⁴⁴⁰). Similar finding was noted in Orava and

colleagues human PET studies (Orava et al 2011¹⁷⁶). These studies implicate BAT's role in DIT, and prolonged activation of BAT from longer duration of meal may possibly explain our study findings of greater DIT in D40 than D10, and also enhanced plasma glucose suppression in D40 than D10 (although only trending towards significance $p=0.07$). Overall, this study provides evidence to suggest that slowing eating rate may, with time result in weight loss through enhanced DIT.

Most reported studies on meal duration have been limited however by reliance upon *subjective* self-reported measures of eating behaviors in a cross-sectional design. Using such an approach, a positive association between BMI and speed of eating has been reported (Otsuka et al 2006¹¹⁰, Maruyama et al 2008¹¹¹, Tanihara et al 2011⁴²⁶, Sasaki et al 2003⁴²⁷). In one of the largest studies to date on a Japanese cohort ($n=7,275$), each subject was divided into one of four groups according to self-reported eating rate: slow, medium, relatively fast and very fast (Ohkuma et al 2013⁴⁴¹). It was demonstrated that the prevalence of obesity increased progressively with increased eating rate. There were also changes in blood pressure, lipid levels and glycaemic control according to eating rate (Ohkuma et al 2013⁴⁴¹). Despite the compelling nature of the data, causality cannot be inferred. One potential mechanism whereby longer meal durations may reduce fat mass is through enhanced DIT, as directly observed in our current study.

With regards to effects of meal duration on food intake and appetite, there is controversy. In one study, it was observed that subjects tend to eat more food with longer meal durations (Pliner et al 2006⁴²⁸). One explanation could be that eating food slowly has been associated with prolonged elevation of postprandial plasma

ghrelin levels (Sobki et al 2010⁴²⁹). Such an effect might be expected to reduce the satiating effects of food and lead to over-eating. Other reported studies showed variable effects of meal duration on postprandial appetitive factors although these were limited by inaccurate replication of normal eating patterns (Karl et al 2013⁴¹⁵, Karl et al 2011⁴⁴²). In a study by Scisco and colleagues, implementation of a slow eating rate through use of a ‘bite-rate counter’ device was shown to *reduce* caloric intake (Scisco et al 2011⁴⁴³). We showed no differences in postprandial ghrelin (AUC data), appetite or subsequent ingestion of an *ad libitum* meal.

The study subjects could be classed as normal metabolically healthy obese and not insulin resistant, and therefore might not have impacted on some of the biochemical changes despite the different transit time of meals. This could explain the equivalent results of endotoxin, a biomarker for metabolic inflammation. Also the meal itself contained 50% carbohydrate, 18% protein, and 32% fat and as such was balanced and not necessarily provoking a considered insult to the system as would a large meal or a high fat or high glucose meal could. Other postprandial gut hormone effects such as elevated PYY and GLP1, noted in previous studies (Kokkinos 2010⁴⁴⁴) were not observed in our study. Whether there appears a blunted effect for these appetite-suppressing hormones in obese women (mean BMI [SD]: 42.1 [4.6]), remains to be clarified with future dedicated studies.

Limitations of our study include the small number of subjects (although comparable to other reported studies in the field). This was necessary due to the detailed phenotyping of subjects. Another limitation was that we only studied the postprandial effects of meal duration. There may be other delayed metabolic and

appetitive effects of meal duration that would not have been identified with our study design. Finally, menstrual cycle phase has been shown to affect appetite and thereby may have influenced *ad libitum* energy intake (Brennan 2009⁴⁴⁵), which was not controlled for this trial. A long-term prospective study on the effects of meal duration on body weight, ectopic fat deposition and future cardiometabolic health would provide invaluable mechanistic insight.

To summarize, these studies have identified the beneficial effects on metabolism (including enhanced DIT, and improved postprandial NEFA and adiponectin profiles) of eating a standard meal slowly. We hypothesize that the divergent effects of meal duration on metabolism over time would influence body fat mass, ectopic fat, insulin resistance and inherent cardiometabolic risk including T2D development. Future prospective studies should focus on the longer-term cardiometabolic effects of meal duration. These studies would provide further data to provide invaluable insight into the complex mechanisms that link meal duration with metabolism and longer-term health. The current availability of high calorific foods and a culture and lifestyle for rapid consumption of such foods poses a challenge. Increased fibre content of food would tend to increase consumption time, and may also impact beneficially on overall metabolic health. This and other cultural, environmental and lifestyle strategies for modifying our eating behavior and adopting a more prolonged, leisurely and sociable ‘Frenchesque’ attitude towards food and mealtimes, are perhaps important public-health messages.

Chapter 6

DISCUSSION

6.1 Introduction

Given the limitations of current therapies, the current global obesity epidemic and escalating incidence of obesity-related deaths, it is imperative to identify novel and effective therapeutic options for obesity. Obesity results when energy intake exceeds expenditure chronically. Therapeutic strategies for obesity have mainly targeted caloric restriction through central appetite suppression and inhibition of fat absorption, and have not been so far successful (Padwal et al 2004, Cochrane review⁴⁴⁶). Centrally acting drugs can potentially cause adverse psychotropic side effects through cross-reactivity with a variety of other receptors within complex central circuits (Padwal et al 2004, Cochrane review⁴⁴⁶). Compared with those acting on central appetite regulation, therapies acting peripherally, termed as '*cellular bioenergetics*', may prove beneficial whilst causing fewer harmful effects, and the most physiological '*cellular bioenergetic*' is exercise (Tseng et al 2010⁴⁴⁷). The concept of increasing energy expenditure through therapeutic manipulation of *peripheral* mechanisms is therefore attractive and worthy of focused research and development. One such strategy is BAT. As outlined in Chapter 1.7.1, BAT's role in beneficial metabolism is persuasive. Two independent but congruent human PET studies estimated an energy expenditure of 200-400 kcal/day, a 10 to 20% rise in daily basal metabolic rate through BAT activation (Yoneshiro et al 2011¹⁹⁶, Muzik et al 2012²⁴⁰). Therefore, the glucose disposal (Orava et al 2011²⁴¹) and triglyceride clearance properties of BAT (Bartelt et al 2011²⁴²), on sustained activation may act as an energy sink, and these properties form an attractive anti-diabesity solution. Appropriately, there is frantic activity in BAT research area, ranging from

characterisation of its physiology to pursuit of BAT-targeted ‘cellular bionergetic’ drugs.

From this background, the thesis sought to undertake exploration of factors that stimulate and activate BAT. The turn of 21st century also marked rejuvenated interest in BAT, purely attributable to a significant technological advancement of integration of PET with CT scan enabling visualization of metabolically active BAT. ¹⁸Fluoro-labelled-2-deoxyglucose Positron Emission Tomography (¹⁸F-FDG PET) is currently the gold standard and the most sensitive method to study BAT and its function. These studies concluded that younger-age, lower body mass index, female sex and cooler outdoor temperatures are strong determinant factors, and non-diabetes state as weak determinant factors of BAT prevalence. These BAT prevalence findings are in line with several PET-series research studies (Saito et al 2009¹⁴³, Cypess et al 2009¹⁴¹, Cronin et al, Pace et al 2011²⁰¹, Persichetti et al 2013³⁸³, Zhang et al 2014³⁸⁵). Information technological advances (MIRADA software) yielded robust calculation of BAT mass, which was strongly determined by younger subjects, females and lower BMI subjects, and weakly determined by previous week’s mean outdoor temperature. BAT activity was stronger in younger subjects, females and lean individuals. Scanning in cooler times of the day and when mean outdoor temperatures are lower were also noted to be weak determinant factors for BAT activity. Major limitation of the study is the inherent nature of PET to detect only metabolically activated BAT; which underestimates true prevalence given the scans are done in thermoneutral conditions which may switch off the BAT activity.

Surprisingly, modest elevation of thyroid hormones in a sustained iatrogenically created thyrotoxic state (levothyroxine and liothyronine replacement therapy for sustained TSH suppression in post-thyroidectomy thyroid cancer patients), did not influence any of the BAT indices of BAT prevalence, activity or mass, contrary to conventional wisdom and recent findings of Lahesmaa and colleagues (Lahesmaa et al 2014³⁹³). Excess thermogenesis from the skeletal route in hyperthyroid patients may centrally inhibit BAT pathway of non-shivering thermogenesis, which is usually modest even in maximal stimulated conditions. D2 levels of skeletal muscle in humans when compared to BAT are far higher than noted in mice, pointing out the diversification of tissue variations between the two species (Salvatore et al 1996³⁹⁵, Croteau et al 1996³⁹⁶). This might explain the failure of replication of animal data in humans, and the conventional hypothesis is based largely on animal studies. This negative finding also should be seen in the context of limitations of PET, which is a suboptimal modality of BAT imaging. Being a retrospective study, thyroid status based on biochemical thyroid function nearer to the scan date was determined, as opposed to thyroid function test on the day of the scan, possibly questioning the credibility of the scan findings in this sub-study. This leads on to the basis of next study, to find a suitable imaging method to identify and characterise BAT in its entirety during active and in inactive state.

It is vital to know BAT's anatomy and physiology, and this would aid achieve a targeted and meaningful therapeutic pursuit. A significant obstacle to the progress of research on human BAT has been the lack of a safe, sensitive, specific and reproducible imaging technique to quantify BAT volume and/or mass. Such a tool would be essential to evaluate the efficacy of novel therapies based on the

manipulation of BAT. Given the presence of ‘beige’, the intermediate type of fat, and the recognised phenomenon of beige transformation of WAT, it is all the more important to unequivocally identify and quantify different types of fat. The IDEAL MRI study first reproduced the experiments done by Hu and colleagues (Hu et al 2010²⁰⁶) on a rat carcass to confirm the validity of IDEAL technique, and subsequently used the same technique on a human volunteer, also providing immunohistochemical confirmation of BAT from a fat sample obtained from the neck surgery. The BAT signals appeared more heterogeneous from the surrounding WAT and this is indeed the pattern that one would expect given the characteristic histological appearance of human BAT often occurring in many islets within surrounding WAT (Cinti et al)¹⁷². Key advantages of MR over PET-CT is that it is safe, measures BAT volume irrespective of activity status, and is not influenced by transient influential factors such as outdoor temperature. Our study thus provided proof of principle that MR can successfully delineate BAT from WAT, and has encouraged a large-scale study in UHCW to validate the methodology. It is possible that adipose tissue may be affected in some way in HPT-JT syndrome, which may in turn affect signal intensity on MR imaging. However, the histological and morphological characteristics of BAT samples obtained were comparable to that of well validated studies (Virtanen et al 2009¹⁴⁰, Cinti et al 2000¹⁷²). Few promising MR studies on BAT imaging have been reported in human subjects following our study, and more evaluation and validation are required at this stage before embarking on large-scale evaluations of BAT quantities (Hu et al 2013⁴⁴⁸, Khanna et al 2012⁴⁴⁹).

It is appropriate to look for new therapeutical solutions for obesity; often, complex problems may have simple solutions. Change in behaviour and lifestyle is a recognized, inexpensive, and beneficial intervention. Recognised stimulators of BAT are cold exposure (Cold induced Thermogenesis-CIT) and diet (DIT). The thesis sought to evaluate manipulation of speed of DIT, and other bio-chemical metabolic factors involved in regulation of hunger, appetite and glucose metabolism. To our knowledge, this is the first-ever reported effort to investigate meal duration in the context of energy expenditure. These set of studies have identified the beneficial effects on metabolism (including enhanced DIT, and improved postprandial NEFA and adiponectin profiles) of eating a standard meal slowly. Limitations include small number and limited to only obese women. However, similar published energy expenditure experiments recruited comparable number of study subjects (Zhang et al 2002²¹⁸, Johnston et al 2002⁴⁵⁰) and detailed phenotyping was required to boost the power of the study; therefore the recruitment limitation to obese caucasian pre-menopausal women. We hypothesize that the divergent effects of meal duration on metabolism over time would influence body fat mass, ectopic fat, insulin resistance and inherent cardiometabolic risk including T2D development.

6.2 Future directions

The thesis provides some useful insights regarding determinant factors of BAT prevalence, including that of lack of thyrotoxicosis effect on human BAT. This may possibly be due to retrospective nature of the study. Dedicated prospective studies exploring effect of thyroid hormones on BAT is advised. Similar to thyrotoxicosis, pheochromocytoma is a hyperadrenergic state and theoretically should enhance

BAT activation. Apart from few case reports and small retrospective study, a dedicated study is lacking (Lean et al 1986²⁵⁰, Simonsen et al 1993²⁴⁸).

HMRU at UHCW offers an excellent opportunity allowing study of 24- hour energy expenditure, and at the same time enabling the accurate assessment of energy intake in the form of Whole Body Calorimeters. Characterising BAT in metabolically relevant conditions such as thyrotoxicosis, phaeochromocytoma, diabetes, polycystic ovarian syndrome, cushings syndrome and various other metabolic states would be useful. The whole body physiology studies such as these are clearly important to study the effects of organ cross-talk during periods of food consumption, exercise and sleep, which cannot be undertaken *in vitro*, with isolated cell systems.

PET-MRI with its capabilities to study thermoregulatory areas like hypothalamus may be able to provide answers for central regulation of brown fat. Functional MRI and other nuclear medicine advances in radiology field holds promising prospects for BAT research.

In addition to augmentation of BAT content and/or enhancement of BAT activity, other approaches include trans-differentiation of non-BAT progenitors into BAT pre-adipocytes, and surgical implantation of BAT. Development of novel BAT-related therapies will require a complete understanding of the embryological and transcriptional mechanisms of BAT specification and development in human models. Several transcriptional regulators of brown adipocyte differentiation are described in rodents, with some revealing promising effects even in human models (Wu et al¹⁴⁶).

6.3 Conclusion

In summary, this thesis provided useful insights into environmental, anthropometrical, behavioural, and hormonal factors regulating BAT. It also provided a proof of principle for an imaging tool to be developed in order to visualise full extent of both metabolically active and inactive BAT, adding evidence for future pursuits of BAT therapeutics to combat the global obesity epidemic. Whilst awaiting solutions for obesity, evidence from this thesis advocates simple behavioural modifications, such as adopting ‘Fletcherism’ (eating only when extremely hungry and chewing food for long durations) and reducing thermostat of indoor living spaces.

BIBLIOGRAPHY

1. WHO global infobase: data on overweight and obesity. 2011. at [http://www.who.int/mediacentre/factsheets/fs311/en/.](http://www.who.int/mediacentre/factsheets/fs311/en/))
2. IASO/IOTB. International Obesity Task Force (2010) The Global Epidemic IASO/IOTB. <http://www.iaso.org/iotf/obesity/obesitytheglobalepidemic/> 2010.
3. 2007 F. Foresight- Tackling obesities, Future Choices Project. Department of Health 2007.
4. Statistics on obesity, physical activity and diet: England, 2010. National Obesity Observatory 2010.
5. Eastwood LST. Statistics on Obesity, Physical Activity and Diet: England 2014. 2014.
6. Padwal R, Li SK, Lau DC. Long-term pharmacotherapy for obesity and overweight. *Cochrane Database Syst Rev* 2004;CD004094.
7. Calle EE, Thun MJ, Petrelli JM, Rodriguez C, Heath CW, Jr. Body-mass index and mortality in a prospective cohort of U.S. adults. *The New England journal of medicine* 1999;341:1097-105.
8. Wannamethee SG, Shaper AG. Weight change and duration of overweight and obesity in the incidence of type 2 diabetes. *Diabetes care* 1999;22:1266-72.
9. Flegal KM, Graubard BI, Williamson DF, Gail MH. Cause-specific excess deaths associated with underweight, overweight, and obesity. *Jama* 2007;298:2028-37.
10. Kenchaiah S, Evans JC, Levy D, et al. Obesity and the risk of heart failure. *N Engl J Med* 2002;347:305-13.
11. Guh DP, Zhang W, Bansback N, Amarsi Z, Birmingham CL, Anis AH. The incidence of co-morbidities related to obesity and overweight: a systematic review and meta-analysis. *BMC public health* 2009;9:88.
12. Basen-Engquist K, Chang M. Obesity and cancer risk: recent review and evidence. *Curr Oncol Rep* 2011;13:71-6.
13. Anandam A, Akinnusi M, Kufel T, Porhomayon J, El-Solh AA. Effects of dietary weight loss on obstructive sleep apnea: a meta-analysis. *Sleep Breath* 2013;17:227-34.
14. Gami AS, Caples SM, Somers VK. Obesity and obstructive sleep apnea. *Endocrinol Metab Clin North Am* 2003;32:869-94.
15. Hryhorczuk C, Sharma S, Fulton SE. Metabolic disturbances connecting obesity and depression. *Front Neurosci* 2013;7:177.
16. Wang YC, McPherson K, Marsh T, Gortmaker SL, Brown M. Health and economic burden of the projected obesity trends in the USA and the UK. *Lancet* 2011;378:815-25.
17. Withrow D, Alter DA. The economic burden of obesity worldwide: a systematic review of the direct costs of obesity. *Obesity reviews : an official journal of the International Association for the Study of Obesity* 2011;12:131-41.
18. Finkelstein EA, Trogon JG, Cohen JW, Dietz W. Annual medical spending attributable to obesity: payer-and service-specific estimates. *Health Aff (Millwood)* 2009;28:w822-31.

19. Whitlock G, Lewington S, Sherliker P, et al. Body-mass index and cause-specific mortality in 900 000 adults: collaborative analyses of 57 prospective studies. *Lancet* 2009;373:1083-96.
20. Berrington de Gonzalez A, Hartge P, Cerhan JR, et al. Body-mass index and mortality among 1.46 million white adults. *N Engl J Med* 2010;363:2211-9.
21. ProspectiveStudiesCollaboration. Body-mass index and cause-specific mortality in 900 000 adults: collaborative analyses of 57 prospective studies. *The Lancet* 2009;373:1083-96.
22. Appropriate body-mass index for Asian populations and its implications for policy and intervention strategies. *Lancet* 2004;363:157-63.
23. Measures of central adiposity as an indicator of obesity. National Obesity Observatory 2009.
24. Pischon T, Boeing H, Hoffmann K, et al. General and abdominal adiposity and risk of death in Europe. *N Engl J Med* 2008;359:2105-20.
25. Koster A, Leitzmann MF, Schatzkin A, et al. Waist circumference and mortality. *Am J Epidemiol* 2008;167:1465-75.
26. Yusuf S, Hawken S, Ounpuu S, et al. Obesity and the risk of myocardial infarction in 27,000 participants from 52 countries: a case-control study. *Lancet* 2005;366:1640-9.
27. Langenberg C, Sharp SJ, Schulze MB, et al. Long-term risk of incident type 2 diabetes and measures of overall and regional obesity: the EPIC-InterAct case-cohort study. *PLoS medicine* 2012;9:e1001230.
28. Pietilainen KH, Kaye S, Karmi A, Suojanen L, Rissanen A, Virtanen KA. Agreement of bioelectrical impedance with dual-energy X-ray absorptiometry and MRI to estimate changes in body fat, skeletal muscle and visceral fat during a 12-month weight loss intervention. *The British journal of nutrition* 2013;109:1910-6.
29. Ginde SR, Geliebter A, Rubiano F, et al. Air displacement plethysmography: validation in overweight and obese subjects. *Obesity research* 2005;13:1232-7.
30. Koda M, Tsuzuku S, Ando F, Niino N, Shimokata H. Body composition by air displacement plethysmography in middle-aged and elderly Japanese. Comparison with dual-energy X-ray absorptiometry. *Ann N Y Acad Sci* 2000;904:484-8.
31. Seidell JC, Oosterlee A, Deurenberg P, Hautvast JG, Ruijs JH. Abdominal fat depots measured with computed tomography: effects of degree of obesity, sex, and age. *Eur J Clin Nutr* 1988;42:805-15.
32. Kaul S, Rothney MP, Peters DM, et al. Dual-energy X-ray absorptiometry for quantification of visceral fat. *Obesity (Silver Spring)* 2012;20:1313-8.
33. Consultation WHOE. Appropriate body-mass index for Asian populations and its implications for policy and intervention strategies. *Lancet* 2004;363:157-63.
34. Dixon JB, Zimmet P, Alberti KG, Rubino F. Bariatric surgery: an IDF statement for obese Type 2 diabetes. *Surg Obes Relat Dis* 2011;7:433-47.
35. Obesity: preventing and managing the global epidemic. Report of a WHO consultation. World Health Organization technical report series 2000;894:i-xii, 1-253.

36. Geldszus R, Mayr B, Horn R, Geithovel F, von zur Muhlen A, Brabant G. Serum leptin and weight reduction in female obesity. *Eur J Endocrinol* 1996;135:659-62.
37. Cummings DE, Weigle DS, Frayo RS, et al. Plasma ghrelin levels after diet-induced weight loss or gastric bypass surgery. *The New England journal of medicine* 2002;346:1623-30.
38. Chearskul S, Delbridge E, Shulkes A, Proietto J, Kriketos A. Effect of weight loss and ketosis on postprandial cholecystokinin and free fatty acid concentrations. *Am J Clin Nutr* 2008;87:1238-46.
39. Buchwald H, Avidor Y, Braunwald E, et al. Bariatric surgery: a systematic review and meta-analysis. *Jama* 2004;292:1724-37.
40. Sjostrom L, Peltonen M, Jacobson P, et al. Bariatric surgery and long-term cardiovascular events. *Jama* 2012;307:56-65.
41. Pontiroli AE, Morabito A. Long-term prevention of mortality in morbid obesity through bariatric surgery. a systematic review and meta-analysis of trials performed with gastric banding and gastric bypass. *Ann Surg* 2011;253:484-7.
42. O'Brien PE, MacDonald L, Anderson M, Brennan L, Brown WA. Long-term outcomes after bariatric surgery: fifteen-year follow-up of adjustable gastric banding and a systematic review of the bariatric surgical literature. *Ann Surg* 2013;257:87-94.
43. Eckel RH, Grundy SM, Zimmet PZ. The metabolic syndrome. *Lancet* 2005;365:1415-28.
44. Stumvoll M, Goldstein BJ, van Haeften TW. Type 2 diabetes: principles of pathogenesis and therapy. *Lancet* 2005;365:1333-46.
45. DeFronzo RA, Tobin JD, Andres R. Glucose clamp technique: a method for quantifying insulin secretion and resistance. *Am J Physiol* 1979;237:E214-23.
46. Borai A, Livingstone C, Kaddam I, Ferns G. Selection of the appropriate method for the assessment of insulin resistance. *BMC Med Res Methodol* 2011;11:158.
47. Buchanan TA, Watanabe RM, Xiang AH. Limitations in surrogate measures of insulin resistance. *J Clin Endocrinol Metab* 2010;95:4874-6.
48. Bergman RN, Finegood DT, Ader M. Assessment of insulin sensitivity in vivo. *Endocr Rev* 1985;6:45-86.
49. Matthews DR, Hosker JP, Rudenski AS, Naylor BA, Treacher DF, Turner RC. Homeostasis model assessment: insulin resistance and beta-cell function from fasting plasma glucose and insulin concentrations in man. *Diabetologia* 1985;28:412-9.
50. Katz A, Nambi SS, Mather K, et al. Quantitative insulin sensitivity check index: a simple, accurate method for assessing insulin sensitivity in humans. *J Clin Endocrinol Metab* 2000;85:2402-10.
51. Wallace TM, Levy JC, Matthews DR. An increase in insulin sensitivity and basal beta-cell function in diabetic subjects treated with pioglitazone in a placebo-controlled randomized study. *Diabet Med* 2004;21:568-76.
52. Hoffman RP. Indices of insulin action calculated from fasting glucose and insulin reflect hepatic, not peripheral, insulin sensitivity in African-American and Caucasian adolescents. *Pediatr Diabetes* 2008;9:57-61.

53. Pfozner A, Weber MM, Forst T. A biomarker concept for assessment of insulin resistance, beta-cell function and chronic systemic inflammation in type 2 diabetes mellitus. *Clin Lab* 2008;54:485-90.
54. Matsuda M, DeFronzo RA. Insulin sensitivity indices obtained from oral glucose tolerance testing: comparison with the euglycemic insulin clamp. *Diabetes care* 1999;22:1462-70.
55. Trikudanathan S, Raji A, Chamarthi B, Seely EW, Simonson DC. Comparison of insulin sensitivity measures in South Asians. *Metabolism* 2013;62:1448-54.
56. DeFronzo RA. Glucose intolerance of aging. Evidence for tissue insensitivity to insulin. *Diabetes* 1979;28:1095-101.
57. Buchanan TA, Metzger BE, Freinkel N, Bergman RN. Insulin sensitivity and B-cell responsiveness to glucose during late pregnancy in lean and moderately obese women with normal glucose tolerance or mild gestational diabetes. *Am J Obstet Gynecol* 1990;162:1008-14.
58. Moran A. Insulin resistance during puberty: results from clamp studies in 357 children. *Diabetes* 1999;48:2039-44.
59. DeFronzo RA. Glucose intolerance and aging: evidence for tissue insensitivity to insulin. *Diabetes* 1979;28:1095-101.
60. Moran A, Jacobs DR, Jr., Steinberger J, et al. Insulin resistance during puberty: results from clamp studies in 357 children. *Diabetes* 1999;48:2039-44.
61. Farooqi I, Beevers G, Lip GY. Insulin resistance, high prevalence of diabetes, and cardiovascular risk in immigrant Asians. *Br Heart J* 1995;73:584.
62. Kramer H, Dugas L, Rosas SE. Race and the insulin resistance syndrome. *Semin Nephrol* 2013;33:457-67.
63. Mory PB, Crispim F, Freire MB, et al. Phenotypic diversity in patients with lipodystrophy associated with LMNA mutations. *Eur J Endocrinol* 2012;167:423-31.
64. Duan C, Yang H, White MF, Rui L. Disruption of the SH2-B gene causes age-dependent insulin resistance and glucose intolerance. *Molecular and cellular biology* 2004;24:7435-43.
65. Farooqi IS, Jebb SA, Langmack G, et al. Effects of recombinant leptin therapy in a child with congenital leptin deficiency. *The New England journal of medicine* 1999;341:879-84.
66. Yasuda K, Hines E, 3rd, Kitabchi AE. Hypercortisolism and insulin resistance: comparative effects of prednisone, hydrocortisone, and dexamethasone on insulin binding of human erythrocytes. *J Clin Endocrinol Metab* 1982;55:910-5.
67. Tebas P. Insulin resistance and diabetes mellitus associated with antiretroviral use in HIV-infected patients: pathogenesis, prevention, and treatment options. *J Acquir Immune Defic Syndr* 2008;49 Suppl 2:S86-92.
68. Reaven GM. Banting lecture 1988. Role of insulin resistance in human disease. *Diabetes* 1988;37:1595-607.
69. DeFronzo RA, Ferrannini E. Insulin resistance. A multifaceted syndrome responsible for NIDDM, obesity, hypertension, dyslipidemia, and atherosclerotic cardiovascular disease. *Diabetes care* 1991;14:173-94.
70. Kaplan NM. The deadly quartet. Upper-body obesity, glucose intolerance, hypertriglyceridemia, and hypertension. *Arch Intern Med* 1989;149:1514-20.

71. Alberti KG, Zimmet PZ. Definition, diagnosis and classification of diabetes mellitus and its complications. Part 1: diagnosis and classification of diabetes mellitus provisional report of a WHO consultation. *Diabet Med* 1998;15:539-53.
72. Balkau B, Charles MA. Comment on the provisional report from the WHO consultation. European Group for the Study of Insulin Resistance (EGIR). *Diabet Med* 1999;16:442-3.
73. Executive Summary of The Third Report of The National Cholesterol Education Program (NCEP) Expert Panel on Detection, Evaluation, And Treatment of High Blood Cholesterol In Adults (Adult Treatment Panel III). *Jama* 2001;285:2486-97.
74. Alberti KG, Zimmet P, Shaw J. The metabolic syndrome--a new worldwide definition. *Lancet* 2005;366:1059-62.
75. Turner RC, Millns H, Neil HA, et al. Risk factors for coronary artery disease in non-insulin dependent diabetes mellitus: United Kingdom Prospective Diabetes Study (UKPDS: 23). *Bmj* 1998;316:823-8.
76. Efficacy of atenolol and captopril in reducing risk of macrovascular and microvascular complications in type 2 diabetes: UKPDS 39. UK Prospective Diabetes Study Group. *Bmj* 1998;317:713-20.
77. Diagnosis and classification of diabetes mellitus. *Diabetes care* 2004;27 Suppl 1:S5-S10.
78. Crowther CA, Hiller JE, Moss JR, McPhee AJ, Jeffries WS, Robinson JS. Effect of treatment of gestational diabetes mellitus on pregnancy outcomes. *The New England journal of medicine* 2005;352:2477-86.
79. Metzger BE, Lowe LP, Dyer AR, et al. Hyperglycemia and adverse pregnancy outcomes. *The New England journal of medicine* 2008;358:1991-2002.
80. Rowan JA, Hague WM, Gao W, Battin MR, Moore MP. Metformin versus insulin for the treatment of gestational diabetes. *The New England journal of medicine* 2008;358:2003-15.
81. Lautatzis ME, Goulis DG, Vrontakis M. Efficacy and safety of metformin during pregnancy in women with gestational diabetes mellitus or polycystic ovary syndrome: A systematic review. *Metabolism* 2013.
82. Revised 2003 consensus on diagnostic criteria and long-term health risks related to polycystic ovary syndrome (PCOS). *Hum Reprod* 2004;19:41-7.
83. Randeve HS, Tan BK, Weickert MO, et al. Cardiometabolic aspects of the polycystic ovary syndrome. *Endocr Rev* 2012;33:812-41.
84. Forget G, Doyon M, Lacerte G, et al. Adoption of american heart association 2020 ideal healthy diet recommendations prevents weight gain in young adults. *Journal of the Academy of Nutrition and Dietetics* 2013;113:1517-22.
85. Randomised trial of cholesterol lowering in 4444 patients with coronary heart disease: the Scandinavian Simvastatin Survival Study (4S). *Lancet* 1994;344:1383-9.
86. Prevention of cardiovascular events and death with pravastatin in patients with coronary heart disease and a broad range of initial cholesterol levels. The Long-Term Intervention with Pravastatin in Ischaemic Disease (LIPID) Study Group. *N Engl J Med* 1998;339:1349-57.
87. Kris-Etherton P, Daniels SR, Eckel RH, et al. Summary of the scientific conference on dietary fatty acids and cardiovascular health: conference

summary from the nutrition committee of the American Heart Association. *Circulation* 2001;103:1034-9.

88. Nutrition SACo. Dietary reference values for energy. 2011.
89. Ebbeling CB, Garcia-Lago E, Leidig MM, Seger-Shippe LG, Feldman HA, Ludwig DS. Altering portion sizes and eating rate to attenuate gorging during a fast food meal: effects on energy intake. *Pediatrics* 2007;119:869-75.
90. Mayer J, Thomas DW. Regulation of food intake and obesity. *Science* 1967;156:328-37.
91. Rennie KL, Jebb SA, Wright A, Coward WA. Secular trends in under-reporting in young people. *The British journal of nutrition* 2005;93:241-7.
92. Kral TV, Rolls BJ. Energy density and portion size: their independent and combined effects on energy intake. *Physiology & behavior* 2004;82:131-8.
93. Rolls BJ, Castellanos VH, Halford JC, et al. Volume of food consumed affects satiety in men. *Am J Clin Nutr* 1998;67:1170-7.
94. Rolls BJ, Bell EA, Waugh BA. Increasing the volume of a food by incorporating air affects satiety in men. *Am J Clin Nutr* 2000;72:361-8.
95. Anson RM, Guo Z, de Cabo R, et al. Intermittent fasting dissociates beneficial effects of dietary restriction on glucose metabolism and neuronal resistance to injury from calorie intake. *Proc Natl Acad Sci U S A* 2003;100:6216-20.
96. Mattson MP. The need for controlled studies of the effects of meal frequency on health. *Lancet* 2005;365:1978-80.
97. Harvie MN, Pegington M, Mattson MP, et al. The effects of intermittent or continuous energy restriction on weight loss and metabolic disease risk markers: a randomized trial in young overweight women. *Int J Obes (Lond)* 2011;35:714-27.
98. Harvie M, Wright C, Pegington M, et al. The effect of intermittent energy and carbohydrate restriction v. daily energy restriction on weight loss and metabolic disease risk markers in overweight women. *The British journal of nutrition* 2013;110:1534-47.
99. Summerbell CD, Moody RC, Shanks J, Stock MJ, Geissler C. Relationship between feeding pattern and body mass index in 220 free-living people in four age groups. *Eur J Clin Nutr* 1996;50:513-9.
100. Crawley H, Summerbell C. Feeding frequency and BMI among teenagers aged 16-17 years. *Int J Obes Relat Metab Disord* 1997;21:159-61.
101. Dreon DM, Fernstrom HA, Campos H, Blanche P, Williams PT, Krauss RM. Change in dietary saturated fat intake is correlated with change in mass of large low-density-lipoprotein particles in men. *Am J Clin Nutr* 1998;67:828-36.
102. Cameron JD, Cyr MJ, Doucet E. Increased meal frequency does not promote greater weight loss in subjects who were prescribed an 8-week equi-energetic energy-restricted diet. *The British journal of nutrition* 2010;103:1098-101.
103. La Bounty PM, Campbell BI, Wilson J, et al. International Society of Sports Nutrition position stand: meal frequency. *Journal of the International Society of Sports Nutrition* 2011;8:4.
104. Farshchi HR, Taylor MA, Macdonald IA. Regular meal frequency creates more appropriate insulin sensitivity and lipid profiles compared with irregular meal frequency in healthy lean women. *Eur J Clin Nutr* 2004;58:1071-7.

105. Farshchi HR, Taylor MA, Macdonald IA. Beneficial metabolic effects of regular meal frequency on dietary thermogenesis, insulin sensitivity, and fasting lipid profiles in healthy obese women. *Am J Clin Nutr* 2005;81:16-24.
106. Andrade AM, Greene GW, Melanson KJ. Eating slowly led to decreases in energy intake within meals in healthy women. *J Am Diet Assoc* 2008;108:1186-91.
107. Martin CK, Anton SD, Walden H, Arnett C, Greenway FL, Williamson DA. Slower eating rate reduces the food intake of men, but not women: implications for behavioral weight control. *Behaviour research and therapy* 2007;45:2349-59.
108. Zandian M, Ioakimidis I, Bergh C, Brodin U, Sodersten P. Decelerated and linear eaters: effect of eating rate on food intake and satiety. *Physiology & behavior* 2009;96:270-5.
109. Hill SW, McCutcheon NB. Contributions of obesity, gender, hunger, food preference, and body size to bite size, bite speed, and rate of eating. *Appetite* 1984;5:73-83.
110. Otsuka R, Tamakoshi K, Yatsuya H, et al. Eating fast leads to obesity: findings based on self-administered questionnaires among middle-aged Japanese men and women. *Journal of epidemiology / Japan Epidemiological Association* 2006;16:117-24.
111. Maruyama K, Sato S, Ohira T, et al. The joint impact on being overweight of self reported behaviours of eating quickly and eating until full: cross sectional survey. *Bmj* 2008;337:a2002.
112. Brindal E, Wilson C, Mohr P, Wittert G. Does meal duration predict amount consumed in lone diners? An evaluation of the time-extension hypothesis. *Appetite* 2011;57:77-9.
113. Cummings DE, Overduin J. Gastrointestinal regulation of food intake. *J Clin Invest* 2007;117:13-23.
114. Guilherme A, Virbasius JV, Puri V, Czech MP. Adipocyte dysfunctions linking obesity to insulin resistance and type 2 diabetes. *Nat Rev Mol Cell Biol* 2008;9:367-77.
115. Unger RH. Lipotoxicity in the pathogenesis of obesity-dependent NIDDM. Genetic and clinical implications. *Diabetes* 1995;44:863-70.
116. Muoio DM, Newgard CB. Mechanisms of disease: molecular and metabolic mechanisms of insulin resistance and beta-cell failure in type 2 diabetes. *Nat Rev Mol Cell Biol* 2008;9:193-205.
117. Ouchi N, Parker JL, Lugus JJ, Walsh K. Adipokines in inflammation and metabolic disease. *Nat Rev Immunol* 2011;11:85-97.
118. Harte AL, Tripathi G, Piya MK, et al. NFkappaB as a potent regulator of inflammation in human adipose tissue, influenced by depot, adiposity, T2DM status, and TNFalpha. *Obesity (Silver Spring)* 2013.
119. Pirola L, Johnston AM, Van Obberghen E. Modulation of insulin action. *Diabetologia* 2004;47:170-84.
120. Tilg H, Moschen AR. Inflammatory mechanisms in the regulation of insulin resistance. *Mol Med* 2008;14:222-31.
121. Kalupahana NS, Moustaid-Moussa N, Claycombe KJ. Immunity as a link between obesity and insulin resistance. *Molecular aspects of medicine* 2012;33:26-34.

122. Shoelson SE, Lee J, Goldfine AB. Inflammation and insulin resistance. *J Clin Invest* 2006;116:1793-801.
123. Vega GL, Adams-Huet B, Peshock R, Willett D, Shah B, Grundy SM. Influence of body fat content and distribution on variation in metabolic risk. *J Clin Endocrinol Metab* 2006;91:4459-66.
124. Snijder MB, Visser M, Dekker JM, et al. Low subcutaneous thigh fat is a risk factor for unfavourable glucose and lipid levels, independently of high abdominal fat. The Health ABC Study. *Diabetologia* 2005;48:301-8.
125. Fox CS, Massaro JM, Hoffmann U, et al. Abdominal visceral and subcutaneous adipose tissue compartments: association with metabolic risk factors in the Framingham Heart Study. *Circulation* 2007;116:39-48.
126. Azuma K, Heilbronn LK, Albu JB, Smith SR, Ravussin E, Kelley DE. Adipose tissue distribution in relation to insulin resistance in type 2 diabetes mellitus. *Am J Physiol Endocrinol Metab* 2007;293:E435-42.
127. St-Pierre J, Lemieux I, Perron P, et al. Relation of the "hypertriglyceridemic waist" phenotype to earlier manifestations of coronary artery disease in patients with glucose intolerance and type 2 diabetes mellitus. *Am J Cardiol* 2007;99:369-73.
128. Alberti KG, Eckel RH, Grundy SM, et al. Harmonizing the metabolic syndrome: a joint interim statement of the International Diabetes Federation Task Force on Epidemiology and Prevention; National Heart, Lung, and Blood Institute; American Heart Association; World Heart Federation; International Atherosclerosis Society; and International Association for the Study of Obesity. *Circulation* 2009;120:1640-5.
129. Despres JP, Lemieux I. Abdominal obesity and metabolic syndrome. *Nature* 2006;444:881-7.
130. Bellary S, O'Hare JP, Raymond NT, et al. Enhanced diabetes care to patients of south Asian ethnic origin (the United Kingdom Asian Diabetes Study): a cluster randomised controlled trial. *Lancet* 2008;371:1769-76.
131. McTernan CL, McTernan PG, Harte AL, Levick PL, Barnett AH, Kumar S. Resistin, central obesity, and type 2 diabetes. *Lancet* 2002;359:46-7.
132. McTernan PG, Fisher FM, Valsamakis G, et al. Resistin and type 2 diabetes: regulation of resistin expression by insulin and rosiglitazone and the effects of recombinant resistin on lipid and glucose metabolism in human differentiated adipocytes. *J Clin Endocrinol Metab* 2003;88:6098-106.
133. Fisher FM, McTernan PG, Valsamakis G, et al. Differences in adiponectin protein expression: effect of fat depots and type 2 diabetic status. *Horm Metab Res* 2002;34:650-4.
134. Harte AL, McTernan PG, McTernan CL, et al. Insulin increases angiotensinogen expression in human abdominal subcutaneous adipocytes. *Diabetes Obes Metab* 2003;5:462-7.
135. Hull D, Segall MM. Distinction of brown from white adipose tissue. *Nature* 1966;212:469-72.
136. Nicholls DG, Locke RM. Thermogenic mechanisms in brown fat. *Physiol Rev* 1984;64:1-64.
137. Feldmann HM, Golozoubova V, Cannon B, Nedergaard J. UCP1 ablation induces obesity and abolishes diet-induced thermogenesis in mice exempt from thermal stress by living at thermoneutrality. *Cell Metab* 2009;9:203-9.

138. Hany TF, Gharehpapagh E, Kamel EM, Buck A, Himms-Hagen J, von Schulthess GK. Brown adipose tissue: a factor to consider in symmetrical tracer uptake in the neck and upper chest region. *Eur J Nucl Med Mol Imaging* 2002;29:1393-8.
139. Nedergaard J, Bengtsson T, Cannon B. Unexpected evidence for active brown adipose tissue in adult humans. *Am J Physiol Endocrinol Metab* 2007;293:E444-52.
140. Virtanen KA, Lidell ME, Orava J, et al. Functional brown adipose tissue in healthy adults. *The New England journal of medicine* 2009;360:1518-25.
141. Cypess AM, Lehman S, Williams G, et al. Identification and importance of brown adipose tissue in adult humans. *The New England journal of medicine* 2009;360:1509-17.
142. van Marken Lichtenbelt WD, Vanhomerig JW, Smulders NM, et al. Cold-activated brown adipose tissue in healthy men. *The New England journal of medicine* 2009;360:1500-8.
143. Saito M, Okamatsu-Ogura Y, Matsushita M, et al. High incidence of metabolically active brown adipose tissue in healthy adult humans: effects of cold exposure and adiposity. *Diabetes* 2009;58:1526-31.
144. Zingaretti MC, Crosta F, Vitali A, et al. The presence of UCP1 demonstrates that metabolically active adipose tissue in the neck of adult humans truly represents brown adipose tissue. *Faseb J* 2009;23:3113-20.
145. Enerback S. Brown adipose tissue in humans. *Int J Obes (Lond)* 2010;34 Suppl 1:S43-6.
146. Wu J, Bostrom P, Sparks LM, et al. Beige adipocytes are a distinct type of thermogenic fat cell in mouse and human. *Cell* 2012;150:366-76.
147. Prusiner SB, Cannon B, Lindberg O. Oxidative metabolism in cells isolated from brown adipose tissue. 1. Catecholamine and fatty acid stimulation of respiration. *Eur J Biochem* 1968;6:15-22.
148. Cannon B, Nedergaard J. Energy dissipation in brown fat. *Experientia Suppl* 1978;32:107-11.
149. Cannon B, Nedergaard J. Brown adipose tissue: function and physiological significance. *Physiol Rev* 2004;84:277-359.
150. Heaton GM, Wagenvoort RJ, Kemp A, Jr., Nicholls DG. Brown-adipose-tissue mitochondria: photoaffinity labelling of the regulatory site of energy dissipation. *Eur J Biochem* 1978;82:515-21.
151. Heaton JM. The distribution of brown adipose tissue in the human. *J Anat* 1972;112:35-9.
152. Rothwell NJ, Stock MJ. A role for brown adipose tissue in diet-induced thermogenesis. *Nature* 1979;281:31-5.
153. Lee P, Swarbrick MM, Ho KK. Brown adipose tissue in adult humans: a metabolic renaissance. *Endocr Rev* 2013;34:413-38.
154. Hatai S. On the presence in human embryos of an interscapular gland corresponding to the so-called hibernating gland in the lower animals. *Anatomischer Anzeiger* 1902;xxi:369.
155. Bonnot E. The Interscapular Gland. *Journal of anatomy and physiology* 1908;43:43-58.
156. Rasmussen A, T. The glandular status of brown multilocular adipose tissue. *Endocrinology* 1922;6:760-70.

157. Silverman WA, Zamelis A, Sinclair JC, Agate FJ. Warm Nap of the Newborn. *Pediatrics* 1964;33:984-7.
158. Dawkins MJ, Scopes JW. Non-shivering thermogenesis and brown adipose tissue in the human new-born infant. *Nature* 1965;206:201-2.
159. Bouillaud F, Combes-George M, Ricquier D. Mitochondria of adult human brown adipose tissue contain a 32 000-Mr uncoupling protein. *Biosci Rep* 1983;3:775-80.
160. Astrup A, Bulow J, Christensen NJ, Madsen J. Ephedrine-induced thermogenesis in man: no role for interscapular brown adipose tissue. *Clin Sci (Lond)* 1984;66:179-86.
161. Hany TF, Gharehpapagh E, Kamel EM, Buck A, Himms-Hagen J, von Schulthess GK. Brown adipose tissue: a factor to consider in symmetrical tracer uptake in the neck and upper chest region. *Eur J Nucl Med Mol Imaging* 2002;29:1393-8.
162. Garcia CA, Van Nostrand D, Majd M, et al. Benzodiazepine-resistant "brown fat" pattern in positron emission tomography: two case reports of resolution with temperature control. *Mol Imaging Biol* 2004;6:368-72.
163. Chiba I, K. Evaluation of human brown adipose tissue using positron emission tomography, computerised tomography and histochemical studies in association with body mass index, visceral fat accumulation and insulin resistance. *Obes Rev* 2006;7.
164. Lee P, Zhao JT, Swarbrick MM, et al. High prevalence of brown adipose tissue in adult humans. *J Clin Endocrinol Metab* 2011;96:2450-5.
165. Lee P, Swarbrick MM, Zhao JT, Ho KK. Inducible brown adipogenesis of supraclavicular fat in adult humans. *Endocrinology* 2011;152:3597-602.
166. Ouellet V, Routhier-Labadie A, Bellemare W, et al. Outdoor temperature, age, sex, body mass index, and diabetic status determine the prevalence, mass, and glucose-uptake activity of 18F-FDG-detected BAT in humans. *J Clin Endocrinol Metab* 2011;96:192-9.
167. Sharp LZ, Shinoda K, Ohno H, et al. Human BAT possesses molecular signatures that resemble beige/brite cells. *PLoS One* 2012;7:e49452.
168. Orava J, Nuutila P, Noponen T, et al. Blunted metabolic responses to cold and insulin stimulation in brown adipose tissue of obese humans. *Obesity (Silver Spring)* 2013;21:2279-87.
169. Chen KY, Brychta RJ, Linderman JD, et al. Brown fat activation mediates cold-induced thermogenesis in adult humans in response to a mild decrease in ambient temperature. *J Clin Endocrinol Metab* 2013;98:E1218-23.
170. van der Lans AA, Hoeks J, Brans B, et al. Cold acclimation recruits human brown fat and increases nonshivering thermogenesis. *J Clin Invest* 2013;123:3395-403.
171. Blondin DP, Labbe SM, Tingelstad HC, et al. Increased brown adipose tissue oxidative capacity in cold-acclimated humans. *J Clin Endocrinol Metab* 2014;99:E438-46.
172. Cinti S. Anatomy of the adipose organ. *Eat Weight Disord* 2000;5:132-42.
173. Napolitano L, Fawcett D. The fine structure of brown adipose tissue in the newborn mouse and rat. *J Biophys Biochem Cytol* 1958;4:685-92.
174. Enerback S, Jacobsson A, Simpson EM, et al. Mice lacking mitochondrial uncoupling protein are cold-sensitive but not obese. *Nature* 1997;387:90-4.

175. Arch JR. The brown adipocyte beta-adrenoceptor. *Proc Nutr Soc* 1989;48:215-23.
176. Orava J, Nuutila P, Lidell ME, et al. Different metabolic responses of human brown adipose tissue to activation by cold and insulin. *Cell Metab* 2011;14:272-9.
177. Vrieze A, Schopman JE, Admiraal WM, et al. Fasting and postprandial activity of brown adipose tissue in healthy men. *J Nucl Med* 2012;53:1407-10.
178. Guerra C, Koza RA, Yamashita H, Walsh K, Kozak LP. Emergence of brown adipocytes in white fat in mice is under genetic control. Effects on body weight and adiposity. *J Clin Invest* 1998;102:412-20.
179. Gossler A, Hrabe de Angelis M. Somitogenesis. *Curr Top Dev Biol* 1998;38:225-87.
180. Atit R, Sgaier SK, Mohamed OA, et al. Beta-catenin activation is necessary and sufficient to specify the dorsal dermal fate in the mouse. *Dev Biol* 2006;296:164-76.
181. Timmons JA, Wennmalm K, Larsson O, et al. Myogenic gene expression signature establishes that brown and white adipocytes originate from distinct cell lineages. *Proc Natl Acad Sci U S A* 2007;104:4401-6.
182. Seale P, Bjork B, Yang W, et al. PRDM16 controls a brown fat/skeletal muscle switch. *Nature* 2008;454:961-7.
183. Wu J, Bostrom P, Sparks LM, et al. Beige Adipocytes Are a Distinct Type of Thermogenic Fat Cell in Mouse and Human. *Cell* 2012.
184. Tang W, Zeve D, Suh JM, et al. White fat progenitor cells reside in the adipose vasculature. *Science* 2008;322:583-6.
185. Billon N, Iannarelli P, Monteiro MC, et al. The generation of adipocytes by the neural crest. *Development* 2007;134:2283-92.
186. Farmer SR. Transcriptional control of adipocyte formation. *Cell Metab* 2006;4:263-73.
187. Puigserver P, Wu Z, Park CW, Graves R, Wright M, Spiegelman BM. A cold-inducible coactivator of nuclear receptors linked to adaptive thermogenesis. *Cell* 1998;92:829-39.
188. Silva JE, Larsen PR. Adrenergic activation of triiodothyronine production in brown adipose tissue. *Nature* 1983;305:712-3.
189. Yeung HW, Grewal RK, Gonen M, Schoder H, Larson SM. Patterns of (18)F-FDG uptake in adipose tissue and muscle: a potential source of false-positives for PET. *J Nucl Med* 2003;44:1789-96.
190. Au-Yong IT, Thorn N, Ganatra R, Perkins AC, Symonds ME. Brown adipose tissue and seasonal variation in humans. *Diabetes* 2009;58:2583-7.
191. Pfannenbergl C, Werner MK, Ripkens S, et al. Impact of age on the relationships of brown adipose tissue with sex and adiposity in humans. *Diabetes* 2010;59:1789-93.
192. Truong MT, Erasmus JJ, Munden RF, et al. Focal FDG uptake in mediastinal brown fat mimicking malignancy: a potential pitfall resolved on PET/CT. *AJR Am J Roentgenol* 2004;183:1127-32.
193. Kim S, Krynycky BR, Machac J, Kim CK. Temporal relation between temperature change and FDG uptake in brown adipose tissue. *Eur J Nucl Med Mol Imaging* 2008;35:984-9.

194. Williams G, Kolodny GM. Method for decreasing uptake of 18F-FDG by hypermetabolic brown adipose tissue on PET. *AJR Am J Roentgenol* 2008;190:1406-9.
195. Stefan N, Pfannenbergs C, Haring HU. The importance of brown adipose tissue. *N Engl J Med* 2009;361:416-7; author reply 8-21.
196. Yoneshiro T, Aita S, Matsushita M, et al. Brown adipose tissue, whole-body energy expenditure, and thermogenesis in healthy adult men. *Obesity (Silver Spring)* 2011;19:13-6.
197. Yoneshiro T, Aita S, Matsushita M, et al. Age-related decrease in cold-activated brown adipose tissue and accumulation of body fat in healthy humans. *Obesity (Silver Spring)* 2011;19:1755-60.
198. Cohade C, Osman M, Pannu HK, Wahl RL. Uptake in supraclavicular area fat ("USA-Fat"): description on 18F-FDG PET/CT. *J Nucl Med* 2003;44:170-6.
199. Cheng WY, Zhu ZH, Ouyang M. [Patterns and characteristics of brown adipose tissue uptake of 18F-FDG positron emission tomograph/computed tomography imaging]. *Zhongguo Yi Xue Ke Xue Yuan Xue Bao* 2009;31:370-3.
200. Jacene HA, Cohade CC, Zhang Z, Wahl RL. The relationship between patients' serum glucose levels and metabolically active brown adipose tissue detected by PET/CT. *Mol Imaging Biol* 2011;13:1278-83.
201. Pace L, Nicolai E, D'Amico D, et al. Determinants of physiologic 18F-FDG uptake in brown adipose tissue in sequential PET/CT examinations. *Mol Imaging Biol* 2011;13:1029-35.
202. Cronin CG, Prakash P, Daniels GH, et al. Brown fat at PET/CT: correlation with patient characteristics. *Radiology* 2012;263:836-42.
203. Zukotynski KA, Fahey FH, Laffin S, et al. Seasonal variation in the effect of constant ambient temperature of 24 degrees C in reducing FDG uptake by brown adipose tissue in children. *Eur J Nucl Med Mol Imaging* 2010;37:1854-60.
204. Hamilton G, Smith DL, Jr., Bydder M, Nayak KS, Hu HH. MR properties of brown and white adipose tissues. *J Magn Reson Imaging* 2011;34:468-73.
205. Cinti S. The adipose organ. *Prostaglandins Leukot Essent Fatty Acids* 2005;73:9-15.
206. Hu HH, Smith DL, Jr., Nayak KS, Goran MI, Nagy TR. Identification of brown adipose tissue in mice with fat-water IDEAL-MRI. *J Magn Reson Imaging* 2010;31:1195-202.
207. Carter BW, Schucany WG. Brown adipose tissue in a newborn. *Proc (Bayl Univ Med Cent)* 2008;21:328-30.
208. van Rooijen BD, van der Lans AA, Brans B, et al. Imaging cold-activated brown adipose tissue using dynamic T2*-weighted magnetic resonance imaging and 2-deoxy-2-[18F]fluoro-D-glucose positron emission tomography. *Invest Radiol* 2013;48:708-14.
209. Blaxter K. *Energy metabolism in animals and man*. 4th ed: Cambridge University Press; 1989.
210. van Marken Lichtenbelt WD, Schrauwen P. Implications of nonshivering thermogenesis for energy balance regulation in humans. *American journal of physiology Regulatory, integrative and comparative physiology* 2011;301:R285-96.
211. Westerterp KR, Wilson SA, Rolland V. Diet induced thermogenesis measured over 24h in a respiration chamber: effect of diet composition. *Int J Obes Relat Metab Disord* 1999;23:287-92.

212. Ravussin E, Burnand B, Schutz Y, Jequier E. Twenty-four-hour energy expenditure and resting metabolic rate in obese, moderately obese, and control subjects. *Am J Clin Nutr* 1982;35:566-73.
213. Prentice AM, Black AE, Coward WA, et al. High levels of energy expenditure in obese women. *Br Med J (Clin Res Ed)* 1986;292:983-7.
214. Ravussin E, Lillioja S, Anderson TE, Christin L, Bogardus C. Determinants of 24-hour energy expenditure in man. Methods and results using a respiratory chamber. *J Clin Invest* 1986;78:1568-78.
215. Riggs AJ, White BD, Gropper SS. Changes in energy expenditure associated with ingestion of high protein, high fat versus high protein, low fat meals among underweight, normal weight, and overweight females. *Nutrition journal* 2007;6:40.
216. Schoffelen PF, Westerterp KR. Intra-individual variability and adaptation of overnight- and sleeping metabolic rate. *Physiology & behavior* 2008;94:158-63.
217. FAO/WHO/UNU. Report of a joint FAO/WHO/UNU Expert Consultation: Energy and Protein Requirements, Technical Report Series No 724. World Health Organization 1985.
218. Zhang K, Sun M, Werner P, et al. Sleeping metabolic rate in relation to body mass index and body composition. *Int J Obes Relat Metab Disord* 2002;26:376-83.
219. Ruml W, Seale JL, Conway JM, Moe PW. Repeatability of 24-h energy expenditure measurements in humans by indirect calorimetry. *Am J Clin Nutr* 1990;51:147-52.
220. Marino S, De Gaetano A, Giancaterini A, et al. Computing DIT from energy expenditure measures in a respiratory chamber: a direct modeling method. *Computers in biology and medicine* 2002;32:297-309.
221. Westerterp KR. Diet induced thermogenesis. *Nutrition & metabolism* 2004;1:5.
222. Kinabo JL, Durnin JV. Thermic effect of food in man: effect of meal composition, and energy content. *The British journal of nutrition* 1990;64:37-44.
223. Tai MM, Castillo P, Pi-Sunyer FX. Meal size and frequency: effect on the thermic effect of food. *Am J Clin Nutr* 1991;54:783-7.
224. Schoffelen PF, Westerterp KR, Saris WH, Ten Hoor F. A dual-respiration chamber system with automated calibration. *Journal of applied physiology* 1997;83:2064-72.
225. Bonomi AG, Soenen S, Goris AH, Westerterp KR. Weight-loss induced changes in physical activity and activity energy expenditure in overweight and obese subjects before and after energy restriction. *PLoS One* 2013;8:e59641.
226. Westerterp KR. Physical activity and physical activity induced energy expenditure in humans: measurement, determinants, and effects. *Frontiers in physiology* 2013;4:90.
227. Jacobsson A, Muhleisen M, Cannon B, Nedergaard J. The uncoupling protein thermogenin during acclimation: indications for pretranslational control. *Am J Physiol* 1994;267:R999-1007.
228. Griggio MA. The participation of shivering and nonshivering thermogenesis in warm and cold-acclimated rats. *Comparative biochemistry and physiology A, Comparative physiology* 1982;73:481-4.

229. Mory G, Ricquier D, Hemon P. Effects of chronic treatments upon the brown adipose tissue of rats. II. Comparison between the effects of catecholamine injections and cold adaptation. *Journal de physiologie* 1980;76:859-64.
230. Mineo PM, Cassell EA, Roberts ME, Schaeffer PJ. Chronic cold acclimation increases thermogenic capacity, non-shivering thermogenesis and muscle citrate synthase activity in both wild-type and brown adipose tissue deficient mice. *Comp Biochem Physiol A Mol Integr Physiol* 2012;161:395-400.
231. Barbatelli G, Murano I, Madsen L, et al. The emergence of cold-induced brown adipocytes in mouse white fat depots is determined predominantly by white to brown adipocyte transdifferentiation. *Am J Physiol Endocrinol Metab* 2010;298:E1244-53.
232. Ouellet V, Labbe SM, Blondin DP, et al. Brown adipose tissue oxidative metabolism contributes to energy expenditure during acute cold exposure in humans. *J Clin Invest* 2012;122:545-52.
233. Muzik O, Mangner TJ, Granneman JG. Assessment of oxidative metabolism in brown fat using PET imaging. *Front Endocrinol (Lausanne)* 2012;3:15.
234. Glick Z, Wickler SJ, Stern JS, Horwitz BA. Regional blood flow in rats after a single low-protein, high-carbohydrate test meal. *Am J Physiol* 1984;247:R160-6.
235. Glick Z, Wickler SJ, Stern JS, Horwitz BA. Blood flow into brown fat of rats is greater after a high carbohydrate than after a high fat test meal. *J Nutr* 1984;114:1934-9.
236. Vosselman MJ, Brans B, van der Lans AA, et al. Brown adipose tissue activity after a high-calorie meal in humans. *Am J Clin Nutr* 2013;98:57-64.
237. Lee P, Zhao JT, Swarbrick MM, et al. High prevalence of brown adipose tissue in adult humans. *J Clin Endocrinol Metab* 2011;96:2450-5.
238. Rothwell NJ, Stock MJ. Luxuskonsumption, diet-induced thermogenesis and brown fat: the case in favour. *Clin Sci (Lond)* 1983;64:19-23.
239. Golozoubova V, Hohtola E, Matthias A, Jacobsson A, Cannon B, Nedergaard J. Only UCP1 can mediate adaptive nonshivering thermogenesis in the cold. *Faseb J* 2001;15:2048-50.
240. Muzik O, Mangner TJ, Granneman JG. Assessment of oxidative metabolism in brown fat using PET imaging. *Front Endocrinol (Lausanne)* 2012;3:15.
241. Orava J, Nuutila P, Lidell ME, et al. Different metabolic responses of human brown adipose tissue to activation by cold and insulin. *Cell Metab* 2011;14:272-9.
242. Bartelt A, Bruns OT, Reimer R, et al. Brown adipose tissue activity controls triglyceride clearance. *Nat Med* 2011;17:200-5.
243. Celi FS, Brychta RJ, Linderman JD, et al. Minimal changes in environmental temperature result in a significant increase in energy expenditure and changes in the hormonal homeostasis in healthy adults. *Eur J Endocrinol* 2010;163:863-72.
244. Cerri M, Morrison SF. Activation of lateral hypothalamic neurons stimulates brown adipose tissue thermogenesis. *Neuroscience* 2005;135:627-38.

245. Fan W, Morrison SF, Cao WH, Yu P. Thermogenesis activated by central melanocortin signaling is dependent on neurons in the rostral raphe pallidus (rRPa) area. *Brain research* 2007;1179:61-9.
246. Fueger BJ, Czernin J, Hildebrandt I, et al. Impact of animal handling on the results of 18F-FDG PET studies in mice. *J Nucl Med* 2006;47:999-1006.
247. Simonsen L, Bulow J, Madsen J, Christensen NJ. Thermogenic response to epinephrine in the forearm and abdominal subcutaneous adipose tissue. *Am J Physiol* 1992;263:E850-5.
248. Simonsen L, Stallknecht B, Bulow J. Contribution of skeletal muscle and adipose tissue to adrenaline-induced thermogenesis in man. *Int J Obes Relat Metab Disord* 1993;17 Suppl 3:S47-51; discussion S68.
249. Ricquier D, Nechad M, Mory G. Ultrastructural and biochemical characterization of human brown adipose tissue in pheochromocytoma. *J Clin Endocrinol Metab* 1982;54:803-7.
250. Lean ME, James WP, Jennings G, Trayhurn P. Brown adipose tissue in patients with phaeochromocytoma. *Int J Obes (Lond)* 1986;10:219-27.
251. English JT, Patel SK, Flanagan MJ. Association of pheochromocytomas with brown fat tumors. *Radiology* 1973;107:279-81.
252. Melicow MM. Hibernating fat and pheochromocytoma. *AMA Arch Pathol* 1957;63:367-72.
253. Bouillaud F, Ricquier D, Mory G, Thibault J. Increased level of mRNA for the uncoupling protein in brown adipose tissue of rats during thermogenesis induced by cold exposure or norepinephrine infusion. *J Biol Chem* 1984;259:11583-6.
254. Hadi M, Chen CC, Whatley M, Pacak K, Carrasquillo JA. Brown fat imaging with (18)F-6-fluorodopamine PET/CT, (18)F-FDG PET/CT, and (123)I-MIBG SPECT: a study of patients being evaluated for pheochromocytoma. *J Nucl Med* 2007;48:1077-83.
255. Wang Q, Zhang M, Ning G, et al. Brown adipose tissue in humans is activated by elevated plasma catecholamines levels and is inversely related to central obesity. *PLoS One* 2011;6:e21006.
256. Klitgaard HM, Dirks HB, Jr., Garlick WR, Barker SB. Protein-bound iodine in various tissues after injection of elemental iodine. *Endocrinology* 1952;50:170-3.
257. Klieverik LP, Coomans CP, Endert E, et al. Thyroid hormone effects on whole-body energy homeostasis and tissue-specific fatty acid uptake in vivo. *Endocrinology* 2009;150:5639-48.
258. Silva JE. Thermogenic mechanisms and their hormonal regulation. *Physiol Rev* 2006;86:435-64.
259. Sheehan TE, Kumar PA, Hood DA. Tissue-specific regulation of cytochrome c oxidase subunit expression by thyroid hormone. *Am J Physiol Endocrinol Metab* 2004;286:E968-74.
260. Lopez M, Varela L, Vazquez MJ, et al. Hypothalamic AMPK and fatty acid metabolism mediate thyroid regulation of energy balance. *Nat Med* 2010;16:1001-8.
261. Bianco AC, Silva JE. Cold exposure rapidly induces virtual saturation of brown adipose tissue nuclear T3 receptors. *Am J Physiol* 1988;255:E496-503.

262. Ribeiro MO, Carvalho SD, Schultz JJ, et al. Thyroid hormone--sympathetic interaction and adaptive thermogenesis are thyroid hormone receptor isoform-specific. *J Clin Invest* 2001;108:97-105.
263. Bryzgalova G, Effendic S, Khan A, et al. Anti-obesity, anti-diabetic, and lipid lowering effects of the thyroid receptor beta subtype selective agonist KB-141. *J Steroid Biochem Mol Biol* 2008;111:262-7.
264. Grover GJ, Egan DM, Sleph PG, et al. Effects of the thyroid hormone receptor agonist GC-1 on metabolic rate and cholesterol in rats and primates: selective actions relative to 3,5,3'-triiodo-L-thyronine. *Endocrinology* 2004;145:1656-61.
265. Lee JY, Takahashi N, Yasubuchi M, et al. Triiodothyronine Induces UCP1 Expression and Mitochondrial Biogenesis in Human Adipocytes. *Am J Physiol Cell Physiol* 2011.
266. Skarulis MC, Celi FS, Mueller E, et al. Thyroid hormone induced brown adipose tissue and amelioration of diabetes in a patient with extreme insulin resistance. *J Clin Endocrinol Metab* 2010;95:256-62.
267. Bostrom P, Wu J, Jedrychowski MP, et al. A PGC1-alpha-dependent myokine that drives brown-fat-like development of white fat and thermogenesis. *Nature* 2012;481:463-8.
268. Kajimura S, Seale P, Kubota K, et al. Initiation of myoblast to brown fat switch by a PRDM16-C/EBP-beta transcriptional complex. *Nature* 2009;460:1154-8.
269. Cederberg A, Gronning LM, Ahren B, Tasken K, Carlsson P, Enerback S. FOXC2 is a winged helix gene that counteracts obesity, hypertriglyceridemia, and diet-induced insulin resistance. *Cell* 2001;106:563-73.
270. Hallberg M, Morganstein DL, Kiskinis E, et al. A functional interaction between RIP140 and PGC-1alpha regulates the expression of the lipid droplet protein CIDEA. *Mol Cell Biol* 2008;28:6785-95.
271. Tseng YH, Kokkotou E, Schulz TJ, et al. New role of bone morphogenetic protein 7 in brown adipogenesis and energy expenditure. *Nature* 2008;454:1000-4.
272. Beenken A, Mohammadi M. The FGF family: biology, pathophysiology and therapy. *Nat Rev Drug Discov* 2009;8:235-53.
273. Wilson-Fritch L, Nicoloso S, Chouinard M, et al. Mitochondrial remodeling in adipose tissue associated with obesity and treatment with rosiglitazone. *J Clin Invest* 2004;114:1281-9.
274. Bordicchia M, Liu D, Amri EZ, et al. Cardiac natriuretic peptides act via p38 MAPK to induce the brown fat thermogenic program in mouse and human adipocytes. *J Clin Invest* 2012;122:1022-36.
275. Harms M, Seale P. Brown and beige fat: development, function and therapeutic potential. *Nat Med* 2013;19:1252-63.
276. Wilding JP. Neuropeptides and appetite control. *Diabet Med* 2002;19:619-27.
277. Wren AM, Bloom SR. Gut hormones and appetite control. *Gastroenterology* 2007;132:2116-30.
278. Williams G, Bing C, Cai XJ, Harrold JA, King PJ, Liu XH. The hypothalamus and the control of energy homeostasis: different circuits, different purposes. *Physiology & behavior* 2001;74:683-701.

279. Cone RD, Cowley MA, Butler AA, Fan W, Marks DL, Low MJ. The arcuate nucleus as a conduit for diverse signals relevant to energy homeostasis. *Int J Obes Relat Metab Disord* 2001;25 Suppl 5:S63-7.
280. Zhang Y, Proenca R, Maffei M, Barone M, Leopold L, Friedman JM. Positional cloning of the mouse obese gene and its human homologue. *Nature* 1994;372:425-32.
281. Halaas JL, Gajiwala KS, Maffei M, et al. Weight-reducing effects of the plasma protein encoded by the obese gene. *Science* 1995;269:543-6.
282. Campfield LA, Smith FJ, Guisez Y, Devos R, Burn P. Recombinant mouse OB protein: evidence for a peripheral signal linking adiposity and central neural networks. *Science* 1995;269:546-9.
283. Pelleymounter MA, Cullen MJ, Baker MB, et al. Effects of the obese gene product on body weight regulation in ob/ob mice. *Science* 1995;269:540-3.
284. Sahu A. Leptin signaling in the hypothalamus: emphasis on energy homeostasis and leptin resistance. *Frontiers in neuroendocrinology* 2003;24:225-53.
285. Farooqi IS, Jebb SA, Langmack G, et al. Effects of recombinant leptin therapy in a child with congenital leptin deficiency. *N Engl J Med* 1999;341:879-84.
286. Maffei M, Halaas J, Ravussin E, et al. Leptin levels in human and rodent: measurement of plasma leptin and ob RNA in obese and weight-reduced subjects. *Nat Med* 1995;1:1155-61.
287. Moon HS, Matarese G, Brennan AM, et al. Efficacy of metreleptin in obese patients with type 2 diabetes: cellular and molecular pathways underlying leptin tolerance. *Diabetes* 2011;60:1647-56.
288. Vazier C, Gautier JF, Vigouroux C. Therapeutic use of recombinant methionyl human leptin. *Biochimie* 2012;94:2116-25.
289. Gualillo O, Gonzalez-Juanatey JR, Lago F. The emerging role of adipokines as mediators of cardiovascular function: physiologic and clinical perspectives. *Trends in cardiovascular medicine* 2007;17:275-83.
290. Lawlor DA, Smith GD, Kelly A, Sattar N, Ebrahim S. Leptin and coronary heart disease risk: prospective case control study of British women. *Obesity (Silver Spring)* 2007;15:1694-701.
291. Sattar N, Wannamethee G, Sarwar N, et al. Leptin and coronary heart disease: prospective study and systematic review. *Journal of the American College of Cardiology* 2009;53:167-75.
292. Scherer PE, Williams S, Fogliano M, Baldini G, Lodish HF. A novel serum protein similar to C1q, produced exclusively in adipocytes. *J Biol Chem* 1995;270:26746-9.
293. Trujillo ME, Scherer PE. Adiponectin--journey from an adipocyte secretory protein to biomarker of the metabolic syndrome. *Journal of internal medicine* 2005;257:167-75.
294. Ouchi N, Kihara S, Arita Y, et al. Novel modulator for endothelial adhesion molecules: adipocyte-derived plasma protein adiponectin. *Circulation* 1999;100:2473-6.
295. Yamauchi T, Kamon J, Waki H, et al. The fat-derived hormone adiponectin reverses insulin resistance associated with both lipoatrophy and obesity. *Nat Med* 2001;7:941-6.

296. Yamauchi T, Kamon J, Waki H, et al. Globular adiponectin protected ob/ob mice from diabetes and ApoE-deficient mice from atherosclerosis. *J Biol Chem* 2003;278:2461-8.
297. Kubota N, Terauchi Y, Yamauchi T, et al. Disruption of adiponectin causes insulin resistance and neointimal formation. *J Biol Chem* 2002;277:25863-6.
298. von Eynatten M, Humpert PM, Bluemm A, et al. High-molecular weight adiponectin is independently associated with the extent of coronary artery disease in men. *Atherosclerosis* 2008;199:123-8.
299. Salmenniemi U, Ruotsalainen E, Pihlajamaki J, et al. Multiple abnormalities in glucose and energy metabolism and coordinated changes in levels of adiponectin, cytokines, and adhesion molecules in subjects with metabolic syndrome. *Circulation* 2004;110:3842-8.
300. Kubota N, Yano W, Kubota T, et al. Adiponectin stimulates AMP-activated protein kinase in the hypothalamus and increases food intake. *Cell Metab* 2007;6:55-68.
301. Kojima M, Hosoda H, Date Y, Nakazato M, Matsuo H, Kangawa K. Ghrelin is a growth-hormone-releasing acylated peptide from stomach. *Nature* 1999;402:656-60.
302. Tschop M, Smiley DL, Heiman ML. Ghrelin induces adiposity in rodents. *Nature* 2000;407:908-13.
303. Wren AM, Seal LJ, Cohen MA, et al. Ghrelin enhances appetite and increases food intake in humans. *J Clin Endocrinol Metab* 2001;86:5992.
304. Wren AM, Small CJ, Abbott CR, et al. Ghrelin causes hyperphagia and obesity in rats. *Diabetes* 2001;50:2540-7.
305. Druce MR, Wren AM, Park AJ, et al. Ghrelin increases food intake in obese as well as lean subjects. *Int J Obes (Lond)* 2005;29:1130-6.
306. Murphy KG, Bloom SR. Gut hormones in the control of appetite. *Experimental physiology* 2004;89:507-16.
307. Weigle DS, Cummings DE, Newby PD, et al. Roles of leptin and ghrelin in the loss of body weight caused by a low fat, high carbohydrate diet. *J Clin Endocrinol Metab* 2003;88:1577-86.
308. Mohlig M, Spranger J, Otto B, Ristow M, Tschop M, Pfeiffer AF. Euglycemic hyperinsulinemia, but not lipid infusion, decreases circulating ghrelin levels in humans. *Journal of endocrinological investigation* 2002;25:RC36-8.
309. English PJ, Ghatei MA, Malik IA, Bloom SR, Wilding JP. Food fails to suppress ghrelin levels in obese humans. *J Clin Endocrinol Metab* 2002;87:2984.
310. Cummings DE, Weigle DS, Frayo RS, et al. Plasma ghrelin levels after diet-induced weight loss or gastric bypass surgery. *N Engl J Med* 2002;346:1623-30.
311. Karamanakos SN, Vagenas K, Kalfarentzos F, Alexandrides TK. Weight loss, appetite suppression, and changes in fasting and postprandial ghrelin and peptide-YY levels after Roux-en-Y gastric bypass and sleeve gastrectomy: a prospective, double blind study. *Ann Surg* 2008;247:401-7.
312. Couce ME, Cottam D, Esplen J, Schauer P, Burguera B. Is ghrelin the culprit for weight loss after gastric bypass surgery? A negative answer. *Obesity surgery* 2006;16:870-8.
313. Garcia-Fuentes E, Garrido-Sanchez L, Garcia-Almeida JM, et al. Different effect of laparoscopic Roux-en-Y gastric bypass and open biliopancreatic

- diversion of Scopinaro on serum PYY and ghrelin levels. *Obesity surgery* 2008;18:1424-9.
314. Wortley KE, del Rincon JP, Murray JD, et al. Absence of ghrelin protects against early-onset obesity. *J Clin Invest* 2005;115:3573-8.
315. Zigman JM, Nakano Y, Coppari R, et al. Mice lacking ghrelin receptors resist the development of diet-induced obesity. *J Clin Invest* 2005;115:3564-72.
316. Foster-Schubert KE, Cummings DE. Emerging therapeutic strategies for obesity. *Endocr Rev* 2006;27:779-93.
317. Batterham RL, Cowley MA, Small CJ, et al. Gut hormone PYY(3-36) physiologically inhibits food intake. *Nature* 2002;418:650-4.
318. Adrian TE, Ferri GL, Bacarese-Hamilton AJ, Fuessl HS, Polak JM, Bloom SR. Human distribution and release of a putative new gut hormone, peptide YY. *Gastroenterology* 1985;89:1070-7.
319. Batterham RL, Cohen MA, Ellis SM, et al. Inhibition of food intake in obese subjects by peptide YY3-36. *N Engl J Med* 2003;349:941-8.
320. Korner J, Bessler M, Cirilo LJ, et al. Effects of Roux-en-Y gastric bypass surgery on fasting and postprandial concentrations of plasma ghrelin, peptide YY, and insulin. *J Clin Endocrinol Metab* 2005;90:359-65.
321. Gantz I, Erondy N, Mallick M, et al. Efficacy and safety of intranasal peptide YY3-36 for weight reduction in obese adults. *J Clin Endocrinol Metab* 2007;92:1754-7.
322. Halatchev IG, Cone RD. Peripheral administration of PYY(3-36) produces conditioned taste aversion in mice. *Cell Metab* 2005;1:159-68.
323. Verdich C, Flint A, Gutzwiller JP, et al. A meta-analysis of the effect of glucagon-like peptide-1 (7-36) amide on ad libitum energy intake in humans. *J Clin Endocrinol Metab* 2001;86:4382-9.
324. Herrmann C, Goke R, Richter G, Fehmann HC, Arnold R, Goke B. Glucagon-like peptide-1 and glucose-dependent insulin-releasing polypeptide plasma levels in response to nutrients. *Digestion* 1995;56:117-26.
325. Kieffer TJ, McIntosh CH, Pederson RA. Degradation of glucose-dependent insulinotropic polypeptide and truncated glucagon-like peptide 1 in vitro and in vivo by dipeptidyl peptidase IV. *Endocrinology* 1995;136:3585-96.
326. Turrel C, Bailbe D, Meile MJ, Kergoat M, Portha B. Glucagon-like peptide-1 and exendin-4 stimulate beta-cell neogenesis in streptozotocin-treated newborn rats resulting in persistently improved glucose homeostasis at adult age. *Diabetes* 2001;50:1562-70.
327. Turton MD, O'Shea D, Gunn I, et al. A role for glucagon-like peptide-1 in the central regulation of feeding. *Nature* 1996;379:69-72.
328. Eng J, Kleinman WA, Singh L, Singh G, Raufman JP. Isolation and characterization of exendin-4, an exendin-3 analogue, from *Heloderma suspectum* venom. Further evidence for an exendin receptor on dispersed acini from guinea pig pancreas. *J Biol Chem* 1992;267:7402-5.
329. Gutzwiller JP, Goke B, Drewe J, et al. Glucagon-like peptide-1: a potent regulator of food intake in humans. *Gut* 1999;44:81-6.
330. Naslund E, Barkeling B, King N, et al. Energy intake and appetite are suppressed by glucagon-like peptide-1 (GLP-1) in obese men. *Int J Obes Relat Metab Disord* 1999;23:304-11.

331. Toft-Nielsen MB, Madsbad S, Holst JJ. Continuous subcutaneous infusion of glucagon-like peptide 1 lowers plasma glucose and reduces appetite in type 2 diabetic patients. *Diabetes care* 1999;22:1137-43.
332. Baggio LL, Huang Q, Brown TJ, Drucker DJ. Oxyntomodulin and glucagon-like peptide-1 differentially regulate murine food intake and energy expenditure. *Gastroenterology* 2004;127:546-58.
333. le Roux CW, Welbourn R, Werling M, et al. Gut hormones as mediators of appetite and weight loss after Roux-en-Y gastric bypass. *Ann Surg* 2007;246:780-5.
334. Ahren B, Winzell MS, Wierup N, Sundler F, Burkey B, Hughes TE. DPP-4 inhibition improves glucose tolerance and increases insulin and GLP-1 responses to gastric glucose in association with normalized islet topography in mice with beta-cell-specific overexpression of human islet amyloid polypeptide. *Regulatory peptides* 2007;143:97-103.
335. Chaudhri OB, Wynne K, Bloom SR. Can gut hormones control appetite and prevent obesity? *Diabetes care* 2008;31 Suppl 2:S284-9.
336. Track NS, McLeod RS, Mee AV. Human pancreatic polypeptide: studies of fasting and postprandial plasma concentrations. *Can J Physiol Pharmacol* 1980;58:1484-9.
337. Lin S, Shi YC, Yulyaningsih E, et al. Critical role of arcuate Y4 receptors and the melanocortin system in pancreatic polypeptide-induced reduction in food intake in mice. *PLoS One* 2009;4:e8488.
338. Malaisse-Lagae F, Carpentier JL, Patel YC, Malaisse WJ, Orci L. Pancreatic polypeptide: a possible role in the regulation of food intake in the mouse. *Hypothesis. Experientia* 1977;33:915-7.
339. Batterham RL, Le Roux CW, Cohen MA, et al. Pancreatic polypeptide reduces appetite and food intake in humans. *J Clin Endocrinol Metab* 2003;88:3989-92.
340. Perry B, Wang Y. Appetite regulation and weight control: the role of gut hormones. *Nutrition & diabetes* 2012;2:e26.
341. Ferrannini E, Camastra S, Coppack SW, Fliser D, Golay A, Mitrakou A. Insulin action and non-esterified fatty acids. The European Group for the Study of Insulin Resistance (EGIR). *Proc Nutr Soc* 1997;56:753-61.
342. Campbell PJ, Carlson MG, Hill JO, Nurjhan N. Regulation of free fatty acid metabolism by insulin in humans: role of lipolysis and reesterification. *Am J Physiol* 1992;263:E1063-9.
343. Golay A, Swislocki AL, Chen YD, Jaspan JB, Reaven GM. Effect of obesity on ambient plasma glucose, free fatty acid, insulin, growth hormone, and glucagon concentrations. *J Clin Endocrinol Metab* 1986;63:481-4.
344. Frayn KN, Williams CM, Arner P. Are increased plasma non-esterified fatty acid concentrations a risk marker for coronary heart disease and other chronic diseases? *Clin Sci (Lond)* 1996;90:243-53.
345. Rosen ED, Spiegelman BM. Adipocytes as regulators of energy balance and glucose homeostasis. *Nature* 2006;444:847-53.
346. McGarry JD, Dobbins RL. Fatty acids, lipotoxicity and insulin secretion. *Diabetologia* 1999;42:128-38.
347. Sako Y, Grill VE. A 48-hour lipid infusion in the rat time-dependently inhibits glucose-induced insulin secretion and B cell oxidation through a process likely coupled to fatty acid oxidation. *Endocrinology* 1990;127:1580-9.

348. Zhou YP, Grill V. Long term exposure to fatty acids and ketones inhibits B-cell functions in human pancreatic islets of Langerhans. *J Clin Endocrinol Metab* 1995;80:1584-90.
349. Mason TM, Goh T, Tchipashvili V, et al. Prolonged elevation of plasma free fatty acids desensitizes the insulin secretory response to glucose in vivo in rats. *Diabetes* 1999;48:524-30.
350. Gremlich S, Bonny C, Waeber G, Thorens B. Fatty acids decrease IDX-1 expression in rat pancreatic islets and reduce GLUT2, glucokinase, insulin, and somatostatin levels. *J Biol Chem* 1997;272:30261-9.
351. Milburn JL, Jr., Hirose H, Lee YH, et al. Pancreatic beta-cells in obesity. Evidence for induction of functional, morphologic, and metabolic abnormalities by increased long chain fatty acids. *J Biol Chem* 1995;270:1295-9.
352. Shimabukuro M, Zhou YT, Levi M, Unger RH. Fatty acid-induced beta cell apoptosis: a link between obesity and diabetes. *Proc Natl Acad Sci U S A* 1998;95:2498-502.
353. Randle PJ, Garland PB, Hales CN, Newsholme EA. The glucose fatty-acid cycle. Its role in insulin sensitivity and the metabolic disturbances of diabetes mellitus. *Lancet* 1963;1:785-9.
354. Basu S, Kwee TC, Surti S, Akin EA, Yoo D, Alavi A. Fundamentals of PET and PET/CT imaging. *Ann N Y Acad Sci* 2011;1228:1-18.
355. Saha G, B. Basics in PET imaging. 2010.
356. Ghonge N, P. Computed Tomography in the 21st Century: Current Status & Future Prospects. *Journal of International Medical Sciences Academy* 2013;26.
357. Goldman LW. Principles of CT and CT technology. *J Nucl Med Technol* 2007;35:115-28; quiz 29-30.
358. Beyer T, Townsend DW, Brun T, et al. A combined PET/CT scanner for clinical oncology. *J Nucl Med* 2000;41:1369-79.
359. Wagner HN, Jr. A brief history of positron emission tomography (PET). *Semin Nucl Med* 1998;28:213-20.
360. Clinical Guidelines on the Identification, Evaluation, and Treatment of Overweight and Obesity in Adults--The Evidence Report. National Institutes of Health. *Obesity research* 1998;6 Suppl 2:51S-209S.
361. Roza AM, Shizgal HM. The Harris Benedict equation reevaluated: resting energy requirements and the body cell mass. *Am J Clin Nutr* 1984;40:168-82.
362. Lucignani G, Paganelli G, Bombardieri E. The use of standardized uptake values for assessing FDG uptake with PET in oncology: a clinical perspective. *Nucl Med Commun* 2004;25:651-6.
363. Thie JA. Understanding the standardized uptake value, its methods, and implications for usage. *J Nucl Med* 2004;45:1431-4.
364. Larson SM, Erdi Y, Akhurst T, et al. Tumor Treatment Response Based on Visual and Quantitative Changes in Global Tumor Glycolysis Using PET-FDG Imaging. The Visual Response Score and the Change in Total Lesion Glycolysis. *Clinical positron imaging : official journal of the Institute for Clinical PET* 1999;2:159-71.
365. Huang Y-C, Chen T-B, Hsu C-C, et al. The relationship between brown adipose tissue activity and neoplastic status: an 18F-FDG PET/CT study in the tropics. *Lipids in health and disease* 2011;10:238.

366. van Marken Lichtenbelt WD, Vanhommerig JW, Smulders NM, et al. Cold-activated brown adipose tissue in healthy men. *N Engl J Med* 2009;360:1500-8.
367. Ross R, Leger L, Guardo R, De Guise J, Pike BG. Adipose tissue volume measured by magnetic resonance imaging and computerized tomography in rats. *Journal of applied physiology* 1991;70:2164-72.
368. Carr H. Free precession techniques in Nuclear Magnetic Resonance. PhD thesis, Harvard 1952.
369. Bitar R, Leung G, Perng R, et al. MR pulse sequences: what every radiologist wants to know but is afraid to ask. *Radiographics* 2006;26:513-37.
370. Buoni C, Barile A. Basics of the magnetic resonance phenomenon. *Italian journal of neurological sciences* 1992;13:91-5.
371. Sands MJ, Levitin A. Basics of magnetic resonance imaging. *Seminars in vascular surgery* 2004;17:66-82.
372. Reeder SB, Pineda AR, Wen Z, et al. Iterative decomposition of water and fat with echo asymmetry and least-squares estimation (IDEAL): application with fast spin-echo imaging. *Magnetic resonance in medicine : official journal of the Society of Magnetic Resonance in Medicine / Society of Magnetic Resonance in Medicine* 2005;54:636-44.
373. Reeder SB, Wen Z, Yu H, et al. Multicoil Dixon chemical species separation with an iterative least-squares estimation method. *Magnetic resonance in medicine : official journal of the Society of Magnetic Resonance in Medicine / Society of Magnetic Resonance in Medicine* 2004;51:35-45.
374. WorldHealthOrganisation. Use of Glycated Haemoglobin (HbA1c) in the Diagnosis of Diabetes Mellitus 2011.
375. Fields DA, Goran MI, McCrory MA. Body-composition assessment via air-displacement plethysmography in adults and children: a review. *Am J Clin Nutr* 2002;75:453-67.
376. Siri WE. Body composition from fluid spaces and density: analysis of methods. 1961. *Nutrition* 1993;9:480-91; discussion , 92.
377. Schoffelen PF, Westerterp KR, Saris WH, Ten Hoor F. A dual-respiration chamber system with automated calibration. *J Appl Physiol* 1997;83:2064-72.
378. Weir JB. New methods for calculating metabolic rate with special reference to protein metabolism. *J Physiol* 1949;109:1-9.
379. Ravn AM, Gregersen NT, Christensen R, et al. Thermic effect of a meal and appetite in adults: an individual participant data meta-analysis of meal-test trials. *Food & nutrition research* 2013;57.
380. Pruessner JC, Kirschbaum C, Meinlschmid G, Hellhammer DH. Two formulas for computation of the area under the curve represent measures of total hormone concentration versus time-dependent change. *Psychoneuroendocrinology* 2003;28:916-31.
381. Elshal MF, McCoy JP. Multiplex bead array assays: performance evaluation and comparison of sensitivity to ELISA. *Methods* 2006;38:317-23.
382. Creely SJ, McTernan PG, Kusminski CM, et al. Lipopolysaccharide activates an innate immune system response in human adipose tissue in obesity and type 2 diabetes. *Am J Physiol Endocrinol Metab* 2007;292:E740-7.
383. Persichetti A, Sciuto R, Rea S, et al. Prevalence, mass, and glucose-uptake activity of (1)(8)F-FDG-detected brown adipose tissue in humans living in a temperate zone of Italy. *PLoS One* 2013;8:e63391.

384. Huang YC, Hsu CC, Wang PW, et al. Review analysis of the association between the prevalence of activated brown adipose tissue and outdoor temperature. *ScientificWorldJournal* 2012;2012:793039.
385. Zhang Z, Cypess AM, Miao Q, et al. The prevalence and predictors of active brown adipose tissue in Chinese adults. *Eur J Endocrinol* 2014;170:359-66.
386. van der Veen DR, Shao J, Chapman S, Leevy WM, Duffield GE. A diurnal rhythm in glucose uptake in brown adipose tissue revealed by in vivo PET-FDG imaging. *Obesity (Silver Spring)* 2012;20:1527-9.
387. al-Adsani H, Hoffer LJ, Silva JE. Resting energy expenditure is sensitive to small dose changes in patients on chronic thyroid hormone replacement. *J Clin Endocrinol Metab* 1997;82:1118-25.
388. Tobin J. Estimation of relationships for limited dependent variables. *Econometrica* 1958;26:24-36.
389. Cypess AM, Kahn CR. The role and importance of brown adipose tissue in energy homeostasis. *Curr Opin Pediatr* 2010;22:478-84.
390. Hamann A, Flier JS, Lowell BB. Decreased brown fat markedly enhances susceptibility to diet-induced obesity, diabetes, and hyperlipidemia. *Endocrinology* 1996;137:21-9.
391. Hamann A, Benecke H, Le Marchand-Brustel Y, Susulic VS, Lowell BB, Flier JS. Characterization of insulin resistance and NIDDM in transgenic mice with reduced brown fat. *Diabetes* 1995;44:1266-73.
392. Lowell BB, V SS, Hamann A, et al. Development of obesity in transgenic mice after genetic ablation of brown adipose tissue. *Nature* 1993;366:740-2.
393. Lahesmaa M, Orava J, Schalin-Jantti C, et al. Hyperthyroidism increases brown fat metabolism in humans. *J Clin Endocrinol Metab* 2014;99:E28-35.
394. Ezaki O. Regulatory elements in the insulin-responsive glucose transporter (GLUT4) gene. *Biochem Biophys Res Commun* 1997;241:1-6.
395. Salvatore D, Bartha T, Harney JW, Larsen PR. Molecular biological and biochemical characterization of the human type 2 selenodeiodinase. *Endocrinology* 1996;137:3308-15.
396. Croteau W, Davey JC, Galton VA, St Germain DL. Cloning of the mammalian type II iodothyronine deiodinase. A selenoprotein differentially expressed and regulated in human and rat brain and other tissues. *J Clin Invest* 1996;98:405-17.
397. Shaw H, B. A contribution to the study of the morphology of adipose tissue. *Journal of anatomy and physiology* 1901.
398. Lunati E, Marzola P, Nicolato E, Fedrigo M, Villa M, Sbarbati A. In vivo quantitative lipidic map of brown adipose tissue by chemical shift imaging at 4.7 Tesla. *J Lipid Res* 1999;40:1395-400.
399. Hamilton G, Smith DL, Jr., Bydder M, Nayak KS, Hu HH. MR properties of brown and white adipose tissues. *J Magn Reson Imaging* 2011;34:468-73.
400. Carpten JD, Robbins CM, Villablanca A, et al. HRPT2, encoding parafibromin, is mutated in hyperparathyroidism-jaw tumor syndrome. *Nat Genet* 2002;32:676-80.
401. Reeder SB, Wen Z, Yu H, et al. Multicoil Dixon chemical species separation with an iterative least-squares estimation method. *Magn Reson Med* 2004;51:35-45.

402. Aquila H, Link TA, Klingenberg M. The uncoupling protein from brown fat mitochondria is related to the mitochondrial ADP/ATP carrier. Analysis of sequence homologies and of folding of the protein in the membrane. *The EMBO journal* 1985;4:2369-76.
403. Sbarbati A, Guerrini U, Marzola P, Asperio R, Osculati F. Chemical shift imaging at 4.7 tesla of brown adipose tissue. *J Lipid Res* 1997;38:343-7.
404. Lunati E, Marzola P, Nicolato E, Fedrigo M, Villa M, Sbarbati A. In vivo quantitative lipidic map of brown adipose tissue by chemical shift imaging at 4.7 Tesla. *J Lipid Res* 1999;40:1395-400.
405. Sbarbati A, Cavallini I, Marzola P, Nicolato E, Osculati F. Contrast-enhanced MRI of brown adipose tissue after pharmacological stimulation. *Magn Reson Med* 2006;55:715-8.
406. Hu HH, Hines CD, Smith DL, Jr., Reeder SB. Variations in T(2)* and fat content of murine brown and white adipose tissues by chemical-shift MRI. *Magn Reson Imaging* 2012;30:323-9.
407. Lee JC, Gupta A, Saifuddin A, et al. Hibernoma: MRI features in eight consecutive cases. *Clin Radiol* 2006;61:1029-34.
408. Hu HH, Tovar JP, Pavlova Z, Smith ML, Gilsanz V. Unequivocal identification of brown adipose tissue in a human infant. *J Magn Reson Imaging* 2012;35:938-42.
409. Danaei G, Finucane MM, Lu Y, et al. National, regional, and global trends in fasting plasma glucose and diabetes prevalence since 1980: systematic analysis of health examination surveys and epidemiological studies with 370 country-years and 2.7 million participants. *Lancet* 2011;378:31-40.
410. Karhunen LJ, Juvonen KR, Huotari A, Purhonen AK, Herzig KH. Effect of protein, fat, carbohydrate and fibre on gastrointestinal peptide release in humans. *Regulatory peptides* 2008;149:70-8.
411. Juvonen KR, Purhonen AK, Salmenkallio-Marttila M, et al. Viscosity of oat bran-enriched beverages influences gastrointestinal hormonal responses in healthy humans. *J Nutr* 2009;139:461-6.
412. Orlet Fisher J, Rolls BJ, Birch LL. Children's bite size and intake of an entree are greater with large portions than with age-appropriate or self-selected portions. *Am J Clin Nutr* 2003;77:1164-70.
413. Levitsky DA, Youn T. The more food young adults are served, the more they overeat. *J Nutr* 2004;134:2546-9.
414. Kral JG, Buckley MC, Kissileff HR, Schaffner F. Metabolic correlates of eating behavior in severe obesity. *Int J Obes Relat Metab Disord* 2001;25:258-64.
415. Karl JP, Young AJ, Rood JC, Montain SJ. Independent and combined effects of eating rate and energy density on energy intake, appetite, and gut hormones. *Obesity (Silver Spring)* 2013;21:E244-52.
416. Burton-Freeman B. Dietary fiber and energy regulation. *J Nutr* 2000;130:272S-5S.
417. McCrory MA, Saltzman E, Rolls BJ, Roberts SB. A twin study of the effects of energy density and palatability on energy intake of individual foods. *Physiology & behavior* 2006;87:451-9.
418. Prentice AM. Manipulation of dietary fat and energy density and subsequent effects on substrate flux and food intake. *Am J Clin Nutr* 1998;67:535S-41S.

419. Ludwig DS, Majzoub JA, Al-Zahrani A, Dallal GE, Blanco I, Roberts SB. High glycemic index foods, overeating, and obesity. *Pediatrics* 1999;103:E26.
420. DiMeglio DP, Mattes RD. Liquid versus solid carbohydrate: effects on food intake and body weight. *Int J Obes Relat Metab Disord* 2000;24:794-800.
421. French SA, Story M, Neumark-Sztainer D, Fulkerson JA, Hannan P. Fast food restaurant use among adolescents: associations with nutrient intake, food choices and behavioral and psychosocial variables. *Int J Obes Relat Metab Disord* 2001;25:1823-33.
422. Clifton PG, Popplewell DA, Burton MJ. Feeding rate and meal patterns in the laboratory rat. *Physiology & behavior* 1984;32:369-74.
423. Sclafani A. Eating rates in normal and hypothalamic hyperphagic rats. *Physiology & behavior* 1994;55:489-94.
424. Lucas GA, Timberlake W. Interpellet delay and meal patterns in the rat. *Physiology & behavior* 1988;43:259-64.
425. Stuart R, B. *Slim Chance in a Fat World: Behavioural Control of Obesity*. Champaign, Illinois Research Press 1972.
426. Tanihara S, Imatoh T, Miyazaki M, et al. Retrospective longitudinal study on the relationship between 8-year weight change and current eating speed. *Appetite* 2011;57:179-83.
427. Sasaki S, Katagiri A, Tsuji T, Shimoda T, Amano K. Self-reported rate of eating correlates with body mass index in 18-y-old Japanese women. *Int J Obes Relat Metab Disord* 2003;27:1405-10.
428. Pliner P, Bell R, Hirsch ES, Kinchla M. Meal duration mediates the effect of "social facilitation" on eating in humans. *Appetite* 2006;46:189-98.
429. Sobki SH, Zaid AA, Khan HA, Alhomida AS, Hilal KA, Khan SA. Significant impact of pace of eating on serum ghrelin and glucose levels. *Clinical biochemistry* 2010;43:522-4.
430. Turer AT, Scherer PE. Adiponectin: mechanistic insights and clinical implications. *Diabetologia* 2012;55:2319-26.
431. Lambert JE, Parks EJ. Postprandial metabolism of meal triglyceride in humans. *Biochim Biophys Acta* 2012;1821:721-6.
432. Farese RV, Jr., Yost TJ, Eckel RH. Tissue-specific regulation of lipoprotein lipase activity by insulin/glucose in normal-weight humans. *Metabolism* 1991;40:214-6.
433. Peterson J, Bihain BE, Bengtsson-Olivecrona G, Deckelbaum RJ, Carpentier YA, Olivecrona T. Fatty acid control of lipoprotein lipase: a link between energy metabolism and lipid transport. *Proc Natl Acad Sci U S A* 1990;87:909-13.
434. Totsuka K, Maeno T, Saito K, et al. Self-reported fast eating is a potent predictor of development of impaired glucose tolerance in Japanese men and women: Tsukuba Medical Center Study. *Diabetes research and clinical practice* 2011;94:e72-4.
435. Sakurai M, Nakamura K, Miura K, et al. Self-reported speed of eating and 7-year risk of type 2 diabetes mellitus in middle-aged Japanese men. *Metabolism* 2012;61:1566-71.
436. Barrows BR, Timlin MT, Parks EJ. Spillover of dietary fatty acids and use of serum nonesterified fatty acids for the synthesis of VLDL-triacylglycerol under two different feeding regimens. *Diabetes* 2005;54:2668-73.

437. Westerterp-Plantenga MS, Rolland V, Wilson SA, Westerterp KR. Satiety related to 24 h diet-induced thermogenesis during high protein/carbohydrate vs high fat diets measured in a respiration chamber. *Eur J Clin Nutr* 1999;53:495-502.
438. Wishnofsky M. Caloric equivalents of gained or lost weight. *Am J Clin Nutr* 1958;6:542-6.
439. Veldhorst M, Smeets A, Soenen S, et al. Protein-induced satiety: effects and mechanisms of different proteins. *Physiology & behavior* 2008;94:300-7.
440. Vosselman MJ, Brans B, van der Lans AA, et al. Brown adipose tissue activity after a high-calorie meal in humans. *Am J Clin Nutr* 2013;98:57-64.
441. Ohkuma T, Fujii H, Iwase M, et al. Impact of eating rate on obesity and cardiovascular risk factors according to glucose tolerance status: the Fukuoka Diabetes Registry and the Hisayama Study. *Diabetologia* 2013;56:70-7.
442. Karl JP, Young AJ, Montain SJ. Eating rate during a fixed-portion meal does not affect postprandial appetite and gut peptides or energy intake during a subsequent meal. *Physiology & behavior* 2011;102:524-31.
443. Scisco JL, Muth ER, Dong Y, Hoover AW. Slowing bite-rate reduces energy intake: an application of the bite counter device. *J Am Diet Assoc* 2011;111:1231-5.
444. Kokkinos A, le Roux CW, Alexiadou K, et al. Eating slowly increases the postprandial response of the anorexigenic gut hormones, peptide YY and glucagon-like peptide-1. *J Clin Endocrinol Metab* 2010;95:333-7.
445. Brennan IM, Feltrin KL, Nair NS, et al. Effects of the phases of the menstrual cycle on gastric emptying, glycemia, plasma GLP-1 and insulin, and energy intake in healthy lean women. *American journal of physiology Gastrointestinal and liver physiology* 2009;297:G602-10.
446. Padwal RS, Majumdar SR. Drug treatments for obesity: orlistat, sibutramine, and rimonabant. *Lancet* 2007;369:71-7.
447. Tseng YH, Cypess AM, Kahn CR. Cellular bioenergetics as a target for obesity therapy. *Nat Rev Drug Discov* 2010;9:465-82.
448. Hu HH, Perkins TG, Chia JM, Gilsanz V. Characterization of human brown adipose tissue by chemical-shift water-fat MRI. *AJR Am J Roentgenol* 2013;200:177-83.
449. Khanna A, Branca RT. Detecting brown adipose tissue activity with BOLD MRI in mice. *Magn Reson Med* 2012;68:1285-90.
450. Johnston CS, Day CS, Swan PD. Postprandial thermogenesis is increased 100% on a high-protein, low-fat diet versus a high-carbohydrate, low-fat diet in healthy, young women. *Journal of the American College of Nutrition* 2002;21:55-61.

APPENDIX

LIST OF PUBLICATIONS ARISING FROM THE THESIS

Identification of brown adipose tissue using MR imaging in a human adult with histological and immunohistochemical confirmation- published January 2014
Narendra Reddy, Terry Jones, Sailesh Sankar, Sudhesh Kumar, Philip McTernan, Gyanendra Tripathi, Harpal Randeva, Charles Hutchinson, Thomas Barber:*
Journal of Clinical Endocrinology and Metabolism.

Brown adipose tissue: endocrine determinants of function and therapeutic manipulation as a novel treatment strategy for obesity- published August 2014
Narendra Reddy, Bee Tan, Thomas Barber, Harpal Randeva:*
Biomed Central Obesity

Enhanced thermic effect of food, postprandial NEFA suppression and raised adiponectin in obese women who eat slowly-published January 2015
Narendra Reddy, Chenjing Peng, Marcos Carreira, Louise Halder, John Hattersley, Milan Piya, Gyanendra Tripathi, Harpal Randeva, Felipe Casanueva, Philip Mcternan, Sudhesh Kumar, Thomas Barber:*
Clinical Endocrinology (Oxf)

LIST OF ABSTRACTS

Identification of brown adipose tissue using MR imaging in a human adult with histological and immunohistochemical confirmation
Narendra Reddy, Terry Jones, Sarah Wayte, Olu Adesanyo, Sailesh Sankar, Sudhesh Kumar, Philip Mcternan, Yen Yeo, Gyanendra Tripathi, Harpal Randeva, Charles Hutchinson, Thomas Barber: OR-151*
73rd Scientific Sessions American Diabetes Association, Chicago, USA June 2013

Eating slowly enhances postprandial NEFA suppression and insulin release but has no effect on appetite and energy expenditure in obese women
Narendra Reddy, Chenjing Peng, John Hattersley, Alison Campbell, Marcos Carreira, Gyanendra Tripathi, Alison Harte, Philip McTernan, Sudhesh Kumar, Harpal Randeva, Thomas Barber: Endocrine Abstracts, 2013, vol 22-*
Joint Meeting of the British Endocrine Societies, Harrogate, UK, March 2013

LIST OF ORAL PRESENTATIONS IN INTERNATIONAL MEETINGS

‘MR imaging of human BAT’- 13th December 2012, The Royal Society, London
Joint meeting of **The Physiological Society** and **The Academy of Medical Sciences**

‘Magnetic Resonance imaging of human brown adipose tissue’- 22nd June 2013, Chicago, United States of America
73rd Scientific Sessions American Diabetes Association

‘Novel insights into manipulation of energy expenditure for obesity treatment’- 9th August 2014, Keble College, University of Oxford
European Association for Study of Diabetes (EASD) Hagedorn Workshop



University Hospitals
Coventry and Warwickshire
NHS Trust

Warwick
Medical School

Patient
name:.....

.....

Patient DOB:.....

Patient
address:.....

Dear Dr.....,

The above patient has given informed consent to be involved in a study looking into the development of biomarkers for human brown adipose tissue. This study is based at the University Hospital in Coventry. The study will involve collection of phenotypic and biochemical data, blood and urine samples, MRI scans and, in some patients (undergoing thyroidectomy for clinical reasons), analyses on fat samples taken peri-operatively from the neck. There may also be more detailed metabolic studies in the future. Confidentiality will be maintained at all times.

Clinically relevant data requiring further investigation and management will be discussed with the patient and, if permission is given, their GP also. Appropriate follow-up will be arranged.

If you have any queries relating to this study, please address them to the chief investigator who is Dr. Tom Barber (based at the WISDEM centre at the University Hospital, Coventry and Warwickshire).

Yours sincerely,

Dr. Tom Barber
Associate Professor in Endocrinology and Diabetes
WISDEM Centre
University Hospital, Coventry and Warwickshire

Dr. Narendra Reddy
NIHR Clinical Lecturer in Endocrinology and Diabetes
WISDEM Centre
University Hospital, Coventry and Warwickshire



**Information sheet for possible participation in the ‘Meal duration study’
based at the University Hospital, Coventry and Warwickshire
Version 1; 05/11/2011
Chief investigator: Dr Tom Barber (WISDEM Centre, UHCW, Coventry)**

Dear Patient,

This is an information sheet containing details about a study on ‘Effect of meal duration on human metabolism’ based here at the University Hospital, Coventry and Warwickshire. We are currently inviting patients who attend clinics at the WISDEM centre and healthy volunteers to take part. This is an important study as the results will provide a clearer understanding of how metabolism in humans (the burning off of ingested calories) is regulated and whether meal duration is a factor that affects metabolism. This study thus provides essential data of enormous public health importance.

We would like to give you an opportunity to be involved in this study. Involvement would in no way compromise your care, data would be kept confidential and you would be kept fully informed at all times. If you are interested in taking part in this study, please indicate this by placing a tick in the box below, complete the requested details, detach this front sheet and either hand it to the clinic receptionist following your clinic appointment today or alternatively send the completed sheet to the Chief Investigator at the address provided at the top of this letter. If you are not interested in taking part, simply leave the box blank.

If you are interested in taking part, it would be helpful if you could also provide your name, date of birth and contact number below so that the Chief Investigator or a member of his research team can contact you to make arrangements to meet up to gain informed consent and to provide an opportunity for you to discuss the study in more detail. Any information you give will be treated confidentially.

In am interested in taking part in this study

My name is.....

My date of birth is.....

My contact number is.....

Yours sincerely,

Dr. Tom Barber, Chief Investigator

Other members of the research team: Dr. Narendra Reddy

Prof. Kumar, Dr. H Randeve, Dr. M Weickert, Dr. J Hattersley, Louise Halder

Information sheet for participation in the 'Effect of Meal Duration on Human Metabolism Study' based at the University Hospital, Coventry and Warwickshire

Version 1; 5th November, 2011

Chief investigator: Dr. Tom Barber

Introduction

You are being invited to take part in a research study. Before you decide if you want to take part, it is important that you understand why the research is being done and what it would involve. Please take time to read the following information carefully and discuss it with others if you wish. There will be an opportunity to ask the Chief Investigator or a member of his research team if there is anything that is not clear or if you would like more information. Take time to decide whether or not you wish to take part. We thank you for taking the time to read this information sheet, and for taking part in this study if you decide to do so.

What is the purpose of this study and why have I been asked to participate?

You are being asked to take part in this study because you are either a patient who attends one of the outpatient clinics at the WISDEM centre or a healthy volunteer with physical attributes that are relevant to this study.

Human metabolic disorders (including obesity) are some of the most important medical problems facing us today. It is crucial to gain a complete understanding of human metabolism so that we can adopt better life style or have a better chance of developing more effective drugs to treat metabolic problems in the future. Your involvement in this study would help us to achieve these goals.

In Meal duration Study, volunteers will have some measurements taken (including height and weight) and will undergo non-invasive fat percentage estimation. This is undertaken with the help of a machine called BODPOD where the volunteer is requested to sit with minimal clothing on for 2-4 minutes. There are no risks or complications involved from undergoing this test, specifically no exposure to radiation involved.

In phase 2, we will select appropriate participants involved in phase 1 to be involved in more detailed metabolic studies on the Human Metabolic Unit (based at the University Hospital Coventry): this will involve attending for one day and having measurements of your fat mass (how much fat you have) and assessment of your metabolic rate (how much energy you use up) during resting, following a meal and following some exercise.

Do I have to take part?

It is up to you to decide whether or not to take part. If you decide to take part you would be asked to sign a consent form. You would still be free to withdraw from the study at any time (and to withdraw your samples)

without giving a reason. A decision to withdraw at any time, or a decision not to take part, would not affect the standard of care you receive. If you do decide to consent to be included in this study, with your consent we would inform your General Practitioner and any other relevant Health Care Professionals of your inclusion in the study.

What would happen if I took part?

There are two phases to this study. All participants shall be invited to take part in phase 1. The phase 2 study is more detailed. You may be invited to take part in this also, although this will only be applicable to some of the participants who take part in the phase 1 study.

Phase 1 study: If you agree, we would ask you to allow us to take a fasting blood sample and urine sample. You would be asked to come to the WISDEM Centre, University Hospital, Coventry to have the blood taken after an overnight fast (we would ask you not to eat or drink anything except for water for 12 hours prior to your morning appointment). Measurements from this blood test would include blood fats, sugars and other factors related to metabolism, in addition to blood to be used for extraction of DNA (discussed in more detail below). During this visit, we would also take a brief medical history from you and perform some measurements including height, weight and an estimation of how much fat you have in your body. Your urine sample and some of your blood samples will be kept in a tissue bank pending ethical approval for future studies. Following the fasting blood samples being taken, we will offer you breakfast.

Phase 2 study: At a later date, we may invite you to attend for more detailed metabolic studies to take place on the Human Metabolic Unit at the University Hospital, Coventry. This would involve you attending for a 24 to 36 hour period. We would take an accurate measurement of how much fat you have and then assess your metabolism over the course of 22.5 to 36 hours (starting at 4pm). To do this, we will ask you to stay in a specially designed room (a 'metabolic chamber') while we measure the gases that you breathe in and out. A plan of the metabolic chamber is shown in figure 1 at the end of this document. To ensure that we can take accurate measurements, you would ideally need to stay in the room for the duration of the study (a maximum of between 22.5 and 36 hours) so it is equipped with a bed, desk and chair, computer access, TV, private toilet and sink. Metabolic rate will be assessed whilst at rest, during and following a 'standard meal' and also possibly during and following some moderate exercise (for 15 minutes on an exercise bike). This latter assessment of exercise metabolism will only be applicable to certain participants who are able and willing to perform this exercise. A 'standard meal' means that the caloric content and quantities of protein, fats and sugars are kept constant and standardised between studies. These types of foods are widely used in both clinical and research practice. Any dietary requirements will be respected and catered for. In addition to these studies, we would also assess your sleep quality with a portable sleep machine whilst you are in the metabolic chamber.

What could be the possible disadvantages and risks of taking part?

There are no obvious disadvantages or risks other than possible discomfort from having blood samples taken. To avoid inconvenience, the blood for research purposes would, if possible, be taken at the same time as any blood samples that are planned as part of your routine medical care.

What could be the possible benefits of taking part?

Your participation in the study is unlikely to provide any direct benefit for yourself. However certain results relevant to your medical care will be fed back (see section on “Will I be told the results” below). Your participation in this study would help us to understand better the determinants of human metabolism. This might help with the development of future treatment options.

What would happen to my samples?

The levels of a number of different hormones, blood fats, sugar and insulin would be measured. Some of those levels are measured routinely in patients who attend the WISDEM clinics and some are being measured for research purposes only. DNA (the body’s genetic blueprint) would be extracted from your blood as well so that we could identify which genes control the levels of these substances and human metabolism. Your samples would only be used to investigate factors related to human metabolism. Some of the blood will be stored within a laboratory in the University Hospital, Coventry until genetic analysis takes place. You have the right to withdraw your samples at any stage. The samples we collect and associated data may be shared with other investigators in the UK and elsewhere (both academic and industrial partners) working to understand the basis of human metabolism. However, when samples are passed to other investigators, no information that would allow personal identification will be shared.

Would taking part in this study be kept confidential?

If you consent to take part in the research, your medical records would be inspected by medical and nursing members of the research team. Information about you might be used when the results of the study are published in a medical journal, but your name would not be revealed. If you give your consent, then your General Practitioner would be notified, by letter, of your participation in the study.

If you consent to take part in this research project, you will be allocated a unique personal identification number for the sole purpose of this study. This number will be used to label your blood samples and also in electronic datasets. This will ensure that all samples/data related to you will be anonymised throughout and will therefore ensure that confidentiality is maintained at all times.

Would I be told the results?

If any of your results have clinical relevance for you (such as results of the routine and research hormones, fats and sugar tests indicating a possible new diagnosis of Diabetes), then we would inform you of these. Your

General Practitioner would receive results of the routine tests and if you wanted, we would also send a copy of the research results to him/her.

As with the other stored blood samples the samples for genetic research will also be anonymised with a unique patient identification code. We do not intend to feed back results of genetic tests to participants or their General Practitioners. However it would be possible for the Chief Investigator to use a participant's genetic data to make associations with their clinical data. The link between a participant's unique identification code and their other data collected during this study will be stored in a secure location within the University Hospital, Coventry. Only the Chief Investigator or a member of his research team will have access to this database. Some of the data and some of the samples collected may be used for future research studies.

What if something goes wrong?

This study is covered by the University of Warwick's Clinical Trial Policy for standard fault claims based on the design of the study. In the event that something does go wrong and you are harmed during the research and this is due to someone's negligence then you may have grounds for a legal action for compensation against University Hospitals Coventry & Warwickshire NHS Trust but you may have to pay your legal costs. The normal National Health Service complaints mechanisms will still be available to you (if appropriate).

Will I receive any payment for taking part in the study?

If you incur any travelling expenses as a result of participating in this study through attending for blood tests or the more detailed metabolic studies then these will be fully reimbursed. You will not receive any other payment for taking part in this study.

Who has reviewed the study?

To ensure that the study is being conducted safely and ethically, the Birmingham East North & Solihull Research Ethics Committee have reviewed the study. This committee is a panel comprising medically qualified people and laypersons from the local community.

Who is funding the study?

The consumable costs are being provided from a variety of grants including existing funds available within the department and from the University of Warwick. The Chief Investigator will not be paid for including you in this study.

Future studies

If you decide to give consent to be involved in this study, you will also be asked to give separate consent for the Chief Investigator to contact you at a later date regarding your possible involvement in future research studies relating to human metabolism that have relevant ethical approval.

Contact for further information

Should you require it, further information can be obtained from Dr. Tom Barber, Chief Investigator, Warwickshire Institute for Diabetes, Endocrinology and Metabolism, University Hospital, Coventry.

If you have any concerns or complaints about the research, staff or conduct, please contact:

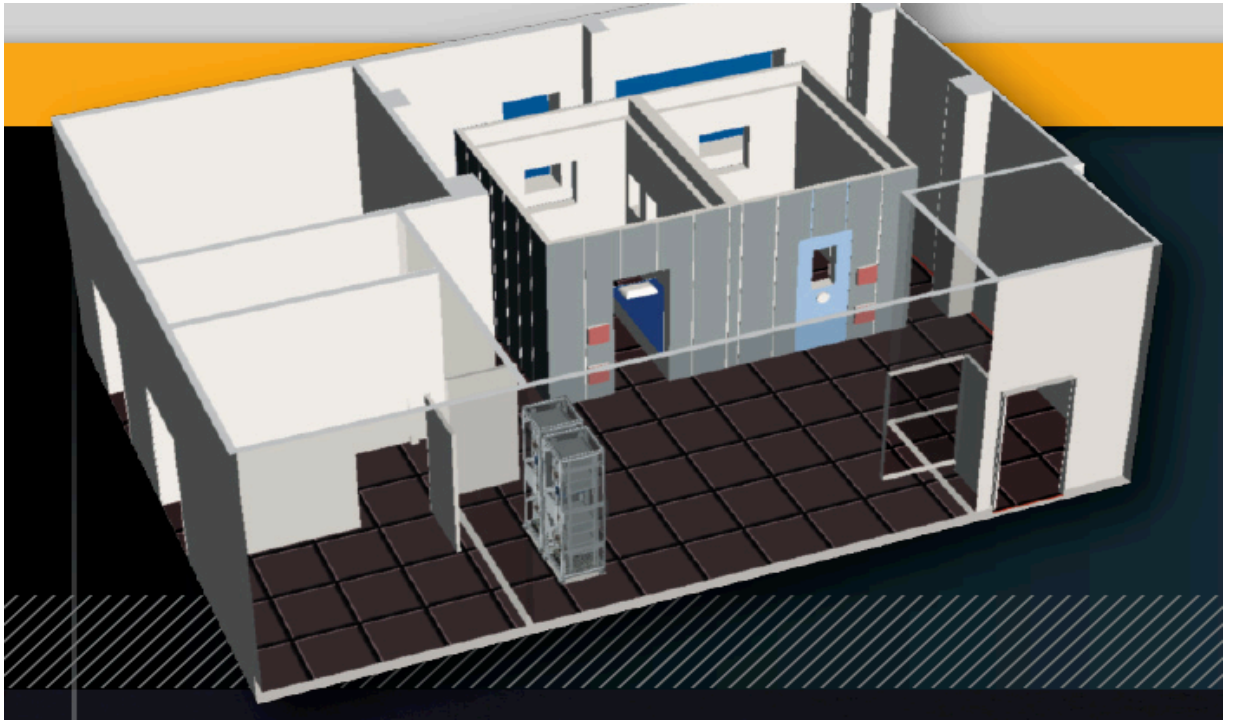
Ms Nicola Owen,
Deputy Registrar,
University of Warwick,
Research Support Services,
University House,
Kirby Corner Road,
Coventry,
CV4 8UW.

E-mail: Nicola.Owen@warwick.ac.uk
Telephone: 024 7652 2785
Fax: 024 7652 4751

Thank you.

Dr. Tom Barber (Chief investigator)
Dr Narendra Reddy (NIHR Clinical Lecturer)
Prof. Sudhesh Kumar,
Dr. Randeve, Dr. Weickert, Dr. Hattersley, Prof. Wilson
University Hospital, Coventry

Figure 1: Plan of the Human Metabolic Research Unit at the University Hospital, Coventry and Warwickshire illustrating the two whole-body metabolic chambers:





**Consent form (phase 2) for participants recruited into the 'Meal Duration Study' based at the University Hospital, Coventry and Warwickshire
Version 2, 05/05/2011**

Chief investigator: Dr. Tom Barber

**Please
initial
boxes**

1. I have already provided informed consent for inclusion in the first part of this study and have already had blood and urine samples taken for storage.

2. I give consent for more detailed metabolic studies to be undertaken, including an assessment of the amount of fat tissue I have, and also my metabolic rate to be measured. I understand that this will involve living in a specially designed room (a 'calorimetry chamber') for between 2 to 36 hours.

3. I give consent for my sleep quality to be assessed during the metabolic assessment in the calorimetry chamber, and understand that this will involve wearing a sensor on my finger, nasal prongs (for airflow assessment) and leads on my chest and head to detect electrical signals during sleep.

4. I understand that I will be free to leave the chamber at any time, although to do so would invalidate the metabolic study results.

5. I confirm that I do not suffer from claustrophobia or isolophobia.

6. I confirm that I have not done any abnormal exercise and have not had any exposure to any radiation within 24 hours of entering the calorimeter chamber, that I do not feel unwell in any way and am not known to be pregnant.

.....
Name of participant Date Signature
(BLOCK CAPITALS)

.....
Name of person taking consent Date Signature
(if different from researcher)

.....
Name of researcher Date Signature

- 1 copy for participant
- 1 copy for researcher
- 1 copy to be kept in hospital notes



Consent form for participants recruited into the ‘Development of Biomarkers for Human Brown Adipose Tissue study’ based at the University Hospital, Coventry and Warwickshire (MRI Study)

Version 2, 23rd March, 2011

Chief investigator: Dr. Tom Barber

**Please
initial
boxes**

1. I have read the information sheet, version 1 dated January 2011, on the above project and have been given a copy to keep. I have had the opportunity to ask questions about the project and understand why the research is being done and any foreseeable risks involved.

2. I give my consent to have MRI scans performed on two separate occasions for research purposes to provide images of fat tissue. I understand that MRI is a safe technique with no associated exposure to harmful ionising radiation and that a check-list of contra-indications (outlined in the information sheet) will be completed just before I have these scans.

3. I give my consent to have blood and urine samples taken for storage.

4. I understand that my participation is voluntary and that I am free to withdraw at any time without giving any reason, without my medical care or legal rights being affected.

5. I understand that relevant sections of my medical notes and data collected during the study, may be looked at by individuals from the research team, from regulatory authorities or from the NHS Trust, where it is relevant to my taking part in this research. I give permission for these individuals to have access to my records.

6. I understand that I will be informed about the results of my medical blood tests if any of these have clinical implications for my health but I shall not be informed about the results of the genetic tests.

7. I understand that I will not benefit financially if this research leads to the development of a new treatment or medical test.

8. I give consent for my General Practitioner to be informed of my involvement in this study and for him/her to be informed of the results of the investigations carried out during this study.

9. I understand that some of my blood and urine samples will be stored within a laboratory in the University Hospital, Coventry and Warwickshire and that future studies with relevant ethical approval, using the samples I give may include genetic research aimed at understanding the

genetic influences on disease, but that the results of these investigations are unlikely to have any implications for me personally.



10. I agree that the samples I have given and the information gathered about me can be looked after and stored in the University Hospital, Coventry for use in future studies with relevant ethical approval, as described in the information sheet. I understand that some of these ethically approved projects may be carried out in the future by researchers other than the study team, including researchers working for commercial companies. However when samples are passed to other investigators, no information that would allow personal identification will be shared.



11. I know how to contact the research team if I need to.



12. I give consent for the Chief Investigator or a member of the research staff working with him at the University Hospital, Coventry to re-contact me at a later date regarding my possible involvement in more detailed human metabolic studies with relevant ethical approval.



13. The following is a safety check-list relating to MRI scans. All the answers need to be answered carefully. They are designed to identify items which may either interfere with the scan or are potentially hazardous in a strong magnetic field:

		Yes	No
1.	Have you had an MRI scan before?		
2.	Do you have or have you ever had a cardiac pacemaker?		
3.	Have you ever had any surgery to your a) heart or chest?		
	b) head or brain? eg. Aneurysm clips or programmable hydrocephalus shunt		
	c) eyes?		
	d) ears?		
4.	Do you have any metal plates, screws or joint replacements?		
5.	Do you have any electronic, mechanical or metal implants in any part of your body?		
6.	Have you had any surgery in the last 8 weeks?		
7.	Have you ever had any incidents to your face or eyes where metal splinters have entered at high speed (eg. While drilling or grinding)? Please tick yes even if these have been removed at an eye hospital.		
8.	Have you had any incidents where bullets, shrapnel or other pieces of metal have entered your body?		
9.	Do you suffer from diabetes, blackouts or epilepsy?		
10.	Do you have any of the following? a) Removable dentures containing metal.		
	b) A hearing aid.		
	c) Body piercing		
	d) Jewellery		
	e) An artificial limb, caliper or corset.		
	f) A transdermal patch.		
	g) Permanent cosmetics (eg. eyeliner)		
	h) Tattoos		
11.	For females of child bearing age a) Are you pregnant?		
	b) Are you breast feeding?		

Tick
box

I confirm that I have been asked the above questions and the information is correct to the best of my knowledge.



.....
Name of participant Date Signature
(BLOCK CAPITALS)

.....
Name of person taking consent Date Signature
(if different from researcher)

.....
Name of researcher Date Signature

- 1 copy for participant
- 1 copy for researcher
- 1 copy to be kept in hospital notes



Information sheet for participants recruited into the ‘Development of Biomarkers for Human Brown Adipose Tissue study’ based at the University Hospital, Coventry and Warwickshire (MRI study)

Version 2, 23rd March, 2011

Chief investigator: Dr. Tom Barber (WISDEM Centre, UHCW, Coventry)

Introduction

You are being invited to take part in a research study. Before you decide if you want to take part, it is important that you understand why the research is being done and what it would involve. Please take time to read the following information carefully and discuss it with others if you wish. There will be an opportunity to ask the Chief Investigator or a member of his research team if there is anything that is not clear or if you would like more information. Take time to decide whether or not you wish to take part. We thank you for taking the time to read this information sheet, and for taking part in this study if you decide to do so.

What is the purpose of this study and why have I been asked to participate?

You are being asked to take part in this study because you are a patient who attends one of the outpatient clinics at the University Hospital in Coventry. Human metabolic disorders (including obesity) are some of the most important medical problems facing us today. It is crucial to gain a complete understanding of human metabolism so that we can have a better chance of developing more effective drugs to treat metabolic problems in the future. Your involvement in this study would help us to achieve these goals.

The Adipose (fat) Tissue Study involves selection of patients to undergo a special scan involving MRI (a safe procedure with no associated exposure to harmful ionising radiation). The purpose of this would be to image fat depots important for metabolism. The scan would be repeated a few months later to see if there has been any change in your fat depots over time. Patients selected for this part of the study will be identified from review of previous images using other techniques (previous images taken for clinical reasons).

Do I have to take part?

It is up to you to decide whether or not to take part. If you decide to take part you would be asked to sign a consent form. You would still be free to withdraw from the study at any time (and to withdraw your samples) without giving a reason. A decision to withdraw at any time, or a decision not to take part, would not affect the standard of care you receive. If you do decide to consent to be included in this study, with your consent we

would inform your General Practitioner and any other relevant Health Care Professionals of your inclusion in the study.

What would happen if I took part?

Following informed consent and an opportunity to discuss the study with the Chief Investigator and to ask any questions, you would be invited to attend for a special Magnetic Resonance Imaging (MRI) scan on two separate occasions (separated by approximately 6 weeks). This will be to image your fat depots. Recruited patients will have already had other imaging taken for clinical reasons. MRI is a safe procedure and there is no exposure to harmful ionising radiation. There is a checklist of contra-indications (provided at the end of this information sheet) that will be completed just prior to each of your scans. Prior to the MRI scan, you will be invited to provide blood and urine samples for further analyses. At this time, we would also request a full medical history to be taken from you and for a non-invasive measurement of body fat mass to be taken, both for the purpose of this study.

What could be the possible disadvantages and risks of taking part?

There are no obvious disadvantages or risks other than possible discomfort from having blood samples taken. To avoid inconvenience, the blood for research purposes would, if possible, be taken at the same time as any blood samples that are planned as part of your routine medical care.

What could be the possible benefits of taking part?

Your participation in the study is unlikely to provide any direct benefit for yourself. However certain results relevant to your medical care will be fed back (see section on “Will I be told the results” below). Your participation in this study would help us to understand better the role of fat tissue in human metabolism. This might help with the development of future treatment options.

What would happen to my samples?

The levels of a number of different hormones, blood fats, sugar and insulin would be measured. Some of those levels are measured routinely and some are being measured for research purposes only. DNA (the body’s genetic blueprint) would be extracted from your blood as well so that we could identify which genes control the levels of these substances and human metabolism. Your samples would only be used to investigate factors related to human metabolism. Some of the blood will be stored within a laboratory in the University Hospital, Coventry until genetic analysis takes place. You have the right to withdraw your samples at any stage. The samples we collect and associated data may be shared with other investigators in the UK and elsewhere (both academic and industrial partners) working to understand the basis of human metabolism. However, when samples are passed to other investigators, no information that would allow personal identification will be shared. **Some of your samples will be kept in long-term storage.**

Would taking part in this study be kept confidential?

If you consent to take part in the research, your medical records would be inspected by medical and nursing members of the research team. Information about you might be used when the results of the study are published in a medical journal, but your name would not be revealed. If you give your consent, then your General Practitioner would be notified, by letter, of your participation in the study.

If you consent to take part in this research project, you will be allocated a unique personal identification number for the sole purpose of this study. This number will be used to label your blood samples and in electronic datasets. This will ensure that all samples/data related to you will be anonymised throughout and will therefore ensure that confidentiality is maintained at all times.

Would I be told the results?

If any of your results have clinical relevance for you (such as results of the routine and research hormones, fats and sugar tests that may indicate a possible new diagnosis of Diabetes), then we would inform you of these. Your General Practitioner would receive results of the routine tests and if you wanted, we would also send a copy of the research results to him/her.

As with the other blood samples taken for storage, samples for genetic research will also be anonymised with unique patient identification codes. We do not intend to feed back results of genetic tests to participants or their General Practitioners. However it would be possible for the Chief Investigator to use a participant's genetic data to make associations with their clinical data. The link between a participant's unique identification code and their other data collected during this study will be stored in a secure location within the University Hospital, Coventry. Only the Chief Investigator will have access to this database. Some of the data and some of the samples collected may be used for future research studies.

What if something goes wrong?

This study is covered by the University of Warwick's Clinical Trial Policy for standard fault claims based on the design of the study. In the event that something does go wrong and you are harmed during the research and this is due to someone's negligence then you may have grounds for a legal action for compensation against University Hospitals Coventry & Warwickshire NHS Trust but you may have to pay your legal costs. The normal National Health Service complaints mechanisms will still be available to you (if appropriate).

Will I receive any payment for taking part in the study?

If you incur any travelling expenses as a result of participating in this study through attending for blood tests or scans then these will be fully reimbursed. You will not receive any other payment for taking part in this study.

Who has reviewed the study?

To ensure that the study is being conducted safely and ethically, a local Research Ethics Committee have reviewed the study. This committee is a panel comprising medically qualified people and laypersons from the local community.

Who is funding the study?

The consumable costs are being provided from a variety of grants including existing funds available within the department and from the University of Warwick. The Chief Investigator will not be paid for including you in this study.

Future studies

If you decide to give consent to be involved in this study, you will also be asked to give separate consent for the Chief Investigator to contact you at a later date regarding your possible involvement in future research studies relating to human metabolism that have relevant ethical approval.

Further information regarding the MRI scans:

Important safety notice

You should notify the Chief Investigator in clinic if you have any of the following:

- Heart pacemaker;
- Heart valve;
- Aneurysm clips in your head;
- Any previous injuries to your eyes involving metal fragments.

Before your scan you must remove all metal objects you are wearing or have in your pockets.

eg. jewellery, watches, keys, credit cards, body piercing, hair clips, hearing aids, coins.

What is MRI?

Magnetic Resonance Imaging (MRI) combines a powerful magnet, radio-waves and an advanced computer to make very clear pictures of any part of the body. MRI does not use X-Rays and there are no known risks provided that the safety form has been correctly filled in.

What do I need to do before the scan?

Unless specifically instructed, you may eat and drink normally.

You can continue with any medication.

Try to wear clothing with no metal fastenings.

You may be asked to change into a gown.

What happens during the scan?

A friend or relative may accompany you into the scan room if necessary.

The scanner is shaped like a large hollow cylinder. It is open at both ends and remains so throughout. Depending on the part of you that is to be scanned, you will enter the magnet either head or feet first.

The machine will make a very loud buzzing or banging noise when scanning. Different scans make different noises. You will be asked to wear earplugs or headphones to protect your ears from the noise.

The radiographer normally takes several sets of pictures, each requiring a few moments to set up, so the machine will be quiet for periods. The radiographer will communicate with you over a microphone at stages throughout the exam. There are microphones within the scanner so you will be able to communicate with the radiographer during the exam as well.

The radiographer is very experienced in looking after nervous patients and has many methods of ensuring that your examination is as comfortable as possible. An average exam takes 20-30 minutes.

What happens after the scan?

The scan has no effect on you and you can leave as soon as you are ready

Contact for further information

Should you require it further information can be obtained from Dr. Tom Barber, Chief Investigator, Warwickshire Institute for Diabetes, Endocrinology and Metabolism, University Hospital, Coventry.

If you have any concerns or complaints about the research, staff or conduct, please contact:

Ms Nicola Owen,
Deputy Registrar,
University of Warwick,
Research Support Services,
University House,
Kirby Corner Road,
Coventry,
CV4 8UW.

E-mail: Nicola.Owen@warwick.ac.uk
Telephone: 024 7652 2785
Fax: 024 7652 4751

Thank you.

Dr. Tom Barber (Chief investigator)
Dr Narendra Reddy, (NIHR Clinical Lecturer)
Prof. Kumar, Dr. Randeve, Dr. Weickert, Dr. Hattersley, Prof. Wilson
University Hospital, Coventry

Chief Investigator: Dr. Tom Barber; Recruitment Pack NMD study; Version 1;
8th February, 2011



Meal Duration Study
University Hospital, Coventry
Participant Recruitment Pack

Signature of researcher taking consent

.....

Unique Participant Identification Number:.....

Meal Duration Study

Medical History

Personal Details

Name DOB.....

Age Tel. no.

Ethnicity Birth weight (*if known*)

Consanguinity?..... Place of birth.....

Birthplace of father..... Birthplace of mother.....

Past Medical History

Endocrine diagnosis:.....

Any history of DM (*type and date of diagnosis*):.....

Any history of IHD, CCF, liver or renal problems (*specify*):.....

Any history of respiratory problems (*specify*):.....

Other past medical history:.....

.....

Family History

Any family history of medical problems?.....

.....

Any family history of DM (*type*):.....

Medications

Insulin or any other oral anti-diabetic drug (*specify*):.....

.....

Steroids or other hormonal therapies (*specify, including OCP*):

.....

Other medication list:.....

.....

.....
Allergies:.....

Social History

Current smoker Ex-smoker Non-smoker

Units of alcohol per week:.....

Systemic Enquiry

Any history of snoring:.....

Any weight change in the last year (give details):.....

.....

Any diets in the last year:.....

.....

Number of hours sun exposure per day (average):.....

Number of times per week for exercise:

Mild exercise (10-30 minutes, no breathlessness or sweating
eg. walking):.....

Moderate exercise (between 10 and 30minutes with sweating
eg. running):.....

Strenuous exercise (>30 minutes with sweating
eg. long run):.....

Menstrual/fertility History (if female)

Last menstrual period (date) Age at menarche
.....

Intervals between menstrual periods in days (*over the last 2 years*)

Shortest intervalLongest interval

Number of days bleeding per menstrual period (*over the last 2
years*)

Shortest duration Longest duration

Any history of hirsutism? (regions
affected):.....

Number of cosmetic treatment(s) for hirsutism needed per
week:.....

(specify treatments):.....

Any history of acne or alopecia? (please specify):.....

Number of pregnancies:.....Number of miscarriages/TOP (specify):.... Chance of current pregnancy?

Current use of contraception? (specify)
.....

Meal Duration Study

Anthropometric and Body Composition Data

Anthropometric measurements

Height (m)

Weight (kg)

BMI

BP (mmHg)

Waist (W) circumference

(mid-point between superior iliac crest and lower costal margin)

Hip (H) circumference

W:H ratio

Body Composition Data

(These data are derived from the Tanita machine that uses foot-to-foot bioimpedance technology)

Lean percentage.....

Fat mass.....

Fat percentage.....

Fasting blood samples for immediate analysis at the UH

Biochemistry: U&E, LFT, fasting lipid profile, glucose, HbA1C

Endocrinology: LH, FSH, Oestradiol, Testosterone, SHBG, Prolactin, TSH, fT4, fT3, IGF1, cortisol (cortisol and testosterone at 9am where possible)

Fasting blood samples for storage at -80 degrees C

Serum samples x3 small tubes

Plasma samples x3 small tubes

EDTA blood sample x2 (for future DNA extraction)

1x sample sent for insulin analysis (for calculation of HOMA measures)

Poster presented in **Warwick Medical School 1st International Symposium in Advances in Human Metabolism Research**

10th November 2011, Scarman House, **University of Warwick, United Kingdom**

Development of the Human Metabolism Research Unit

Barber, TM; Reddy, N; Halder, L; Hattersley, J; Kumar, S

University of Warwick and University Hospitals Coventry and Warwickshire, Clifford Bridge Road, Coventry, CV2 2DX

The Human Metabolism Research Unit (HMRU) is a £1.5 million investment funded by a variety of sources including Science City and the University of Warwick. Based at the University Hospitals Coventry and Warwickshire, HMRU will prove an invaluable resource for University of Warwick-based clinical research into human metabolism

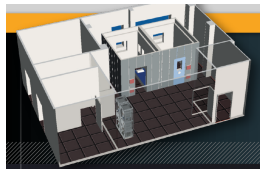


Figure 1: Plan of the Human Metabolism Research Unit, showing two whole-body calorimeters

A major feature of the HMRU is two whole-body calorimeters. These are hermetically-sealed chambers that are capable of precisely measuring human metabolic rate in real-time through the use of indirect calorimetry. Gas concentrations of CO₂ and O₂ are measured accurately for this purpose.



Figure 2: Subject inside chamber. Each chamber is equipped with a pull-down bed, sink, toilet, chair, desk, phone and computer with internet access. There is also an intercom system for communication with the outside, and ports for delivery of food

The HMRU also houses a BodPod. This measures body volume precisely through use of Boyles Law (P1V1 = P2V2). Through precise measurements of body volume and weight, it is possible to calculate body composition, including fat mass.



Figure 3: The BodPod. Inside is the BBC Health Correspondent, Jane Hughes during the recent media profile of HMRU

Through calculation of metabolic rate from CO₂ and O₂ concentrations, data from the whole body calorimeters within HMRU are used to produce metabolic profiles. These provide an assessment of energy expenditure during the resting and post-prandial states, and can be used for comparison between subjects.

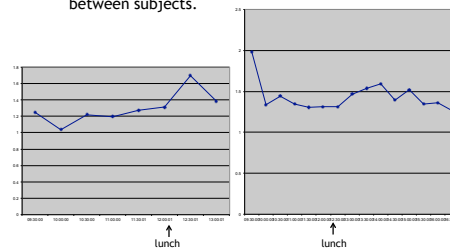


Figure 4: Metabolic profiles. On the left is a lean male control subject showing resting energy expenditure and post-prandial energy expenditure. On the right is the profile of a lean female with untreated hyperthyroidism. Units on y-axis are Kcal per minute. Time is shown on x-axis. This profile clearly demonstrates heightened resting energy expenditure in the hyperthyroid state which is probably one reason why weight loss is a characteristic feature of hyperthyroidism

The HMRU facility holds great potential for important research into human metabolism. In addition to the study of the aetiology and management of obesity through food-based solutions and novel therapeutic strategies, HMRU will also provide a unique opportunity to gain insight into the endocrine determinants of human energy expenditure, and the complexities of the gut-brain-metabolic axis.



Figure 5: 'Does eating slowly help you to lose weight?' This is an ongoing HMRU study into the effects of meal duration on post-prandial energy expenditure and appetite. Through a simple design, each subject will act as their own control. The data will have important public health implications. This study was recently profiled on BBC national news

Figure 6: Professor Kumar during a recent interview on BBC news, discussing obesity and the potential of HMRU for tackling the most important health issue of our age



Poster presented in **Warwick Medical School 2nd International Symposium in Advances in Human Metabolism Research**

17th May 2013, Scarman House, **University of Warwick, United Kingdom**

Brown adipose tissue activation thresholds in lean and overweight men

University Hospitals **NHS**
Coventry and Warwickshire
NHS Trust

Philip Auckland, Narendra Reddy, Terry Jones, Sarah Wayte, Gyanendra Tripathi, John Hattersley, Alison Campbell, Philip McTernan, Charles Hutchinson, Thomas M Barber

Warwick
Medical School

Department of Metabolic and Vascular Health, Clinical Sciences Research Laboratories, Warwick Medical School

Introduction

Brown adipose tissue (BAT) enables the maintenance of body temperature significantly above ambient temperature via **nonshivering thermogenesis**. Originally thought to involve in early childhood, its significance in adult humans has been underestimated. Recently PET-CT scans using ¹⁸F-FDG have identified significant BAT depots in supraclavicular and perirenal regions in adults¹ (fig 1). Prevalence estimates based on these scans vary from 3.1%² to 96%³ in men. It has been estimated that 50g of BAT maximally stimulated would account for 20% of daily energy expenditure. Therefore it could be targeted by **antiobesity therapeutics** aiming to create a negative energy balance⁴.

Aims

The aim of this study was to assess the effect of cold on facultative energy expenditure, a component of which is BAT activation, and correlate this with BAT volume calculated using IDEAL MRI.

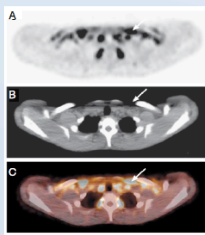


Fig 1 Transverse PET (A), CT (B), and integrated PET-CT (C) scans, with BAT location indicated.

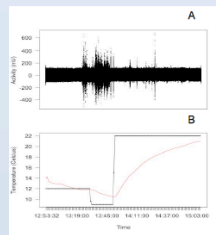


Fig 2 (A) Electrical profile of pectoral shivering. (B) Temperature of chamber during shiver test.

Methods

Metabolic Assessment: The body composition of eight male subjects with BMIs of $26.1\text{kg/m}^2 \pm 5.8\text{kg/m}^2$ was measured using the BopPod. Following overnight fast, each subject underwent 8.5 hours of energy expenditure measurements in whole body calorimeter. Subjects wore surgical scrubs to standardize insulation. Following 90 minutes of immobility to calculate resting metabolic rate, the temperature was decreased in 1.5°C steps over three hours to 13°C (tab 1). Core temperature, blood pressure, and heart rate were taken at 30 minute intervals.

Electromyography (EMG) Assessment: EMG recordings were taken at 1000Hz from both pectoralis major muscles to monitor and minimize shivering. Previous assessment of shivering at 10°C identified the associated electrical profile (fig 2).

IDEAL MRI: To confirm the presence and volume of BAT each subject was scanned using IDEAL MRI, a technique that distinguishes fat types based on water content.

Time	08:30 – 10:00	10:00 – 10:30	10:30 – 11:00	11:00 – 11:30	11:30 – 12:00	12:00 – 12:30	12:30 – 13:00	13:00 – 17:00
Target temperature (°C)	22	20.5	19	17.5	16	14.5	13	22

Table 1 Temperature curve

Results

- The preliminary findings have been taken from 2 participants (P1 & P2) with BMIs of 20.3kg/m² and 27.8kg/m² respectively.
- As the temperature decreases an increase in energy expenditure is observed. However, this increase is initiated at a higher temperature in P1 (17.4°C) than in P2 (16.04°C), indicating that BMI may affect BAT activity (fig 3).
- Compared to rest, the proportional increase in energy expenditure was very similar for P1 and P2, 74.3% and 70% respectively. The overall higher energy expenditure in P2 is likely due to a larger lean body mass, 64kg compared to 53.3kg.
- Heart rate and core temperature remained constant. A peak in blood pressure at 14.5°C was observed in P1 due to vasoconstriction.
- Core temperature in P1 was maintained closer to 37°C than in P2, potentially due to differences in BAT activity.

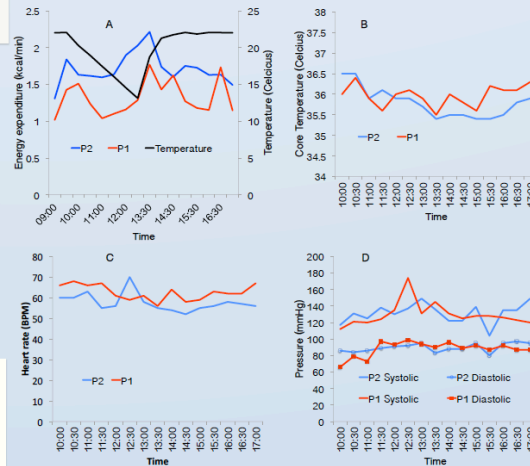


Fig 3 Energy expenditure (A), core temperature (B), heart rate (C), and blood pressure (D) of P1 (red) and P2 (blue), and chamber temperature (black), over eight and seven hour periods in the whole body calorimeter respectively. Core temperature and cardiovascular recordings were not taken in the first hour as the subject was required to be immobile for resting metabolic rate calculation.

Conclusions

We have shown that in the absence of shivering and increased cardiovascular output, energy expenditure increases reciprocally with a gradual reduction in temperature. It is likely that BAT activation in response to exposure to cold environmental temperature is one contributor to this enhanced facultative energy expenditure. The metabolic data will be analysed with data from BAT imaging to explore any associations between BAT content and metabolic responses to cold exposure.

References

- Sven Enerback. (2010). *Cell Metabolism*, 7, 248 – 252
- Cypess, A.M., et al. (2009). *New England Journal of Medicine*, 360, 1509–1517
- Wouter D. van Marken Lichtenbelt, et al. (2009). *New England Journal of Medicine*, 360, 1500 – 1508
- Rothwell, N.J., et al. (1983). *Clinical Science*, 64, 19–23







Shorter meal duration is associated with augmented overall exposure to glucose and NEFA in the post-prandial phase, but has no effect on energy expenditure in obese women

Narendra L Reddy^{1,2}, Chenjing Peng², Saboor Aftab^{1,2}, Alison Campbell¹, John Hattersley¹, Louise Halder², Alison Harte¹, Milan Piya¹, Gyanendra Tripathi¹, Philip G McTernan¹, Harpal S Randeva^{1,2}, Sudhesh Kumar^{1,2}, Thomas M Barber^{1,2}

*Warwick Medical School¹, University of Warwick, Clinical Sciences Research Laboratories, Coventry, UK
University Hospitals of Coventry & Warwickshire², UK*

Aim

The global obesity epidemic has promoted the search for novel solutions. One approach is through modification of eating-related behaviours. Our aim was to explore the effects of meal duration on energy expenditure, appetite and excursions of molecules associated with insulin sensitivity in the post-prandial phase.

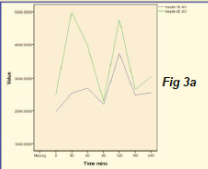



Figure 1: Plan of the Human Metabolism Research Unit, showing two whole-body calorimeters

Figure 2: Subject inside chamber. Each chamber is equipped with a pull-down bed, sink, toilet, chair, desk, phone and computer with internet access. There is also an intercom system for communication with the outside, and ports for delivery of food

Results

Post-prandial energy expenditures were equivalent between the two meal durations (range 80-120kcal/hour). Regarding buffet selection (t=240-minutes), the total number/composition of calories ingested were equivalent between the meal durations. Overall, following the 10- vs 40-minute meals, there were significant differences in post-prandial plasma glucose (mean 6.4mmol/l [SD 1.4] vs 6.0mmol/l [SD 1.3] respectively, P=0.01) and serum NEFA concentrations (mean 243µmol/l [SD 224] vs 191µmol/l [SD 171] respectively, P=0.005). There was a trend towards greater post-prandial insulin resistance following the 10- vs 40-minute meals (HOMA2 IR 2.1 [SD 2.0] vs 1.9 [SD 1.7] respectively, P=NS).







Methodology


Normoglycaemic, pre-menopausal, Caucasian obese women (n=8) were recruited from the Obesity clinic at Warwickshire Institute for the Study of Diabetes, Endocrinology and Metabolism (WISDEM, UHCW). Whole-body indirect calorimetry (6-hours) was performed on each subject on two separate occasions, with standard lunch (763kcal: 37.7% carbohydrate) ingested over 10- vs 40-minutes. Blood tests (spun for serum) were taken at baseline (fasting) and at 30, 60, 90, 120, 180 and 240 minutes following mid-meal, and analysed for glucose, insulin and non-esterified fatty acids (NEFA). Appetite for standard buffet meal (240-minutes) was assessed. Paired-sample t-tests were used. P<0.05 was considered statistically significant.

Conclusion

We demonstrate for the first time that in obese normoglycaemic women, meal duration has no effect on post-prandial energy expenditure or appetite for next meal. Shorter meal duration is associated with a greater overall exposure to glucose and NEFA, and a trend towards augmented insulin resistance during the post-prandial phase. Longer meal durations may therefore facilitate maintenance of metabolic health.

Funded by: Warwick Strategic Grant- University of Warwick

Acknowledgements: Maastricht instruments



REFERENCES:

[1] Karl JP, Young AJ, Montain SJ (2011) *Physiol Behav*, 28;102(5):524-31.

[2] Sobki SH, Zaid AA, Khan HA, Alhomida AS, Hlail KA, Khan SA (2010) Significant impact of pace of eating on serum ghrelin and glucose levels. *Clinical Biochemistry* 43: 522-524

University Hospitals
Coventry and Warwickshire
NHS Trust

Unequivocal identification of brown adipose tissue in an adult human using MRI

Narendra L Reddy¹, Terence A Jones¹, Sarah C Wayte², Oludolapo Adesanya³, Yen Yeo⁴, Harpal Randeve¹, Sudhesh Kumar¹, Charles E Hutchinson^{1,3}, Thomas M Barber¹
*Warwick Medical School¹, University of Warwick, Clinical Sciences Research Laboratories, Coventry, UK
 Departments of Medical Physics², Radiology³ & Histopathology⁴, University Hospitals of Coventry & Warwickshire, UK*

Aim

Manipulation of human brown adipose tissue (BAT) represents a novel therapeutic option for type 2 diabetes mellitus and obesity. The aim of our study was to develop and test a novel Magnetic Resonance Imaging (MR) based method to identify human BAT and delineate it from white adipose tissue (WAT), and validate it by providing histological and immunohistochemical confirmation of BAT

Methods

Initial scanning with ¹⁸F-FDG PET-CT radiotracer uptake on a 25-year old Caucasian female with primary hyperparathyroidism, showed avid uptake within mediastinum, neck, supraclavicular fossae and axillae, consistent with BAT. Subsequently, serial MR scans were performed using 3-echo IDEAL (iterative decomposition of water and fat with echo asymmetry and least-squares estimation) sequence. Retrospectively, regions of interest (ROIs) were identified on MR corresponding to PET-CT. Prospectively, ROIs were identified on MR images based on signal intensity and appearance, and compared with PET-CT. Immunohistochemical staining using uncoupling protein-1 antibody was performed on fat samples corresponding to low MR-signal, obtained during parathyroidectomy.

Figure 1: Variation in BAT_{retro}/WAT_{retro} signal ratio according to anatomical location, with significantly lower signal ratio within mediastinum and neck. The shaded area represents a ratio >1 (i.e. WAT_{retro} signal > BAT_{retro} signal).

Figure 2: (a) ¹⁸F-FDG uptake within the suprasternal notch on PET-CT (arrow); (b) fat:IDEAL MR at the same level showing corresponding low signal in suprasternal notch; (c) Haematoxylin-Eosin staining and (d) UCP1 immunostaining providing confirmation of BAT obtained from this area.

Anatomical region	No of BAT_{retro} ROIs with lower MR signal than adjacent fat	No of BAT_{retro} ROIs with similar MR signal to adjacent fat	Total number of ROIs	Total area of ROIs (mm ²)
All regions	93	18	111	9030
Mediastinum	25	0	25	2348
Supraclavicular	31	10	41	3313
Neck	29	2	31	1451
Axillae	8	6	14	1918

Table 1: For each anatomical region number of BAT_{retro} ROIs with low and normal signal intensity on MR are tabulated. The ROIs were retrospectively drawn on MR from areas of corresponding high ¹⁸F-FDG uptake on PET-CT

Results

111 retrospectively identified ROIs from PET-CT scans: 88 (79%) showed corresponding low signal on MR images: 100% in mediastinum, 29/31 (93.5%) in neck, 31/41 (75.6%) supraclavicular, and 8/14 (57%) in axillae. Prospectively, 87% of ROIs identified on MR scans corresponded to increased areas of uptake on PET-CT. Histology and immunohistochemistry confirmed BAT.

Conclusion

We provide the first ever report that MR can be used reliably to identify BAT in a human adult, with histological and immunohistochemical confirmation. Our data demonstrate proof of concept to support the development of MR, a safe and reproducible imaging modality, as a biomarker for human BAT.

Acknowledgements: Sean James, Mirada Medical Ltd & MR Radiographers in UHCW: Study funded by Strategic Impact Fund grant from University of Warwick

REVIEW

Open Access

Brown adipose tissue: endocrine determinants of function and therapeutic manipulation as a novel treatment strategy for obesity

Narendra L Reddy^{1,2†}, Bee K Tan^{1,3†}, Thomas M Barber^{1,2†} and Harpal S Randeva^{1,2*†}

Abstract

Introduction: Recent observation of brown adipose tissue (BAT) being functional in adult humans provides a rationale for its stimulation to increase energy expenditure through 'adaptive thermogenesis' for an anti-obesity strategy. Many endocrine dysfunctions are associated with changes in metabolic rate that over time may result in changes in body weight. It is likely that human BAT plays a role in such processes.

Review: In this brief review article, we explore the endocrine determinants of BAT activity, and discuss how these insights may provide a basis for future developments of novel therapeutic strategies for obesity management. A review of electronic and print data comprising original and review articles retrieved from PubMed search up to December 2013 was conducted (Search terms: brown adipose tissue, brown fat, obesity, hormone). In addition, relevant references from the articles were screened for papers containing original data.

Conclusion: There is promising data to suggest that targeting endocrine hormones for BAT modulation can yield a cellular bioenergetics answer for successful prevention and management of human obesity. Further understanding of the physiological link between various endocrine hormones and BAT is necessary for the development of new therapeutic options.

Keywords: Brown adipose tissue, Obesity, Hormone

Introduction

According to the World Health Organization (WHO) report, worldwide obesity rates have more than doubled since 1980. Global figures from 2008 showed that 1.5 billion adults were overweight and that obesity affected 200 million men and 300 million women, with the numbers expected to rise exponentially [1]. Obesity is associated with significant morbidity and mortality that result from the related complications of type 2 diabetes mellitus (T2DM), non-alcoholic fatty liver disease, cardiovascular events, obstructive sleep apnoea, musculoskeletal and psychiatric diseases, and various malignancies [2]. In 2010,

overweight and obesity were estimated to cause 3.4 million deaths, 3.9% of years of life lost, and 3.8% of disability-adjusted life-years (DALYs) worldwide [3]. Obesity, in 1980's was limited to affluent countries such as North America, Western Europe and Australasia, but now manifests as a true pandemic, with its increasing prevalence in developing countries such as India, China and Brazil, and spreading even to sub-Saharan Africa [4,5], placing an enormous financial burden on the global economy.

The management of obesity through lifestyle is notoriously difficult and the resulting effects on weight are variable and often transient. Weight regain following weight loss is common and results from a number of mechanisms that redress any loss of energy storage capacity. Such mechanisms include changes in the levels of appetite-regulating hormones following weight loss that encourage weight recovery [6]. Weight loss also reduces energy expenditure [7] and brown adipose tissue (BAT) activity, and this combined with enhanced appetite promotes weight regain. Current therapeutic options for obesity management are

* Correspondence: Harpal.Randeva@warwick.ac.uk

†Equal contributors

¹Clinical Sciences Research Laboratories, Division of Metabolic and Vascular Health, Warwick Medical School, University of Warwick, University Hospitals Coventry and Warwickshire, Clifford Bridge Road, Coventry CV2 2DX, UK

²Warwickshire Institute for Study of Diabetes, Endocrinology and Metabolism, University Hospitals Coventry and Warwickshire NHS Trust, Clifford Bridge Road, Coventry CV2 2DX, UK

Full list of author information is available at the end of the article

limited following recent withdrawals of sibutramine and rimonabant amid safety concerns, and problems relating to the supply, unacceptable side-effect profile and long-term efficacy of orlistat [8]. Despite its effectiveness as a weight-loss intervention, bariatric surgery is only applicable to a sub-group of obese patients who meet funding criteria and as such, does not represent a practical solution to the global obesity epidemic [9]. Given the limitations of current therapies, the current global obesity epidemic and escalating incidence of obesity-related deaths, it is imperative to identify novel and effective therapeutic options for obesity.

Obesity results when energy intake exceeds expenditure chronically. Therapeutic strategies for obesity have mainly targeted caloric restriction through central appetite suppression and inhibition of fat absorption [10]. Compared with those acting on central appetite regulation, therapies acting peripherally may prove beneficial whilst causing fewer harmful effects [11]. The body is, by default, genetically predisposed to store energy in preparation for prolonged periods of starvation [12]. Even minor weight-loss through appetite suppression is often redressed through multiple peripheral counter-regulatory mechanisms to maintain 'isoenergetic' conditions [6]. Centrally acting drugs can potentially cause adverse psychotropic side effects through cross-reactivity with a variety of other receptors within complex central circuits (such as the endocannabinoid receptor blocker, Rimonabant) [10]. The concept of increasing energy expenditure through therapeutic manipulation of *peripheral* mechanisms is therefore attractive and worthy of focused research and development.

The main physiological function of BAT, to generate heat for the organism to protect against development of hypothermia, has been well understood for nearly 50 years [13]. Recent studies using ¹⁸F-fluoro-labelled 2-deoxyglucose (FDG) positron emission tomography computed tomography (PET-CT) have demonstrated the presence of BAT depots in the axillary, paravertebral, supraclavicular and cervical regions in adult humans [14-16]. Data from various animal studies have demonstrated that through BAT activation, triglyceride stores within white adipose tissue (WAT) can be utilized for heat generation through modulation of adaptive thermogenesis [17]. Therapeutic manipulation of human BAT therefore represents a novel mechanism to promote weight-loss. It is noted that endocrine disorders such as pheochromocytoma and thyrotoxicosis play a role in activating BAT [18,19]. To maximize its future therapeutic potential, it is important to appreciate the mechanisms by which endocrine dysfunction influences human BAT activity. In this brief review article, we explore the main mechanisms linking various endocrine hormones and human energy expenditure, mediated by effects on BAT activity.

BAT energetics

There are two main types of adipose tissue, white adipose tissue (WAT) and BAT that have evolved for completely different purposes: to survive famine and prevent hypothermia respectively. WAT and BAT, as energy storage and thermogenic tissues respectively, therefore evolved to protect mammalian organisms from important environmental threats, including lack of food and exposure to cold climates [20]. In addition to WAT and BAT, a third intermediate-type of adipose tissue that is termed 'beige' has recently been identified. Adipocytes from beige adipose tissue (BeAT) depots resemble white adipocytes but possess the classical properties of brown adipocytes. Partial success noted in animal models in converting WAT to BeAT, has set a tone in BAT research field to replicate the concept in humans too [21,22]. The characteristic features of WAT, BAT and BeAT, and the origin of BAT are shown in Table 1 and Figure 1 respectively.

Heat production plus external work account for the average daily metabolic rate or total energy expenditure (TEE). TEE can be classically divided into resting metabolic rate (RMR; normally 55–65% of TEE), activity related energy expenditure (AEE; normally 25–35% of TEE), and diet-induced thermogenesis (DIT) (about 10% of TEE) [23,24]. Alternative classification is obligatory energy expenditure, which includes RMR, involuntary AEE and obligatory part of DIT, and facultative energy expenditure, which includes voluntary AEE, cold-induced non-shivering thermogenesis (NST), cold-induced shivering thermogenesis, and facultative part of DIT [23].

Cold-induced activation of BAT has resulted in a high incidence (60% to 96%) of detection as shown in recent PET studies [25,26]. The presence of the 32 kDa uncoupling protein-1 (UCP1) in BAT mitochondria enables heat dissipation rather than generation of adenosine triphosphate (ATP) [27], thereby resulting in non-shivering thermogenesis (NST). Although controversial, BAT is thought to influence DIT through sympathetic nervous system activity via UCP1 [27,28]. Using PET studies with radio-labeled fatty acid tracers, Ouellet *et al.* quantified BAT oxidative metabolism, glucose and non-esterified fatty acid (NEFA) turnover in 6 healthy human subjects, demonstrating unequivocally that BAT contributes to energy expenditure in humans [29]. Extrapolating rodent experiments of thermogenic potential of BAT (300 W/kg), Rothwell and Stock calculated that 40-50 g of BAT in humans, might account for 20% of total energy expenditure [30]. Human PET studies estimated that maximal activation of 63 g of BAT would result in 4.1 kg of weight loss during one year [14]. Two independent but congruent human studies estimated an energy expenditure of 200–400 kcal/day, a 10 to 20% rise in daily basal metabolic rate through BAT activation [31,32]. Therefore, the glucose disposal [33] and triglyceride clearance

Table 1 Morphological features of BAT, WAT and BeAT

	WAT	BAT	BeAT
Cell shape	Variable, but classically spherical	Polygonal	Resembles WAT
Cell size	Variable, but large (25-200 μ m)	Comparatively small (15-60 μ m)	Variable
Nucleus	Peripheral, flattened	Central, round or oval in shape	To be determined
Cytoplasm	Thin, peripheral rim	Large volume evenly distributed throughout cell	To be determined
Lipid content	Single large droplet occupying up to 90% of cell volume	Multiple small lipid droplets	To be determined
Mitochondria	Few	Abundant	Intermediate
Endoplasmic reticulum (ER)	Little, but recognizable as rough and smooth ER	Present, but poorly developed	To be determined
Tissue organization	Small lobules of densely packed cells	Lobular, gland-like	To be determined
Cell content	Multiple other cell types present	Few other cell types present	Few other cell types present
Vascularity	Adequate	Highly vascularised	To be determined
Gene expression	PPAR-gamma, aP2, Adiponectin, adipisin, perilipin	UCP-1, PGC-1alpha, β -3 adreno receptor (ARB3), PRDM16, de-iodinase type II (D2)	Low UCP1, but activated by cAMP stimulation
Cell markers	CD34, ABCG2, ALDH	EVA1, EBF3, FBXO31	CD137, TMEM26, TBX1

properties of BAT [34], when fully utilized may act as an energy sink. There are three ways in which enhanced energy expenditure through manipulation of BAT could be theoretically achieved: i) maximal and continual activation of BAT; ii) trans-differentiation of WAT to BAT (to form BeAT), and; iii) transplantation of BAT stem cells.

The presence of BAT in adult humans represents a potentially important therapeutic target for future novel weight-loss strategies. The origins and functions of BAT, WAT and BeAT differ in important ways, and studies on the energetics of BAT have shown promising results. In the next sections, we discuss the main endocrine determinants of human BAT activity, and how each of these mechanisms could be therapeutically manipulated for promotion of weight-loss.

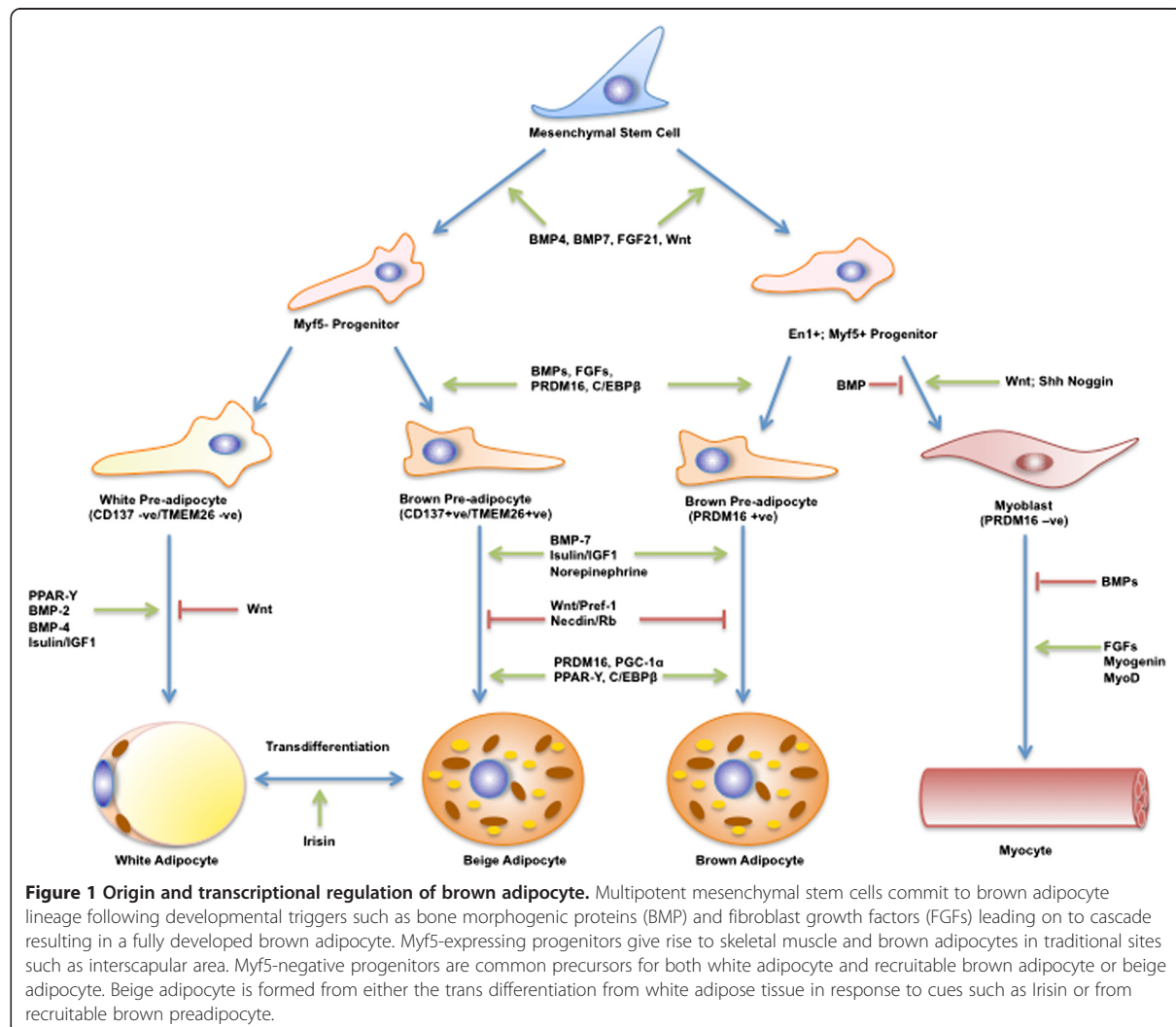
Review of endocrine determinants of BAT activity Thyroid and BAT

We have known for over a century that thyroid hormone (TH) increases metabolic rate and thermogenesis in homeothermic species, and hence is an important physiological modulator of energy homeostasis [35,36] TH stimulates both obligatory and facultative thermogenesis [37] and plays an important role in the regulation of lipid metabolism within adipose tissue [38,39]. TH also enhances oxidative phosphorylation through induction of mitochondrial biogenesis and modulation of the expression of genes implicated in the regulation of the mitochondrial respiratory chain [40]. The weight gain and decreased cold tolerance observed in individuals with hypothyroidism, and the weight loss and sweating/heat intolerance observed in patients with hyperthyroidism, are predictable clinical manifestations of alterations in BAT activity [41]. It follows therefore that differences in BAT quantity and/or activity

between individuals may also influence the clinical manifestations of hypo- or hyperthyroid states. This may also explain the inter-individual variability of weight changes and heterogeneity of other clinical manifestations of dys-thyroid states.

The physiological effects of TH are exerted at the level of transcription through the thyroid receptors (TR): TR α and TR β [42]. TR β mediates thyronine (T3) induced *UCP1* gene expression, whilst the TR α isoform through T3 regulates facultative thermogenesis in BAT [43]. Type 2 deiodinase (D2) plays an essential role in mediating the full thermogenic response of BAT to adrenergic stimulation via increased thyroxine (T4) to T3 conversion within this tissue [44]. From a therapeutic perspective, it would be desirable to selectively activate TR β for UCP1 stimulation to avoid the widespread unwanted effects of TR α , the predominant receptor in non-BAT tissues. Thyroid hormone analogues have been explored with variable outcomes. GC-1 compound, a selective TR β agonist, induces *UCP1* gene expression in rats [43], improves glucose homeostasis [45], increases energy expenditure and reduces fat mass and plasma cholesterol [46]. High-fat feeding and concurrent treatment with the TR β -selective agonist GC-24 (with a 40-fold higher affinity for TR β than TR α) resulted in only a partial improvement in metabolic control, probably related to acceleration of resting metabolic rate [47]. Treatment with another TR β -selective agonist, KB-41 in rats resulted in a 6-8% weight-loss with significant improvements in glucose homeostasis, cholesterol and triglyceride levels without affecting heart rate, probably due to lack of TR α effects [45].

There are also some promising data from human studies that implicate thyroid hormones having important effects on BAT activity. T3 treatment of differentiated human



multipotent adipose-derived stem cells *in vitro* induces UCP1 expression and mitochondrial biogenesis through effects on TR β [48]. Following thyroidectomy and subsequent treatment with thyroxine replacement therapy in a patient with papillary carcinoma, BAT activity was enhanced with concurrent weight-loss and remission of T2DM [49]. Thyroxine may cause 'brownification' of WAT [48], and holds immense potential given the mechanism of action in BAT, and hence needs to be robustly tested in humans.

Catecholamines and BAT

Epinephrine causes vasodilatation and enhances glucose and oxygen consumption in skeletal muscle [50] whilst also enhancing thermogenesis in humans [51]. BAT is also activated in patients with pheochromocytoma, (excess catecholamine producing benign adrenal medullary tumour) with increased UCP1 expression similar to levels in cold-

exposed rodents [18,52]. BAT activity is greater in patients with pheochromocytoma [53,54] due to over-activity of the sympathetic nervous system and elevated levels of circulating catecholamines, that in turn stimulate β_3 adrenergic receptors, thereby activating *UCP1* expression via cyclic adenosine monophosphate (cAMP) and protein kinase-A (PKA) pathways [55]. Hadi *et al.* demonstrated active BAT to be present in 27% (26/96) of pheochromocytoma patients undergoing FDG PET-CT scans [56], indicating higher detection rates compared to 5.37% (106/1972) of all cause PET-CT studies reported by Cypess and colleagues [16]. Recent human observational studies demonstrate a correlation between plasma metanephrine levels and BAT activity [57].

Nor-epinephrine action on β_3 -adrenergic receptor in mature human brown adipocyte is the most studied pathways. β_3 -adrenergic receptor would appear to be a convenient

therapeutic target based on evidence from rodent studies using “selective” β 3-agonists (CL-316,243) [58] and knock-out mouse models [59]. β 3-agonists have not yielded desirable results in humans due to differences in β 3-receptor binding properties in humans and rodents. Second-generation β 3-agonist trials in humans were unsuccessful due to poor oral bioavailability and unfavorable pharmacokinetics [60]. Another β 3-agonist, L-796568, showed an initial increase in energy expenditure effect in 12 healthy obese subjects that failed to be sustained beyond 28 days [61,62]. Catecholamines may also ‘brownify’ WAT. Two case reports of extensive brown fat deposits in omental and mesenteric regions detected on human FDG-PET scans indicate a possible role for catecholamines in the ‘browning’ of WAT [63,64]. Therapeutically, catecholamine-like molecules may trans-differentiate WAT into BeAT, but such an approach would need to avoid the associated sympathomimetic effects to be safe.

Glucocorticoids and BAT

Both BAT and WAT contain glucocorticoid receptors [65]. Excessive levels of glucocorticoids increase WAT mass and result in weight gain [66]. Conversely, glucocorticoids have an *inhibitory* effect on BAT activity in rodent models [67]. Glucocorticoids enhance appetite, stimulate lipolysis, suppress thermogenesis [68] (specifically *facultative* thermogenesis [69]) and profoundly suppress norepinephrine-induced *UCPI* activation [67]. Glucocorticoids also inhibit the expression and function of β 1 and β 3 adrenergic receptors within BAT. [70,71] Corticosterone reduces NST and increases lipid storage within BAT in an *in vivo* rodent study, possibly as a result of steroid-induced hyperinsulinaemia [69]. Within rodent models, it has been observed that adrenalectomy results in stimulation of BAT thermogenesis and also weight-loss [72]. This mechanism is probably mediated through removal of glucocorticoid-induced hypothalamic inhibitory influences on BAT activity, and is reversed following glucocorticoid administration [72,73]. A similar reduction in body fat mass was seen in a 46-year old female with Cushing’s syndrome following adrenalectomy [74]. The therapeutic challenge here would be to develop the beneficial effects of steroid depletion on metabolism and adipose-regulation whilst avoiding its potentially life-threatening effects.

Mineralocorticoid and BAT

Mineralocorticoid receptors in rodent BAT, were first demonstrated by Zennaro and colleagues [75]. Following aldosterone treatment of a T37i cell line derived from hibernoma in mice, there was increased expression of adipogenic genes such as *Lpl* (lipoprotein lipase), *PPAR- γ* (Peroxisome proliferator receptor activated-gamma) (*PPAR- γ*) and *aP2* (adipocyte-specific fatty acid binding protein)

[75,76]. Treatment with aldosterone also results in inhibition of *Ucp1* expression, favouring lipid storage rather than heat dissipation [77,78]. Within WAT, aldosterone induces inflammation resulting in the release of pro-inflammatory cytokines such as Interleukin-6 (IL-6), tumour necrosis factor-alpha (TNF- α) and Monocyte chemo attractant protein (MCP-1) [79]. Aldosterone also appears to inhibit thermogenesis within BAT, and also inhibits the differentiation of WAT into BAT [80]. Given that mineralocorticoids have a negative effect on BAT, it follows that aldosterone antagonists may represent a combined therapy for both hypertension and obesity (through possible activation of BAT). This also supports the findings that high aldosterone levels are noted in obesity-induced hypertension in humans, which reverses on weight loss [81].

Growth hormone/Insulin Growth Factor-1 and BAT

BAT-status in growth hormone (GH)-deficient patients and acromegalics remains unknown. GH replacement in GH-deficient humans results in sustained improvement of body composition and reduction of insulin resistance [82,83]. Conversely, GH excess in acromegalics promotes insulin resistance [82], resulting in dysglycaemia and hyperlipidaemia. GH replacement (1 mg/kg/day) for 10 days in experimental mice resulted in significant reduction of WAT mass, increased skeletal weight and reduction of insulin resistance. Despite an increase in *Ucp-1* mRNA by 2.8 fold, there was no change in the inter-scapular brown fat mass [84], although a substantial increase (2 to 6 fold) in inter-scapular brown fat mass was noted at higher doses of GH (3.5 mg/kg/day).

Insulin Growth Factor-1 (IGF-1) receptors are highly expressed in the plasma membrane of rat brown adipocytes [85]. *In vitro* studies in murine foetal brown adipocytes have shown that IGF-1 is intensely mitogenic and prevents TNF- α induced apoptosis [86,87]. IGF-1 induces the expression of *Ucp-1* and CCAAT/enhancer binding protein alpha (C/EBP- α) in rat brown adipocyte primary-cell cultures [88]. Transient up-regulation of *Igf-1* gene expression and BAT hyperplasia was noted in rats exposed to cold (4°C) in the first 48 hours [89]. One of the factors influencing the dramatic rise in human foetal UCP-1 content during late gestation, especially prior to birth, is thought to be due to increased IGF-1 and IGF-2 levels [90]. There may therefore be a role for IGF-1 in BAT differentiation and activation, although the precise molecular mechanisms remain unclear. As a therapeutic strategy, the effect of GH or recombinant human IGF-1 (or truncated IGF-1) on BAT and WAT functioning is worth exploring.

Prolactin and BAT

Functional prolactin receptors (PRLR) are highly expressed in both WAT and BAT and are essential for adipogenesis

and adaptive thermogenesis [91]. Prolactin plays important roles in carbohydrate metabolism through its effects on pancreatic β -cell mass and energy homeostasis through lipid metabolism [92]. Prolactin suppression, through use of dopamine agonists in hyperprolactinaemic patients, results in metabolic effects [93]. Lactation in experimental mice is strongly and negatively associated with expression of thermogenic genes in BAT [94]. PRLR $^{-/-}$ male mice subjected to a high fat diet for 16 weeks exhibited resistance to weight-gain and a reduction in WAT compared to wild-type mice. These mice also showed 2–3 fold increased expression of BAT-specific markers (PR domain containing 16 [PRDM16], UCP1, PPAR-coactivator 1-alpha [PGC1 α] and brown-like adipocyte foci, indicating a possible role in BeAT differentiation from WAT [95]. Further studies are required to establish whether prolactin blockade by either dopamine agonists or pure prolactin receptor antagonists may represent a targeted approach for browning of human WAT.

Sex hormones and BAT

Androgen and oestrogen receptors (ER α) are expressed in BAT in both sexes [96]. Furthermore, sex hormones play an important role in the BAT thermogenic program by acting at several steps of the lipolytic signal cascade and on UCP1 transcription control. Observations such as cessation of ovarian function at menopause resulting in weight-gain, loss of insulin sensitivity and increased incidence of cardiovascular disease [97], coupled with greater BAT activity in young females in PET-CT studies [16], fuel the argument that ovarian hormones probably influence BAT function. Ovariectomy in female rodents reduced BAT mitochondrial functionality through reduction in the oxidative capacity and anti-oxidant defenses. Furthermore, 17- β oestradiol (E2) supplementation partially reversed these effects indicating oestrogen's partial influence on BAT [98]. There may also be non-oestrogenic ovarian signals stimulating BAT activity [98]. Interestingly, *in vitro* cell culture studies by Rodriguez-Cuenca show a dual effect of 17- β oestradiol on the mitochondrial biogenic program [99,100].

Addition of testosterone reduced norepinephrine-induced *Ucp1* mRNA expression in a dose-dependent manner in cultured rodent brown adipocytes, and these effects were reversed by flutamide (an androgen receptor antagonist) [101]. Furthermore, testosterone reduces the thermogenic and lipolytic capacity of BAT [100]. In contrast, progesterone is shown to have the opposite effect to that of testosterone on brown adipocytes [101] by positively stimulating mitochondriogenesis and BAT differentiation as demonstrated by an increase in the mRNA expression of the *GABPA-TEFAM* axis and *PPAR- γ* , respectively [99]. These apparent opposite influences of testosterone and progesterone on BAT activity may explain the gender

dimorphism displayed by BAT in human PET studies [16,102]. Dehydroepiandrosterone (DHEA, a precursor sex steroid), when administered to obese and lean rats caused reduced food intake and enhanced energy expenditure resulting in weight-loss through increased expression of *Pgc-1 α* , *Ucp1* and *β 3-*Ar** [103].

In summary, these animal studies demonstrate variable effects of sex hormones on BAT activity: testosterone appears to have a negative influence, oestrogen probably has a dual effect and progesterone and DHEA both appear to have positive influences on BAT activity. However, the increase in both, BAT amount and BAT activity in both sexes in human adolescents, (during peak surge of sex hormones) [104] fuels speculation that sex hormones may have a strong influence on BAT. Therefore it is worth exploring the influences of flutamide, selective oestrogen-receptor modulators (SERMs) and DHEA on human BAT activity.

Insulin and BAT

In cultured murine brown and white adipose tissue, insulin has a role in differentiation of pre-adipocytes into adipocytes [105]. Furthermore, insulin-signaling in BAT is similar to that of WAT and other tissues, displaying similar anabolic effects of glucose uptake and lipid accretion [106]. The studies suggest that uptake of glucose into BAT is both insulin-mediated (mainly occurring in non-thermogenic conditions) and norepinephrine-mediated (occurring during thermogenic conditions) [107]. In rodent models, BAT is shown to be one of the most insulin-responsive tissues with respect to glucose-uptake [108] and is mediated via GLUT4, similar to that in WAT [109].

Animal studies suggest that chronic insulin deficiency reduces the thermogenic capacity of BAT [110,111]. Furthermore, in type 1 diabetes mellitus glucose homeostasis is reverted to normalcy by increasing BAT quantity [112]. Contrarily, compensatory hyperinsulinaemia induces apoptosis of endothelial cells in rat BAT, thereby reducing BAT quantity [113]. This may explain reduced BAT activity observed in insulin-resistant states such as human obesity and T2DM in human PET-case series [16,102]. In human PET studies, insulin-mediated glucose-uptake by BAT increased 5-fold (independent of perfusion) in comparison to WAT, and gene expression of *GLUT4* (Glucose transporter type 4) was higher in BAT than WAT [33]. In summary, it appears that insulin is required in maintenance of BAT thermogenic capacity, but the potential therapeutic role of insulin and insulin-related molecules in BAT manipulation is yet to be determined.

Central or peripheral intravenous leptin administration in rats is shown to increase insulin stimulated glucose utilisation, and to favour expression of uncoupling proteins predominantly through central pathways of increasing sympathetic tone [114,115]. However, the lack of success

of human recombinant leptin infusions on weight loss in obese subjects [116], and adverse cardiovascular profile of hypertension, left ventricular dysfunction, and possible cardiovascular risk [117] may need to be factored in for contemplating leptin route of BAT activation. Adiponectin is noted to inhibit UCP-1 gene expression by suppression of β 3-adrenergic receptor in rats [118]. Conversely, adiponectin levels were significantly higher in BAT compared to WAT in active pheochromocytoma patients, and consequently serum adiponectin levels reduced markedly following adrenalectomy [119]. The relation between BAT and adiponectin in humans is yet to be clarified before considering on therapeutic prospects.

Endocannabinoids and BAT

Acting centrally and peripherally, the endocannabinoid system positively regulates appetite and energy balance [120] and has a role in adipose tissue metabolism [121], mainly through cannabinoid receptors (CB1 and CB2), and their natural endogenous ligands anandamide and 2-arachidonoyl glycerol [120]. In rodents, weight-loss associated with chronic CB1 antagonism was accompanied by increased energy expenditure, enhanced insulin-stimulated glucose utilisation, and marked activation of BAT thermogenesis [122]. Similar mice studies have shown a sustained increase of BAT temperature and up-regulation of UCP1 on CB1 blockade [123]. Through peripheral CB1 receptor inhibition, *in vitro* murine white adipocytes trans-differentiate into a mitochondria rich, thermogenic BAT phenotype [124]. Experiments with BAT denervation have attenuated such browning responses, indicating that central regulation is essential. Recent withdrawal of rimonabant from the market owing to concerns regarding an adverse psychotropic profile, poses a problem for CB1 being a target for activation of brown fat, unless a more

selective peripheral blocker of CB1 is identified. Table 2 enlists effect of various hormones on BAT and possible therapeutic options through manipulation of individual hormonal actions.

Current trends in BAT therapeutics

Given that adult humans have BAT, it is important to explore BAT manipulation as a means of promoting weight-loss through enhanced energy expenditure via BAT manipulation. In addition to augmentation of BAT content and/or enhancement of BAT activity, other approaches include trans-differentiation of non-BAT progenitors into BAT pre-adipocytes, and surgical implantation of BAT. Development of novel BAT-related therapies will require a complete understanding of the embryological and transcriptional mechanisms of BAT specification and development in human models. We also need to characterize and confirm the physical and genetic attributes of BAT including anatomical and histological distributions of human BAT. Further challenges will be to develop a sustained long-term BAT stimulating or recruiting molecular circuit with adequate knowledge of counter-regulatory mechanisms for an acceptable safety profile, and to identify a reliable and safe imaging modality to monitor the effects of such therapies on BAT once developed and administered.

Several transcriptional regulators of brown adipocyte differentiation are described in rodents, with some revealing promising effects even in human models. Irisin is a 112-amino-acid polypeptide hormone, and is a cleaved and secreted fragment of fibronectin type III domain containing 5 (FNDC5) membrane protein, in turn released by muscle through increased PGC-1 α expression following exercise in both rodents and humans [125]. Irisin showed a powerful browning effect on certain white adipose tissues in mice, both in culture and *in vivo* [125]. Human irisin is

Table 2 Effect of hormones on BAT and possible therapeutic options

Hormone	Influence on BAT	Probable BAT therapeutic suggestions
Epinephrine	+ve	Selective human β 3 receptor agonists
T3	+ve	TR β selective agonists- GC-40, KB-41
Testosterone	-ve	To be determined
Estradiol	+/- (? dual effect)	Selective estrogen receptor modulators (SERM)
Progesterone	+ve	To be determined
DHEA	+ve	To be determined
IGF-1	Probably +ve	Recombinant human IGF-1 or truncated IGF-1
GH	+ve at higher dose	To be determined
Insulin	Unclear	To be determined
Cortisol	-ve	To be determined
Prolactin	-ve	Bromocriptine, pure prolactin receptor antagonists eg., Δ 1-9-G129R- hPrI (Δ 1-9)
Aldosterone	-ve	Eplerenone, Spironolactone
Endocannabinoids	-ve	Peripheral CB1 antagonists

believed to be identical to mouse irisin, and in healthy adult subjects showed a 2-fold increase in plasma levels following 10 weeks of supervised endurance exercise training, as compared to the non-exercised state [125]. This PGC-1 α dependent myokine alludes to the super-added beneficial effects of exercise via BAT, which need to be further explored.

The PRDM16-C/EBP- β transcriptional complex acts in Myogenic Factor-5 (Myf5) positive myoblastic precursors or pre-adipocytes to drive the thermogenic program with co-activation of PPAR- γ and PGC-1 α [126,127]. The cAMP-dependent thermogenic program is potentiated by Forkhead Box Protein C2 (FOXO2) [128] and PRDM16 and repressed by receptor-interacting protein-140 (RIP140) [129] (Figure 1). Other transcriptional regulators of Bone Morphogenic Protein-7 (BMP7) [130], Fibroblast Derived Growth Factor-21 (FGF21) [131], PPAR- γ ligands [132] and Atrial Natriuretic Peptide (ANP) [133], have been described in rodents. The transcribed cells through these various regulators are termed as BeAT as opposed to classical BAT and the success of these compounds depend upon extrapolating the gains in human models.

The discovery of brown adipocyte stem/progenitor cells, CD34+ in skeletal muscle [134] and human multipotent adipose derived stem cells (hMADS) in subcutaneous tissue [135] in adult humans, serve as novel molecular targets for the development of BAT therapeutics as they have self-renewing capacity, and hence are expandable. In response to specific agents, muscle-derived CD34+ cells differentiate exclusively into brown adipocytes [134]. The WAT-derived hMADS, in contrast, first differentiate into WAT and following chronic exposure to PPAR- γ co-activators, gain brown adipose phenotype [135]. These human cell models provide a unique opportunity to study the formation and energy dissipation functions of human brown adipocytes, whilst simultaneously exploring therapeutic options. Such cells can potentially be externally induced into BAT, expanded and implanted back as an autologous implantation for metabolic beneficial effects as shown in recent mouse models [136]. Subcutaneous transplantation of embryonic BAT corrected type 1 diabetes in immune-competent mice as evidenced by reversal of diabetes symptoms, weight regain and normalization of glucose tolerance and the mice that remained euglycaemic 6-months following the procedure [137].

Conclusion

There is compelling evidence to suggest that targeting cellular bioenergetics will yield an effective anti-obesity therapy. There are also complex practical concerns to be addressed. Recent key advances in the fields of molecular cell biology and metabolic science have raised relevant questions relating to the duration of the acquired

BAT-like properties of cells following transcriptional regulation, the long-term fate of transcriptionally converted non-BAT (BeAT) tissues, the total amount of inactive BAT in humans and the fate of inter-scapular BAT in infants. Compensatory enhancement of appetite through central feedback regulation via complex neurological circuits following sustained chronic peripheral energy loss is a concern. Therefore, combining novel therapies that enhance BAT activity with an appetite-suppressant may be required. Therapeutic manipulation of peripheral energy expenditure through increasing BAT quantity and/or activity remains one of the most promising strategies for the successful prevention and management of human obesity. Although there are significant hurdles, there is also great potential for BAT manipulation to promote weight-loss through enhanced facultative metabolism.

Abbreviations

BAT: Brown adipose tissue; WHO: World Health Organization; T2DM: Type 2 diabetes mellitus; FDG: 18-Fluoro-labelled- 2-deoxyglucose; PET-CT: Positron Emission Tomography- Computed Tomography; WAT: White adipose tissue; BeAT: Beige adipose tissue; UCP-1: Uncoupling protein- 1; ATP: Adenosine tri-phosphate; AEE: Activity energy expenditure; TEE: Total energy expenditure; RMR: Resting metabolic rate; NST: Non-shivering thermogenesis; DIT: Diet-induced thermogenesis; NEFA: Non-esterified fatty acids; TH: Thyroid hormone; TR: Thyroid receptor; D2: type-2-deiodinase; T4: Thyroxine; T3: Thyronine; c-AMP: cyclic adenosine-mono-phosphate; PKA: Protein kinase-A; Lpl: Lipoprotein lipase; PPAR- γ : Peroxisome proliferator receptor activated-gamma; aP2: Adipocyte-specific fatty acid binding protein; IL-6: Interleukin-6; TNF- α : Tumour necrosis factor-alpha; MCP-1: Monocyte chemoattractant protein; GH: Growth Hormone; IGF-1: Insulin Growth Factor-1; C/EBP- α : CCAAT-enhancer binding protein- alpha; PRDM-16: PR domain containing 16; PGC-1 α : Peroxisome proliferator activated receptor gamma coactivator 1- alpha; CB-1: Cannabinoid receptor-1; ER- α : Oestrogen receptor-alpha; E2: 17- β -Oestradiol; NRF-1: Nuclear respiratory transcriptional factor-1; GABPA: GA-binding protein transcription protein- alpha; TFAM: Mitochondrial transcription factor-A; PTEN: Phosphatase and tensin homolog deleted on chromosome 10; AR: Adrenergic receptor; SERMs: Selective oestrogen receptor modulators; GLUT-4: Glucose transporter type 4; FNDC-5: Fibronectin type 3 domain containing 5; Myf-5: Myogenic factor-5; FOXO2: Forkhead box protein C2; RIP140: Receptor interacting protein-140; BMP-7: Bone morphogenic protein-7; FGF21: Fibroblast derived growth factor-21; hMADS: Human multi-potent adipocyte derived stem cells.

Competing interests

The authors declare that they have no competing interests.

Authors' contributions

NLR researched the data, contributed to discussion, wrote, reviewed and edited the manuscript. BKT and TMB contributed to discussion and edited the manuscript. HSR contributed to conception/design, data interpretation and manuscript preparation. All authors read and approved the final manuscript.

Authors' information

NLR is a Clinical Lecturer in Division of Metabolic and Vascular Health (DMVH), University of Warwick, and Honorary Consultant in Diabetes & Endocrinology, University Hospitals Coventry and Warwickshire NHS Trust (UHCW). BKT is an Associate Professor in Warwick Medical School, University of Warwick, and Consultant in Department of Obstetrics and Gynaecology, Birmingham Heartlands Hospital, Heart of England NHS Foundation Trust, Birmingham, UK. TMB is an Associate Professor in DMVH, University of Warwick and Consultant in Diabetes & Endocrinology, UHCW. HSR is a Senior Lecturer in DMVH, University of Warwick and Clinical Director/Consultant in Diabetes & Endocrinology, UHCW.

Acknowledgements

We would like to acknowledge the many patients, nurses, scientists and doctors who have contributed towards ascertaining the data referred to in this review.

Author details

¹Clinical Sciences Research Laboratories, Division of Metabolic and Vascular Health, Warwick Medical School, University of Warwick, University Hospitals Coventry and Warwickshire, Clifford Bridge Road, Coventry CV2 2DX, UK. ²Warwickshire Institute for Study of Diabetes, Endocrinology and Metabolism, University Hospitals Coventry and Warwickshire NHS Trust, Clifford Bridge Road, Coventry CV2 2DX, UK. ³Obstetrics and Gynaecology, Birmingham Heartlands and Solihull Hospitals, Heart of England NHS Foundation Trust, Birmingham B9 5SS, UK.

Received: 27 January 2014 Accepted: 18 July 2014

Published: 22 August 2014

References

1. WHO global infobase: data on overweight and obesity. <http://www.who.int/mediacentre/factsheets/fs311/en/>.
2. Larsson B, Svardsudd K, Welin L, Wilhelmsen L, Bjorntorp P, Tibblin G: Abdominal adipose tissue distribution, obesity, and risk of cardiovascular disease and death: 13 year follow up of participants in the study of men born in 1913. *Br Med J (Clin Res Ed)* 1984, **288**:1401–1404.
3. Lim SS, Vos T, Flaxman AD, Danaei G, Shibuya K, Adair-Rohani H, Amann M, Anderson HR, Andrews KG, Aryee M, Lim SS, Vos T, Flaxman AD, Danaei G, Shibuya K, Adair-Rohani H, Amann M, Anderson HR, Andrews KG, Aryee M, Atkinson C, Bacchus LJ, Bahalim AN, Balakrishnan K, Balmes J, Barker-Collo S, Baxter A, Bell ML, Blore JD, Blyth F, *et al*: A comparative risk assessment of burden of disease and injury attributable to 67 risk factors and risk factor clusters in 21 regions, 1990–2010: a systematic analysis for the Global Burden of Disease Study 2010. *Lancet* 2012, **380**:2224–2260.
4. Ng M, Fleming T, Robinson M, Thomson B, Graetz N, Margono C, Mullany EC, Biryukov S, Abbafati C, Abera SF, Abraham JP, Abu-Rmeileh NM, Achoki T, AlBuhairan FS, Alemu ZA, Alfonso R, Ali MK, Ali R, Guzman NA, Ammar W, Anwar P, Banerjee A, Barquera S, Basu S, Bennett DA, Bhutta Z, Blore J, Cabral N, Nonato IC, Chang JC: Global, regional, and national prevalence of overweight and obesity in children and adults during 1980–2013: a systematic analysis for the Global Burden of Disease Study 2013. *Lancet* 2014, e-publication ahead of print.
5. Scott A, Ejikeme CS, Clotey EN, Thomas JG: Obesity in sub-Saharan Africa: development of an ecological theoretical framework. *Health Promot Int* 2013, **28**:4–16.
6. Sumithran P, Prendergast LA, Delbridge E, Purcell K, Shulkes A, Kriketos A, Proietto J: Long-term persistence of hormonal adaptations to weight loss. *N Engl J Med* 2011, **365**:1597–1604.
7. Rosenbaum M, Hirsch J, Gallagher DA, Leibel RL: Long-term persistence of adaptive thermogenesis in subjects who have maintained a reduced body weight. *Am J Clin Nutr* 2008, **88**:906–912.
8. Padwal R, Li SK, Lau DC: Long-term pharmacotherapy for obesity and overweight. *Cochrane Database Syst Rev* 2004, **3**:CD004094.
9. Dixon JB, Zimmet P, Alberti KG, Rubino F: Bariatric surgery: an IDF statement for obese Type 2 diabetes. *Surg Obes Relat Dis* 2011, **7**:433–447.
10. Padwal RS, Majumdar SR: Drug treatments for obesity: orlistat, sibutramine, and rimonabant. *Lancet* 2007, **369**:71–77.
11. Tseng YH, Cypess AM, Kahn CR: Cellular bioenergetics as a target for obesity therapy. *Nat Rev Drug Discov* 2010, **9**:465–482.
12. Wells JC: Thrift: a guide to thrifty genes, thrifty phenotypes and thrifty norms. *Int J Obes (Lond)* 2009, **33**:1331–1338.
13. Fawcett DW, Jones IC: The effects of hypophysectomy, adrenalectomy and of thiouracil feeding on the cytology of brown adipose tissue. *Endocrinology* 1949, **45**:609–621. *illust*.
14. Virtanen KA, Lidell ME, Orava J, Heglind M, Westergren R, Niemi T, Taittonen M, Laine J, Savisto NJ, Enerback S, Nuutila P: Functional brown adipose tissue in healthy adults. *N Engl J Med* 2009, **360**:1518–1525.
15. Hany TF, Gharehpapagh E, Kamel EM, Buck A, Himms-Hagen J, von Schulthess GK: Brown adipose tissue: a factor to consider in symmetrical tracer uptake in the neck and upper chest region. *Eur J Nucl Med Mol Imaging* 2002, **29**:1393–1398.
16. Cypess AM, Lehman S, Williams G, Tal I, Rodman D, Goldfine AB, Kuo FC, Palmer EL, Tseng YH, Doria A, Kolodny GM, Kahn CR: Identification and importance of brown adipose tissue in adult humans. *N Engl J Med* 2009, **360**:1509–1517.
17. Guerra C, Koza RA, Yamashita H, Walsh K, Kozak LP: Emergence of brown adipocytes in white fat in mice is under genetic control: effects on body weight and adiposity. *J Clin Invest* 1998, **102**:412–420.
18. Lean ME, James WP, Jennings G, Trayhurn P: Brown adipose tissue in patients with pheochromocytoma. *Int J Obes (Lond)* 1986, **10**:219–227.
19. Lahesmaa M, Orava J, Schalin-Jantti C, Soinio M, Hannukainen JC, Noponen T, Kirjavainen A, Iida H, Kudomi N, Enerback S, Virtanen KA, Nuutila P: Hyperthyroidism increases brown fat metabolism in humans. *J Clin Endocrinol Metab* 2014, **99**:E28–E35.
20. Enerback S: Brown adipose tissue in humans. *Int J Obes (Lond)* 2010, **34**(Suppl 1):S43–S46.
21. Wu J, Bostrom P, Sparks LM, Ye L, Choi JH, Giang AH, Khandekar M, Virtanen KA, Nuutila P, Schaart G, Huang K, Tu H, Van Marken Lichtenbelt WD, Hoeks J, Enerback S, Schrauwen P, Spiegelman BM: Beige adipocytes are a distinct type of thermogenic fat cell in mouse and human. *Cell* 2012, **150**:366–376.
22. Whittle AJ, Lopez M, Vidal-Puig A: Using brown adipose tissue to treat obesity - the central issue. *Trends Mol Med* 2011, **17**:405–411.
23. van Marken Lichtenbelt WD, Schrauwen P: Implications of nonshivering thermogenesis for energy balance regulation in humans. *Am J Physiol Regul Integr Comp Physiol* 2011, **301**:R285–R296.
24. Westerterp KR, Wilson SA, Rolland V: Diet induced thermogenesis measured over 24 h in a respiration chamber: effect of diet composition. *Int J Obes Relat Metab Disord* 1999, **23**:287–292.
25. Saito M, Okamatsu-Ogura Y, Matsushita M, Watanabe K, Yoneshiro T, Nio-Kobayashi J, Iwanaga T, Miyagawa M, Kameya T, Nakada K, Kawai Y, Tsujisaki M: High incidence of metabolically active brown adipose tissue in healthy adult humans: effects of cold exposure and adiposity. *Diabetes* 2009, **58**:1526–1531.
26. van Marken Lichtenbelt WD, Vanhommerig JW, Smulders NM, Drossaerts JM, Kemerink GJ, Bouvy ND, Schrauwen P, Teule GJ: Cold-activated brown adipose tissue in healthy men. *N Engl J Med* 2009, **360**:1500–1508.
27. Nicholls DG, Locke RM: Thermogenic mechanisms in brown fat. *Physiol Rev* 1984, **64**:1–64.
28. Kozak LP: Brown fat and the myth of diet-induced thermogenesis. *Cell Metab* 2010, **11**:263–267.
29. Ouellet V, Labbe SM, Blondin DP, Phoenix S, Guerin B, Haman F, Turcotte EE, Richard D, Carpentier AC: Brown adipose tissue oxidative metabolism contributes to energy expenditure during acute cold exposure in humans. *J Clin Invest* 2012, **122**:545–552.
30. Rothwell NJ, Stock MJ: Luxuskonsumption, diet-induced thermogenesis and brown fat: the case in favour. *Clin Sci (Lond)* 1983, **64**:19–23.
31. Yoneshiro T, Aita S, Matsushita M, Kameya T, Nakada K, Kawai Y, Saito M: Brown adipose tissue, whole-body energy expenditure, and thermogenesis in healthy adult men. *Obesity (Silver Spring)* 2011, **19**:13–16.
32. Muzik O, Mangner TJ, Granneman JG: Assessment of oxidative metabolism in brown fat using PET imaging. *Front Endocrinol (Lausanne)* 2012, **3**:15.
33. Orava J, Nuutila P, Lidell ME, Oikonen V, Noponen T, Viljanen T, Scheinin M, Taittonen M, Niemi T, Enerback S, Virtanen KA: Different metabolic responses of human brown adipose tissue to activation by cold and insulin. *Cell Metab* 2011, **14**:272–279.
34. Bartelt A, Bruns OT, Reimer R, Hohenberg H, Itrich H, Peldschus K, Kaul MG, Tromsdorf UJ, Weller H, Waurisch C, Eychmüller A, Gordts PL, Rinninger F, Bruegelmann K, Freund B, Nielsen P, Merkel M, Heeren J: Brown adipose tissue activity controls triglyceride clearance. *Nat Med* 2011, **17**:200–205.
35. Klitgaard HM, Dirks HB Jr, Garlick WR, Barker SB: Protein-bound iodine in various tissues after injection of elemental iodine. *Endocrinology* 1952, **50**:170–173.
36. Klieverik LP, Coomans CP, Endert E, Sauerwein HP, Havekes LM, Voshol PJ, Rensen PC, Romijn JA, Kalsbeek A, Fliers E: Thyroid hormone effects on whole-body energy homeostasis and tissue-specific fatty acid uptake in vivo. *Endocrinology* 2009, **150**:5639–5648.
37. Silva JE: Thermogenic mechanisms and their hormonal regulation. *Physiol Rev* 2006, **86**:435–464.
38. Jiang W, Miyamoto T, Kakizawa T, Sakuma T, Nishio S, Takeda T, Suzuki S, Hashizume K: Expression of thyroid hormone receptor alpha in 3 T3-L1

- adipocytes; triiodothyronine increases the expression of lipogenic enzyme and triglyceride accumulation. *J Endocrinol* 2004, **182**:295–302.
39. Viguerie N, Millet L, Avizou S, Vidal H, Larrouy D, Langin D: **Regulation of human adipocyte gene expression by thyroid hormone.** *J Clin Endocrinol Metab* 2002, **87**:630–634.
40. Sheehan TE, Kumar PA, Hood DA: **Tissue-specific regulation of cytochrome c oxidase subunit expression by thyroid hormone.** *Am J Physiol Endocrinol Metab* 2004, **286**:E968–E974.
41. Lopez M, Varela L, Vazquez MJ, Rodriguez-Cuenca S, Gonzalez CR, Velagapudi VR, Morgan DA, Schoenmakers E, Agassandian K, Lage R, Martinez de Morentin PB, Tovar S, Nogueiras R, Carling D, Lelliott C, Gallego R, Oresic M, Chatterjee K, Saha AK, Rahmouni K, Diéguez C, Vidal-Puig A: **Hypothalamic AMPK and fatty acid metabolism mediate thyroid regulation of energy balance.** *Nat Med* 2010, **16**:1001–1008.
42. Brent GA: **The molecular basis of thyroid hormone action.** *N Engl J Med* 1994, **331**:847–853.
43. Ribeiro MO, Carvalho SD, Schultz JJ, Chiellini G, Scanlan TS, Bianco AC, Brent GA: **Thyroid hormone-sympathetic interaction and adaptive thermogenesis are thyroid hormone receptor isoform-specific.** *J Clin Invest* 2001, **108**:97–105.
44. Bianco AC, Silva JE: **Cold exposure rapidly induces virtual saturation of brown adipose tissue nuclear T3 receptors.** *Am J Physiol* 1988, **255**:E496–E503.
45. Bryzgalova G, Effendic S, Khan A, Rehnmark S, Barbounis P, Boulet J, Dong G, Singh R, Shapses S, Malm J, Webb P, Baxter JD, Grover GJ: **Anti-obesity, anti-diabetic, and lipid lowering effects of the thyroid receptor beta subtype selective agonist KB-141.** *J Steroid Biochem Mol Biol* 2008, **111**:262–267.
46. Grover GJ, Egan DM, Sleph PG, Beehler BC, Chiellini G, Nguyen NH, Baxter JD, Scanlan TS: **Effects of the thyroid hormone receptor agonist GC-1 on metabolic rate and cholesterol in rats and primates: selective actions relative to 3,5,3'-triiodo-L-thyronine.** *Endocrinology* 2004, **145**:1656–1661.
47. Amorim BS, Ueta CB, Freitas BC, Nassif RJ, Gouveia CH, Christoffolete MA, Moriscot AS, Lancellotti CL, Llimona F, Barbeiro HV, de Souza HP, Catanosi S, Passarelli M, Aoki MS, Bianco AC, Ribeiro MO: **A TRbeta-selective agonist confers resistance to diet-induced obesity.** *J Endocrinol* 2009, **203**:291–299.
48. Lee JY, Takahashi N, Yasubuchi M, Kim YI, Hashizaki H, Kim MJ, Sakamoto T, Goto T, Kawada T: **Triiodothyronine induces UCP1 expression and mitochondrial biogenesis in human adipocytes.** *Am J Physiol Cell Physiol* 2011, **302**:463–472.
49. Skarulis MC, Celi FS, Mueller E, Zemskova M, Malek R, Hugendubler L, Cochran C, Solomon J, Chen C, Gorden P: **Thyroid hormone induced brown adipose tissue and amelioration of diabetes in a patient with extreme insulin resistance.** *J Clin Endocrinol Metab* 2010, **95**:256–262.
50. Simonsen L, Bulow J, Madsen J, Christensen NJ: **Thermogenic response to epinephrine in the forearm and abdominal subcutaneous adipose tissue.** *Am J Physiol* 1992, **263**:E850–E855.
51. Simonsen L, Stallknecht B, Bulow J: **Contribution of skeletal muscle and adipose tissue to adrenaline-induced thermogenesis in man.** *Int J Obes Relat Metab Disord* 1993, **17**(3):S47–S51. discussion S68.
52. Ricquier D, Nechad M, Mory G: **Ultrastructural and biochemical characterization of human brown adipose tissue in pheochromocytoma.** *J Clin Endocrinol Metab* 1982, **54**:803–807.
53. English JT, Patel SK, Flanagan MJ: **Association of pheochromocytomas with brown fat tumors.** *Radiology* 1973, **107**:279–281.
54. Melicow MM: **Hibernating fat and pheochromocytoma.** *AMA Arch Pathol* 1957, **63**:367–372.
55. Bouillaud F, Ricquier D, Mory G, Thibault J: **Increased level of mRNA for the uncoupling protein in brown adipose tissue of rats during thermogenesis induced by cold exposure or norepinephrine infusion.** *J Biol Chem* 1984, **259**:11583–11586.
56. Hadi M, Chen CC, Whatley M, Pacak K, Carrasquillo JA: **Brown fat imaging with (18)F-6-fluorodopamine PET/CT, (18)F-FDG PET/CT, and (123)I-MIBG SPECT: a study of patients being evaluated for pheochromocytoma.** *J Nucl Med* 2007, **48**:1077–1083.
57. Wang Q, Zhang M, Ning G, Gu W, Su T, Xu M, Li B, Wang W: **Brown adipose tissue in humans is activated by elevated plasma catecholamines levels and is inversely related to central obesity.** *PLoS One* 2011, **6**:e21006.
58. Himms-Hagen J, Cui J, Danforth E Jr, Taatjes DJ, Lang SS, Waters BL, Claus TH: **Effect of CL-316,243, a thermogenic beta 3-agonist, on energy balance and brown and white adipose tissues in rats.** *Am J Physiol* 1994, **266**:R1371–R1382.
59. Susulic VS, Frederick RC, Lawitts J, Tozzo E, Kahn BB, Harper ME, Himms-Hagen J, Flier JS, Lowell BB: **Targeted disruption of the beta 3-adrenergic receptor gene.** *J Biol Chem* 1995, **270**:29483–29492.
60. Arch JR: **The discovery of drugs for obesity, the metabolic effects of leptin and variable receptor pharmacology: perspectives from beta3-adrenoceptor agonists.** *Naunyn Schmiedebergs Arch Pharmacol* 2008, **378**:225–240.
61. Larsen TM, Toubro S, van Baak MA, Gottesdiener KM, Larson P, Saris WH, Astrup A: **Effect of a 28-d treatment with L-796568, a novel beta(3)-adrenergic receptor agonist, on energy expenditure and body composition in obese men.** *Am J Clin Nutr* 2002, **76**:780–788.
62. van Baak MA, Hul GB, Toubro S, Astrup A, Gottesdiener KM, DeSmet M, Saris WH: **Acute effect of L-796568, a novel beta 3-adrenergic receptor agonist, on energy expenditure in obese men.** *Clin Pharmacol Ther* 2002, **71**:272–279.
63. Joshi PV, Lele VR: **Unexpected visitor on FDG PET/CT—brown adipose tissue (BAT) in mesentery in a case of retroperitoneal extra-adrenal pheochromocytoma: is the BAT activation secondary to catecholamine-secreting pheochromocytoma?** *Clin Nucl Med* 2012, **37**:e119–e120.
64. Cheng W, Zhu Z, Jin X, Chen L, Zhuang H, Li F: **Intense FDG activity in the brown adipose tissue in omental and mesenteric regions in a patient with malignant pheochromocytoma.** *Clin Nucl Med* 2012, **37**:S14–S15.
65. Feldman D: **Evidence that brown adipose tissue is a glucocorticoid target organ.** *Endocrinology* 1978, **103**:2091–2097.
66. Strack AM, Sebastian RJ, Schwartz MW, Dallman MF: **Glucocorticoids and insulin: reciprocal signals for energy balance.** *Am J Physiol* 1995, **268**:R142–R149.
67. Soumano K, Desbiens S, Rabelo R, Bakopanos E, Camirand A, Silva JE: **Glucocorticoids inhibit the transcriptional response of the uncoupling protein-1 gene to adrenergic stimulation in a brown adipose cell line.** *Mol Cell Endocrinol* 2000, **165**:7–15.
68. Garrel DR: **Glucocorticoids and energy expenditure: relevance to the regulation of energy balance in man.** *Nutrition* 1997, **13**:482–483.
69. Strack AM, Bradbury MJ, Dallman MF: **Corticosterone decreases nonshivering thermogenesis and increases lipid storage in brown adipose tissue.** *Am J Physiol* 1995, **268**:R183–R191.
70. Feve B, Baude B, Krief S, Strosberg AD, Pairault J, Emorine LJ: **Inhibition by dexamethasone of beta 3-adrenergic receptor responsiveness in 3 T3-F442A adipocytes. Evidence for a transcriptional mechanism.** *J Biol Chem* 1992, **267**:15909–15915.
71. Kiely J, Hadcock JR, Bahouth SW, Malbon CC: **Glucocorticoids down-regulate beta 1-adrenergic-receptor expression by suppressing transcription of the receptor gene.** *Biochem J* 1994, **302**(Pt 2):397–403.
72. Vander Tuig JG, Ohshima K, Yoshida T, Romsos DR, Bray GA: **Adrenalectomy increases norepinephrine turnover in brown adipose tissue of obese (ob/ob) mice.** *Life Sci* 1984, **34**:1423–1432.
73. Berthiaume M, Sell H, Lalonde J, Gelinias Y, Tchernof A, Richard D, Deshaies Y: **Am J Physiol Regul Integr Comp Physiol.** *Am J Physiol Regul Integr Comp Physiol* 2004, **287**:R1116–R1123.
74. Ashizawa N, Takagi M, Seto S, Suzuki S, Yano K: **Serum adiponectin and leptin in a patient with Cushing's syndrome before and after adrenalectomy.** *Intern Med* 2007, **46**:383–385.
75. Zennaro MC, Le Menuet D, Viengchareun S, Walker F, Ricquier D, Lombes M: **Hibernoma development in transgenic mice identifies brown adipose tissue as a novel target of aldosterone action.** *J Clin Invest* 1998, **101**:1254–1260.
76. Penforis P, Viengchareun S, Le Menuet D, Cluzeaud F, Zennaro MC, Lombes M: **The mineralocorticoid receptor mediates aldosterone-induced differentiation of T37i cells into brown adipocytes.** *Am J Physiol Endocrinol Metab* 2000, **279**:E386–E394.
77. Viengchareun S, Penforis P, Zennaro MC, Lombes M: **Mineralocorticoid and glucocorticoid receptors inhibit UCP expression and function in brown adipocytes.** *Am J Physiol Endocrinol Metab* 2001, **280**:E640–E649.
78. Kraus D, Jager J, Meier B, Fasshauer M, Klein J: **Aldosterone inhibits uncoupling protein-1, induces insulin resistance, and stimulates proinflammatory adipokines in adipocytes.** *Horm Metab Res* 2005, **37**:455–459.
79. Hoppmann J, Perwitz N, Meier B, Fasshauer M, Hadaschik D, Lehnert H, Klein J: **The balance between gluco- and mineralo-corticoid action critically**

- determines inflammatory adipocyte responses. *J Endocrinol* 2010, **204**:153–164.
80. Marzolla V, Armani A, Zennaro MC, Cinti F, Mammi C, Fabbri A, Rosano GM, Caprio M: **The role of the mineralocorticoid receptor in adipocyte biology and fat metabolism.** *Mol Cell Endocrinol* 2012, **350**:281–288.
81. Feraco A, Armani A, Mammi C, Fabbri A, Rosano GM, Caprio M: **Role of mineralocorticoid receptor and renin-angiotensin-aldosterone system in adipocyte dysfunction and obesity.** *J Steroid Biochem Mol Biol* 2013, **137**:99–106.
82. Al-Shoumer KA, Page B, Thomas E, Murphy M, Beshyah SA, Johnston DG: **Effects of four years' treatment with biosynthetic human growth hormone (GH) on body composition in GH-deficient hypopituitary adults.** *Eur J Endocrinol* 1996, **135**:559–567.
83. Hoffman AR, Kuntze JE, Baptista J, Baum HB, Baumann GP, Biller BM, Clark RV, Cook D, Inzucchi SE, Kleinberg D, Klibanski A, Phillips LS, Ridgway EC, Robbins RJ, Schlechte J, Sharma M, Thorner MO, Vance ML: **Growth hormone (GH) replacement therapy in adult-onset gh deficiency: effects on body composition in men and women in a double-blind, randomized, placebo-controlled trial.** *J Clin Endocrinol Metab* 2004, **89**:2048–2056.
84. Hioki C, Yoshida T, Kogure A, Takakura Y, Umekawa T, Yoshioka K, Shimatsu A, Yoshikawa T: **Effects of growth hormone (GH) on mRNA levels of uncoupling proteins 1, 2, and 3 in brown and white adipose tissues and skeletal muscle in obese mice.** *Horm Metab Res* 2004, **36**:607–613.
85. Lorenzo M, Valverde AM, Teruel T, Benito M: **IGF-I is a mitogen involved in differentiation-related gene expression in fetal rat brown adipocytes.** *J Cell Biol* 1993, **123**:1567–1575.
86. Valverde AM, Benito M, Lorenzo M: **Proliferation of fetal brown adipocyte primary cultures: relationship with the genetic expression of glucose 6 phosphate dehydrogenase.** *Exp Cell Res* 1991, **194**:232–237.
87. Porras A, Alvarez AM, Valladares A, Benito M: **TNF-alpha induces apoptosis in rat fetal brown adipocytes in primary culture.** *FEBS Lett* 1997, **416**:324–328.
88. Guerra C, Benito M, Fernandez M: **IGF-I induces the uncoupling protein gene expression in fetal rat brown adipocyte primary cultures: role of C/EBP transcription factors.** *Biochem Biophys Res Commun* 1994, **201**:813–819.
89. Duchamp C, Burton KA, Geloan A, Dauncey MJ: **Transient upregulation of IGF-I gene expression in brown adipose tissue of cold-exposed rats.** *Am J Physiol* 1997, **272**:E453–E460.
90. Symonds ME, Mostyn A, Pearce S, Budge H, Stephenson T: **Endocrine and nutritional regulation of fetal adipose tissue development.** *J Endocrinol* 2003, **179**:293–299.
91. Viengchareun S, Servel N, Feve B, Freemark M, Lombes M, Binart N: **Prolactin receptor signaling is essential for perinatal brown adipocyte function: a role for insulin-like growth factor-2.** *PLoS One* 2008, **3**:e1535.
92. Ben-Jonathan N, LaPensee CR, LaPensee EW: **What can we learn from rodents about prolactin in humans?** *Endocr Rev* 2008, **29**:1–41.
93. Pijl H, Ohashi S, Matsuda M, Miyazaki Y, Mahankali A, Kumar V, Pipek R, Iozzo P, Lancaster JL, Cincotta AH, DeFronzo RA: **Bromocriptine: a novel approach to the treatment of type 2 diabetes.** *Diabetes Care* 2000, **23**:1154–1161.
94. Krol E, Martin SA, Huhtaniemi IT, Douglas A, Speakman JR: **Negative correlation between milk production and brown adipose tissue gene expression in lactating mice.** *J Exp Biol* 2011, **214**:4160–4170.
95. Julien Auffret SV, Adeline M, Bruno F, Marc L, Nadine B: **Mice lacking prolactin receptor resist high-fat diet-induced obesity by browning of adipose tissue.** *Endocr Rev* 2011, **32**:p1–p787.
96. Rodriguez-Cuenca S, Monjo M, Frontera M, Gianotti M, Proenza AM, Roca P: **Sex steroid receptor expression profile in brown adipose tissue: effects of hormonal status.** *Cell Physiol Biochem* 2007, **20**:877–886.
97. Gaspard U: **Hyperinsulinaemia, a key factor of the metabolic syndrome in postmenopausal women.** *Maturitas* 2009, **62**:362–365.
98. Nadal-Casellas A, Proenza AM, Llado I, Gianotti M: **Effects of ovariectomy and 17-beta estradiol replacement on rat brown adipose tissue mitochondrial function.** *Steroids* 2011, **76**:1051–1056.
99. Rodriguez-Cuenca S, Monjo M, Gianotti M, Proenza AM, Roca P: **Expression of mitochondrial biogenesis-signaling factors in brown adipocytes is influenced specifically by 17beta-estradiol, testosterone, and progesterone.** *Am J Physiol Endocrinol Metab* 2007, **292**:E340–E346.
100. Monjo M, Rodriguez AM, Palou A, Roca P: **Direct effects of testosterone, 17 beta-estradiol, and progesterone on adrenergic regulation in cultured brown adipocytes: potential mechanism for gender-dependent thermogenesis.** *Endocrinology* 2003, **144**:4923–4930.
101. Rodriguez AM, Monjo M, Roca P, Palou A: **Opposite actions of testosterone and progesterone on UCP1 mRNA expression in cultured brown adipocytes.** *Cell Mol Life Sci* 2002, **59**:1714–1723.
102. Ouellet V, Routhier-Labadie A, Bellemare W, Lakhal-Chaieb L, Turcotte E, Carpentier AC, Richard D: **Outdoor temperature, age, sex, body mass index, and diabetic status determine the prevalence, mass, and glucose-uptake activity of 18 F-FDG-detected BAT in humans.** *J Clin Endocrinol Metab* 2011, **96**:192–199.
103. Ryu JW, Kim MS, Kim CH, Song KH, Park JY, Lee JD, Kim JB, Lee KU: **DHEA administration increases brown fat uncoupling protein 1 levels in obese OLETF rats.** *Biochem Biophys Res Commun* 2003, **303**:726–731.
104. Gilsanz V, Hu HH, Kajimura S: **Relevance of brown adipose tissue in infancy and adolescence.** *Pediatr Res* 2013, **73**:3–9.
105. Tseng YH, Kraucunas KM, Kokkoto E, Kahn CR: **Differential roles of insulin receptor substrates in brown adipocyte differentiation.** *Mol Cell Biol* 2004, **24**:1918–1929.
106. Tanti JF, Gremeaux T, Brandenburg D, Van Obberghen E, Le Marchand-Brustel Y: **Brown adipose tissue in lean and obese mice. Insulin-receptor binding and tyrosine kinase activity.** *Diabetes* 1986, **35**:1243–1248.
107. Shimizu Y, Kielar D, Minokoshi Y, Shimazu T: **Brown adipose tissue in culture by a mechanism different from that of insulin.** *Biochem J* 1996, **314**(Pt 2):485–490.
108. Storlien LH, James DE, Burleigh KM, Chisholm DJ, Kraegen EW: **Fat feeding causes widespread in vivo insulin resistance, decreased energy expenditure, and obesity in rats.** *Am J Physiol* 1986, **251**:E576–E583.
109. Shimizu Y, Nikami H, Tsukazaki K, Machado UF, Yano H, Seino Y, Saito M: **Increased expression of glucose transporter GLUT-4 in brown adipose tissue of fasted rats after cold exposure.** *Am J Physiol* 1993, **264**:E890–E895.
110. Rothwell NJ, Stock MJ: **A role for insulin in the diet-induced thermogenesis of cafeteria-fed rats.** *Metabolism* 1981, **30**:673–678.
111. Shibata H, Perusse F, Bukowiecki LJ: **The role of insulin in nonshivering thermogenesis.** *Can J Physiol Pharmacol* 1987, **65**:152–158.
112. Gunawardana SC, Piston DW: **Reversal of type 1 diabetes in mice by brown adipose tissue transplant.** *Diabetes* 2012, **61**:674–682.
113. Markelic M, Velickovic K, Golic I, Otasevic V, Stancic A, Jankovic A, Vucetic M, Buzadzic B, Korac B, Korac A: **Endothelial cell apoptosis in brown adipose tissue of rats induced by hyperinsulinaemia: the possible role of TNF-alpha.** *Eur J Histochem* 2011, **55**:e34.
114. Rouru J, Cusin I, Zakrzewska KE, Jeanrenaud B, Rohner-Jeanrenaud F: **Effects of intravenously infused leptin on insulin sensitivity and on the expression of uncoupling proteins in brown adipose tissue.** *Endocrinology* 1999, **140**:3688–3692.
115. Enriori PJ, Sinnayah P, Simonds SE, Garcia Rudaz C, Cowley MA: **Leptin action in the dorsomedial hypothalamus increases sympathetic tone to brown adipose tissue in spite of systemic leptin resistance.** *J Neurosci* 2011, **31**:12189–12197.
116. Heymsfield SB, Greenberg AS, Fujioka K, Dixon RM, Kushner R, Hunt T, Lubina JA, Patane J, Self B, Hunt P, McCamish M: **Recombinant leptin for weight loss in obese and lean adults: a randomized, controlled, dose-escalation trial.** *Jama* 1999, **282**:1568–1575.
117. Koh KK, Park SM, Quon MJ: **Leptin and cardiovascular disease: response to therapeutic interventions.** *Circulation* 2008, **117**:3238–3249.
118. Qiao L, Yoo H, Bosco C, Lee B, Feng GS, Schaack J, Chi NW, Shao J: **Adiponectin reduces thermogenesis by inhibiting brown adipose tissue activation in mice.** *Diabetologia* 2014, **57**:1027–1036.
119. Iacobellis G, Di Gioia C, Petramala L, Chiappetta C, Serra V, Zinmanosca L, Marinelli C, Ciardi A, De Toma G, Letizia C: **Brown fat expresses adiponectin in humans.** *Int J Endocrinol* 2013, **2013**:126751.
120. Rinaldi-Carmona M, Barth F, Heaulme M, Shire D, Calandra B, Congy C, Martinez S, Maruani J, Neliat G, Caput D, Ferrara R, Soubrié P, Brière JC, Le Fur G: **SR141716A, a potent and selective antagonist of the brain cannabinoid receptor.** *FEBS Lett* 1994, **350**:240–244.
121. Muccioli GG, Naslain D, Backhed F, Reigstad CS, Lambert DM, Delzenne NM, Cani PD: **The endocannabinoid system links gut microbiota to adipogenesis.** *Mol Syst Biol* 2010, **6**:392.
122. Bajzer M, Olivieri M, Haas MK, Pfluger PT, Magrisso IJ, Foster MT, Tschöp MH, Krawczewski-Carhuatana KA, Cota D, Obici S: **Cannabinoid receptor 1**

- (CB1) antagonism enhances glucose utilisation and activates brown adipose tissue in diet-induced obese mice. *Diabetologia* 2011, **54**:3121–3131.
123. Verty AN, Allen AM, Oldfield BJ: **The effects of rimonabant on brown adipose tissue in rat: implications for energy expenditure.** *Obesity (Silver Spring)* 2009, **17**:254–261.
 124. Pervitz N, Wenzel J, Wagner I, Buning J, Drenckhan M, Zarse K, Ristow M, Lillenthal W, Lehnert H, Klein J: **Cannabinoid type 1 receptor blockade induces transdifferentiation towards a brown fat phenotype in white adipocytes.** *Diabetes Obes Metab* 2010, **12**:158–166.
 125. Bostrom P, Wu J, Jedrychowski MP, Korde A, Ye L, Lo JC, Rasbach KA, Bostrom EA, Choi JH, Long JZ, Kajimura S, Zingaretti MC, Vind BF, Tu H, Cinti S, Højlund K, Gygi SP, Spiegelman BM: **A PGC1-alpha-dependent myokine that drives brown-fat-like development of white fat and thermogenesis.** *Nature* 2012, **481**:463–468.
 126. Seale P, Bjork B, Yang W, Kajimura S, Chin S, Kuang S, Scime A, Devarakonda S, Conroe HM, Erdjument-Bromage H, Tempst P, Rudnicki MA, Beier DR, Spiegelman BM: **PRDM16 controls a brown fat/skeletal muscle switch.** *Nature* 2008, **454**:961–967.
 127. Kajimura S, Seale P, Kubota K, Lunsford E, Frangioni JV, Gygi SP, Spiegelman BM: **Initiation of myoblast to brown fat switch by a PRDM16-C/EBP-beta transcriptional complex.** *Nature* 2009, **460**:1154–1158.
 128. Cederberg A, Gronning LM, Ahren B, Tasken K, Carlsson P, Enerback S: **FOXC2 is a winged helix gene that counteracts obesity, hypertriglyceridemia, and diet-induced insulin resistance.** *Cell* 2001, **106**:563–573.
 129. Hallberg M, Morganstein DL, Kiskinis E, Shah K, Kralli A, Dilworth SM, White R, Parker MG, Christian M: **A functional interaction between RIP140 and PGC-1alpha regulates the expression of the lipid droplet protein CIDEA.** *Mol Cell Biol* 2008, **28**:6785–6795.
 130. Tseng YH, Kokkotou E, Schulz TJ, Huang TL, Winnay JN, Taniguchi CM, Tran TT, Suzuki R, Espinoza DO, Yamamoto Y, Ahrens MJ, Dudley AT, Norris AW, Kulkarni RN, Kahn CR: **New role of bone morphogenetic protein 7 in brown adipogenesis and energy expenditure.** *Nature* 2008, **454**:1000–1004.
 131. Beenken A, Mohammadi M: **The FGF family: biology, pathophysiology and therapy.** *Nat Rev Drug Discov* 2009, **8**:235–253.
 132. Wilson-Fritch L, Nicoloso S, Chouinard M, Lazar MA, Chui PC, Leszyk J, Straubhaar J, Czech MP, Corvera S: **Mitochondrial remodeling in adipose tissue associated with obesity and treatment with rosiglitazone.** *J Clin Invest* 2004, **114**:1281–1289.
 133. Bordinchia M, Liu D, Amri EZ, Ailhaud G, Dessi-Fulgheri P, Zhang C, Takahashi N, Sarzani R, Collins S: **Cardiac natriuretic peptides act via p38 MAPK to induce the brown fat thermogenic program in mouse and human adipocytes.** *J Clin Invest* 2012, **122**:1022–1036.
 134. Crisan M, Casteilla L, Lehr L, Carmona M, Paoloni-Giacobino A, Yap S, Sun B, Leger B, Logar A, Penicaud L, Schrauwen P, Cameron-Smith D, Russell AP, Péault B, Giacobino JP: **A reservoir of brown adipocyte progenitors in human skeletal muscle.** *Stem Cells* 2008, **26**:2425–2433.
 135. Elabd C, Chiellini C, Carmona M, Galitzky J, Cochet O, Petersen R, Penicaud L, Kristiansen K, Bouloumie A, Casteilla L, Dani C, Ailhaud G, Amri EZ: **Human multipotent adipose-derived stem cells differentiate into functional brown adipocytes.** *Stem Cells* 2009, **27**:2753–2760.
 136. Stanford-RJ-WM KI, Ding AN, Kristy T, Hitchcox KM, Dae Young J, Yong Jin L, Kim JK, Hirshman MF, Yu-Hua T, Goodyear LJ: *Transplantation of Brown Adipose Tissue Exerts Beneficial Effects on Glucose Homeostasis.* San Diego: American Diabetes Association, 71st Scientific Session; 2011.
 137. David W, Piston SCG: *Reversal of Type 1 Diabetes by Brown Adipose Tissue Transplant.* San Diego: American Diabetes Association, 71st Scientific Session; 2011.

doi:10.1186/s40608-014-0013-5

Cite this article as: Reddy et al.: Brown adipose tissue: endocrine determinants of function and therapeutic manipulation as a novel treatment strategy for obesity. *BMC Obesity* 2014 **1**:13.

Submit your next manuscript to BioMed Central and take full advantage of:

- Convenient online submission
- Thorough peer review
- No space constraints or color figure charges
- Immediate publication on acceptance
- Inclusion in PubMed, CAS, Scopus and Google Scholar
- Research which is freely available for redistribution

Submit your manuscript at
www.biomedcentral.com/submit



Identification of Brown Adipose Tissue Using MR Imaging in a Human Adult With Histological and Immunohistochemical Confirmation

Narendra L. Reddy, Terence A. Jones, Sarah C. Wayte, Oludolapo Adesanya, Sailesh Sankar, Yen C. Yeo, Gyanendra Tripathi, Philip G. McTernan, Harpal S. Randeva, Sudhesh Kumar, Charles E. Hutchinson, and Thomas M. Barber

Clinical Sciences Research Laboratories (N.L.R., T.A.J., S.S., G.T., P.G.M., H.S.R., S.K., C.E.H., T.M.B.), Warwick Medical School, University of Warwick, and Departments of Medical Physics (S.C.W.), Radiology (O.A., C.E.H.), and Histopathology (Y.C.Y.), University Hospitals of Coventry and Warwickshire, Coventry CV2 2DX, United Kingdom

Objective: Manipulation of human brown adipose tissue (BAT) represents a novel therapeutic option for diabetes. The aim of our study was to develop and test a novel magnetic resonance (MR) imaging-based method to identify human BAT, delineate it from white adipose tissue, and validate it through immunohistochemistry.

Design: A 25-year old Caucasian female with hyperparathyroidism-jaw tumor syndrome underwent parathyroidectomy. An ^{18}F fluoro-2-deoxyglucose positron emission tomography (PET)-computed tomography (CT) scan performed after surgery ruled out malignancy but showed avid uptake within the mediastinum, neck, supraclavicular fossae, and axillae, consistent with BAT. Immunohistochemical staining using uncoupling protein-1 antibody was performed on one fat sample obtained from the suprasternal area during parathyroidectomy. Subsequently, serial MR scans were performed. Retrospectively, regions of interest (ROIs) were identified on MR corresponding to areas of high uptake on PET-CT. Prospectively, ROIs were identified on MR based on signal intensity and appearance and compared with PET-CT.

Results: Of 111 retrospectively identified ROIs from PET-CT, 93 (83.8%) showed corresponding low MR signal: 25 of 25 mediastinum (100%), 29 of 31 neck (93.5%), 31 of 41 supraclavicular (75.6%), and 8 of 14 axillae (57%). Prospectively, 47 of 54 ROIs identified on MR (87%) showed a corresponding increased uptake on PET-CT. Serendipitously, the sample obtained at surgery corresponded with high uptake and low signal on subsequent PET and MR, respectively, and immunohistochemistry confirmed BAT.

Conclusion: We provide the first report for the reliable use of MR to identify BAT in a living human adult, with histological/immunohistochemical confirmation. Our data demonstrate proof of concept to support the development of MR as a safe, reproducible imaging modality for human BAT. (*J Clin Endocrinol Metab* 99: E117–E121, 2014)

Recently, active brown adipose tissue (BAT) was identified in human adults for the first time (1). The clinical relevance is that BAT activation should promote weight loss (2, 3) and may account for 10%–20% increase in energy expenditure (4, 5). BAT activity may also improve glucolipid status (6, 7).

Most studies on human BAT have used ^{18}F -fluoro-2-deoxyglucose (^{18}F -FDG)-positron emission tomography (PET) (1, 3). This technique is excellent for the assessment of BAT activity. However, there are limitations that include signal variability resulting from changes in BAT activity in response to environmental temperature (necessitating careful control of environmental temperature). Magnetic resonance (MR)-based images of human BAT may overcome this problem and improve reproducibility. MR would provide data on anatomy and BAT content rather than activity that in turn would provide insight into the presence of BAT among the adult human population and also could potentially be used in the assessment of future therapies that manipulate BAT content. Furthermore, MR does not use ionizing radiation.

The rationale for exploring MR to identify human adult BAT is based on the premise that BAT and white adipose tissue (WAT) differ in their water to fat ratio (due to differences in mitochondrial and triglyceride content) (8). The MR technique of iterative decomposition of water and fat with echo asymmetry and least-squares estimation (IDEAL MR) has been shown in rats to delineate BAT from WAT, with fat fraction ranges being 37%–70% and 90%–93%, respectively (9). However, this technique has not been demonstrated to identify BAT conclusively in a living human adult.

The aim of our study was to demonstrate proof of concept that the identification of BAT in a living human adult is possible using the technique of IDEAL MR.

Materials and Methods

The case

A 25-year-old nonobese Caucasian female (phenotype shown in Supplemental Table 1) was diagnosed with hyperparathyroidism-jaw tumor syndrome (heterozygous mutation: T to C nucleotide substitution in exon 2 of *CDC73* [c.191T>C], encoding parafibromin) (10). There were no regular medications and no other medical history of note. A right-sided mandibular lesion (giant cell granuloma) was identified and resected. After a successful enucleation of a 5-mm right inferior parathyroid adenoma, the serum PTH level was transiently elevated. Subsequent ^{18}F -FDG PET-computed tomography (CT) scan was negative for malignancy but revealed multiple areas of high ^{18}F -FDG uptake within suprasternal and mediastinal fat (Supplemental Figure 1A). Informed consent for study recruitment was obtained. Ethical approval was obtained from the regional ethics committee.

Positron emission tomography scanning

The subject was fasted for 6 hours. A total of 375 MBq of ^{18}F -FDG radiotracer was injected 1 hour prior to PET scan (GE Discovery STE PET-CT scanner; General Electric Medical Systems). Two sets of emission data were obtained for 3 minutes in each bed position; from skull base to midhigh (arms elevated); and the head and neck protocol (without arm elevation). PET images were reconstructed using CT data for attenuation correction.

Magnetic resonance scanning

A baseline MR scan using 3-echo IDEAL sequence (11, 12) on a 3T GE-HDxt scanner (General Electric Medical Systems) was performed in the same month as the PET scan. Axial images with 5-mm slice thickness were obtained from upper cervical to midthoracic level. The T1-weighted IDEAL sequence parameters were as follows: repetition time, 440 milliseconds; echo time, 10.8 milliseconds; acquisition matrix size, 320×256 ; number of excitations, 3; and field of view, 30 cm. This generated water-only and fat-only (fat-IDEAL) images. The latter were used for subsequent analyses. A second MR was performed 2 months later using identical imaging parameters to determine temporal variation in BAT distribution.

Retrospective image analysis

PET-CT and fat-IDEAL MR images were transposed and coregistered using image fusion software Mirada XD 4.3 (Mirada Medical Ltd).

In the fused images, BAT areas identified on PET (greater than background levels of ^{18}F -FDG uptake within adipose tissue) were drawn on fat-IDEAL MR images (Supplemental Figure 1C) and will be referred to as $\text{BAT}_{\text{retro}}$. Radiotracer uptake in the paravertebral regions was not assessed due to the difficulties of accurately identifying these areas on MR. Image analysis was then performed on the enhanced MR images possessing mapped $\text{BAT}_{\text{retro}}$ regions, using ImageJ 1.45s (National Institutes of Health).

MR signals within $\text{BAT}_{\text{retro}}$ areas were compared with those from immediately adjacent adipose tissue ($\text{WAT}_{\text{retro}}$) to determine differences in signal intensity. The MR images were scrutinized with regard to adjacent image slices to ensure that any perceived variation in MR signal did not represent partial volume artifact. Differences in signal intensity in $\text{BAT}_{\text{retro}}$ and $\text{WAT}_{\text{retro}}$ areas were compared using the Wilcoxon matched-pairs test (paired *t* test) using GraphPad Prism version 5.00 (GraphPad Software). One-way ANOVA was performed to determine the variation of the $\text{BAT}_{\text{retro}}$ to $\text{WAT}_{\text{retro}}$ signal ratios according to the anatomical location.

Prospective image analysis

Two radiologists independently drew BAT areas on unmapped fat-IDEAL MR images ($\text{BAT}_{\text{prosp}}$) based on differences in signal intensity observed between $\text{BAT}_{\text{retro}}$ and $\text{WAT}_{\text{retro}}$ during retrospective analyses 4 months after the retrospective analysis (to reduce any recall bias). The regions of interest (ROIs) were restricted to adipose tissue within the upper mediastinum, base of neck, and supraclavicular fossae.

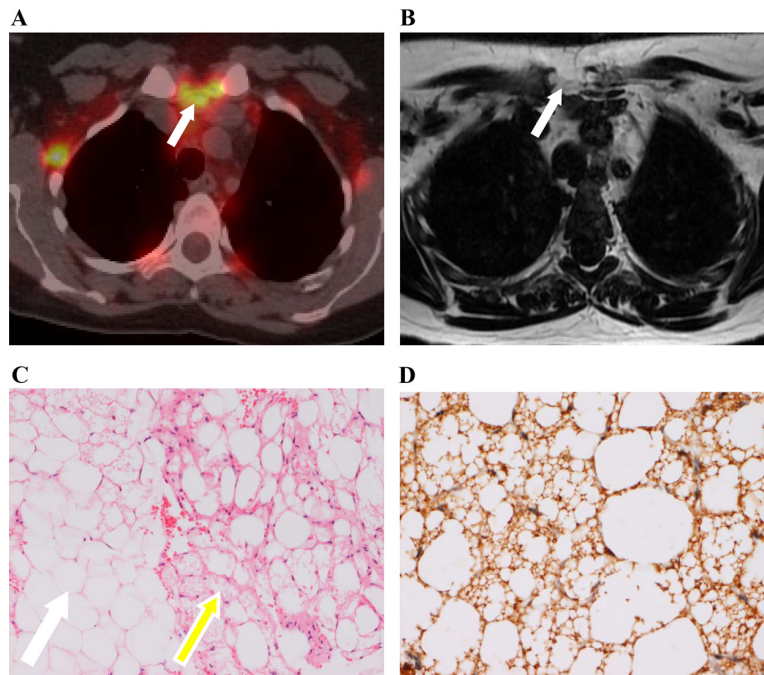


Figure 1. A, ^{18}F -FDG uptake within the suprasternal notch on PET-CT (arrow). B, fat-IDEAL MR at the same level showing corresponding low signal in the suprasternal notch. Hematoxylin-eosin staining (C) and UCP1 immunostaining (D) provide confirmation of BAT obtained from this area.

Histology and immunohistochemistry

The single fat sample obtained during parathyroidectomy underwent histological and immunohistochemical analysis (no other samples were taken). The Vectastain Elite ABC kit (Vector Laboratories; PK-6101) and rabbit antiuncoupling protein-1 (UCP1; 1:500, U6382; Sigma) were used according to the manufacturer's protocol.

Results

Retrospective image analyses

One hundred eleven ROIs of ^{18}F -FDG uptake on PET were identified, which were consistent with BAT (Figure 1A and Supplemental Figure 1A): upper mediastinum ($n = 25$); supraclavicular fossae ($n = 41$); neck ($n = 31$); and axillae ($n = 14$) (Table 1). These ROIs of increased ^{18}F -FDG uptake had a total cumulative surface area of

9031 mm², of which the majority occurred within the mediastinum and supraclavicular regions. Visual comparison of the MR signal within these BAT_{retro} areas and adjacent WAT_{retro} revealed consistently lower signal intensity and were often delineated by a discrete margin, as shown in Figure 1B and Supplemental Figure 1B.

Overall, 93 of the 111 BAT_{retro} ROIs (83.8%) had a lower MR signal than adjacent WAT_{retro}, although this did vary according to anatomical site (Table 1). Twenty-five of 25 of the BAT_{retro} ROIs in the upper mediastinum (100%) had a lower MR signal than adjacent adipose tissue, 29 of 31 in the neck (93.5%), 31 of 41 in the supraclavicular fossae (75.6%), and 8 of 14 in the axillae (57%). A significant difference was found between MR signal within BAT_{retro} and WAT_{retro} ROIs (Table 1) using Wilcoxon

matched-pairs test in all but the axillary region. The signal intensity varied considerably along the B0 axis (cranio-caudal direction), with a 10-fold difference in signal intensity between cranial (neck) images and caudal (mediastinal) images (Supplemental Figure 2). This was due to the signal variation from the receiver coil because the distance between the receiver coil and the body was greater in the cervical region than the mediastinum. However, the BAT_{retro} to WAT_{retro} signal ratio remained constant with slice position (Supplemental Figure 3). There was variation in the BAT_{retro} to WAT_{retro} signal ratio according to the anatomical region (Table 1 and Supplemental Figure 4), with a significantly lower signal ratio ($P < .0001$, one way ANOVA) within the mediastinum and neck (ie, lower BAT signal with respect to WAT) than in the supraclavic-

Table 1. For Each Anatomical Region, the Number of BAT_{retro} ROIs With Low and Normal Signal Intensity on MR, the Variation in BAT_{retro} and WAT_{retro} MR Signal Intensity, and BAT-WAT Signal Ratio Are Tabulated

Anatomical Regions	BAT _{retro} ROIs With Lower MR Signal Than Adjacent Fat, n	BAT _{retro} ROIs With Similar MR Signal to Adjacent Fat, n	Total ROI, n	Mean BAT _{retro} MR Signal	Mean WAT _{retro} MR Signal	Significance	Signal BAT to WAT Ratio
All regions	93	18	111	485 (± 229)	549 (± 260)	$P < .0001$	0.89 \pm 0.12
Mediastinum	25	0	25	586 (± 145)	750 (± 197)	$P < .0001$	0.79 \pm 0.11
Supraclavicular	31	10	41	541 (± 68)	594 (± 90)	$P < .0001$	0.92 \pm 0.12
Neck	29	2	31	196 (± 116)	219 (± 125)	$P < .0001$	0.89 \pm 0.09
Axillae	8	6	14	783 (± 189)	788 (± 184)	$P = .76$	0.99 \pm 0.08

The BAT_{retro} ROIs were retrospectively drawn on MR from areas of corresponding high ^{18}F -FDG uptake on the PET-CT images.

ular fossae and axillae. The repeat IDEAL MR scan (Supplemental Figure 5) demonstrated little change in the distribution of low signal regions (Supplemental Figure 1B).

Prospective image analyses

Fifty-four ROIs were prospectively identified on un-mapped MR by two investigators (T.A.J. and O.A.) on the basis of having discrete areas of low signal intensity with respect to adjacent adipose tissue and were presumed to represent BAT (BAT_{prosp}). The total cumulative surface area of these BAT_{prosp} ROIs was 6207 mm², compared with 5661 mm² in the mediastinum and supraclavicular fossae in BAT_{retro} ROIs (the majority of ROIs occurring within centrally located regions due to favorable signal to noise ratio). The surface area of 54 BAT_{prosp} ROIs comprised 2.4% of the total surface area of adipose tissue examined (257,181 mm²). Comparison between BAT_{prosp} ROIs and PET-CT scans showed that 47 of 54 ROIs (87%) coincided with areas of ¹⁸F-FDG uptake. Cohen's kappa coefficient of interrater agreement was 0.61.

Histology and immunohistochemistry

Hematoxylin-eosin staining of the fat tissue obtained from the suprasternal area (white arrowhead, Figure 1B) demonstrated smaller multilocular cells with multiple small lipid droplets (yellow arrowhead, Figure 1C), consistent with BAT in contrast to larger unilocular droplets in WAT (white arrowhead, Figure 1C) (8). BAT was unequivocally confirmed on immunostaining with antiserum against rabbit UCP1 (Figure 1D), a unique marker for BAT (13). Although the fat sample was collected prior to imaging, there was morphological and immunohistochemical correlation between the suprasternal ROIs corresponding to BAT in PET and MR images, confirming the presence of BAT.

Discussion

We report the first proof of concept of MR in the identification of BAT in a living human adult, with immunohistochemical and histological confirmation. Using MR, we demonstrated unequivocal differences in signal intensities between BAT and adjacent WAT.

BAT was identified using MR in mice (14, 15) and in human postmortem studies (16), including a 3-month-old infant [with lower fat fraction for BAT (41.9% ± 6.25%) vs WAT (>90%)] (17). Presumed BAT was identified in a premature 13-day-old live neonate based on MR (18). In contrast to previous studies though, we demonstrate the first conclusive identification of BAT using MR in a living human adult.

We show data on one human adult, and future studies should validate this technique, including obese adults. Although retrospective and prospective analyses were separated by 4 months, there may have still been some recall bias, and this could be better controlled for in subsequent validations. The anatomical variation in MR signal results from differences in signal to noise ratio between centrally and more laterally located tissues. Furthermore, small areas of BAT (such as in paravertebral regions) were difficult to identify. These factors may limit the usefulness of MR as an accurate quantifier of BAT in human adults. Finally, we had immunohistochemistry from only one sample. Future validations should assess multiple samples of BAT and WAT.

It seems unlikely that MR signals from adipose tissue are abnormal in hyperparathyroidism-jaw tumor syndrome because immunohistochemistry showed characteristic features of BAT (3). Furthermore, although (minimally invasive) surgery preceded the imaging, we believe that this is unlikely to have affected the MR signal from this region, given that there was little surgical damage to tissues, and the appearance and signal from BAT in this region was similar to that in other centrally located BAT areas. The potential bias from transposing areas of ¹⁸F-FDG uptake on PET-CT onto MR images was limited by scans being performed with the patient adopting a similar position (arms down) as per standard protocols.

In summary, we provide proof of concept of an MR-based novel method for demonstrating BAT with clear delineation from adjacent WAT, in a living human adult. Future studies should focus on developing and validating IDEAL MR imaging as a clinical and research tool, including obese adults, for use in future assessments and quantification of human BAT.

Acknowledgments

We acknowledge Sean James (Department of Histopathology, University Hospitals of Coventry and Warwickshire) for the assistance in immunohistochemical staining of the adipose tissue sample. We also acknowledge the patient who consented for inclusion and contributed towards the data presented in this manuscript. We thank the University Hospitals of Coventry and Warwickshire MR radiographers, in particular Eddie Ngandwe, for the assistance with the study. We also thank MIRADA Medical Ltd (Oxford) for assistance with the Mirada XD 4.3 software. We acknowledge the UK Meteorological Office for providing meteorological data.

All authors contributed toward this manuscript.

Address all correspondence and requests for reprints to: Dr Thomas M. Barber, Clinical Sciences Research Laboratories, Department of Metabolic and Vascular Health, University of

Warwick, University Hospitals of Coventry and Warwickshire, Clifford Bridge Road, Coventry CV2 2DX, United Kingdom. E-mail: t.barber@warwick.ac.uk.

This work was supported by a Strategic Impact Fund grant from the University of Warwick.

Disclosure Summary: The authors have nothing to declare, and there is no duality of interest.

References

1. Cypess AM, Lehman S, Williams G, et al. Identification and importance of brown adipose tissue in adult humans. *N Engl J Med*. 2009;360:1509–1517.
2. Rothwell NJ, Stock MJ. A role for brown adipose tissue in diet-induced thermogenesis. *Nature*. 1979;281:31–35.
3. Virtanen KA, Lidell ME, Orava J, et al. Functional brown adipose tissue in healthy adults. *N Engl J Med*. 2009;360:1518–1525.
4. Yoneshiro T, Aita S, Matsushita M, et al. Brown adipose tissue, whole-body energy expenditure, and thermogenesis in healthy adult men. *Obesity (Silver Spring)*. 2011;19:13–16.
5. Muzik O, Mangner TJ, Granneman JG. Assessment of oxidative metabolism in brown fat using PET imaging. *Front Endocrinol (Lausanne)*. 2012;3:15.
6. Cooney GJ, Caterson ID, Newsholme EA. The effect of insulin and noradrenaline on the uptake of 2-[1-¹⁴C]deoxyglucose in vivo by brown adipose tissue and other glucose-utilising tissues of the mouse. *FEBS Lett*. 1985;188:257–261.
7. Bartelt A, Bruns OT, Reimer R, et al. Brown adipose tissue activity controls triglyceride clearance. *Nat Med*. 2011;17:200–205.
8. Cinti S. Anatomy of the adipose organ. *Eat Weight Disord*. 2000;5:132–142.
9. Hu HH, Smith DL Jr, Nayak KS, Goran MI, Nagy TR. Identification of brown adipose tissue in mice with fat-water IDEAL-MRI. *J Magn Reson Imaging*. 2010;31:1195–1202.
10. Carpten JD, Robbins CM, Villablanca A, et al. HRPT2, encoding parafibromin, is mutated in hyperparathyroidism-jaw tumor syndrome. *Nat Genet*. 2002;32:676–680.
11. Reeder SB, Wen Z, Yu H, et al. Multicoil Dixon chemical species separation with an iterative least-squares estimation method. *Magn Reson Med*. 2004;51:35–45.
12. Reeder SB, Pineda AR, Wen Z, et al. Iterative decomposition of water and fat with echo asymmetry and least-squares estimation (IDEAL): application with fast spin-echo imaging. *Magn Reson Med*. 2005;54:636–644.
13. Bouillaud F, Ricquier D, Mory G, Thibault J. Increased level of mRNA for the uncoupling protein in brown adipose tissue of rats during thermogenesis induced by cold exposure or norepinephrine infusion. *J Biol Chem*. 1984;259:11583–11586.
14. Hu HH, Hines CD, Smith DL Jr, Reeder SB. Variations in T(2)* and fat content of murine brown and white adipose tissues by chemical-shift MRI. *Magn Reson Imaging*. 2012;30:323–329.
15. Sbarbati A, Guerrini U, Marzola P, Asperio R, Osculati F. Chemical shift imaging at 4.7 tesla of brown adipose tissue. *J Lipid Res*. 1997;38:343–347.
16. Heaton GM, Wagenvoort RJ, Kemp A Jr, Nicholls DG. Brown-adipose-tissue mitochondria: photoaffinity labelling of the regulatory site of energy dissipation. *Eur J Biochem*. 1978;82:515–521.
17. Hu HH, Tovar JP, Pavlova Z, Smith ML, Gilsanz V. Unequivocal identification of brown adipose tissue in a human infant. *J Magn Reson Imaging*. 2012;35:938–942.
18. Carter BW, Schucany WG. Brown adipose tissue in a newborn. *Proc (Bayl Univ Med Cent)*. 2008;21:328–330.



Renew your Society membership by Dec. 31
to maintain access to your Society member benefits.

www.endocrine.org/renew



ORIGINAL ARTICLE

Enhanced thermic effect of food, postprandial NEFA suppression and raised adiponectin in obese women who eat slowly

Narendra L. Reddy^{*†}, Chenjing Peng[†], Marcos C. Carreira[‡], Louise Haldert[†], John Hattersley[†], Milan K. Piya^{*†}, Gyanendra Tripathi^{*}, Harpal S. Randeva^{*†}, Felipe F. Casanueva^{‡§}, Philip G. McTernan^{*}, Sudhesh Kumar^{*†} and Thomas M. Barber^{*†}

^{*}Division of Translational and Systems Medicine, Warwick Medical School, The University of Warwick, Clinical Sciences Research Laboratories, University Hospitals Coventry and Warwickshire, [†]Warwickshire Institute for the Study of Diabetes, Endocrinology and Metabolism, University Hospitals Coventry and Warwickshire, Coventry, UK, [‡]CIBER Fisiopatología Obesidad y Nutrición (CB06/03), Instituto de Salud Carlos III (ISCIII), and [§]Department of Medicine, Santiago de Compostela University, Complejo Hospitalario Universitario de Santiago (CHUS), Santiago de Compostela, Spain

Summary

Objective Meal duration may influence cardiometabolic health. The aim of this study was to explore postprandial effects of meal duration on human metabolism and appetite.

Design Postprandial comparisons following a standard meal eaten slowly over 40 min ('D40') and the same meal eaten quickly over 10 min ('D10') on a different day. Each participant therefore acted as their own control, thereby limiting confounding factors.

Patients Obese premenopausal Caucasian women ($n = 10$) with confirmed normoglycaemia were recruited from an obesity clinic at UHCW, Coventry UK. Subjects underwent whole-body calorimetry (8-h) on two separate days.

Measurements Following standard lunch (D40 vs D10), 4-h postprandial analysis included thermic effect of food (TEF) and bloods taken at predefined times (including baseline fasting). Analytes included lipid profile, adiponectin, insulin, glucose, ghrelin, leptin, endotoxin, gut and pancreatic hormones. Appetite was measured using visual-analogue scales and *ad libitum* food intake at subsequent meal. Paired sample *t*-tests [including area under the curve (AUC)] were used to compare D40 and D10 trials.

Results Postprandial TEF (over 240-min) was significantly greater for D40 than D10 [mean (SEM): 80.9 kcal (3.8) vs 29.9 kcal (3.4); 10.6% vs 3.9%, respectively, $P = 0.006$; AUC 71.7 kcal.h vs 22.4 kcal.h, respectively, $P = 0.02$]. Postprandial plasma NEFA was significantly lower, and adiponectin levels were significantly higher for D40 than D10 [AUC (SEM): NEFA 627 $\mu\text{mol.h/l}$ (56) vs 769 $\mu\text{mol.h/l}$ (60), respectively, $P = 0.02$; adiponectin 33.4 $\mu\text{g.h/ml}$ (3.9) vs 27.3 $\mu\text{g.h/ml}$ (3.8), respec-

tively, $P = 0.04$]. Other postprandial analytes and appetite measures were equivalent.

Conclusions In obese women, eating slowly associates with enhanced TEF, elevated serum adiponectin and suppressed NEFA.

(Received 13 September 2014; returned for revision 12 October 2014; finally revised 23 October 2014; accepted 31 October 2014)

Introduction

The global obesity epidemic shows no signs of abating.¹ Obesity and its associated problems including type 2 diabetes mellitus (T2D) constitute the biggest threat to global health and healthcare economies.² Novel strategies implemented in multifaceted ways are required: development of novel pharmacological therapies; redesign of our obesogenic living spaces; policies to improve our diet particularly for our children; and cultural change.

Diet, a major determinant of fat mass, is an obvious target for obesity prevention and management.³ Although macronutrient composition⁴ and food viscosity⁵ are important considerations, other eating-related behaviours such as meal duration merit investigation. Faster eating has been shown to associate with increased energy intake during single meals,^{6–8} and higher BMI,^{9–11} thereby potentially influencing body weight. Although meal duration may influence metabolism and appetite (and therefore body weight) via effects on adipokines and gut and pancreatic neuro-endocrine signals,¹² this remains speculative.^{10,11,13,14}

A clear understanding of how meal duration influences human metabolism [including thermic effect of food (TEF)] and appetite would provide invaluable insight into obesity pathogenesis and potential strategies for prevention and management of obesity through modification of eating-related behaviour. We define TEF as overall energy expenditure in the 4-h postprandial period following a meal, incorporating obligatory energy requirements of food digestion, absorption, metabolism and storage, and facultatively,

Correspondence: Thomas M Barber, Division of Translational and Systems Medicine, Warwick Medical School, The University of Warwick, Clinical Sciences Research Laboratories, University Hospitals Coventry and Warwickshire, Clifford Bridge Road, Coventry, CV2 2DX, UK. Tel.: 02476 28591; Fax: 02476 968653; E-mail: t.barber@warwick.ac.uk

tive energy expenditure (EE), mediated at least in part by the sympathetic nervous system.⁴ The aim of this study was to explore in obese, normoglycaemic women the postprandial effects of meal duration on metabolism [including TEF and excursions of glucose, insulin, endotoxin and nonesterified fatty acids (NEFA)] and appetite (including excursions of appetite-related hormones such as ghrelin).

Methods and procedures

Subjects

All subjects ($n = 10$) were recruited from the Obesity clinic at the Warwickshire Institute for the Study of Diabetes, Endocrinology and Metabolism (WISDEM) centre at the University Hospitals Coventry and Warwickshire (UHCW). All subjects were obese ($\text{BMI} > 30 \text{ kg/m}^2$) premenopausal (based on menstrual history and absence of clinical features suggestive of peri- or postmenopausal status), white, Caucasian women, with normoglycaemia (based on fasting and postprandial plasma glucose measurements, and no past history of dysglycaemia). All subjects were nonsmokers, and none had any other medical problems including weight-related conditions such as polycystic ovary syndrome, Cushing's syndrome, obstructive sleep apnoea or other adverse metabolic sequelae. Exclusion criteria included prior bariatric surgery, weight-loss medication or actual weight-loss of $>2.5 \text{ kg}$ up to 3 months prior to recruitment. All subjects had received standard lifestyle advice from a specialist dietician prior to inclusion in the study as part of their clinical care. All clinical investigations were conducted in accordance with the guidelines in the Declaration of Helsinki. All subjects provided fully informed written consent, and a local Research Ethics Committee in the United Kingdom approved the study.

Anthropometry, calorimetry and meal duration

Following informed consent, each subject was invited to undergo metabolic studies on two separate days at the Human Metabolism Research Unit (HMRU), a University of Warwick and UHCW NHS Trust facility. HMRU houses two whole-body calorimeters (WBCs) ($2 \text{ m} \times 3 \text{ m} \times 2.5 \text{ m}$), each hermetically sealed to the outside environment and replicating free-living environments. Double-doored hatches allow food to be delivered into and waste out of each WBC. Accurate minute-by-minute measurements of CO_2 and O_2 from air entering and leaving the WBCs enable EE (including TEF) to be calculated in real time using Weir's formula: $\text{EE (kcal)} = [3.941 \times \text{O}_2 \text{ consumed (L)}] + [1.106 \times \text{CO}_2 \text{ produced (L)}]$.¹⁵ Thermoneutral temperature ($24 \text{ }^\circ\text{C}$) and relative humidity (57%) were kept constant.

The two WBC metabolic studies were executed within 2 weeks of each other. Subjects were instructed to avoid caffeine ingestion and strenuous physical activity for 24-h preceding each visit, and to adhere to their normal diet and physical activity schedules. Subjects were fasted for 12 h prior to commencement of each metabolic study. On each study day morning, the subject arrived at HMRU in a fasted state. Prior to metabolic studies,

waist circumference, BMI and body composition (body fat mass and fat percentage) was measured, the latter with a BodPod using air displacement plethysmography (Cosmed Inc, USA).¹⁶ Baseline fasting blood tests were taken. Subjects then entered WBC at 0900 h and lay still on the bed for 120 min, to allow for equilibration and estimation of resting EE. During postprandial periods, subjects had minimal activity or ambulation.

For each study day, standard lunch was provided at 1200 h. The same standardized lunch (designed and prepared by a specialist weight-management dietician) was served for all the metabolic studies. The standard lunch (ham sandwich, yoghurt, banana, biscuit and orange juice drink) contained a total of 763 kcal; 50% carbohydrate, 18% protein and 32% fat. On their first metabolic assessment day, each subject was served standard lunch, with caloric content of the meal divided equally into eight separate food boxes, the food contents of each box eaten over 5 min for a total meal duration of 40 min (the lunch being completed by 1240 h). This trial is referred to as 'D40'. For the second metabolic assessment (on a different day), an identical protocol was followed except that the duration of the standard lunch was 10 min rather than 40 min. For this assessment, the caloric content of the standard meal was divided into two halves, with the food contents of each box being eaten over 5 min for a total meal duration of 10 min (the lunch being completed by 1210 h). This trial is referred to as 'D10'. Subjects were provided with timers and were monitored by study investigators to ensure compliance with eating rate. Subjects were instructed to vary chewing speed accordingly.

Postprandial phase

During the 4-h postprandial phase, subjects were requested to remain seated in the WBC with minimal activity and to refrain from ingestion of food or drink. Blood tests were taken at predefined time-points (at baseline, 30-, 60-, 90-, 120-, 180- and 240-min intervals). The timing of the postprandial blood tests was determined by the *end-point* of the standard meal (to avoid taking any bloods during the D40 meal), that is time '0' was defined by the *end* of the meal for D40 at 1240 h and for D10 at 1210 h. Blood was taken from an arm placed through a hatch of the WBC, a plastic cover used to avoid any air exchange with the WBC. All samples were spun in a centrifuge immediately, and serum samples frozen at $-80 \text{ }^\circ\text{C}$. Appetite was assessed just prior to each blood test through use of visual analogue scale (VAS). At 1700 h, subjects were invited to leave the WBC and offered an *ad libitum* standard buffet meal, consisting of cold foods (sandwiches, chocolate bars, fruit, sausage rolls and drinks). The caloric content and macronutrient composition of the *ad libitum* food ingested was calculated. TEF was calculated using validated methods reported in literature, and also expressed in percentage of energy intake [(Postprandial EE - Baseline EE)/Amount of calories ingested].¹⁷

Biochemical evaluation

Fasting baseline serum samples were analysed for lipid profile (total cholesterol, LDL cholesterol, HDL cholesterol and triglyce-

rides), HbA1C, glucose, 0900 h cortisol, insulin-like growth factor 1 (IGF1), thyroid-stimulating hormone (TSH), free T4, testosterone, sex hormone-binding globulin (SHBG) and 25-hydroxycholecalciferol. Postprandial and prelunch blood samples (D40 and D10) were analysed for ghrelin, leptin, PYY, GLP-1, adiponectin, cortisol, insulin, glucose, total cholesterol, LDL cholesterol, HDL cholesterol, triglycerides, endotoxin and NEFA. 4-(2-aminoethyl)-benzenesulfonylfluoride hydrochloride (Pefabloc SC) and dipeptidyl peptidase-IV inhibitor were added to chilled EDTA tubes for measurements of pancreatic and gut hormones. Serum insulin was measured with a chemiluminescent assay (DPC immulite 2500 machine), and plasma glucose with a hexokinase assay (ADVIA 2400 analyser). Serum testosterone and SHBG were measured with chemiluminescent assays (Immulite 2000 analyser). Serum ghrelin (total) was measured with a radioimmunoassay (LINCO Research, St. Charles, MO, USA) with lower limit of detection 100 pg/ml. (intra-assay coefficient of variation for all assays used <7%). Serum endotoxin was analysed using a commercially available QCL-1000 LAL Endpoint Assay (Lonza Inc., Allendale, NJ, USA) and validated as previously described.¹⁸

Statistical analyses and power calculations

Statistical analyses were conducted in SPSS (version 21 Windows; SPSS Inc., Chicago, IL, USA) and Microsoft Excel. Paired sample *t*-tests were used for comparisons of 4-h postprandial 'area under the curve' (AUC) metabolic and biochemical data between D40 and D10. Each subject acted as their own control thereby limiting confounding. We had >80% power to detect a between meal duration difference exceeding 50% of a standard deviation (SD) for plasma glucose from D40 to D10 ($\alpha = 0.05$). A *P*-value < 0.05 was considered significant. Data are shown as mean and SEM unless otherwise stated. AUC was calculated using the validated trapezoid method in Excel.

Results

Baseline anthropometric, clinical and biochemical data

Baseline anthropometric, clinical and fasting biochemical data are shown in Table 1. Mean age was 41.8 years (SD 6.7). Mean BMI was 42.1 kg/m² (SD 4.6). Mean body fat percentage was 50.7% (SD 7.4). By definition, all subjects had normal fasting glucose and HbA1C and were biochemically euthyroid and normoandrogenaemic.

Postprandial biochemical data

Postprandial biochemical data are shown in Table 2. For each analyte, AUC (SEM) data from the 4-h postprandial period are shown. Plasma NEFA in the postprandial period was significantly lower for D40 than D10 [AUC (SEM): NEFA 627 $\mu\text{mol.h/l}$ (56) vs 769 $\mu\text{mol.h/l}$ (60), respectively, *P* = 0.02]. Postprandial adiponectin was significantly higher for D40 than D10 [Adiponectin AUC (SEM) 33.4 $\mu\text{g.h/ml}$ (3.9) vs 27.3 $\mu\text{g.h/ml}$

Table 1. Baseline anthropometric, clinical and biochemical (fasting) data for subjects (*n* = 10) taken prior to entry into WBC at first metabolic study

Variable	Mean	SD
Age (years)	41.8	6.7
Weight (kg)	116.5	16.2
BMI (kg/m ²)	42.1	4.6
Waist circumference (m)	1.20	0.09
Hip circumference (m)	1.35	0.13
Waist: hip ratio	0.90	0.1
Fat mass (kg)	59.5	14.5
Lean mass (kg)	57.0	8.7
Fat %	50.7	7.4
Glucose (mmol/l)	4.7	0.6
Total Cholesterol (mmol/l)	5.0	0.9
LDL Cholesterol (mmol/l)	3.2	0.8
HDL Cholesterol (mmol/l)	1.3	0.1
Triglycerides (mmol/l)	1.2	0.3
Haemoglobin A1C (%)	5.6	0.3
9am Cortisol (nmol/l)	356	165
IGF1 (ng/ml)	20.7	5.8
TSH (mIU/l)	2.4	1.1
Free T4 (pmol/l)	15.2	1.6
Testosterone (nmol/l)	0.8	0.6
SHBG (nmol/l)	54.4	31.5
25-hydroxycholecalciferol (nmol/l)	36	18

BMI, body mass index; kg, kilogram; SHBG, sex hormone-binding globulin; TSH, thyroid-stimulating hormone; IGF1, insulin-like growth factor-1; HDL, high-density lipoprotein; LDL, low-density lipoprotein; SD, standard deviation.

To convert glucose mmol/l to mg/dl, divide by 0.0555; to convert triglyceride mmol/l to mg/dl, divide by 0.0113; to convert cholesterol mmol/l to mg/dl, divide by 0.0259; to convert cortisol nmol/l to microgram/dl, divide by 27.59; to convert testosterone nmol/l to ng/dl, divide by 0.0347; to convert 25-hydroxycholecalciferol nmol/l to ng/ml, divide by 2.496; to convert SHBG nmol/l to $\mu\text{g/ml}$, divide by 8.896; to convert IGF1 nmol/l to ng/ml, divide by 0.131; to convert free T4 pmol/l to ng/dl, divide by 12.871.

(3.8), respectively, *P* = 0.04]. Postprandial insulin, ghrelin and glucose levels (and all other analytes) were statistically equivalent between D40 and D10 (Table 2).

TEF

TEF was significantly greater in D40 than D10 [TEF mean over 240-min postprandial period (SEM): 80.9 kcal (3.8) vs 29.9 kcal (3.4), respectively, *P* = 0.006, Table 3; TEF AUC 71.7 kcal.h vs 22.4 kcal.h, respectively, *P* = 0.02, Fig. 1]. As a proportion of energy intake during the meal, TEF was significantly greater in D40 than D10 (10.6% vs 3.9%, respectively, *P* = 0.006).

Postprandial appetite (Visual Analogue Scale and ad libitum evening buffet)

Postprandial data on appetite (VAS) and evening buffet consumption are shown in Table 3. Appetite was greatest premeal and was most suppressed in the early postprandial phase

Table 2. Postprandial biochemical data of study subjects following each standard meal (D10 vs D40) ($n = 10$)

Analyte	D40 AUC (SEM)	D10 AUC (SEM)	D40 Mean (SEM)	D10 Mean (SEM)
Glucose (mmol/l)	23.8 (0.7)	25.2 (0.9)	6.0 (0.4)	6.4 (0.3)
Insulin (pmol/l)	2416 (301)	2853 (537)	615 (143)	693 (130)
NEFA (μ mol/l)	627* (56)	769* (60)	191* (50)	242* (69)
Ghrelin (pg/ml)	305 (77)	226 (43)	78* (5.3)	54* (5.7)
Leptin (η g/ml)	74 291 (15 718)	69 645 (19 352)	17 837 (1194)	17 154 (693)
GLP1 (pg/ml)	274 (29)	292 (34)	67 (3.3)	72 (3.2)
PYY (pg/ml)	503 (34)	535 (37)	127 (6.4)	132 (6.2)
Adiponectin (μ g/ml)	33.4* (3.9)	27.3* (3.8)	8.4 (1.3)	6.9 (0.4)
Cortisol (η mol/l)	1575 (93)	1424 (241)	438 (64)	387 (45)
Total Cholesterol (mmol/l)	18.8 (1.1)	18.9 (0.8)	4.7 (0.01)	4.7 (0.03)
LDL Cholesterol (mmol/l)	11.8 (1.0)	12.0 (0.8)	3.0 (0.02)	3.0 (0.04)
HDL Cholesterol (mmol/l)	4.1 (0.2)	4.1 (0.1)	1.03 (0.01)	1.03 (0.01)
Triglycerides (mmol/l)	5.7 (1.3)	5.7 (1.3)	1.4 (0.06)	1.4 (0.05)
Endotoxin (EU/ml)	23.2 (3.5)	23.4 (3.5)	5.9 (0.4)	6.0 (0.4)

*Significant difference ($P < 0.05$) between D10 and D40 values.

AUC, area under the curve; HDL cholesterol, high-density lipoprotein cholesterol; LDL cholesterol, low-density lipoprotein cholesterol; NEFA, nonesterified fatty acids; GLP1, glucagon-like peptide 1; PYY, peptide YY; For the AUC data, the units are multiplied by time (hours). To convert insulin from pmol/l to μ IU/ml divide by 7.175.

To convert glucose mmol/l to mg/dl, divide by 0.0555; to convert triglyceride mmol/l to mg/dl, divide by 0.0113.

To convert cholesterol mmol/l to mg/dl, divide by 0.0259; to convert cortisol η mol/l to μ g/dl, divide by 27.59.

Table 3. Data showing measures of appetite (visual analogue scales) in the postprandial phase, consumption of *ad libitum* evening meal data and energy expenditure in the postprandial phase ($n = 10$)

	D40 Mean (SD)	D10 Mean (SD)
Premeal (SL) appetite VAS	7.5 (2.6)	7.4 (2.4)
Early postprandial appetite VAS (0–90 mins)	1.6 (1.1)	1.7 (0.9)
Late postprandial appetite VAS (120–240 mins)	3.2 (2.2)	3.3 (2.1)
Postbuffet VAS	2.6 (3.0)	4.1 (3.1)
Buffet total calories ingested (kcal)	482 (274)	448 (243)
Buffet total protein ingested (g)	24 (7.6)	21 (9.0)
Buffet total CHO ingested (g)	45 (29.6)	41 (24.1)
Buffet total fat ingested (g)	23 (17.6)	23 (16.4)
Resting metabolic rate (kcal/h)	37.4 (2.5)	38.6 (3.7)
Total TEF for 240 min (kcal)	80.9* (3.8)	29.9* (3.4)

*significant difference ($P < 0.05$) between D10 and D40 values.

SL, standard lunch; VAS, visual analogue scale (0 = no hunger and fully satiated; 10 = extremely hungry); g, grams; CHO, carbohydrate; kcal, kilocalories; mins, minutes; SD, standard deviation; D10, data for the 10-min standard lunch study; D40, data for the 40-min standard lunch study; EE, energy expenditure; TEF, thermic effect of food.

(0–90 min). Comparisons between appetite VAS for D40 and D10 were equivalent throughout (Table 3). For the early evening *ad libitum* buffet following the standard lunch, total calories ingested and macroconstituent food fractions for D40 and D10 were equivalent [mean (SD) total calories ingested 482Kcal (274) vs 448 kcal (243), respectively, $P = NS$].

Discussion

We demonstrate objectively that duration of a standard meal influences TEF, postprandial NEFA suppression and adiponectin levels in obese women. To our knowledge, our study is the first to report on effects of meal duration in the free-living environment of a WBC.

Given beneficial metabolic effects of adiponectin,¹⁹ eating slowly may improve insulin sensitivity through adiponectin effects, although this remains speculative. This hypothesis is, however, consistent with evidence from the literature that shows acute effects of changes in adiponectin levels on insulin sensitivity (through effects on AMP kinase, GLUT4 transporters, fatty acid oxidation and gluconeogenesis).²⁰ The differences in NEFA suppression between the D40 and D10 trials may be explained, at least in part by differences in adiponectin, mediated via possible effects on insulin sensitivity and peripheral lipoprotein lipase activity.²¹ We hypothesize that the relatively higher levels of adiponectin for D40 compared with D10 may facilitate enhanced action of insulin on NEFA suppression through enhanced peripheral lipoprotein lipase activity; this may be an explanation

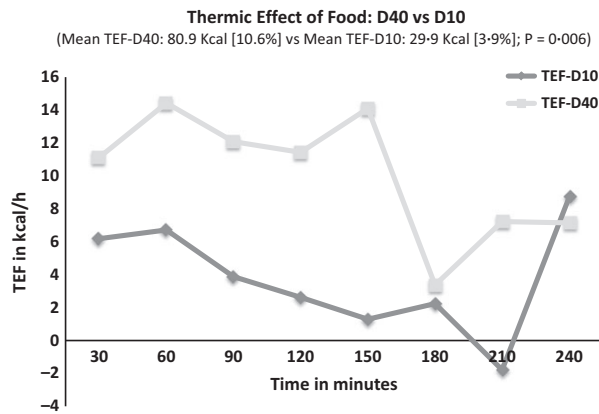


Fig. 1 Time course of thermic effect of food (TEF) calculated for the two trials D40 and D10 during postprandial phase (240-min).

for differences in NEFA suppression between D40 and D10 despite equivalent postprandial insulin levels. Speculatively, improved postprandial NEFA suppression associated with eating slowly may, over time result in improved ectopic fat deposition. Consistent with this hypothesis is a report of an association between short meal duration and T2D.²² The equivalence of endotoxin data (a biomarker for metabolic inflammation) between trials may simply be a reflection that although subjects were obese, they were also young and healthy. Also, the standard meal was balanced with avoidance of a high fat or high carbohydrate load that would usually be required to provoke an endotoxin response.²³

Ingestion of food results in increased oxygen consumption and body temperature primarily from digestive processes accounting for TEF.²⁴ Between D40 and D10 trials, a mean difference in TEF of 51Kcal per 763Kcal standard lunchtime meal was observed during the 4-h postprandial period. Assuming that a similar standard lunch with equivalent caloric and macronutrient content were ingested each day over an entire year, the extrapolated difference in TEF between eating this meal each day slowly over 40 min *vs* quickly over 10 min would be in excess of 18 600 kcal. Assuming that 3500 kcal is equivalent to 395 g of fat,²⁵ this energy difference equates to a difference in body weight of 2.1 kg/year.

Our data are consistent with objective data from Hamada and colleagues that demonstrated correlation between meal duration and postprandial energy expenditure in healthy normal-weight subjects.²⁶ It was hypothesized that number of chews and splanchnic blood flow (both of which correlated with meal duration) may have contributed towards observed differences in postprandial expenditure.²⁶ Most other reported studies on meal duration have relied upon *subjective* self-reported measures of eating behaviours in cross-sectional designs. In one study on young people, the validity of a self-questionnaire about eating rate was supported, with self-reports being related to objective measurements of number of chews and duration of chewing.²⁷ Using subjective measures of eating behaviours, speed of eating and BMI have been reported to be positively correlated in some

studies.^{10,11,13} In one of the largest studies to date on a Japanese cohort ($n = 7275$), prevalence of obesity, blood pressure, lipid levels and glycaemic control all correlated with self-reported speed of eating.²⁸ Whilst it is tempting to speculate that slow-eaters have favourable body weight through beneficial effects on TEF, this remains speculative and causality cannot be inferred from the observational studies outlined here.

The effects of slow eating rate on food intake and appetite are incompletely understood. Data are conflicting, with one study reporting that eating slowly (with long meal duration) associates with *increased* food ingestion²⁹ (possibly resulting from prolonged elevation of postprandial plasma ghrelin levels³⁰), and another showing *anorexic* effects of eating slowly.³¹ In one study by Scisco and colleagues, implementation of a slow eating rate through use of a 'bite-rate counter' device was shown to *reduce* caloric intake.³² Conversely, in a study on subjects with Prader-Willi syndrome, a *faster* rate of eating was more effective than slow eating at stimulating anorexigenic gut peptides (including PYY release) and promoting satiety, a pattern that was not evident in age-matched subjects with simple obesity.³³

We showed no differences in appetite or *ad libitum* meal ingestion in relation to speed of eating a standard meal. One explanation is that all subjects in our study were obese women with similar postprandial profiles of ghrelin, PYY and GLP1 between meal duration trials. PYY and ghrelin response to food was shown in one study to be blunted in obese female adolescents.³⁴ Our data are in contrast to those from another study that showed *elevations* of PYY and GLP1 in response to eating slowly.³¹ The differences in anorexigenic gut peptide response to speed of food ingestion between our study and other reports in the literature may be due to differences in inclusion criteria between studies: we only studied obese women who were also healthy, despite >50% body fat, representing a unique metabolic scenario.

Our study is limited by a relatively small number of subjects, therefore with potential for type 1 errors in the analyses for the exploratory outcome measures of adiponectin and NEFA, with AUC differences for these measures that were just significant between meal duration trials. However, the number of subjects included in our study was comparable to that of other reported studies in this field. Although our sample size was calculated from *a priori* calculations based on changes in postprandial plasma glucose levels, we showed no differences in postprandial glucose levels between the meal duration trials. We speculate this may be due to the inclusion of *healthy* obese subjects, and the relative sensitivities of glucose (compared with NEFA) to the effects of insulin and adiponectin in the postprandial phase. A further limitation of our study is the potential for phase of menstrual cycle to have influenced TEF, demonstrated previously in lean women.³⁵ The design of our study precluded any assessment of delayed metabolic and appetitive effects beyond the initial 4-h postprandial phase. We only included healthy obese women. Future studies should include men, and subjects with a range of BMI to explore the effects of meal duration in men *vs* women and lean *vs* obese subjects. A further limitation of our study was the lack of randomization to the order of the D40 and D10 trials. Finally, our measurement of expenditure was

based on TEF, which reflects energy expenditure required to digest food.²⁴ Although the D40 group spent longer engaging in eating activity for the standard meal, it is important to emphasize that for both trials (D40 and D10), subjects consumed exactly the same food (total calories and macronutrient content), and the postprandial period for each trial started once the activity of eating had stopped, to avoid any confounding from eating activity. During postprandial phases, subjects remained inactive.

To summarize, we have shown preliminary evidence that duration of a standard meal influences TEF, postprandial NEFA suppression and adiponectin levels in obese women. Eating a meal slowly appears to confer beneficial metabolic effects in terms of energy expenditure, metabolic profile and lipid handling. Future studies are required to validate our findings, including prospective studies that focus on how these demonstrable acute postprandial effects of meal duration translate into longer term cardiometabolic effects, including body weight, ectopic fat deposition and future development of T2D.

Acknowledgements

The authors wish to acknowledge Alison Campbell, HMRU Research Nurse, UHCW, for significant technical contribution to the experiments. The authors wish to acknowledge all the subjects who took part in this study.

Competing interests/financial disclosure

The authors have nothing to declare.

Author contributions

N. L. R and T. M. B have made primary contributions in study design conception, data collection, analyses and manuscript preparation. All authors were involved with drafting the article or revising it critically for important intellectual content, and all authors had final approval of the submitted and published versions.

References

- Danaei, G., Finucane, M.M., Lu, Y. *et al.* (2011) National, regional, and global trends in fasting plasma glucose and diabetes prevalence since 1980: systematic analysis of health examination surveys and epidemiological studies with 370 country-years and 2.7 million participants. *Lancet*, **378**, 31–40.
- Masters, R.K., Reither, E.N., Powers, D.A. *et al.* (2013) The impact of obesity on US mortality levels: the importance of age and cohort factors in population estimates. *American Journal of Public Health*, **103**, 1895–1901.
- Forget, G., Doyon, M., Lacerte, G. *et al.* (2013) Adoption of American Heart Association 2010 ideal healthy diet recommendations prevents weight gain in young adults. *Journal of the Academy of Nutrition and Dietetics*, **113**, 1517–1522.
- Karhunen, L.J., Juvonen, K.R., Huotari, A. *et al.* (2008) Effect of protein, fat, carbohydrate and fibre on gastrointestinal peptide release in humans. *Regulatory Peptides*, **149**, 70–78.
- Juvonen, K.R., Purhonen, A.K., Salmenkallio-Marttila, M. *et al.* (2009) Viscosity of oat bran-enriched beverages influences gastrointestinal hormonal responses in healthy humans. *Journal of Nutrition*, **139**, 461–466.
- Andrade, A.M., Greene, G.W. & Melanson, K.J. (2008) Eating slowly led to decreases in energy intake within meals in healthy women. *Journal of the American Dietetic Association*, **108**, 1186–1191.
- Martin, C.K., Anton, S.D., Walden, H. *et al.* (2007) Slower eating rate reduces the food intake of men, but not women: implications for behavioral weight control. *Behaviour Research and Therapy*, **45**, 2349–2359.
- Zandian, M., Ioakimidis, I., Bergh, C. *et al.* (2009) Decelerated and linear eaters: effect of eating rate on food intake and satiety. *Physiology & Behavior*, **96**, 270–275.
- Hill, S.W. & McCutcheon, N.B. (1984) Contributions of obesity, gender, hunger, food preference, and body size to bite size, bite speed, and rate of eating. *Appetite*, **5**, 73–83.
- Maruyama, K., Sato, S., Ohira, T. *et al.* (2008) The joint impact on being overweight of self reported behaviours of eating quickly and eating until full: cross sectional survey. *British Medical Journal*, **337**, a2002.
- Otsuka, R., Tamakoshi, K., Yatsuya, H. *et al.* (2006) Eating fast leads to obesity: findings based on self-administered questionnaires among middle-aged Japanese men and women. *Journal of Epidemiology*, **16**, 117–124.
- Wren, A.M. & Bloom, S.R. (2007) Gut hormones and appetite control. *Gastroenterology*, **132**, 2116–2130.
- Tanihara, S., Imatoh, T., Miyazaki, M. *et al.* (2011) Retrospective longitudinal study on the relationship between 8-year weight change and current eating speed. *Appetite*, **57**, 179–183.
- Brindal, E., Wilson, C., Mohr, P. *et al.* (2011) Does meal duration predict amount consumed in lone diners? An evaluation of the time-extension hypothesis. *Appetite*, **57**, 77–79.
- Weir, J.B. (1949) New methods for calculating metabolic rate with special reference to protein metabolism. *Journal of Physiology*, **109**, 1–9.
- Fields, D.A., Goran, M.I. & McCrory, M.A. (2002) Body-composition assessment via air-displacement plethysmography in adults and children: a review. *American Journal of Clinical Nutrition*, **75**, 453–467.
- Ravn, A.M., Gregersen, N.T., Christensen, R. *et al.* (2013) Thermic effect of a meal and appetite in adults: an individual participant data meta-analysis of meal-test trials. *Food & Nutrition Research*, **57**, doi:10.3402/fnr.v57i0.19676.
- Harte, A.L., Varma, M.C., Tripathi, G. *et al.* (2012) High fat intake leads to acute postprandial exposure to circulating endotoxin in type 2 diabetic subjects. *Diabetes Care*, **35**, 375–382.
- Turer, A.T. & Scherer, P.E. (2012) Adiponectin: mechanistic insights and clinical implications. *Diabetologia*, **55**, 2319–2326.
- Fisman, E.Z. & Tenenbaum, A. (2014) Adiponectin: a manifold therapeutic target for metabolic syndrome, diabetes, and coronary disease? *Cardiovascular Diabetology*, **13**, doi:10.1186/1475-2840-13-103.
- Lambert, J.E. & Parks, E.J. (2012) Postprandial metabolism of meal triglyceride in humans. *Biochimica et Biophysica Acta*, **1821**, 721–726.

- 22 Sakurai, M., Nakamura, K., Miura, K. *et al.* (2012) Self-reported speed of eating and 7-year risk of type 2 diabetes mellitus in middle-aged Japanese men. *Metabolism*, **61**, 1566–1571.
- 23 Herieka, M. & Erridge, C. (2014) High-fat meal induced postprandial inflammation. *Molecular Nutrition and Food Research*, **58**, 136–146.
- 24 Westerterp-Plantenga, M.S., Rolland, V., Wilson, S.A. *et al.* (1999) Satiety related to 24 h diet-induced thermogenesis during high protein/carbohydrate vs high fat diets measured in a respiration chamber. *European Journal of Clinical Nutrition*, **53**, 495–502.
- 25 Wishnofsky, M. (1958) Caloric equivalents of gained or lost weight. *American Journal of Clinical Nutrition*, **6**, 542–546.
- 26 Hamada, Y., Kashima, H. & Hayashi, N. (2014) The number of chews and meal duration affect diet-induced thermogenesis and splanchnic circulation. *Obesity*, **22**, E62–E69.
- 27 Ekuni, D., Furuta, M., Takeuchi, N. *et al.* (2012) Self-reports of eating quickly are related to a decreased number of chews until first swallow, total number of chews, and total duration of chewing in young people. *Archives of Oral Biology*, **57**, 981–986.
- 28 Ohkuma, T., Fujii, H., Iwase, M. *et al.* (2013) Impact of eating rate on obesity and cardiovascular risk factors according to glucose tolerance status: the Fukuoka Diabetes Registry and the Hisayama Study. *Diabetologia*, **56**, 70–77.
- 29 Pliner, P., Bell, R., Hirsch, E.S. *et al.* (2006) Meal duration mediates the effect of “social facilitation” on eating in humans. *Appetite*, **46**, 189–198.
- 30 Sobki, S.H., Zaid, A.A., Khan, H.A. *et al.* (2010) Significant impact of pace of eating on serum ghrelin and glucose levels. *Clinical Biochemistry*, **43**, 522–524.
- 31 Kokkinos, A., le Roux, C.W., Alexiadou, K. *et al.* (2010) Eating slowly increases the postprandial response of the anorexigenic gut hormones, peptide YY and glucagon-like peptide-1. *Journal of Clinical Endocrinology and Metabolism*, **95**, 333–337.
- 32 Scisco, J.L., Muth, E.R., Dong, Y. *et al.* (2011) Slowing bite-rate reduces energy intake: an application of the bite counter device. *Journal of the American Dietetic Association*, **111**, 1231–1235.
- 33 Rigamonti, A.E., Bini, S., Grugni, G. *et al.* (2014) Unexpectedly increased anorexigenic postprandial responses of PYY and GLP-1 to fast ice cream consumption in adult patients with Prader-Willi syndrome. *Clinical Endocrinology*, **81**, 542–550.
- 34 Stock, S., Lechner, P., Wong, A.C. *et al.* (2005) Ghrelin, peptide YY, glucose-dependent insulinotropic polypeptide, and hunger responses to a mixed meal in anorexic, obese, and control female adolescents. *Journal of Clinical Endocrinology and Metabolism*, **90**, 2161–2168.
- 35 Tai, M.M., Castillo, T.P. & Pi-Sunyer, F.X. (1997) Thermic effect of food during each phase of the menstrual cycle. *American Journal of Clinical Nutrition*, **66**, 1110–1115.



National Research Ethics Service
Birmingham, East, North and Solihull Research Ethics Committee

REC Offices
Prospect House
Fishing Line Road
Enfield
Redditch
B97 6EW

Telephone: 01527 582534
Facsimile: 01527 582540

31 January 2011

Dr. Thomas M Barber
Associate Professor in Clinical Endocrinology and Diabetes
Clinical Sciences Research Institute
University Hospital,
Clifford Bridge Road
Coventry
CV22 5PX

Dear Dr. Barber

Study Title: Investigation of metabolism in human participants
REC reference number: 11/H1206/3
Protocol number: HMU1

Thank you for your letter of 27 January 2011, responding to the Committee's request for further information on the above research and submitting revised documentation.

The further information has been considered on behalf of the Committee by the Chair.

Confirmation of ethical opinion

On behalf of the Committee, I am pleased to confirm a favourable ethical opinion for the above research on the basis described in the application form, protocol and supporting documentation as revised, subject to the conditions specified below.

Ethical review of research sites

The favourable opinion applies to all NHS sites taking part in the study, subject to management permission being obtained from the NHS/HSC R&D office prior to the start of the study (see "Conditions of the favourable opinion" below).

The Committee has not yet been notified of the outcome of any site-specific assessment (SSA) for the non-NHS research site(s) taking part in this study. The favourable opinion does not therefore apply to any non-NHS site at present. I will write to you again as soon as one Research Ethics Committee has notified the outcome of a SSA. In the meantime no study procedures should be initiated at non-NHS sites.

Conditions of the favourable opinion

The favourable opinion is subject to the following conditions being met prior to the start of the study.

Management permission or approval must be obtained from each host organisation prior to the start of the study at the site concerned.

For NHS research sites only, management permission for research ("R&D approval") should be obtained from the relevant care organisation(s) in accordance with NHS research governance arrangements. Guidance on applying for NHS permission for research is available in the Integrated Research Application System or at <http://www.rdforum.nhs.uk>.

Where the only involvement of the NHS organisation is as a Participant Identification Centre (PIC), management permission for research is not required but the R&D office should be notified of the study and agree to the organisation's involvement. Guidance on procedures for PICs is available in IRAS. Further advice should be sought from the R&D office where necessary.

Sponsors are not required to notify the Committee of approvals from host organisations.

It is the responsibility of the sponsor to ensure that all the conditions are complied with before the start of the study or its initiation at a particular site (as applicable).

Approved documents

The final list of documents reviewed and approved by the Committee is as follows:

<i>Document</i>	<i>Version</i>	<i>Date</i>
Covering Letter		03 December 2010
GP/Consultant Information Sheets	1	02 December 2010
Investigator CV		
Participant Information Sheet	1	02 December 2010
Protocol	1	02 December 2010
Evidence of insurance or indemnity		03 August 2010
Referees or other scientific critique report		24 November 2010
Advertisement	1	02 December 2010
Letter from funder - Trust R&D Letter		24 November 2010
Recruitment Pack	1	02 December 2010
Participant Consent Form	1	02 December 2010
Participant Consent Form	2	24 January 2011
Participant Consent Form: Phase 2	1	02 December 2010
REC application	IRAS 3.0	02 December 2010
Response to Request for Further Information		27 January 2011
Participant Information Sheet	2	24 January 2011

Statement of compliance

The Committee is constituted in accordance with the Governance Arrangements for

This Research Ethics Committee is an advisory committee to West Midlands Strategic Health Authority
The National Research Ethics Service (NRES) represents the NRES Directorate within the National Patient Safety Agency and
Research Ethics Committees in England

Research Ethics Committees (July 2001) and complies fully with the Standard Operating Procedures for Research Ethics Committees in the UK.

After ethical review

Now that you have completed the application process please visit the National Research Ethics Service website > After Review

You are invited to give your view of the service that you have received from the National Research Ethics Service and the application procedure. If you wish to make your views known please use the feedback form available on the website.

The attached document "*After ethical review – guidance for researchers*" gives detailed guidance on reporting requirements for studies with a favourable opinion, including:

- Notifying substantial amendments
- Adding new sites and investigators
- Progress and safety reports
- Notifying the end of the study

The NRES website also provides guidance on these topics, which is updated in the light of changes in reporting requirements or procedures.

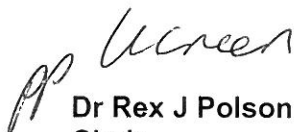
We would also like to inform you that we consult regularly with stakeholders to improve our service. If you would like to join our Reference Group please email referencegroup@nres.npsa.nhs.uk.

11/H1206/3

Please quote this number on all correspondence

With the Committee's best wishes for the success of this project

Yours sincerely



Dr Rex J Polson
Chair

Email: Karen.Green@westmidlands.nhs.uk

Enclosures: "After ethical review – guidance for researchers"

<i>Copy to:</i>	Dr. Peter Hedges Director of Research Support Services Research Support Services University of Warwick University of House Kirby Corner Road Coventry CV4 8UW	Mrs Ceri Jones Head of R & D First Floor Rotunda University Hospitals Coventry & Warwickshire NHS Trust Clifford Bridge Road Coventry CV2 2DX
-----------------	--	--



Health Research Authority

NRES Committee West Midlands – Solihull

East Midlands REC Centre
The Old Chapel
Royal Standard Place
Nottingham
NG1 6FS

Tel: 0115 8839437

15 April 2013

Dr. Thomas M Barber
Associate Professor in Clinical Endocrinology and Diabetes
University of Warwick
Clinical Sciences Research Institut
University Hospital,
Clifford Bridge Road, Coventry
CV22 5PX

Dear Dr. Barber

Study title: Investigation of metabolism in human participants
REC reference: 11/H1206/3
Protocol number: HMU1
Amendment number: Amendment 3 7th Feb 2013
Amendment date: 27 February 2013
IRAS project ID: 66666

The above amendment was reviewed 03 April 2013 by the Sub-Committee in correspondence.

Ethical opinion

The members of the Committee taking part in the review gave a favourable ethical opinion of the amendment on the basis described in the notice of amendment form and supporting documentation.

Approved documents

The documents reviewed and approved at the meeting were:

Document	Version	Date
Participant Consent Form: HMU phase 2 consent form	4	07 February 2013
Participant Information Sheet: HMU Information Sheet	5	07 February 2013
Protocol	HMU Research Proposal revised v4	07 February 2013
Notice of Substantial Amendment (non-CTIMPs)	Amendment 3 7th Feb 2013	27 February 2013
Covering Letter		

Membership of the Committee

The members of the Committee who took part in the review are listed on the attached sheet.

R&D approval

All investigators and research collaborators in the NHS should notify the R&D office for the relevant NHS care organisation of this amendment and check whether it affects R&D approval of the research.

Statement of compliance

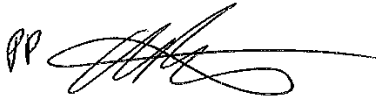
The Committee is constituted in accordance with the Governance Arrangements for Research Ethics Committees and complies fully with the Standard Operating Procedures for Research Ethics Committees in the UK.

We are pleased to welcome researchers and R & D staff at our NRES committee members' training days – see details at <http://www.hra.nhs.uk/hra-training/>

11/H1206/3:

Please quote this number on all correspondence

Yours sincerely



Rex Polson
Chair

E-mail: NRESCommittee.WestMidlands.Solihull@nhs.net

Copy to:

Mrs. Ceri Jones, University Hospital of Coventry and Warwickshire
Dr. Peter Hedges

Welcome to the Human Metabolism Research Unit BodPod

Information Guide

**You have been asked to have a measurement in the BodPod.
Please read this information carefully before your visit.**

The BodPod is located in the Human Metabolism Research Unit on the ground floor of University Hospital, outside Ward 2

What is a BodPod?



The BodPod is a very accurate method of measuring your body composition. It does this by calculating your weight and volume (measured by air displacement) to determine body density. Your body fat percentage is determined from density and this and other measurements will be used by your researcher.

What will I be asked to do in the BodPod Room?

You will first be asked to change into swimwear or close fitting underwear. There is a screen and couch provided and no one will be permitted to enter the room while testing takes place.

You will be asked to stand on some weighing scales with your back towards the wall. It is very important that you stand very still for this measurement.

You will then be asked to sit very still in the BodPod for approximately five minutes in total while measurements are being taken.



Patient Information

At the end of the test you are free to get dressed and leave the room.

What do I need to wear?

- Please bring close fitting swimsuit or underwear.
- A cap will be provided to cover your hair

How safe is the Bodpod?

The BodPod equipment is very safe and used only by those with appropriate training.

The operator will open and close the door several times during the procedure. **Please do not try to help. Keep your hands on your lap and away from the door at all times.**

There is an emergency button if you want the door to open at any time.

The BodPod is very quiet, however, when the door is closed a 'popping' sound can be heard after approximately 30 seconds.



We hope this information will help to prepare you for your visit to the BodPod at the Human Metabolism Research Unit. If you have any further questions, please do not hesitate to contact the staff at the Unit on 024 7696 5621

Comments

If you have any comments on your visit to the HMRU BodPod then please let your researcher or HMRU staff know. We would like to use your experience to help future users of the Unit.

We look forward to meeting you.

Patient Information

The Trust has access to interpreting and translation services. If you need this information in another language or format please contact 024 7696 5621 and we will do our best to meet your needs.

The Trust operates a smoke free policy.



Document History

Author	Alison Campbell
Department	Research and Development
Contact Tel	25621
Published	January 2012
Reviewed	
Review	January 2013
Version	1
Reference No	HIC/LFT/1398/12

Welcome to the Human Metabolism Research Unit (HMRU)

Information Guide

You have been asked by your researcher to attend University Hospital's Human Metabolism Research Unit. Please read this information carefully before your visit.

What is the Human Metabolism Research Unit (HMRU)

The Human Metabolism Research Unit (HMRU) is a dedicated research unit run by University Hospitals Coventry and Warwickshire NHS Trust (UHCW) in partnership with Warwick Medical School. It includes a unique two room Whole Body Calorimeter.

HMRU is located on the ground floor of University Hospital, outside Ward 2

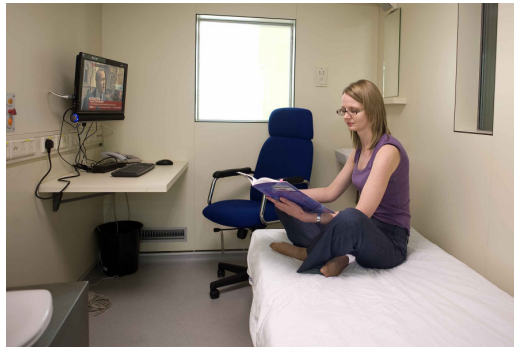
What facilities are there during my stay?

The Whole Body Calorimeter has two bedsit rooms, a shower room and monitoring area. On arrival you will be given an outline of the timetable for your stay. You will have a tour with full instructions about your room and its facilities.

Each room has a **desk, chair, fold down bed, toilet, sink, telephone** and an internet connected **computer/television**. An **exercise step** is provided for light exercise or as directed by your researcher. There is an intercom to speak to the resident in the second room as well as the staff.

There are three windows; one with an outside view, one to the neighbouring room and one in the door.

There are three two-way hatches which are air locked. These are used for passing food, urine samples and taking blood tests. Only one side of the hatch can be opened at a time.



Patient Information

What do I need to bring with me?

- Reading materials if desired, such as book, newspaper etc
- Nightwear and toiletries - **no aerosols** please
- Usual medication, if any
- Towel and change of clothing if you wish to shower at the end of your stay
- Outdoor clothing and extra belongings can be stored in a secure locker
- Do not bring any food or drinks – these will be provided

You have been asked by your researcher to stay on the unit for a set time, usually between 8 and 36 hours. **During this time you will be required to stay in your room with the door closed.** This enables very accurate measurements to be taken from the surrounding air.

Fresh air is constantly circulating and temperature and humidity is regulated. Please inform the staff if you are too warm or cold.

There is a fire alarm in your room. You will be given instructions as to what to do in an emergency.

You may, of course, leave at any time if you no longer wish to participate. Simply open the **door**, it is **never locked**.

Are there any special preparations required?

- Please do not exercise for 24 hours
- Arrive by public transport or car, do not walk any distance to the Unit
- While in the HMRU you will not be able to drink caffeinated drinks (for example, tea or coffee), alcohol and fizzy drinks – you may want to gradually reduce your intake of these before this if necessary.
- Do not eat or drink anything except water for **12 hours before** arrival.

Comments

If you have any comments, positive or negative, about your stay in the HMRU, please let your researcher or HMRU staff know. We would like to use your experience to help future users of the Unit.

We look forward to meeting you.

We hope this information will help to prepare you for your visit to the Human Metabolism Research Unit. If you have any further questions, please do not hesitate to contact the staff at the Unit on 024 7696 5621

The Trust has access to interpreting and translation services. If you need this information in another language or format please contact 024 7696 5621 and we will do our best to meet your needs.

The Trust operates a smoke free policy.

Patient Information



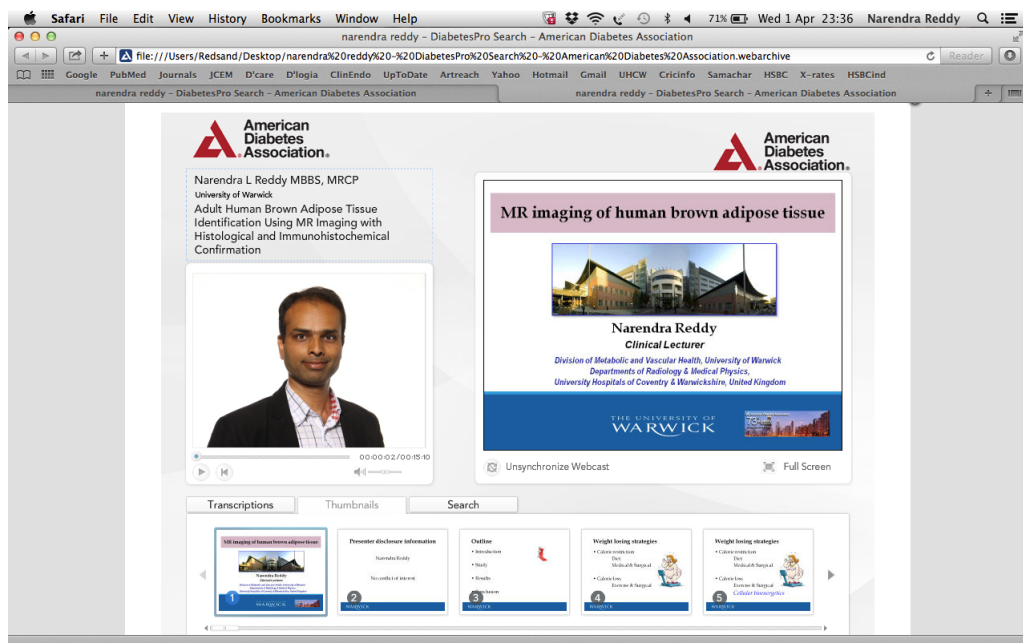
www.advantagewm.co.uk

Document History

Author	Alison Campbell
Department	Research and Development
Contact Tel	25621
Published	January 2012
Reviewed	
Review	January 2013
Version	1
Reference No	HIC/LFT/1399/12

Oral presentation in 73rd Scientific Sessions American Diabetes Association

22nd June 2013, Chicago, United States of America



Prizes

2nd prize for poster presentation – Certificate and cash reward

‘MR imaging of human BAT’

13th December 2012, The Royal Society, London

Joint meeting of **The Physiological Society** and **The Academy of Medical Sciences**

1st prize for oral presentation – Certificate and cash reward

‘Metabolic significance of Brown fat in humans’

8th February 2013, National Exhibition Centre, Birmingham

Midlands Endocrine Club

★ **The Midlands Endocrine Club** ★

First Prize

is presented to

Dr Narendra Reddy

for

'Brown adipose tissue identification in an adult human using
IDEAL MRI'

J. Tol
Signature

8th February 2013
Date